Cues Triggering Formation and Germination of Resting Stages in Marine Diatoms

Thesis

Cues triggering formation and germination of resting stages in marine diatoms

Angela Pelusi

Doctor of Philosophy (PhD)

in School of Life, Health and Chemical Sciences

September 2018

Abstract

The project of my PhD thesis was focused on understanding the factors that induce spore formation and germination in the marine planktonic diatom *Chaetoceros socialis*. Among the candidate triggers of spore formation, nitrogen depletion is the most common while light is the principal trigger of spore germination. The link between spore formation and nitrogen starvation in the natural environment is however elusive and this lead me to test other factors, such as cell crowding and viral infections, which were never tested before.

The results of my experimental work show that nitrogen depletion is not the only factor that induces the formation of resting spores, even though it remains the most effective in laboratory experiments. Spore formation was in fact induced when nitrogen and other nutrients were still available; it was induced by culture medium conditioned by the presence of high cell density, by culture medium obtained after killing cells by sonication. This is evidence for the presence of chemical compound/s that induced the formation of spores. Moreover, spores were produced in nutrient replete cultures infected by a species-specific virus. A transcriptomic approach in which the differential expression of genes in key time points during spore formation *versus* the control (exponentially growing cells), provided insights on the molecular mechanisms involved in this life cycle transition.

I evaluated the role of blue, red and white light at very low intensity (1.2 µmol m^2 sec^{-1}) below the threshold for photosynthesis and slight higher white light (20 µmol m^2 sec^{-1}) in inducing spore germination. Results showed significantly higher germination rates only at higher light levels, while low and similar germination rates although germination occurred in other conditions including the controls in the dark. This study adds new and relevant information for understanding how and why spores are formed, underlying their potential importance in population dynamics and, in turn, in the ecosystem functioning.

Acknowledgements

I would like to thank the Open University (OU) and Stazione Zoologica Anton Dohrn for the opportunity and fellowship to pursue my Ph.D.

This thesis will never been written without the help of my research supervisors: I would like to express my deep gratitude to Dr. Marina Montresor for being my landmark over these three years, guiding me with kindness and honest criticism. I would also like to extend my thanks to Dr. Anna Godhe, Dr. Mariella Ferrante and Dr. Maurizio Ribera d'Alcalà for their valuable and constructive suggestions during the planning and the development of this research, for sharing with me their knowledge and experience and keeping my progress on schedule, I could wish nothing better of all of them.

My grateful thanks are also to Dr. Elio Biffali, Dr.Pasquale de Luca and Dr. Giovanna Benvenuto for their assistance in molecular and microscopic analysis; learning new techniques has been one of the important achievements of this experience and they made it even more pleasant. I am grateful to Dr. Laura Entrambasagueas for the bioinformatic analysis and her constant availability. I would also thank all the other technicians and colleagues of Stazione Zoologica for their help and the

Special thanks to Greta and Massimiliano for being partners of this challenge from its beginning I could not explain how grateful I am for your friendship.

Thank to my crazy Naepolitan family, "I Casucci" (Bea, Gio, Luca and Elena and I sesti) for being so brave to live with me every day. Beside the work all of them made my Neapolitan experience special.

And finally thanks to my family for teaching me that passion and enthusiasm are essential components of everyday life, I wish to make them always proud of me.

List of contents

List of contents i

List of figures v

List of tables xiii

Chapter 1

Introduction 1

The resting strategy 3

Phytoplankton: a brief introduction 6

Phytoplankton life histories 8

Diatoms 10

Resting stages in diatoms 12

Resting stages in diatom:formation 14

Resting stages in diatom:germination 23

The model species for my PhD project: the centric diatom Chaetoceros socialis 28

The questions addressed in this thesis 31

Chapter 2

Spore formation and germination: microscopic investigation 35

Introduction 37

Materials and Methods 38

Culture isolation and maintenance 38

Genetic characterization of the strains 39

Time lapse microscopy 40

Confocal laser scanning microscopy 41

Results 43

Vegetative cell division 43

Spore formation 46

Spore germination 53

Discussion 56
Vegetative division 56
Spore formation 56
Spore germination 59
Chapter 3
Factors inducing spore formation: nitrogen limitation and cell density 61
Introduction 63
Materials and Methods 64
Experiment 1: nitrogen limitation as a factor for the induction of spore formation 64
Experiment 2: cell density as a factor for the induction of spore formation 66
Experiment 3: spore formation in high-cell-density conditioned medium 68
Experiment 4a and 4b: short-term experiment with high-cell-density conditioned medium 70
Results 71
Experiment 1: nitrogen limitation as a factor for the induction of spore formation 71
Experiment 2: cell density as a factor for the induction of spore formation 80
Experiment 3: spore formation in high cell density conditioned medium 86
Experiment 4a and 4b: short-term experiment with high-cell-density conditioned medium 88
Discussion *92*
Nitrogen-limitation as a factor inducing spore formation 92
The possible role of density in inducing spore formation 93
Spore formation mediated by a chemical signal? 96
Conclusion 98
Chapter 4
Effect of viral infection on spore formation 99
Introduction 101

Ecological role of virus-phytoplankton interactions 101
Diatom viruses 103
Material and Methods 104
Algal and virus isolation and maintenance 104
Experimental set-up 104
Calibration to assess cell viability 105
Sample preparation for Transmission Electron Microscopy 106
Viral genome extraction, primer design and preparation of the standard curve 107
qPCR assay conditions and total viral genome copy number enumeration 108
Most Probable Number (MPN) assay 109
Results 111
Effect of viral infection on cell concentration and spore formation 111
Evidence for the presence of viruses: TEM preparations 116
Viral concentration assessed by qPCR 119
Viral concentration assessed by MPN 121
Discussion 121
Chapter 5
Differential gene expression analysis during spore formation 125
Introduction 127
Nitrogen limitation 129
Materials and methods 131
Experimental set up and transcriptome sequencing 131
RNA extraction 132
De novo transcriptome assembly, functional annotation and differential gene expression analysis 133
Genes related to specific processes 134
Results and discussion 135
Spore formation in the experiment for transcriptomic analysis 135

Differential gene expression and Gene Ontology enrichment analysis 136
Common and unique transcripts 150
Expression patterns of genes related to specific processes 150
Conclusions 170

Chapter 6

Spore germination 173
Introduction 175
Spectral modification of light 175
Light perception 177
Material and methods 179
Absorption spectra 179
Spore germination at different irradiances and wavelengths 180
Results 181
Absorption spectra 181
Spore germination at different irradiances and wavelengths 183
Discussion 187

Conclusions and perspectives 191
Future perspectives 198

References 201

Appendix 233

List of figures

Figure 1.1: CLSM images of *C. socialis* "*sensu stricto*", strain APC2. A) Traditional tertiary structure of colonies. Scale bar 100 µm. B) Spores still attached to one parental valve. The arrowhead shows spines typical of this species. Scale bar 10 µm. 29

Figure 1.2: Weekly abundances (cells ml^{-1}) of *C. socialis* at the LTER MareChiara station in the Gulf of Naples from 1984 to 2010 (courtesy of Diana Sarno, Stazione Zoologica Anton Dohrn). 30

Figure 1.3: Life cycle of *C. diadema* (French III & Hargraves, 1985). 31

Figure 2.1: Schematic representation of the three spore types in diatoms as defined by the position of the spore relative to the pa rental valves (based on Round et al., 1990): endogenous spore (A), semi- endogenous spore (B), exogenous spore (C). 37

Figure 2.2: Schematic drawings of the confocal laser scanning microscope. The laser emits the light that is directed by rotating scanning mirrors; the pinhole, a single small aperture, allows the passage of the light; the detector filter (blue arrow) catches the light emitted by the sample. Filters are selected based on the wavelengths required for the excitation of the specific fluorochrome (excitation filters) and the detection of the specific wavelengths emitted by the stained or auto fluorescent sample (detector filters). 41

Figure 2.3: Time-lapse frames of vegetative divisions. Two colonies of strain APC2 at time 0 (the colony on the left moved away during the recording period) (A). Colony after 3 hours of observation (B). All cells in the chain duplicated and there are visible also short setae in elongation (arrowheads). Scale bars = 50 µm. 44

Figure 2.4: CLSM images of strain APC2 stained with PDMPO and SYBER Green (A) and in transmitted light (B). A chain of vegetative cells in division with nuclei stained with SYBER Green (in blue) and newly synthesized frustules stained with PDMPO (in green). The neo-synthesized valves after mitotic division are arrowed Arrowheads mark two cells in which cytokinesis just occurred but the daughter valves were not formed yet. Scale bars = 10 µm. 45

Figure 2.5: CLSM images of strain APC2 stained with PDMPO (A) and in transmitted light (B). In figure A are visible vegetative cells whose newly synthesized valves and setae are stained in green; chloroplasts are red. The overlapping of the different staining can result in a yellow coloration. Scale bars = 50 µm. 45

Figure 2.6: Frames extracted from the first time-lapse showing the formation of four spores in strain APC12. On the top-right time: hours, minutes, seconds. The cells that turned into spores are marked with arrows (A). Frames showing several steps of spore formation (see text for details) (B-F). On the left the entire chain and on the right magnification of the first two spores formed. Frame at the end of recording with all seven spores marked with arrows (G). Scale bars = 50 µm. 47-48

Figure 2.7: Frame extracted from the second time-lapse showing the formation of two spores in strain APC2. Colony at time zero with a cell undergoing vegetative division (arrowhead) (A). The two cells that are transforming into spores (arrows). The one on the bottom is already forming the primary spore valve (B). Spore formation in one of the daughter cells (arrowhead) (C). Spores completely formed (D); Scale bars = 50 µm. 49

Figure 2.8: CLSM images of strain APC2 stained with PDMPO (A) and in transmitted light (B). In figure A spores and vegetative cells with neo-synthesized valves stained in green are visible. Chloroplast are in red. Scale bars = 50 µm. 50

Figure 2.9: CLSM images of strain APC12. Vegetative cells stained with the nuclear stain SYBER Green (A). The primary valve of a spore stained with PDMPO (arrowed) close to a vegetative cell in which the two SYBER green-stained nuclei just completed mitosis (B). Vegetative cells and spores in formation stained with PDMPO and SYBER Green (C and D). Chain of spores stained with PDMPO and SYBER Green; the secondary valve of each spore is visible but the nucleus is visible in only two spores (arrows) (E). The same image in transmitted light (F). Scale bars = 10 µm. 51

Figure 2.10: CLSM images of strain APC12. Spores stained with SYBER Green (blue) and PDMPO (green); two nuclei are visible in the second spore in formation (arrowhead) (A). The same image in which also chloroplasts (red) have been visualized (B). Scale bars = 10 µm. 52

Figure 2.11: CLSM images of strain APC12 showing a chain of spores. Spores stained with SYBER Green (blue) and PDMPO (green); chloroplasts (red) (A). The same image in which only the nuclei are visualized; the red circle marks two nuclei in the same spore (B). Scale bars = 10 µm. 52

Figure 2.12: CLSM images of strain APC2 showing a chain of spores in which are visible the newly synthesized secondary valve and the chloroplast. A) Spores stained with PDMPO and B) in transmitted light. Scale bars =10 µm. 53

Figure 2.13: Frames extracted from time-lapse that show the germination of a spore. On the left frames time is reported: hours, minutes, seconds (on the top-right). The white box is the portion expanded on the pictures on the right. Beginning of time-lapse (A). The cytoplasm movement and the formation of the first vegetative valve (B). Beginning of the second vegetative valve formation (C). Detachment of the spore valves (D). Scale bars = 50 µm. 54

Figure 2.14: Frames extracted from time-lapse that show the germination of a spore with hours, minutes, and seconds on the top-right. The white box marks the portion expanded on the pictures on the right. Free vegetative cell (A). End of cellular division (B). Elongation of setae (C). Scale bars = 50 µm. 55

Figure 2.15: Frame of second experiment showing the first vegetative epivalve formation. Scale bar = 50 µm. 56

Figure 2.16: Schematic drawings of the formation of endogenous spores in C. *socialis*. A mitotic division with the degeneration of one nucleus precedes the formation of both spore's valves. **58**

Figure 3.1: Schematic representation of the experimental set up for Experiment 2. ..... **68**

Figure 3.2: Schematic representation of the experimental set up used for Experiment. **69**

Figure 3.3: Total cell concentration of strain APC12 in semi-continuous growth, at high cell density with full strength medium (+N) in Experiment 2 (red) and during the semi-continuous acclimation growth of the cultures used to prepare the high-cell-density conditioned medium (blue). Data represent average values ± S.D. (n=3). **69**

Figure 3.4: Growth curves of strain APC1 (A, B) and APC2 (C, D) in low nitrogen medium (A, C; blue) and in high nitrogen medium (B, D; orange). Data shown as average ± S.D. (n=3). **72**

Figure 3.5: Average percentages (n=3) of spores and vegetative cells in strains APC1 (A, B) and APC2 (C, D) grown in low nitrogen medium (A, C; blue) and in high nitrogen medium (B, D; orange). **73**

Figure 3.6: Maximum exponential growth rate of the two strains, APC1 (A) and APC2 (B), grown in low-nitrogen medium (blue bars) and high-nitrogen medium (orange bars); the exponential phase lasted two days. Data shown as average ± S.D. (n=3). Daily growth rate of the two strains APC1 (C) and APC2 (D) grown in low-nitrogen medium (blue bars) and high-nitrogen medium (orange bars) during the entire experiment. Values on the x axis show the time interval over which growth rate was measured, i.e. 1= growth rate between day 0 and day 1. Data shown as average ± S.D. (n=3). **74**

Figure 3.7: Concentration of: nitrates (NO_3; A, B), silicates (SiO_2; C, D) and orthophosphates (PO_4; E, F) in strains APC1 (A, C, E) and APC2 (B, D, and F) grown in low nitrogen medium (blue) and in high nitrogen medium (orange). Data shown as average ± S.D. (n=3). Note that NO_3 concentration for the low nitrogen condition is represented on the right axis. **75**

Figure 3.8: Intracellular nitrogen content (A, B), carbon content (C, D) in strain APC1 (A, C) and APC2 (B, D) grown in low nitrogen medium (blue) and in high nitrogen medium (orange). Data shown as average ± S.D. (n=3). Treatment and control values for each sampling time have been compared with a t-test. **76**

Figure 3.9: C:N ratio in strain APC1 (A,) and APC2 (B,) grown in low nitrogen medium (blue) and high nitrogen medium (orange). Data shown as average ± S.D. (n=3). **77**

Figure 3.10: Nitrogen (A, B) silicate (C, D) and phosphate (E, F) uptake rate per day, during the exponential growth phase, in strains APC1 and APC2 (right) grown in

depleted (blue) and full strength (orange) medium. Data shown as average ± S.D. (n=3). 79

Figure 3.11: Total cell concentration (vegetative cells and spores) of strain APC12 in semi-continuous growth with full strength medium (orange) and medium depleted in nitrogen (blue), at three different cell densities (high, A; medium, B; low, C). Data represent average values ± S.D. (n=3); the error bars is not visible in most time points because it was lower than the symbol. 81

Figure 3.12: Spore percentage of strain APC12 in semi-continuous growth with full strength medium (orange) and medium depleted in nitrogen (blue), at three different cell densities (high, A; medium, B; low, C). Data represent average values ± S.D. (n=3). .84

Figure 3.13: Growth curves of high (A, B) medium (C, D) and low (E, F) density in low nitrogen medium (A, C, E; blue) and in high nitrogen medium (B, D, F; orange). Data shown as average ± S.D. (n=3). Note that in panels D and F values equal to zero are missing. 85

Figure 3.14: Total cell concentration (vegetative cells and spores) of strain APC12 in semi-continuous growth, at low cell density with full strength medium in Experiment 2 (red) and with the high-cell-concentration conditioned medium in Experiment 3 (blue). Data represent average values ± S.D. (n=3). 86

Figure 3.15: Concentration of vegetative cells and spores in Experiment 3 where cultures were inoculated in high-cell-density conditioned medium (A). Percentage of spores in Experiment 3 (blue) and in Experiment 2 at low cell density with full strength medium (red). Data represent average values ± S.D. (n=3).). Note that in panel A equal to zero are missing. 87

Figure 3.16: Results of Experiment 4a in which strain APC12 was inoculated in high-cell-density conditioned medium obtained by filtration (filtered medium) and by sonication and filtration (sonicated medium) and in the control (full strength f/2 medium). Total cell concentration (A), percentage of spore (B) in the treatments and control, concentration of vegetative cells and spores in control (C), filtered medium (D) and sonicated medium (E). Data are shown as average ± S.D. (N=3). 89

Figure 3.17: Results of Experiment 4b in which strain APC12 was inoculated in high-cell-density conditioned medium obtained by filtration (filtered medium), by filtration with the addition of nutrients (filtered medium+ nutr.), by sonication and filtration (sonicated medium), by sonication and filtration with the addition of nutrients (sonicated medium+ Nutr.) and in the control (full strength f/2 medium). Total cell concentration (A), percentage of spore formation in the treatments and control (B), concentration of vegetative cells and spores in control (C), filtered medium (D), filtered medium + Nutr. (E), sonicated medium (F), sonicated medium + nutr (G).Data are shown as average ± S.D. (N=3). 91

Fig 3.18: Estimates of nitrates (A), phosphates (B) and silicates (C) concentration in the medium of cultures growth at the three cell densities in nitrogen depleted (blue) and full strength medium (orange). Data represent average values ± S.D. (n=3). 94

Figure 4.1: Schematic drawing of 10-fold serial diluitions of the viral lysate and MPN assay. Drawing provided by K. Thamatrakoln 110

Figure 4.2: Fluorescence curves of control cultures (blue) and cultures infected by viruses (red) for the Neapolitan (A) and Japanese (B) strains during four days after the infection in Exp#001. Green arrows show the day of infection. Data shown as average ± SD (n=3). Thamatrakoln 111

Figure 4.3: Cell densities (cells ml-1) of control cultures (blue) and cultures infected by viruses (red) for the Neapolitan (A) and Japanese (B) strains during four days after the infection in Exp#001. Green arrows show the day of infection. Data shown as average ± SD (n=3). 112

Figure 4.4: Vegetative cells (blue) and spores (red) concentration in Neapolitan (A, B) and Japanese (bottom, D) strains in control (A, C) and infected (B, D) cultures in Exp#001. Data shown as average ± S.D. (n=3). 113

Figure 4.5: Fluorescence measurements in control cultures (blue) and in cultures infected by viruses (red) for the Neapolitan (A) and the Japanese (B) strains during four days after the infection in Exp#002. Green arrows show the day of infection. Data shown as average ± SD (n=3). 114

Figure 4.6: Total cell numbers in control cultures (blue) and in cultures infected by viruses (red) for the Neapolitan (A) and Japanese (B) strain during four days after the infection in Exp#002. Green arrows show the day of infection. Data shown as average ± S.D. (n=3). 114

Figure 4.7: Vegetative cells (blue) and spores (red) concentration Neapolitan (A, B) and Japanese (C, D) strains in control (A, C) and infected (B, D) cultures in Exp#002. Data shown as average ± S.D. (n=3). 115

Figure 4.8: Spore percentage (number of spores of total number of alive cells + spores) in control condition (blue) and infected (red) cultures of the Neapolitan strain (A, C) and Japanese strain (B, D) in Exp#001 (A, B) and in Exp#002 (C, D). Data shown as average ± S.D. (n=3).Statistical analysis performed considering values over time.). 116

Figure 4.9: TEM micrograph of infected vegetative cell of strain APC12 with degraded cytoplasm (A). Detail of (A) with arrows indicating viral particles (B). n=nucleus, chl= chloroplast. Scale bars = 1 (A) and 0.5 µm (B). 117

Figure 4.10: Micrograph of TEM ultrathin-section of a spore of the Neapolitan strain APC12. Vc= vacuole chl=chloroplast, m=mitochondria, s= storage compounds. Scale bar = 3 µm. 118

Figure 4.11: TEM micrograph of viral lysate produced by filtration of an infected culture of strain APC12. Viral particles are encircled in red. Scale bar = 0.1 µm. 118

Figure 4.12: Gel of the PCR to test the two primers with viral genomic RNA. B1: blank for the first primer-pair, P1: primer1, B2: blank for the second primer-pair, P2: primer2 and the ladder where the values for 100 and 200 bp are indicated. 119

Figure 4.13: Standard curve used for the direct quantification of initial lysate used for the infection and final lysate of the Neapolitan and Japanese strains. It represents is the Ct values of three technical replicates. Data shown as average ± S.D (n=3). 120

Figure 4.14: Quantification by qPCR of viral copy number·mL-1of initial lysate (green), final lysate of the Neapolitan (blue) and Japanese (red) strains. The latter two values are the average of the triplicate samples and are shown as average ± SD. 120

Figure 4.15: Infectious units calculated with MPN assay; initial lysate (Ti) in Neapolitan (light red) and Japanese (light blue) strains and final lysates (Tf) in Neapolitan (red) and (blue). Average data ± SD (n=3). 121

Figure 5.1: Cell density (A, B) and percentage (C, D) of vegetative cells and spores in cultures grown in low nitrogen (treatment, A, C) and nutrient replete (control, B, D) medium. Red circles indicate sampling points for the differential gene expression analysis. Data in panels A and B are shown as average ± S.D. (n=3). 136

Figure 5.2: Dimensional plot of PCA components 1 and 2 (x and y axis, respectively) of expression values of *C. socialis.* 137

Figure 5.3: Number of differentially expressed genes (red), annotated with at least one GO term (blue), and the percentage of GO annotated on the total genes. 138

Figure 5.4: Biological processes up (upper panel) and down (lower panel) regulated in T2, T3 and T4 versus control (T2C). The size of the grey circles on the right side of each panel represent the frequency of the GO term in the underlying GO databases (more general terms have larger circles) and the colour code represents the level of statistical significance (log 10 p value). The plots representing the comparisons between T3/T4 and the control are in next two pages. 144,145,146

Figure 5.5: Biological processes down (upper panel) and up (lower panel) regulated in T3 and T4 versus treatment (T2T) and each other. The size of the grey circles on the right side of each panel represent size indicates the frequency of the GO term in the underlying GO databases (general terms have larger circles) and the colour code represents the level of statistical significance (log 10 p value). The plots representing the comparisons between T4 and T2/T3 are in next two pages. 147,148,149

Figure 5.6: Number of up (A) and down-regulated (B) genes common and unique in T3T and T4T compared to the control condition (T2C). 150

Figure 5.7: Differential expression of genes involved in nitrogen metabolism and TCA (Tricarboxyilic Acid) cycle pathway in nitrogen-stressed cultures *vs* control condition at T2T, T3T and T4T. 155

Figure 5.8: Differential expression level of genes involved in Pentose Phosphate Pathway in nitrogen-limited cultures *vs* control condition during at T2T, T3T and T4T. 161

Figure 5.9: Differential expression level of genes involved in TAG biosynthesis in nitrogen-stressed cultures *vs* control condition during at T2T, T3T and T4T. **162**

Figure 5.10: Ammonia fermentation pathway. Image taken from Catalanotti *et al.*, 2013. Ald: alcohol dehydrogenase; AddaA: acetaldehyde dehydrogenase; Ack: acetate kinase. **165**

Figure 6.1: Underwater profile of different light wavelengths. Profile provided by dr. Maurizio Ribera d'Alcalà. **176**

Figure 6.2: Absorption spectra of vegetative cells (A 1, 2), fresh spores (B 1, 2) expressed as absorption·cell1; the old-fresh spores ratio of absorption spectra (C). Panels on the right side are enlargements of the portion marked in red of the panels on the left. Lines represent loess fitted curves and halos the standard error (n=3). **182**

Figure 6.3: Agglomerates found in cultures maintained in the dark for three months, spores and spore valves are marked with arrows (A); two valves and two dead vegetative cells found in one sample kept in the dark (C). Scale bars: 10 µm. **183**

Figure 6.4: Percentage variation of the increase or decrease of full spores, valve pairs and vegetative cells in the different experimental conditions as compared to the values recorded at t0 after 3 (blue) and 7 (red) days. In the upper row cultures incubated at different wavelengths (A) in the lower row, the respective control in the dark (B). Data represent average values ± S.D. (n=3). **185**

List of tables

Table 1.1: The most relevant publications in which the factors inducing the formation of spores have been studied in laboratory, ... **18**

Table 1.2: The most relevant publications in which the factors inducing the formation of spores have been studied in the natural environment, ... **22**

Table 1.3: Main studies evaluating viability and /or factors influencing germination of resting stages using cultures or natural sediment samples (N= nitrogen; P=phosphorus; T=temperature) **26**

Table 2.1: Wavelengths of excitation laser (Ex. laser) and type of emission filter (Filter Em.) used for each fluorochrome during observations in CLSM. The absorbance (Abs.) and emission (Em) wavelength range for the different fluorochromes are also indicated. **42**

Table 3.1: Concentration of the main nutrients in the Low N medium (treatment) and High N medium (control) used in Experiment 1. ..... **66**

Table 3.2: Concentration of nutrients in the two media used in Experiment 2. .... **67**

Table 3.3: Hypotheses at the base of experiment #2. ..... **80**

Table 3.4: Growth rates (specific absolute growth rate· (day^{-1}) estimated over the time interval between two subsequent dilutions (two days) for each cell density and media treatment. Values shown as average ± S.D. (n=3). * Data statistically different to all other conditions ($P<0.005$). **82**

Table 3.5: pH values at different time points in the cultures grown at high density in '+N' medium. Values shown as average ± S.D. (n=3). **82**

Table 4.1. Primer sequences used to prepare the standard curve and qPCR. **108**

Table 5.1: Overview of papers in which molecular responses to nitrogen starvation were examined in diatoms. **129**

Table 5.2: Basic statistics of the *de novo* transcriptome of *C. socialis* **137**

Table 5.3: Number of differentially expressed (DE) genes in the comparisons between the control (T2C) and the treatments at three time points (T2T, T3T, T4T) and between pairs of treatments. For each comparison, the number of DEGs, the number of the individual GO terms (BP= biological processes; MF= molecular functions; CC= cellular compartments),in common between categories (BP_MF _CC, MF_CC, BP_CC, BF_MF); the number and percentage of annotated GO terms are listed for both up- and down-regulated genes and functions (GO annotated). **140**

Table 5.4: Differential expression of genes related to resting stage formation; log fold change in the different time point comparisons. **152**

Table. 5.6: Differential expression of genes related to autophagy; log fold change in the different time point comparisons. **157**

Table 5.7: Differential expression of genes related to the metabolism of crysolaminarin; log fold change in the different time point comparisons. **160**

Table 5.8: Differential expression of photoreceptors; log fold change in the different time point comparisons. **164**

Table 5.9: Differential expression of metacaspases; log fold change in the different time point comparisons. **167**

Table 5.10: Differential expression of genes related to synthesis of flagella and meiosis; log fold change in the different time point comparisons. **168**

Table 6.1: One-way Anova performed on the variation of spore percentages in samples collected at day $t_{3.}$ Values significantly different (P value < 0.05) are reported in red. **186**

Table 6.2: One-way Anova performed on the variation of spores in samples collected at day $t_{7.}$ Values significantly different (P value < 0.05) are reported in red. **186**

Chapter 1
Introduction

The research carried out within my PhD project addresses various questions concerning the production of resting spores in the marine planktonic diatom *Chaetoceros socialis,* from the modality in which they are produced at the cellular level, to the factors that induce their formation, to the genes activated during spore formation, and, finally, to the condition in which resting spores can germinate. In this Chapter, I will provide: a brief overview on the resting strategy as an important trait in the life history of many organisms, an illustration of planktonic microalgae and diatoms in particular with information of the main features of their life histories, an overview on the information available on formation and germination of diatom resting stages. At the end of the chapter, I present the main questions addressed in this thesis.

The resting strategy

The fact that resting stages are a widespread strategy suggests that in the natural environment a considerable fraction of microorganisms might be metabolically inactive. For example, it has been estimated that in natural samples of bacteria from 20 to 80% of cells are metabolically inactive (Cole, 1999). The capability to switch from an active growing stage to a dormant one allows them to survive to adverse conditions and might be interpreted as the key of their success, abundance and of their diversity (Stevenson, 1977; Lennon & Jones, 2011).

When an organism enters a reversible stage of low metabolic activity, the stage is defined ‘resting’. The terminology used to describe these stages is often confusing and I will use here the terms used in plant biology. There are two kinds of resting stages, basically distinguished by the cause that determines the ‘resting period’ and its termination. The mandatory suspension of growth determined by the organism’s internal clock is defined ‘dormancy’, while it is called ‘quiescence’ when its duration is influenced by external environmental factors such as light, temperature, or nutrient availability. In the first case, even if the conditions become favourable, the organism does not germinate until the end of a refractory period that is species-specific. This mechanism explains the seasonal appearance of some higher plants that can germinate only after a defined period of dormancy and that anticipate the adverse season producing dormant seeds. In the second case, the organism produces a resting stage in response to environmental cues but can return to growth given the appropriate environmental signals. The presence of resting stages is known for a large number of organisms living in different habitats and belonging to different lineages, from plants, to

animals, to protists and bacteria. Also in the marine environment many studies on resting strategies have been carried out, for instance on copepods (Marcus, 1996), rotifers (Snell *et al.*, 1983), dinoflagellates (Figueroa *et al.*, 2018) and diatoms (McQuoid & Hobson, 1996).

Several bacteria can produce resting stages and they represent the most studied taxa due to their important role as pathogens for humans and other organisms (Lennon & Jones, 2011). A particular form of dormancy is represented by the so-called 'persister cells', which can just stop growing and become spontaneously dormant, apparently without the need of an external trigger (Wood *et al.*, 2013). The persister cells show resistance to antibiotics, which is not heritable by the progeny.

The resting mechanism can be different within the same group of organisms, and copepods are a good example: depending on the species they may arrest the metabolic activity during embryonic, naupliar, copepodite or adult phase. Moreover, copepods may produce diapausing eggs, whose hatching depends on the internal clock, or quiescent eggs when hatching is determined by external conditions (Marcus, 2005).

Also molecular and cellular pathways differ among taxa. More investigations have been carried out on the molecular mechanisms that regulate dormancy in bacteria, in reason of their implication in dangerous diseases, as tuberculosis and cholera (Coates, 2003). Often the formation of resting stages in bacteria is related to environmental factors such as low nutrient concentration, light, temperature and crowding (Jones & Lennon, 2010). The first signal implicated in the perception of these factors is a trans-membrane histidine kinase sensor that perceives external changes and promotes the intracellular reorganization through a highly structured regulatory network that ends with the formation of the resting stage. Looking at gene expression, bacteria remain the most studied microbes: searching orthologues of genes involved in dormancy, showed that there are presumably several genetic networks behind resting stages formation (Lennon & Jones, 2011).

The formation of a resting stage requires energy because it implies an intracellular chemical reorganisation, with an increase in storage compounds and a modification of cell stoichiometry. Cyanobacteria's akinetes contain high concentration of phycocyanin and glycogen (Sutherland *et al.*, 1979) used as N- and C-source, respectively. These storage compounds ensure the minimum metabolic activity required during the resting period and determine the survival time of the resting stages that can potentially be very

long, as proved for *Anabaena* akinetes revived after 64 years (Livingstone & Jaworski, 1980).

Germination seems to be almost always triggered by the presence of favourable environmental conditions for growth even when a mandatory period of dormancy is required; i.e., also when the mandatory dormancy period is completed germination occurs only at specific conditions. In some bacteria, germination might be a density dependent event, and a *quorum* of individuals has to be reached before that transition can happen (Lennon & Jones, 2011). The molecular mechanism that determines the *quorum sensing* germination is the resuscitation promoting factor (Rpf) that is secreted in the environment by the randomly awake cells in the population; if conditions are favourable the concentration of Rpf increases and induces the germination of the other dormants (Lennon & Jones, 2011). This mechanism has been observed the first time in *Micrococcus luteus* (Mukamolova *et al.*, 1998) but common to many other bacteria belonging to Actinobacteria.

Resting stages act as "seed banks", ensuring the persistence in time of genotypes and populations, allowing them to withstand periods of adverse conditions, with important ecological implications for population dynamics. For instance, the formation of resting stages can increase biodiversity at different levels: it promotes the intraspecific genetic variability (assuring the revival of genomes after long time of dormancy or transported from different areas), allowing the coexistence of different species in the same environment, ensuring their persistence in a certain environment when they are absent in the water column (as in the seasonal succession of planktonic species), determining ecologically important phenomena as bloom initiation and termination, and influencing biogeographic distribution patterns. Resting stages thus have the function of stabilizing an ecosystem that has to cope with more or less fluctuating environmental conditions.

Classical models of plankton productivity look at benthic-pelagic coupling only in terms of nutrient cycling, without considering the importance that resting stages may have on energy flow, plankton production, population dynamics and on biodiversity (Anderson, 2005). At least for phytoplankton, the main part of studies is based on coastal areas, especially because they are more easily accessible. The permanence of resting stages in the sediment may be short but there are records of spores germinating after very long time (Ellegaard & Ribeiro, 2018). The recruitment in the water column depends on their physiological features, for instance how much storage compounds they

have accumulated and how much has been consumed during the dormant period, but also on the capability of resting stages to perceive environmental signals such as light availability or oxygen concentration.

Phytoplankton: a brief introduction

A huge number of organisms responsible for half of global primary production are unicellular and are known as phytoplankton. Evolutionary speaking, they belong to different lineages and have an extreme diversity, both in terms of morphological and physiological characteristics and in terms of habitats where they live. They are single cells, prokaryotes or eukaryotes, which share the capability to do oxygenic photosynthesis. If in the marine environment photosynthetic prokaryotes are represented by Cyanobacteria, for the domain of Eukarya, a mixture of phylogenetically diverse organisms deriving from different endosymbiotic events represents marine microalgae. A primary endosymbiotic event involved a heterotrophic organism and a cyanobacterium that became the chloroplast of Archaeplastida, i.e. green algae, red algae and Glaucophyta. A secondary endosymbiotic event that involved a eukaryote and an Archaeplastida originated other lineages, e.g., Haptophyta, Cryptophyta, Stramenopiles and Dinophyta (Not *et al.*, 2012).

Several features make phytoplankton an interesting but also complex subject of research. Classically the biodiversity of phytoplankton has been assessed using microscopes and was based on morphological characters; there is now evidence that estimates of biodiversity based on morphology is largely underestimated (de Vargas *et al.*, 2015). Difficulties to identify the different phytoplankton species are manifold. Phytoplankton species have a broad range of size, from 0.2 μm to 2 mm, which requires different tools for their identification and quantification; smaller species are more difficult to identify. The identification of species belonging to different microalgal lineages is based on different characters. As an example, diatoms are identified based on the gross and fine morphology of their siliceous frustule, dinoflagellates based on cell morphology, number and pattern of the organic thecal vesicles that surround the cell, haptophyes based on the morphology of thin organic scales or, in the case of coccolithophores, of the calcareous coccoliths. Moreover, the cell shape may be affected by environmental characteristics such as nutrient concentration, or by physical dynamics, or by the life strategy of the species. As an example, the formation of

coenobia in *Scenedesums acutus* is related to phosphorus availability in addition to the presence of grazers (O'Donnell *et al.*, 2013). While unicellular chlorophyceae and diatoms are mainly phototrophic organisms, other lineages include mixotrophic species, i.e. capable of performing photosynthesis but also to ingest other organisms by phagotrophy; in the case of dinoflagellates include also many purely heterotrophic taxa.

The use of molecular approaches based, on sequences of various regions of the ribosomal DNA permitted in the last decades the discovery of cryptic or pseudo-cryptic species. Those are species that share the same morphology, or can be distinguished only by very minor ultrastructural features in the case of pseudo-cryptic species, but are genetically different. The use of a molecular approach provided clarifications in many instances, but also raised additional questions as, for instance, about the traditional definition of species. This field is in rapid evolution but, until now, objective and applicable criteria to define a species are not available at least for many microalgae (Not *et al.*, 2012).

In reason of their widespread presence and abundance, it is evident that microalgae are active actors in ecosystems. Microalgae play an important role, being at the base of the marine food webs, being food for zooplankton, but also in biogeochemical cycles. In fact, fixing carbon and assimilating nitrogen and phosphorus, they rule the global cycles of these elements. Some of them, in addition to the biotransformation of macronutrients, are involved in the cycle of particular elements due to their special chemical composition; this is the case of the role of diatoms in the silica cycle. The relative abundance of different taxa differs between environments and along the annual cycle. In eutrophic zones (coastal and continental shelf waters), diatoms, dinoflagellates and coccolithophores can form large blooms with high impact on earth chemistry, while small cells, as haptophytes and prasinophytes, are better adapted in oligotrophic areas because of their higher surface to volume ratio (Finkel *et al.*, 2010). Diatoms can fix up to 20% of global photosynthetic carbon per year, which is more than what is fixed by tropical rainforests (Boyd *et al.*, 2000).

Blooms are ephemeral events in which the microalgae grow massively and their biomass exceeds that of heterotrophic organisms; this situation occurs only in certain environmental conditions, when nutrients are non-limiting and light is available. Besides the role played in carbon cycle, blooms have important consequences for the entire ecosystem and directly or indirectly for human beings. For example, they can be associated to anoxic events (mainly in freshwater environments) and some species can

produce toxins, dangerous for fishes but sometimes also for humans. The formation of blooms seems to be mainly related to nutrients: in general, algal growth is driven by the limiting nutrient, different in different environments. It is generally accepted that nitrogen is the limiting nutrient in iron-rich coastal areas, phosphorus in freshwaters and oligotrophic areas, while iron can be limiting in several open ocean zones (Assmy & Smetacek, 2009). This means that blooms occur when these nutrients are abundant, playing a bottom–up control on phytoplankton growth. The rest of the time, phytoplankton must survive under fluctuating and often limiting nutrient conditions and be able to rapidly recover when favourable conditions appear. The bloom-forming species are only a small percentage of total species described until now, but these species should have particular life cycle characteristics that allow their success and these features need to be clarified if we want to understand cues that trigger their advent (Assmy & Smetacek, 2009).

Phytoplankton life histories

The mechanisms regulating microalgal species abundance and succession, and the role played by different life strategies are still largely unknown (Marcus & Boero, 1998) but necessitate to be elucidated to better understand many aspects of ocean functioning (von Dassow & Montresor, 2011). The major part of phytoplankton is characterized by a heteromorphic life cycle that may include morphologically and physiologically different phases, selected during their evolutionary history that can give us information about species ecology.

During vegetative growth, cells divide mitotically and, based on the ploidy of the dominant life cycle stage, the life cycle can be haplontic (1n), diplontic (2n) o haplo-diplontic (alternation of 1n and 2n) and this feature is conserved in the large taxonomic groups with few exceptions. Chlorophyte and dinoflagellates are mostly haplontic, prymnesiophyceae are haplo-diplontic and diatoms are diplontic. Switch from the haploid to the diploid phase in organisms with a haplo-diplontic life cycle has implications for the morphology and behaviour of the specie with consequences, sometimes, for the whole ecosystem. *Emiliania huxleyi*, a coccolithophore (Prymnesiophyceae) known to form extensive blooms, can shift from a 1n to 2n stages, which have different morphology: the diploid coccoid stage is surrounded by coccoliths, while organic scales surround the flagellate haploid stage. Even if sexuality links these

stages to each other, both of them are able to grow through mitotic divisions (Von Dassow *et al.*, 2015). The relative abundance of each of them may facilitate the adaptation of the specie to different environmental conditions and pressures and influence indirectly global dynamics as the carbon flow. As an example, it has been shown that only the coccoid calcareous stage is affected by viral attacks; switching to the haploid stage thus represents an escape to the virus's lysis (Frada *et al.*, 2008).

Cells of each species share the same genome but different genes are expressed in the different stages and phases of their life cycle. In any species' life cycle it is possible to identify an actively growth phase, i.e. cells with high metabolic activity and programmed to divide, which are probably the most studied. There are also other phases, less studied but equally important, such as the sexual phase and the resting phase. The capability to have a heteromorphic life cycle can increase the range of conditions in which the specie can survive.

Sexual reproduction seems to be an ancestral and widespread feature in eukaryotes, including unicellular organisms, and more and more species are reported to have a sexual phase in their life cycle (Speijer *et al.*, 2015). Recent evidences have shown that sex is an example of evolutionary convergence in eukaryotes and, although it seems energetically not convenient, it is widespread. The mating system is defined homothallic, when gametes of opposite mating type are produced within a single clonal culture, or heterothallic if they are produced by strains belonging to distinct mating types.

Often the sexual phase is induced when the population moves from an active growth to a stationary state or when it is exposed to a particular kind of stress, such as oxidative stress deriving from temperature increase for the green alga *Volvox* (Nedelcu, 2005). Since it is difficult to observe sexual stages in the natural environment and to identify the right triggers for sexualisation in laboratory, detailed information on sexual reproduction is available only for few microalgal species (Montresor *et al.*, 2016). For instance, even for a well-known organism as the protozoan *Trypanosoma brucei* that has been studied since a long time because it causes sleeping illness, the sexuality is a recent discovery (Peacock *et al.*, 2014). Genomic studies now allow the detection of gene clusters associated with meiosis or gamete conjugation, showing that they are present in many micro-eukaryotes including microalgae (Speijer *et al.*, 2015).

Resting stages can be present in the life cycle of several species all over the phylogenetic diversity of microalgae. The main characters are their incapability to reproduce themselves - as vegetative cells do - and the fact that they are physiologically and often morphologically modified, so to stay dormant or quiescent for a period of variable length. Victor Hensen was one of the first scientists to recognize the existence of resting stages in phytoplankton and their potential role in determining species' seasonal patterns (Hensen, 1887), and Gran hypothesized that they are formed in the water column when nutrients are poor and then sink to sediments where they stay as benthic stages (Gran, 1912).

The production of resting stages can be linked to the sexual phase. This is the case of unicellular haplontic chlorophytes (e.g. *Chlamydomonas*) where the zygote produced after gamete fusion is transformed into a resting spore. Also dinoflagellates cysts have been interpreted as an obligatory step after sexual reproduction; however, it has been recently shown that the planozygote does not necessarily transform into a cyst but, depending on environmental conditions, it can undergo meiosis and resume the vegetative phase (Figueroa *et al.*, 2018). In cyst-forming species, several morphological changes occur in the planozygote until the formation of a cyst that enters in a dormant period. Cysts are generally resistant to adverse conditions and their germination can be triggered by environmental cues (e.g. temperature or light availability), or can also be independent from them and driven by an internal clock (Ellegaard & Ribeiro, 2018). This is the case of *Alexandrium fundyense*, which, when kept at constant and favourable environmental conditions, germinates only in a specific time window of the annual cycle (Matrai *et al.*, 2005). Resting stages (akinetes) are also known in filamentous cyanobacteria where their formation is induced by environmental signals such as low temperature or nutrient starvation (Kaplan-Levy *et al.*, 2010). Various studies showed that resting stages are present mainly in sediments, while vegetative forms are planktonic. However, they both belong to the same species, highlighting the fact that benthic and planktonic compartments are strictly interconnected.

Diatoms

Diatoms (class Bacillariophyta) belong to Stamenopiles (also called Heterokontophyta) together with the golden-brown microalgae and the brown macroalgae. The principal feature of Stramenopiles is the ultrastructure of their flagella

(one smooth and the other presenting thin fibrils). Flagella have been lost in diatoms with the only exception of spermatozoids of centric diatoms that have one flagellum. Diatoms are present in all kind of aquatic environments where they play a key role in the carbon, nitrogen and silica cycles with about 10^5 species (Kooistra *et al.*, 2007). This class of protists is responsible for blooms in coastal and open oceanic waters producing 20% of global organic carbon. Species with a wide dimensional size (from <10 to >200 μm) and several morphological features are included in this group (Kooistra *et al.*, 2007). Diatoms are characterized by a siliceous cell wall, the frustule, made by two parts, called epitheca (upper part) and hypotheca (lower part). Frustules are composed of the hypotheca smaller than the epitheca put together as a lid with its box. Based on the symmetry of their frustule, diatoms can be divided in 4 groups: radial centrics, the oldest one (appeared in Jurassic), followed by multipolar centrics (Early Cretaceous), araphid pennates and the youngest raphid pennates (in Late Cretaceous). There are evidences from paleontological observations of their high capability to survive and have a fast recovery after the mass extinction at the end of Cretaceous (K/T- boundary), and this was probably due to the formation of resting stages. During cell division, each cell uses its own thecae to form the lid (epitheca) of the two daughter cells' frustules, while the smaller hypotheca is newly synthesized, causing a progressive reduction of the population cell size. Valves are produced in few hours and derive from the fusion of silica deposition vesicles (SDVs) with cell plasmalemma; the deposition starts immediately after nuclear mitotic division. This group of microalgae represents a particular case where cell size determines sexualisation. In fact, there is a species-specific window, generally 30-40% of maximum size (Edlund & Stoermer, 1997), after which cells can undergo sexual reproduction. In diatoms gametes fusion restores the diploid phase and the zygote transforms into a particular structure, called auxospore, which is deprived of the rigid siliceous frustule. Within the soft auxospore, a cell of the maximum size is produced. Centric diatoms have a homothallic mating system, i.e. sexual reproduction can occur in a clonal culture where both male and female gametes are produced, while pennates have almost always a heterothallic mating system, i.e. male and female gametes are produced in strains of opposite mating type and sex can occur only when strains of the opposite mating type are in contact (Montresor *et al.*, 2016). The size is not the unique parameter required to have sex; in *Pseudo-nitzschia multistriata,* for instance, a threshold cell density is required (Scalco *et al.*, 2014). Also external factors may play a role as triggers, amongst which environmental stress conditions. For instance, salinity shifts trigger sexual reproduction in *Skeletonema marinoi* (Godhe *et al*., 2014). In addition to size, external parameters seem to be

essential factors for inducing sexualisation in the case of phylogenetically older centric diatoms, while in heterothallic pennates sex is mostly linked to endogenous mechanisms and to the production of pheromones for the communication between mating types (Montresor *et al.*, 2016).

Asexual enlargement appears to be common amongst centric diatoms and consists in the production of an auxospore-like cell with the same function of cell-size restitution; however the auxospore-like structure is not formed following the conjugation of gametes. This mechanism, discovered by von Stosch (1965), allows the species to save the energy and risks required for sexual reproduction but information about this aspect is scarce because asexual enlargement is an ephemeral event and easily overlooked using routine approaches.

Resting stages in diatoms

Two main types of resting stages are known for diatoms: resting cells, which differ from vegetative cells mainly in their physiology, and spores in which also the morphology is different (McQuoid & Hobson, 1996).

The term resting cells was used for the first time by Lund (1954) to define cells with condensed cytoplasm, less pigments in shrunken chloroplasts and thicker frustule than vegetative cells, but with the same shape. Spores, instead, have a thick frustule, sometimes ornamented with spines and other protuberances; they have such a different morphology from vegetative cells that they were not recognized until found attached to vegetative parental cells (Round *et al.*, 1990). Pennates and freshwater species are known to form mainly resting cells while marine centric diatoms produce mainly resting spores (McQuoid & Hobson, 1996) and only in some species both types can be formed (Kuwata *et al.*, 1993) .

Both in freshwater and in seawater resting stages allow the species to survive in periods of stress such as ice cover, nutrient depletion and anoxic conditions. Resting stages can potentially remain viable for decades (Sicko-Goad *et al.*, 1989; McQuoid & Hobson, 1996) up to one century, as demonstrated by the capability to resume vegetative growth of *Skeletonema marinoi* resting cells isolated from laminated sediment cores (Härnström *et al.*, 2011).

In diatoms, resting stages seem to be produced mostly asexually (Round *et al*., 1990), with the only exception of *Leptocylindrus danicus* and *Chaetoceros eibenii* (von Stosch *et al.*, 1973, French III & Hargraves, 1985). The cytological reorganization behind resting stage formation is well documented only for spores of a few species; it has been demonstrated that valve formation is always preceded by a mitotic nuclear division that may or may not be associated to cytokinesis (Round *et al.*, 1990).

In order to survive in the sediments for long time and resting stages should have considerable amounts of storage materials. Studies about chemical composition and metabolic activity have shown that both resting cells and spores are characterized by a higher content of storage compounds that results in higher C:N and C:chl *a* ratio (French & Hargraves, 1980; Doucette & Fryxell, 1983; Kuwata *et al.*, 1993), low photosynthetic activity and a respiration rate that is ~20% less than in vegetative cells (Anderson, 1976; Kuwata *et al.*, 1993). In *Chaetoceros pseudocurvisetus* this carbon is mainly accumulated as carbohydrates (glucose in mono- oligosaccharides and glucan in polysaccharides) in spores and neutral lipids (saturated and monosaturated fatty acids) in resting cells (Anderson, 1976; Doucette & Fryxell, 1983). The content of ATP, ADP, AMP and UTP seems to be lower in spores, whereas that of photoprotective pigments seems to be higher, at least in *Chaetoceros pseudocurvisetus* (Oku & Kamatani, 1999). It was proved that spores' sinking rate in the water column is 5-6 times higher than that of vegetative cells (Davis *et al.*, 1980). All these features allow spores to sink faster to the bottom and confirm their role to "rest" in colder and dark condition, i.e. the bottom sediments (Durbin, 1978; Doucette & Fryxell, 1983; McQuoid & Godhe, 2004).

Various functions were attributed to diatom resting stages, such as capability to resist digestion by grazers and to be transported over long distances, either by currents or in the stomach of grazers. On the other side, resting stages represent a way to 'anchor' a species to a certain environment, as in the case of Mariager Fjord in Denmark, where resting cells of *Skeletonema marinoi* contribute to maintain a distinct population inside the fjord, which is genetically different from that outside it (Härnström *et al.*, 2011). Resting stages also contribute to carbon flux to the bottom, and in productive areas this percentage may be important as proved in South Georgia (Rembauville *et al.*, 2016) or in the naturally iron-fertilized areas, where it has been estimated to be responsible for 60% of POC export (Rembauville *et al.*, 2015)

Diatom resting stages: formation

Laboratory studies

I will present an overview of the most relevant scientific publications in which the factors that induce spore formation in marine diatoms have been investigated (Table 1.1). Particular attention will be placed on papers that examined spore formation in species of the genus *Chaetoceros*. The information has been summarized in Table 1.1 where I also reported an evaluation of the experimental set up, i.e., if the external and internal nutrient concentration were measured, if control conditions were tested, if there was information on the time course of spore formation.

The first studies illustrating the results of laboratory experiments with cultures aimed to assess the factors that determine the formation of resting spores date back to the late 1970s. Nitrogen depletion was applied to induce spore formation in the cold-water diatom *Thalassiosira nordenskioeldii* under a range of temperature conditions (0-15 °C) and high percentages of spore formation were detected only at the lowest temperatures, suggestion that spore formation may be a strategy to overcome nitrogen limitation at the end of the bloom and allow survival during the winter season (Durbin, 1978).

French & Hargraves (1980) tested five diatoms (*Leptocylindrus danicus, Chaetoceros diadema, C. teres, C. socialis,* and *Stephanopyxis turris*). Nitrogen, phosphorus and silicon-depleted media were used, together with temperature stress and darkness, but only nitrogen starvation induced the formation of spores in considerable number. The treatment involved the use of ammonia as unique source of nitrogen with a concentration of 15 µM. In that study, also physiological parameters such as dark respiration rate, electron transport system, photosynthetic rate and chlorophyll, carbon and nitrogen cell content were estimated. C:N ratio was higher in spores, which also had higher chlorophyll content in the dark; carbon fixation was occurring in spores in the dark and respiration rates were low, all features supporting the conclusion that spores can survive adverse conditions.

Five years later, French III & Hargraves (1985) described the entire life cycle of two of the species investigated in the previous publication, *Leptocylindrus danicus* and *C. diadema.* The formation of spores was induced by transferring the cultures in low-

nitrogen medium (T medium). In *C. diadema*, spores were formed asexually in cells of all sizes, while in *L. danicus* only cells below a diameter of 8 µm went through a sexual phase, formed auxospores that turned into spores.

Kuwata and Takahashi (1990) carried out a study during a natural bloom of *C. pseudocurvisetus* (see below) and, to support their observations, the authors tested the role of nitrogen depletion as a cue to induce spore production using unialgal cultures. Results confirmed that nitrogen depletion was a key factor for the induction of spore formation and also showed that this process requires a substantial uptake of silicic acid.

Kuwata *et al.* (1993) tested the production of resting spores and resting cells in cultures of *C. pseudocurvisetus*. To obtain spores, the f/2 medium was depleted in nitrogen (10 µM) but contained excess Si (140 µM), while the concentration of both nitrate and silicic acid was drastically diminished to obtain resting cells (10 and 20 µM, respectively). The formation of resting spores started on day 3 in concomitance with exhaustion of nitrate in the culture medium and, by day 5, almost all cells turned into spores. In the experimental set up to induce the formation of resting cells, both nitrate and silicic acid were depleted by day 2 and 3, respectively and cells acquired a shrunken cytoplasm; less than 0.1% of spores were formed in those conditions. The authors also estimated various physiological parameters. Gross photosynthesis, assessed as oxygen production, was similar and very low (1.3-1.4 pg O_2 $cell^{-1}$ h^{-1}) in both spores and resting cells, dark respiration in resting spores and resting cells reached about 10 and 30%, respectively, of that of vegetative cells. Spores contained about double the amount of carbon than vegetative cells, while they contained about half the amount of nitrogen. Resting cells contained similar amounts of carbon and half the amount of nitrogen of vegetative cells. The C:N ratio of resting spores was 4 times higher than that of vegetative cells, and 2 times higher than that of resting cells. The silicic acid concentration in the spores was 2-3 times higher than in vegetative cells and resting cells. While internal nutrients concentration and physiological parameters were measured in vegetative cells in the exponential growth phase, it is not stated if spores were recorded in this control condition.

Oku and Kamatani (1995) used the same species, *C. pseudocurvisetus,* to study spore formation, testing not only N-depleted medium but also P-depleted medium and also assessed the internal phosphorus pool in the experiments carried out with the two culture media. The depletion of N induced the formation of spores starting from day 4, after the depletion of nitrate in the medium; by day 5 about 84% of the cells were

transformed in spores and this ratio persisted till the end of the experiment (day 10). The timing of spore formation was similar in P-depleted medium, but the fraction of cells transformed into spores was lower (65%). Interestingly, spores were produced also in control conditions, but with lower percentages (ca 34%). There was no evidence for super-storage of orthophosphate and/or polyphosphate in cultures with high percentages of spores, i.e. in N and P depleted conditions. In a further study Oku and Kamatani (1999) tested the composition of various nucleotides (AMP, ADP, ATP and UTP) as well as chlorophyll and accessory pigments in cultures of *C. pseudocurvisetus* grown in nitrogen and silica-limited conditions. Also in these experiments, spore formation, although at lower percentages, was detected also in control conditions with full strength medium, confirming the results obtained by Oku and Kamatani (1995). High spore formation was obtained in N depleted medium, as expected, while spores were not produced when both Si and N were limiting. The total nucleotide content decreased in the order: vegetative cells>nutrient-starved cells (resting cells?)>resting spores, showing that the two resting stages have different metabolism. The cellular ratios of diadinoxanthin: chl a and of diatoxanthin:chl a were higher in resting spores and nutrient-starved vegetative cells than in nutrient-replete vegetative cells.

Other studies manipulated other factors together with nitrogen starvation. Spore formation in *C. anastomosans* was tested in f/2 medium with low concentration of N (10 and 20µM, respectively) and at a range of salinities spanning from 6.9 to 48.2 (Oku & Kamatani, 1997). Cell growth was recorded only at salinities comprised between 32 and 48, and the maximum abundance of spores between salinities of 40 and 48. A second time course experiment was carried out with the same nutrient depleted medium at two salinities values (34.5 and 42.7). This second experiment showed that spore formation was higher at the higher salinity and it started around day 9 or 10 when nitrate in the medium was already exhausted, but not the other nutrients.

In the freshwater diatom *Aulacoseira skvortzowii* spores were observed in cultures within 2 days of exponential growth ceasing and 72% of cells turned into spores in phosphate depleted medium while only 15% of cells turned into spores in nitrogen-limited medium (Jewson *et al.*, 2008).

Sugie and Kuma (2008) investigated spore formation *Thalassiosira nordenskioeldii* and, besides N-depleted conditions, they also tested Fe-depletion as trigger of spore formation. Also in this case the percentage of spores obtained was much higher in N-deprived cultures (100%) than in the ones deprived of Fe (60%).

In synthesis, the results of laboratory investigations carried out on resting stage formation in planktonic diatoms, including various *Chaetoceros* species, show that nitrogen limitation is the most effective factor inducing the shift from vegetative cells to resting spores. Only one study was produced using cultures of *C. socialis* (French & Hargraves, 1980). Other environmental factors can further modulate spore formation induced by nitrogen deprivation, such as salinity (*Chaetoceros anastomosans*, Oku & Kamatani, 1997) and temperature (*Thalassiosisra nordenskioeldii* and *Detonula confervacea*, Durbin 1978). In some species, phosphorus depletion (*Chaetoceros pseudocurvisetus*, Oku & Kamatani 1995) or iron depletion (*Thalassiosira nordenskioeldi*, Sugie & Kuma 2008) were also effective, but the percentage of spore produced was always lower as compared to nitrogen depletion. Another important information is that spore formation requires high silicate concentration in the culture medium (Kuwata *et al.*, 1993). A notable exception on the role of the lack of nitrate in inducing the formation of resting cells was the freshwater diatom *Aulacoseira skvortzowii*, where resting stage formation was much higher under P-depletion (Jewson *et al.*, 2008). The experimental set up in the different investigations was however extremely different and only the studies by Oku & Kamatani (1995) and Sugie & Kuma (2008) included time course experiments in which both the external and internal nutrient pools were measured, and control conditions without nutrient limitation.

Table 1.1: The most relevant publications in which the factors inducing the formation of spores have been studied in laboratory, including: reference, studied species, treatment applied to induce spore formation, experimental procedure applied (C = control conditions; INP = internal nutrient pool; ENC = external nutrient concentration; TC = time course) and a short synthesis of the results obtained. N= nitrogen; P=phosphorus; Fe= iron; T= temperature.

STUDIES WITH CULTURES				
References	**Species**	**Treatment**	**C: YES/NO INP: YES/NO ENC: YES/NO TC: YES/NO**	**Results**
Durbin (1978)	*Thalassiosira nordenskioeldii*	T: 0, 5, 10, 15°C f/2 with 25 µM $NaNO_3$l	C: NO INP: NO ENC:NO TC: NO	N depletion effective; 77% of spores at 0°C; 85% at 5 °C; 46.5% at 10 °C; 0% at 15 °C
French & Hargraves (1980)	*Leptocylindrus danicus, Chaetoceros diadema, C. teres, C. sociale, Stephanopyxis turris*	T medium: 15µM NH_4, 7 µM P; 50 µM Si other factors tested: T stress; P and Si depletion; darkness	C: NO INP:YES (C, N) ENC: NO TC: NO	Only N depletion induced spore formation; C:N higher in spores; low dark respiration; cholorophyll higher in spores
French III & Hargraves (1985)	*Chaetoceros diadema, Leptocylindrus danicus*	T medium: 15 µM NH_4, 7 µM P, 50 µM Si	C: NO INP: NO ENC:NO TC: NO	*C. diadema:* spores in cells of all sizes *L. danicus*: spores only in cells below a certain size
Kuwata & Takahashi (1990)	Natural surface sample (see below) and culture of *Chaetoceros pseudocurvisetus*	N-limited medium (10 µM NO_3)	C: NO INP:NO ENC:YES TC:YES	Resting stages formed in low N medium

Kuwata *et al*. (1993)	*Chaetoceros pseudocurvisetus*	To induce spores: f/2 with 10 µM NO_3 and 140 µM Si To induce resting cells: with 10 µM NO_3 and 20 µM Si	C: NO INP:YES ENC:YES TC:YES	Spore formation requires high Si besides N limitation. Carbon accumulation as lipids in spores.
Oku & Kamatani (1995)	*Chaetoceros pseudocurvisetus*	N:P:Si (µM) N limited: 12:10:170 P limited: 120:2:170 Full medium: 120:10:170	C: YES INP: YES (P) ENC:YES TC: YES	Spores produced in both N and P depleted conditions and also in control conditions (lower %)
Oku & Kamatani (1997)	*Chaetoceros anastomosans*	N:P:Si (µM) N limited: 10 or 20:5:100 Salinity from 6.9 to 48.2	C: NO INP: NO ENC:YES TC: YES	Spores at higher salinity and when nitrate was exhausted
Oku & Kamatani (1999)	*Chaetoceros psedocurvisetus*	N:P:Si (µM) N limited: 20:10:180 N and Si limited: 20:10:27 Full medium: 120:10:180	C: YES INP:NO ENC:YES TC: YES	Spores in controls and in – N medium. No spores in – N and –Si; xanthophylls higher in spores
Jewson *et al*.. (2008)	*Aulacoseira skvortzowii*	P-limited culture medium N-limited culture medium	C: NO INP:NO ENC:NO TC: YES	75% of spores in P-depleted 15% in N-depleted
Sugie & Kuma (2008)	*Thalassiosira nordenskioeldi* (neritic and oceanic strains)	N limited and Fe limited at 5 and 10 °C	C: YES INP:YES (N,Si) ENC:YES TC: YES	High % of spore formation in N-depletion at both temperatures; in Fe-depleted medium only the neritic strains produced up to 60% of spores

Field studies

A summary of the information concerning investigations carried out in the natural environment and addressing the factors that induce spore formation is presented in Table 1.2.

The dynamics of natural populations of *Leptocylindrus danicus* was studied in coastal waters at Saanich Inlet (British Columbia, Canada) within a cylindrical mesocosm open on the bottom that isolated 1,300 m^3 of seawater, from surface to a depth of 20 m. During a natural bloom, a large number of spores were produced, when nitrogen was almost completely depleted, and sank to the bottom (Davis *et al.*, 1980). A subsample of the natural community dominated by *L. danicus* cells was also incubated in outdoor continuous cultures; spore formation was only observed when the addition of nutrients was stopped, whereas no spores were produced in the same community kept with regular addition of nutrients. A third support was provided by experiments carried out with a batch culture in the lab: also in this case, spores were produced when the culture became N-depleted.

The abundances of *Chaetoceros* spp. vegetative cells and spores were monitored over two years in the coastal waters of Monterey Bay (US) (Garrison, 1981). Several spore-forming species were detected and they did not show a marked seasonality since vegetative cells were recorded over almost all the sampling period. Spore formation was generally observed near the peak of abundance of the individual species. The dynamic and percentages of spore formation was different in the two years, with a major event in the spring of the first year that involved *C. debilis* and *C. vanheurkii*. The highest abundances of spores were recorded when nitrogen concentration in the surface layer became lower, but were still measurable; however, the correlation between spore formation and nutrient limitation was not clear since spores were detected in most of the samples (>80%) also when nutrients were present at relatively high concentration. For the two species mentioned above, spore formation was observed in concomitance with the presence of cells in poor physiological conditions. The data support the role of spores as benthic stages, but they could not provide evidence for their role in the initiation of the species-specific blooms.

Besides relatively shallow coastal waters, *Chaetoceros* species are often abundant in upwelling regions and the study by Pitcher (1986) assessed the composition of vegetative cells and spores in the water column and in two sediment traps deployed for

2 and 3 days, respectively, along the South African Coast during a summer upwelling event. A considerable fraction of *Chaetoceros* species was recorded as spores in the deepest samples (more or less at the level of the thermocline) in the sediment traps and at the water-sediment interface. There was no evidence for nutrient or light limitation during the study (sediment traps were shallow, deployed just below the thermocline). The distribution of vegetative cells and spores of *C. pseudocurvisetus* was studies in another upwelling area off the Izu Islands in Japan. Stations were sampled after the upwelling event when nutrient concentration started decreasing. High percentages of spores (up to 75% and 100%) were found in the deep layers of the water column (100-200 m). The presence of unhealthy vegetative cells in the surface layer suggested that the population was affected by nutrient depletion, several cells turned to spores and sank to the deeper layers (Kuwata & Takahashi, 1990).

A considerable amount of resting spores of several *Chaetoceros* (but mainly *C. diadema)* was found in sediment traps deployed between 200 and 750 m depth in the sup polar area of North Atlantic (Rynearson *et al.*, 2013). The only nutrient found to be limiting in the surface layer was silicic acid that, as demonstrated by experiment presented above, does not induce spore formation. Spores of *C. diadema* were not recorded in the surface waters and it is thus plausible that they are formed along the sinking path, where the concentration of silicic acid was higher.

In sediment traps deployed in the Kerguelen plateau, an area of the Southern Ocean that is naturally enriched in iron, two short fluxes of spores of *Chaetoceros* spp. (up to 7.8×10^7 cells $m^{-2}d^{-1}$) and *Thalassiosira antarctica* were recorded during spring-summer (Rembauville *et al.*, 2015). Spores were responsible for more than 60% of the annual flux of particulate organic carbon. The same diatom spore assemblage was recorded in another study carried out with sediment traps in the naturally iron-fertilized waters close to South Georgia (Southern Ocean) (Rembauville *et al.*, 2016).

Table 1.2: The most relevant publications in which the factors inducing the formation of spores have been studied in the natural environment, including references, approach to the study, and a short synthesis of the results obtained.

References	Species	Treatment	Results
Davis *et al.* (1980)	Natural community with 80% of *Leptocylindrus. danicus*	Mesocosm experiment and continuous cultures	Spore formation under N- limitation The same result with continuous culture of the natural community
Garrison (1981)	Natural populations, with mainly *Chaetoceros debile* and *C. vanheurckii*	Cells and spores monitored for 2 years	Spores formed during or after the species peaks; link to nutrient limitation not always evident
Pitcher (1986)	Natural community dominated by *Chaetoceros spp.*	Water samples and sediment traps during upwelling	Spores produced when nutrients and light were not limiting
Kuwata & Takahashi (1990)	Natural samples and cultures of *Chaetoceros pseudocurvisetus*	Cells and spores counted in transects of the upwelling zone	Spores recorded at depth; incubated natural pop. produced 20% of spores
Rynearson *et al.* (2013)	Natural community	Water samples and sediment traps till 750 m	Spores of *C. aff. diadema* ormed in the mesopelagic zone
Rembauville *et al.* (2015)	Natural community in the Kerguelen Plateau (, Southern Ocean)	Sediment traps	Spores of *Chaetoceros* spp. and *Thalassiosira antarctica*
Rembauville *et al.* (2016)	Natural community off South Georgia (Southern Ocean)	Sediment traps	Spores of *Chaetoceros* spp. and *Thalassiosira antarctica*

Diatom resting stages: germination

In Table 1.3, are listed the main studies on the factors that induce the germination of diatom resting stages. Talking about germination two main aspects need to be taken into account: the factors causing the transition from the resting to the vegetative phase and those that influence spore viability after variable time periods of storage.

Factors inducing germination

Spores and resting cells of *C. pseudocurvisetus* stored for 22 days in the N-depleted medium in which they were formed showed different levels of degradation, which was higher for resting cells (only ca. 10% of them were viable at the end of the observation period) than for spores (50%) (Kuwata & Takahashi, 1999). The viability of spores was always higher than that of resting cells over a range of temperature ranging from 5 to 30°C. Spore germination can be influenced by the intensity, duration but also the composition of light, which is not only carrier of energy but also of information (Ragni & Ribera D'Alcalà, 2004). However, experiments on the role of photoperiod conducted with resting stages from natural sediments showed contrasting results. A strong signal was apparently found in resting stages from a Norwegian fjord, where germination seemed to occur at more than 11 hours of light (Eilertsen *et al.*, 1995). In these experiments, however, it is difficult to disentangle germination success from differences in growth rates at the various photoperiods, which makes results somehow questionable. In the Gulf of Naples the germination pattern of resting stages was assessed with the serial dilution culture (SDC) coupled with the most probable number (MPN) approach (Montresor *et al.*, 2013). Sediments were exposed to 8, 12 and 16 h of light but no significant differences were recorded in the germination success of different species. Different photoperiods in combination with different temperatures were tested to understand the role of these factors in the germination dynamics on spore forming species abundant in a Swedish fjord (McQuoid 2002). The author determined 'germination time' (the number of days until cells entered exponential division) and two diatoms (*Chaetoceros similis* and *Odontella aurita*) showed faster germination and growth at warm temperature and long photoperiod (20°C, 16L), two other species *C. didymus* and *C. cinctus* at intermediate conditions (15°C, 14L), *Ditylum brightwellii* performed in a similar way under all conditions, while no consistent germination patterns were recorded for *Thalassiosira rotula.* Also in this experiment it is however difficult to disentangle germination from growth

Light has a complex spectrum with wavelengths that have a specific energetic composition, and the light spectrum can change also in a few meters in the water column (Ragni & Ribera D'Alcalà, 2004). The effect of irradiance was tested on *Chaetoceros didymus*, *C. diadema* and *C. vanheurckii*: the lowest irradiance at which germination was recorded was 1.3 μM photons $m^{-2}sec^{-1}$. Germination was also recorded in both continuous light and with a 11L:13D photoperiod within irradiances ranging from 30 to 290 μM photons $m^{-2}sec^{-1}$ (Hollibaugh *et al.*, 1981). Light availability seems to be independent from nutrient concentration since spores of the three *Chaetoceros* species germinated with the same success when inoculated in f/2 medium and in seawater with much lower nutrient concentrations. The only exception to the role of light for spore germination is *Aulacoseira skvortzowii,* a freshwater diatom in which germination of spores isolated from the natural environment was observed in the light at low irradiances (12 μM photons m^{-2} s^{-2}) but also in the dark (Jewson *et al.*, 2008)

The study of phytoplankton species succession in Japanese coastal waters prompted Shikata *et al.* (2009) to test germination and growth of different spore-forming diatoms at six different wavelengths with same intensity and photoperiod, including darkness as a control. Natural sediment samples, in which the abundance of viable resting stages was assessed with the SDC method, were used for the experiment. None of the species (*Skeletonema costatum, Thalassiosira minima, Chaetoceros* sp.) germinated in the dark and violet light seemed to be the optimal wavelengths for germination to proceed. The same authors went deeper in understanding the role of light in germination testing different levels of irradiance and the same wavelengths on spores produced in a laboratory culture of *Leptocylindrus danicus* (Shikata *et al.*, 2011). They arrived to the conclusion that germination is strictly related to photo-perception. It occurred only at intensity of 3 μM photons $m^{-2}sec^{-1}$ and using 3-(3, 4-dichlorophenyl)-1,1-dimethylurea (DCMU) that blocks photosynthetic electron transport, germination was prevented. Clear evidence that spores perceive light has been provided by the fact that germination was occurring only when spores were exposed to irradiances of 440 nm and 680 nm, which match with the absorption spectra of chlorophyll *a*. All these observations demonstrated the importance of light to return to the vegetative phase.

Survival of resting stages

An important point investigated in a few studies is the survival time of diatom resting stages. This aspect is very important in fluctuating coastal environments because species with benthic cells viable for longer time would be more successful. The first experiments testing spore survival were made with two cold-water species, *Thalassiosira nordenskioeldii* and *Detonula cnofervacea,*¸whose resting stages were incubated in the dark at temperatures ranging between 0 and 20 °C (Durbin, 1978). At 0 °C, spores of *T. nordenskioeldii* survived for more than 500 days, while at 20 °C they only survived for a few days.

Spores of *Leptocylindrus danicus* produced within a mesocosm experiment with a natural population were stored in the dark and germination was still observed after 97 days, while after 200 days almost no germination was recorded (Davis *et al.,* 1980); no detailed information on the experimental procedure was provided. The authors hypothesized that anoxia and/or high concentration of organic matter could impair spore viability. Spores produced by cultures of various *Chaetoceros* species incubated in nitrogen limited media were able to germinate in high percentages up to 167 days but after that time, only a minor fraction of the spores could germinate (Hollibaugh *et al.,* 1981). After 645 days only 10% of *Chaetoceros didymus* and *C. vanheurckii* spores and 1% of *C. diadema* spores germinated.

Sediment samples collected along the Scottish coast were stored in the dark at 5 °C; resting stages of *Skeletonema costatum* were still viable after 73 months and even longer survival times, 96 months, were recorded for various *Chaetoceros* species among which there was also *C. socialis* (Lewis *et al.,* 1999). Additional information on long term spore viability was provided by incubations of sediment samples from different layers of sediment cores collected in a Swedish fjord (McQuoid *et al.,* 2002). *Chaetoceros diadema, C. simplex, C.socialis., Denotula confervacea, Skeletonema costatum* germinated from 55 years old layers. Even a longer survival time was detected for *Skeletonema marinoi* resting stages recorded in anoxic laminated natural sediments dating back 100 years (Härnström *et al.*, 2011).

To summarize: light availability seems the key factor that induces **germination of diatom resting stages,** which do not seem to have mandatory dormancy. Few studies have tested the minimum amount of irradiance to elicit germination; Hollibaugh *et al.* (1981) and Shikata *et al.* (2011) found effective irradiances as low as 1.3 and 3 μM

photons $m^{-2}sec^{-1}$, respectively. The wavelength at which germination occurs was tested only for *Leptocylindrus danicus* (Shikata *et al.*, 2011): irradiances of 440 nm and 680 nm, which match with the absorption spectra of chlorophyll *a*. The effect of photoperiod on germination is contradictory and this most probably reflects the difficulty to carry out experiments that can discriminate between germination of the single spores and the subsequent growth of the vegetative cells, which are the stages that were enumerated in the various studies.

Notwithstanding the lack of a mandatory dormancy, diatom resting stages seem to **remain viable in the sediments** for very long periods of time. This was demonstrated by studies in which sediment samples, either stored in the dark at cold temperatures for long time or collected from deep sediment layers, were incubated in the light and produced vegetative cells.

Table 1.3: Main studies evaluating viability and /or factors influencing germination of resting stages using cultures or natural sediment samples (N= nitrogen; P=phosphorus; T=temperature).

Reference	Species	Results
Durbin (1978)	*Thalassiosira nordenskioeldii* and *Denotula confervacea* Incubated in the dark at 0,5, 10, 15, 20 °C	Survival time is inversely related to T Maximum survival time: 576 days at 0°C for *T. nordenskioeldii*
Davis *et al.*, (1980)	*Leptocylindrus danicus* Spores produced in the mesocosm experiment stored in the dark	Survival time: after 97 days the majority of spores germinated but at 214 days only 1% germinated.
Hollibaugh *et al.*, (1981)	*Chaetoceros didymus, C. diadema, C. vanheurckii*	Light: the most important germination trigger. Survival: decreases over time but a few spores could germinate up to after 645 days.
McQuoid & Hobson, (1995)	*Chaetoceros cinctus, C.didymus, C. similis, Ditylum brightwellii, Odontella aurita, Thalassiosira rotula*	Species- specific temperature and photoperiod combination for germination

Lewis (1999)	Sediment samples incubated in the dark at 5 °C	Diatom resting stages were viable after 73 (*S. costatum)* - 96 months *(Chaetoceros* spp.)
Kuwata & Takahashi, (1999)	*Chaetoceros pseudocurvisetus*	Spores survive for longer time as compared to resting cells
Eilertsen *et al.,* (1995)	Natural assemblages in sediments incubated at various temperature and photoperiods	Photoperiod: max. germination at >11 h light
McQuoid *et al.,* (2002)	Sediment samples from a dated core incubated at different temperature	*Chaetoceros diadema, C. simplex, C.socialis, Denotula confervacea, Skeletonema* costatum collected in ca. 55 years-old sediments were able to germinate.
Jewson *et al.,* (2008)	*Aulacoseira skvortzowii*	Germination in the dark and in the light, but at low irradiance
Shikata *et al.,* (2009)	Especially *Chaetoceros spp, Thalassiosira minima* and *Skeletonema costatum*	Violet light induced germination in all species
Shikata *et al,,* (2011)	*Leptocylindrus danicus*	Blue and red light induce germination
Härnström *et al.,* (2011)	*Skeletonema marinoi*	Survival time: one century
Montresor *et al.* (2013)	Natural assemblages in sediments incubated at various photoperiods	Photoperiod does not have an effect on germination success

The model species for my PhD project: the centric diatom *Chaetoceros socialis*

Chaetoceros is a species-rich genus with a high number of cryptic and pseudo-cryptic species (Hasle & Syvertsen, 1997). They are characterized by hollow spine-like extensions, called setae, which protrude from the valve face or margin. Many species form chains in which cells are joined by the basal portion of setae. *Chaetoceros* species are exclusively marine.

Chaetoceros socialis has been reported in various studies but only recently it has been clearly defined taxonomically (Chamnansinp *et al.*, 2013). *C. socialis* colonies are curved, fan-shaped due to the presence in each cell of a longer seta; these long setae are connected at their tips to form the ribs of the fan. The curved colonies are organized to produce a three-dimensional sphaerical colony that is a distinctive character of *C. socialis* and the closely related cryptic species; for long time it was interpreted as a clear example of ecological plasticity due to its cosmopolitan distribution but molecular phylogenetic approaches revealed an unexpected diversity within this taxon. Various cryptic or pseudo-cryptic species have been described recently by molecular approaches (Gaonkar *et al.*, 2017).

Chaetoceros socialis was described by Lauder (1864) from the Hong Kong waters. Lauder described the vegetative cell of this species without giving information about the presence of spores. Spore morphology became however important to distinguish this species (spiny spore) from the phylogenetically close related ones (smooth spore) (Cleve, 1896). These two species were later merged together and classified as two varieties of the same species, *C. socialis* var, *socialis* and *C. socialis* var. *radians*. Their fate was then clarified in 2013 by using a molecular approach (Chamnansinp *et al.*, 2013). Two different species, the warm water *C. socialis* and the cold water *C. gelidus* were defined not only by spores morphology but based on their distinct genetic profile, as determined by sequencing ribosomal genes and studying the fine characteristics of vegetative cells. *C. radians* became the new *C. socialis* "*sensu stricto*" with spines on spores and living in warm waters (Fig1.1 B). Besides *C. socialis* and *C gelidus,* two other genetically different species, *C. dichatoensis* and *C. sporotruncatus,* were described in the *C. socialis* species complex (Gaonkar *et al.*, 2017). Vegetative cells are very similar to those of *C. socialis* and *C. gelidus,* but spores are different.

C. socialis "*sensu stricto*" has large hexagonal windows, often with a slight central constriction between two adjacent cells. Setae are ornamented with poroids and spines and large, lengthened, solitary pores. Spores are biconvex with spines on each valve

face, and one valve is less convex than the other. In all cells there is only one chloroplast (Chamnansinp *et al.*, 2013).

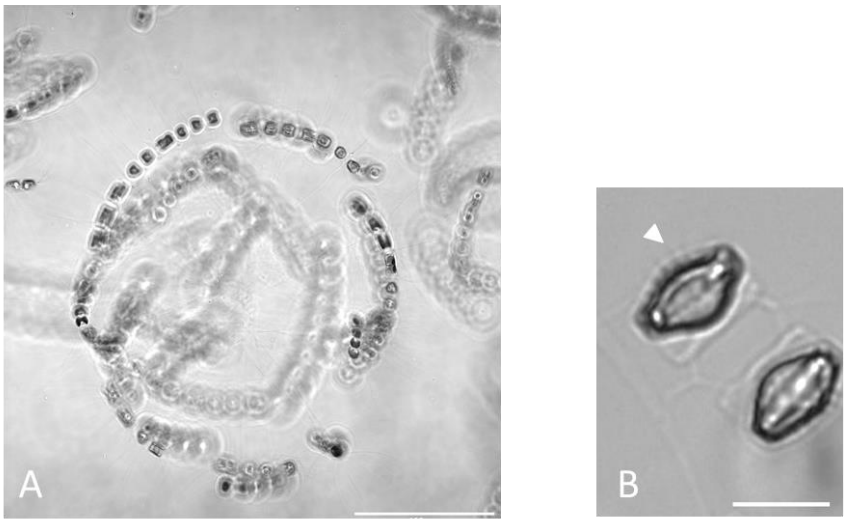

Figure 1.1: CLSM images of C. socialis "sensu stricto", strain APC2. A) Traditional tertiary structure of colonies. Scale bar 100 µm. B) Spores still attached to one parental valve. The arrowhead shows spines typical of this species. Scale bar 10 µm.

This genus *Chaetoceros* is ecologically important and widespread, as shown by the results of the Tara-Oceans expedition (Malviya *et al.*, 2016) and by data from globally distributed marine coastal Long Term Ecological Research stations (Harrison *et al.*, 2015) . This genus is dominant in spring blooms at mid and high latitudes (e.g., Bresnan *et al.*, 2009; Degerlund & Eilertsen, 2010; Rynearson *et al.*, 2013). *Chaetoceros socialis* is common in the water column of the Gulf of Naples, where it forms seasonal blooms, usually with a bimodal trend with one peak in late spring and the other in late autumn (Fig. 1.2) (Ribera d'Alcalà *et al.*, 2004). Numerous resting spores are present in the sediments of the Gulf of Naples (Montresor *et al.* 2013), where its presence has been confirmed also by a HTS metabarcoding approach using the V4 region of 18S rDNA (Piredda *et al.*, 2017).

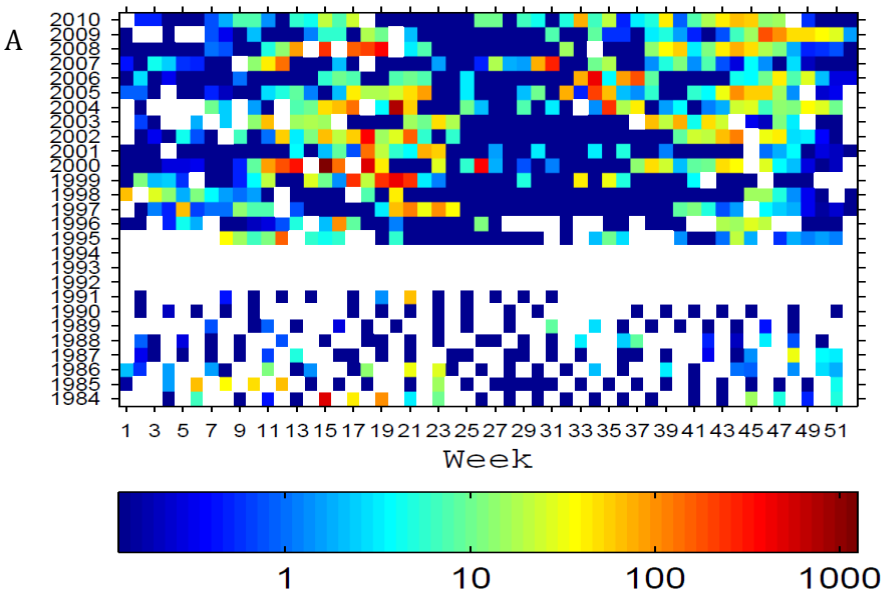

Figure 1.2: Weekly abundances (cells ml-1) of *C. socialis* at the LTER MareChiara station in the Gulf of Naples from 1984 to 2010 (courtesy of Diana Sarno, Stazione Zoologica Anton Dohrn).

Chaetoceros socialis as all other centric diatoms should have a life cycles including sexual reproduction and spore formation. Although it is widely abundant, no information in literature is available on sexual reproduction, neither on cell size window in which it happens or if external triggers are involved. Nothing is known also regarding the cytological processes that lead to spore formation. *Chaetoceros socialis* produces them during its vegetative phase: As an example, the life cycle of *C. diadema* is illustrated in Figure 1.3. When the cell size threshold for sexualisation is reached, cells produce gametes (from a to i); gametes conjugate (j) giving an auxospore that does not transform into a spore (as only done by the centric *Leptocylindrus danicus*, French III & Hargraves, 1985) but produces directly the maximum-sized cell (from k to b). The spore is produced asexually (from b to n) and it will generate a new vegetative cell when conditions return favourable (from o to b).

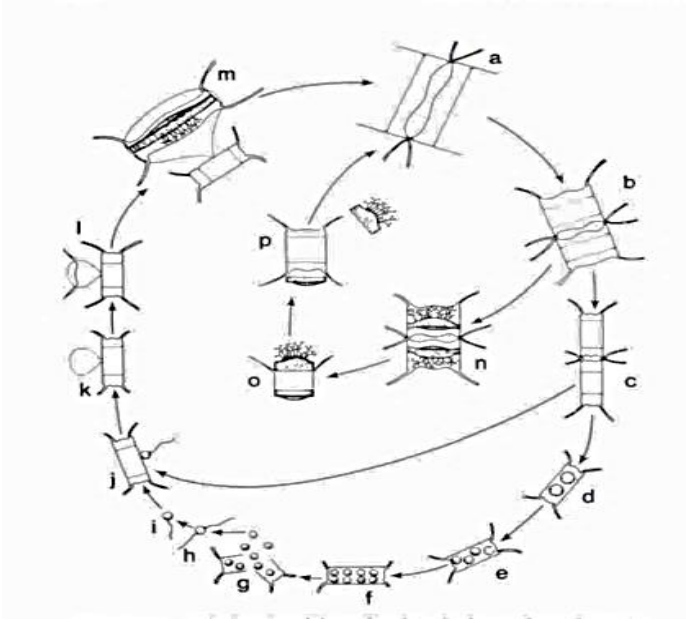

Figure 1.3: Life cycle of *C. diadema* (French III & Hargraves, 1985).

The questions addressed in this thesis

In this section I present the questions that have driven my PhD project, starting with the contrasting and sometimes incomplete information obtained by previous studies illustrated in this Chapter. Every question has been addressed with a*d hoc* approaches and I give a short summary of the results obtained.

As shown above, also in the same genus of spore formers, the cues are not always the same. In synthesis: although several publications investigated the factors that can induce the formation of resting stages, information is often partial: e.g., control conditions were seldom tested, time course of nutrient concentration in the culture medium or intracellular nutrient concentrations were not included. In order to gain information on the dynamics of this life cycle transition and to understand the cues that induce this shift, it is important to design a careful experimental set up.

1) How are spore formed in C. socialis?

Background: No information is present on how spores are formed within the colonies of *C. socialis.* It has been assumed that spores are formed asexually but there is no information about the timing needed by a cell to turn into spore or about the pattern followed by cells in the colony during spore formation. Nothing is known also on spore

germination, neither on the time needed to produce a new vegetative cell nor on the cytological changes. These considerations, together with the hope to find a particular morphological feature that marks cells undergoing this transition, prompted a detailed study on the morphological changes during the transition from vegetative cell to spore and during germination.

In chapter 2 I will present observations conducted with a microscopic approach. Thanks to the use of fluorescent stains, I described the division of cells within a colony, spore formation and spore germination. I also demonstrated that spore formation and spore germination are short timespan processes once the cues are perceived by the cell.

2) What does induce the formation of resting spores in Chaetoceros socialis?

Background: Although there is variability in the factors that induce the formation of spores in different species of marine diatoms, nitrogen deficiency has been often reported as the main trigger. However, the set-up of the experiments carried out mostly 30-40 years ago is seldom complete and often several details are lacking and contradictory results are reported in natural environment.

The aim of chapter 3 was to obtain a straightforward experimental set up in which the main variables during spore formation could be analysed is. I started confirming the role of N-depletion as primary factor in inducing the formation of spores; besides monitoring cell and spore concentration, I monitored the internal pool of nutrients and the dissolved nutrients in the culture medium at the moment of this transition. However, a considerable number of spores were found also in control conditions when cell density was high and nutrients not limiting indicating a role of cell density and allelopathic interactions in spore formation. Although the percentage of spores obtained was lower than that recorded with nitrogen starvation, there are several evidences that intraspecific interactions within the population are involved.

3) Are spores produced as a defence strategy against viruses?

Background: Besides the capability of resting stages to overcome harsh environmental conditions, it has been proved that they are immune to digestion from their predators, the copepods. The effect of their presence is so strong that when present in the medium, the feeding behaviour of copepods changes (Kuwata & Tsuda, 2005). In

additions to predation, phytoplankton mortality can be induced also by viral infection. Little is known about their role in inducing spore formation, even though their presence could explain why there are many spores in non-limiting conditions in natural environments.

In chapter 4 are described experiments assessing the role of viruses in inducing spore formation. For the first time the production of spore has been related to the presence of a species-specific virus. A time course of infection was obtained using two geographically distant strains, proving also the potential of viral infection in inducing spore formation. These experiments highlight the role of interspecific relationships and also of the different life cycle stages in shaping the population dynamic of a species

4) What are the genetic changes that characterised the spore formation?

Background: As reported above, several are the physiological modifications of a cell that is turning in a spore. The modifications at the level of genes that characterize this life cycle transition are completely unknown. An increasing information are obtained with genomic and transcriptomic approaches, especially in for species that have economic and/or medical importance. In the last years, thanks also to the 'Marine Microbial Eukaryote Transcriptome Project' founded by the Moore Foundation, transcriptomes of a large number of marine unicellular microalgae became available.

Insights in the principal molecular pathways involved in spore formation are described in chapter 5. In order to follow this process cells were grown in nitrogen-depleted medium and were sampled at three time points, before and during spore formation; a control was grown in nutrient replete conditions. The main reasons why I used this trigger were two: i) the solid experimental set-up implemented in chapter 2 gave the highest percentage of spores and high repeatability also with different strains; 2) the response of diatoms to nitrogen stress is one of the best studied with a molecular approach. I thus had the opportunity to carry out a comparative study with other non-spore forming diatoms under the same stress conditions. The results presented in this chapter highlighted the differential expression of a set of genes involved in various pathways during spore formation and provided the basis to potentially identify the process in metatranscriptomic dataset obtained from the natural environment.

5) What triggers spore germination?

Background: The careful review of available information in the literature showed that spores can apparently stay ‘quiescent’ for years but they do not have a mandatory dormancy and can germinate when light is available. The role of light remains however poorly explored. Light is carrier of energy but it is also a carrier of information; it has a complex spectrum that can ‘inform’ phytoplankton on the distance from the surface or can induce their migration to avoid a photochemical damage. A growing number of evidences show that different photoreceptors play an important role in the perception to environmental cues by diatoms. Nothing is known about their role in resting stage germination. In addition, experiments made until now were not always able to discriminate between vegetative growth and the germination of individual spores.

In chapter 6 I tested the role of very low irradiance levels provided by different wavelengths in inducing spore germination. These experiments required a very careful planning and were not easy to carry out. In spite of methodological limitations, I can exclude the role of photoreceptors in germination. From my results, it seems that germination can occur also in darkness. Germination can be favoured and enhanced by the presence of light that is crucial to allow the survival of the new vegetative cells formed.

The aim of my PhD project was to find what signals trigger transition from the vegetative phase to the resting stage and *vice versa* getting a solid experimental set up that will be useful, in the future, to investigate the same processes in other species. The results of the experiments contribute to understand ecological events such as seasonal patterns of bloom formation and termination, the capability of diatoms to ‘perceive’ and respond to environmental (nutrients, irradiance) and/or biological (cell density, predators) cues. The results of my experiments will hopefully represent the base for investigations of the functional mechanisms that regulate the transition from vegetative cell to spore and their ecological impact. These results will be also useful for modelling applications on the population dynamics of diatom species and their impact on ecosystem functioning.

Chapter 2

Spore formation and germination: microscopic investigation

Most of the studies on the modalities of spore formation in diatoms were carried out about 50-70 years ago and cytological information are available only for a few species, i.e. *Stephanopyxis turris, Bacteriastrum hyalinum, Chaeetoceros didymus* (Round *et al.*, 1990). From these observations, it was possible to conclude that the formation of spores takes place during a 'modified' vegetative division in which a morphologically differentiated emi-theca is formed instead of the normal hypotheca of the vegetative cell. This division follows the general rule that a valve is formed after a nuclear division (von Stosch & Kowallik, 1969). This division may or may not be associated with cytokinesis. Another factor that determines the kind of spores is the fact that one of the two nuclei produced by mitotic division can degenerate. As a consequence one vegetative cell can produces one or more spores. All these characteristics allow defining different types of resting spores (Syvertsen, 1979, Round *et al*., 1990) (Fig. 2.1):

A. surrounded by both parental valves: endogenous spores;
B. attached to only one parental valve: semi-endogenous spores;
C. without the parental frustule: exogenous spores.

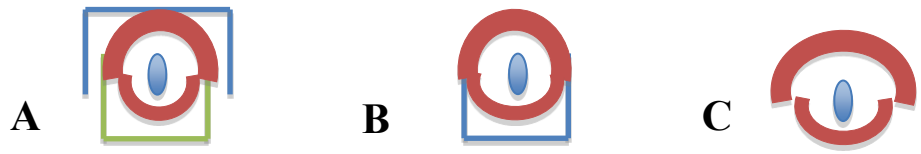

Figure 2.1: Schematic representation of the three spore types in diatoms as defined by the position of the spore relative to the parental valves (based on Round *et al*., 1990): endogenous spore (A), semi- endogenous spore (B), exogenous spore (C).

The formation of endogenous spores has been reported for some species of the genera *Bacterastrium, Urosolenia, Acanthoceras* and *Chaetoceros* (von Stosch *et al*., 1973, Edlund *et al*., 1996). In *Chaetoceros didymus*, the plasmalemma is contracted in the portion of cell where the new spore valve will be synthesized and one nucleus degenerates after the formation of each new spore valve (von Stosch *et al*., 1973). Spores of *C. socialis* are known to be endogenous (Hargraves, 1979, Syvertsen, 1979, Garrison, 1981, Pitcher, 1986), however, details of spore formation in this species are unknown. It has been stated that spore formation in *C. socialis* occurs in two adjacent cells that undergo the same process (McQuoid & Hobson, 1996) but the ontogeny of the spore is not always related to its appearance. For instance, spores of *C. didymus* appear

as semi-endogenous but their formation is endogenous (von Stosch *et al*., 1973).

The time needed to form a spore is variable among species and can take several hours, e.g., from 6 to 48h in C. *dydimus* (von Stosch *et al*., 1973). It has been suggested that individual cells are "pre-determined" to become spore one division before spore formation by their physiological state (von Stosch *et al*., 1973).

Also the modalities through which spore germination occurs have been reported for very few species. In *Stephanopyxis turris*, the spore elongates and, after mitosis, it divides forming two heteromorphic daughter cells with one valve of the spore and a newly synthesized vegetative valve (von Stosch & Drebes, 1964). In *C. didymus*, spore germination includes two acytokinetic nuclear divisions with the formation of the two new valves of the vegetative cell inside the spore, which than opens and its valves are eliminated soon after (von Stosch *et al*., 1973). Germination does not require a mandatory period of dormancy as in dinoflagellates, but it occurs after a variable time from the perception of external cue (Hargraves & French, 1983).

Aim of this chapter, is to describe the process of vegetative cell division, spore formation and spore germination in the model species *Chaetoceros socialis*. Information has been gained with observations of culture material with imaging time-lapse microscopy and using different fluorochromes on confocal laser scanning microscopy (CLSM). Especially on spore formation, these approaches could help to detect any morphological change useful to recognize vegetative cells programmed to became spores.

Materials and Methods

Culture isolation and maintenance

Strains of *Chaetoceros socialis* have been established from the germination of spores in surface sediments. Sediment cores were collected at the LTER MareChiara station in the Gulf of Naples (Italy) at the 4th of December 2015. The first centimetre of the sediment sample was placed in 50 mL centrifuge tubes (Corning Incorporated, NY, USA) with 1 mL of autoclaved seawater, filtered through 0.22 μm pore-diameter filters and with salinity adjusted to 36, in order to avoid sediment desiccation. Tubes were then stored in the dark at a temperature of about 4 °C for two weeks to ensure that only resting stages were present in the sample. Small amounts of the sediment slurry were placed in 6-wells culture plates (Corning Incorporated, NY, USA) containing f/4

medium prepared using f/2 + Si medium (Guillard 1975) diluted 1:1 (v:v) with sterile sea water and were incubated at an irradiance of 55 µmol·m^{-2}·sec^{-1}, 12:12 hrs dark:light cycle and at a temperature of 20 °C. Culture plates were inspected daily with a LEICA DM IL inverted microscope until short chains of C. *socialis* were detected. At this point, some of them were isolated with a micropipette and placed in wells of a 24-well culture plate (Corning Incorporated, NY, USA) filled with f/4 medium. When the cell density increased, the content of two wells (then called APC1, APC2) were transferred to 25-cm^2 (50 ml) polystyrene cell culture flasks (Corning Inc., NY, USA) filled with 30 ml of f/2+Si medium and maintained at the same light and temperature conditions described above. The same procedure was followed to isolate the strain APC12 in September 2016 from the same sediment sample.

Genetic characterization of the strains

Genomic DNA was extracted from all isolated strains for their genetic characterization. An 1mL of each exponentially growing culture was collected from the flask in a 1.5 ml sterile Eppendorf tube and centrifuged at 12,000 rpm for 5 min to obtain a pellet. DNA was extracted following the extraction protocol modified from Doyle & Doyle (1987) and Cullings (1992): 500 µl of CTAB Lysis buffer (AppliChem GmbH, Darmstadt, Germany) and 12 µl of β-mercaptoethanol (Sigma-Aldrich, Missouri, USA) were added to the pellet under a fume hood and energetically mixed. This homogenous mixture was then incubated in a pre-heated water bath at 65 °C for 1 h; samples were vortexed for few seconds every 15 min during incubation. At the end of this step, the suspension was placed in an ice bath for 5 min and 500 µl of SEVAG solution (chloroform: isoamyl alcohol at 24:1 vol:vol) was added and mixed. This solution was then centrifuged at 14,000 rpm for 30 min at 4 °C, which sorted the mixture to separate into three layers; the top aqueous layer with nucleic acids and hydrosoluble carbohydrates, the middle layer containing proteins and other cell debris and the bottom one, which comprises the chloroform with all the liposoluble cell components such as chlorophyll. Approximately 400 µl of the undisturbed upper aqueous layer were collected in a new tube with 400 µl of ice-cold isopropanol and gently mixed by inverting the tube upside down; the tube was then incubated at 4 °C overnight. The DNA was then pelleted by centrifuging the mixture at 14,000 rpm for 30 min at 4 °C and washed with 400 µl of 75% ice-cold ethanol to remove any salt. Ethanol was removed centrifuging at 14,000 rpm for 15 min at 4 °C and drying the DNA pellet under a fume hood. The obtained DNA pellet was then suspended in sterile milliQ water and stored at -20 °C. Molecular identification has been made by

sequencing the D1-D3 region (ca 750 bp) of the nuclear encoded large subunit (LSU or 28S rDNA). It was PCR-amplified in 25 µl-volumes containing 1x Roche diagnostics PCR reaction buffer (Roche Diagnostics, GmbH, Mannheim, Germany), and 1 unit Taq DNA Polymerase (Roche), DNA pellet, 1 mM dNTPs, 0.5 µM of the D1R forward primer and 0.5 µM of the D3Ca reverse primer. Before starting with PCR cycles, the thermocycler (C1000 Touch, BioRad, California, USA) was preheated at 98 °C. PCR analysis included an initial step of 3 min at 94 °C, 35 cycles of 94 °C for 35 s, 54 °C for 35 s, and 72 °C for 2 min, tailed by a final extension at 72 °C for 15 min and a final hold at 12 °C. A total of 1 µL of the PCR products was visualized using 1 % agarose gel electrophoresis with TBE buffer against 100 bp standard ladder in order to check quality and length of them. PCR products were then sequenced through the BigDye Terminator Cycle Sequencing technology (Applied Biosystems, Foster City, CA), purified using a 'Biomek FX' (Beckman Coulter, Fullerton, CA, USA) robotic station, and analysed on an Automated Capillary Electrophoresis Sequencer '3730 DNA Analyzer' (Applied Biosystems, CA, USA) by the Molecular Biology Unit at SZN. Forward and reverse sequences were combined into contigs in BioEdit (Ibis Biosciences, Carlsbad CA, USA). Sequence analysis and alignment was made using as references sequences of other strains of *C. socialis*.

Time lapse microscopy

Time-lapse microscopy is time-lapse photography applied to microscopy. A sequence of images taken with a photo camera with a certain frequency is recorded. When the sequence is viewed at a great speed, it provides a sort of movie of the microscopic process.

The observations were carried out on the following life history phases of *C. socialis* strain APC2:

- vegetative cell division;
- spore formation, using the experimental set up illustrated in Chapter 3. The observation of the samples started on day 2 from the incubation in nitrogen deficient medium;
- spore germination. Spores obtained with the experimental set-up illustrated in Chapter 3 were diluted in full strength medium for 10 hours. Sub-samples were then used for recording germination in time-lapse using a multipoint set-up for the acquisition of images.

Samples were placed in micro well dish (MatTek Corporation, Ashland, MA, USA) covered with a cover slip. For the observations in time-lapse microscopy, bright field images were recorded using a Leica DMI6000B microscope (Leica Microsystems, Wetzlar, Germany) at 20x magnification. A frame has been recorded every 90 seconds for at least 12 hours. All pictures and movies were then processed by Fiji (Schindelin *et al.*, 2012) and Adobe Photoshop CS5.1.

Confocal laser scanning microscopy

In epifluorescence microscopy, the light source hits the entire specimen and all its parts are excited at the same time. That means that the resulting emitted fluorescence detected by the microscope camera includes a large unfocused background. On the contrary, confocal laser scanning microscopy (CLSM) is an imaging technique that allows optical sectioning of the sample. This is possible by the presence of a pinhole, positioned before the photo-detector that eliminates the out-of-focus light. Another advantage of CLSM is the illumination with a laser that is a single wavelength light source (Fig. 2.2). The optical resolution of images is much better than that of epifluorescence microscopy since only the fluorescence coming by a single focal plane can be detected. As result, the single image derives only from a thin section of the sample and, by scanning many thin sections; it is possible to build a very clean three-dimensional image of the sample.

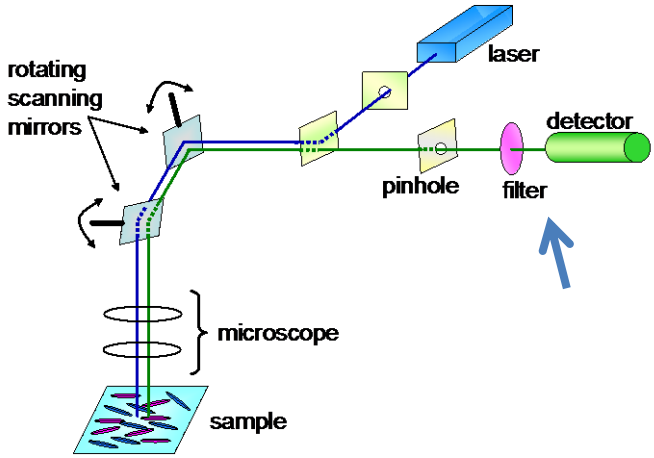

Figure 2.2: Schematic drawings of the confocal laser scanning microscope. The laser emits the light that is directed by rotating scanning mirrors; the pinhole, a single small aperture, allows the passage of the light; the detector filter (blue arrow) catches the light emitted by the sample. Filters are selected based on the wavelengths required for the excitation of the specific

fluorochrome (excitation filters) and the detection of the specific wavelengths emitted by the stained or auto fluorescent sample (detector filters).

Two different fluorochromes were used for the observations in CLSM: LysoSensor™ and SYBR Green I.

- LysoSensor™ Yellow/Blue (DND-160, Invitrogen, Paisley, UK), 2-(4-pyridyl)-5-((4-(2-dimethylaminoethylaminocarbamoyl-methoxy-phenyl-oxazole (PDMPO). This fluorochrome binds to the newly deposited silica (Shimizu *et al.*, 2001). The stock was a PDMPO solution dissolved in anhydrous DMSO (1 mM). It was stored at -20 °C until use. The working solution was prepared with the stock solution diluted 1:10 with MilliQ water. One µL of working solution was added to each mL of sample for a final dilution of 1:10,000. The samples were then incubated for a variable length of time, from 2 to 24 h, and then fixed with neutralized formaldehyde and analysed with CLSM. The PDMPO-stained frustules appear green in the micrographs included in this thesis.

- SYBR Green I (S7567, Invitrogen, Milano, Italy). It is a nuclear dye. As stock solution was used the SYBR Green I (10,000 concentrate in DMSO) sold by Invitrogen and stored at -20° C. The working solution was prepared diluting 1:10 the stock solution in 4-Morpholinepropanesulfonic acid buffer (MOPS) 200 nM, pH 7.5-8. It was then split in 0.5 mL Eppendorf vials and kept at -20 °C in the dark. One µL of working solution was added to each mL of cultures to reach a final dilution 1:10,000. The culture was incubated for at least 15 min in the dark before observation. The SYBR Green-stained nuclei appear blue in the micrographs included in this thesis.

An aliquot of the stained and fixed sample was placed into a glass bottom microwell dish (MatTek Corporation, Ashland, MA, USA), covered with a cover slip to avoid evaporation, and observed with ZEISS CLSM 510 or ZEISS LSM 700 (Zeiss, Oberkochen, Germany) using the wavelength set up and the filters illustrated in Table 2.1. The CLSM pictures were processed with Photoshop CS5.1.

Table 2.1: Wavelengths of excitation laser (Ex. laser) and type of emission filter (Filter Em.) used for each fluorochrome during observations in CLSM. The absorbance (Abs.) and emission (Em) wavelength range for the different fluorochromes are also indicated.

	Ex. laser (nm)	Filter Em.	Abs. (nm)	Em. (nm)
SYBR Green I	488	BP 500-550	290-380	497-520

PDMPO	488	BP 500-550	290-380	497-520
Chlorophyll	405	BP 650-710	400-450 and 625-645	650-750

The observations were carried out with *C. socialis* strains APC2 and APC12.

a) *Vegetative cell division*

A subsample of an exponentially growing culture was incubated with PDMPO for 24 hours and then observed in CLSM.

b) Spore formation

Observations were done following the experimental set-up used to obtain spores illustrated in Chapter 3. Cells were incubated with PDMPO, on day 2, i.e. one day before the shift from vegetative cells to spores. In a first experiment, subsamples of 1 mL were fixed with formaldehyde after 24 hours from the incubation.

In a second experiment, cells stained with PDMPO were collected and fixed at 2, 4 and 8 hours from the beginning of the incubation. This time, each sample was also stained with SYBER Green I. Pictures were acquired in fluorescence excitation and in transmitted light using 20x, 25x or 40x objectives. The CLSM was also used with a time-lapse setting to record both bright field and fluorescent images of cultures incubated with PDMPO. The stain was added one hour before the start of time-lapse and images were recorded for 12 hours.

Results

The strains used in these experiments belong to *C. socialis sensu stricto* since their LSU sequences could be perfectly aligned and showed 99% of identity to the reference sequence for this species (Gaonkar *et al.*, 2017).

Vegetative cell division

With time-lapse observations it has been possible to record the division of vegetative cells in a chain. During the first hour several cells, in different positions of the chain, started to elongate (Fig. 2.3A) and cytoplasmic movements were visible within cells. Even though the nuclear division was not visible, a cytoplasmic separation

occurred and preceded the cellular division with the formation of the valves of two daughter cells. After cell division was completed new setae were formed. A single cell division required about 75 minutes (starting from cell elongation to the completion of cell division) and all cells of the chain divided. In some cells newly formed setae still in the elongation process were visible (arrowheads in Fig 2.3 B).

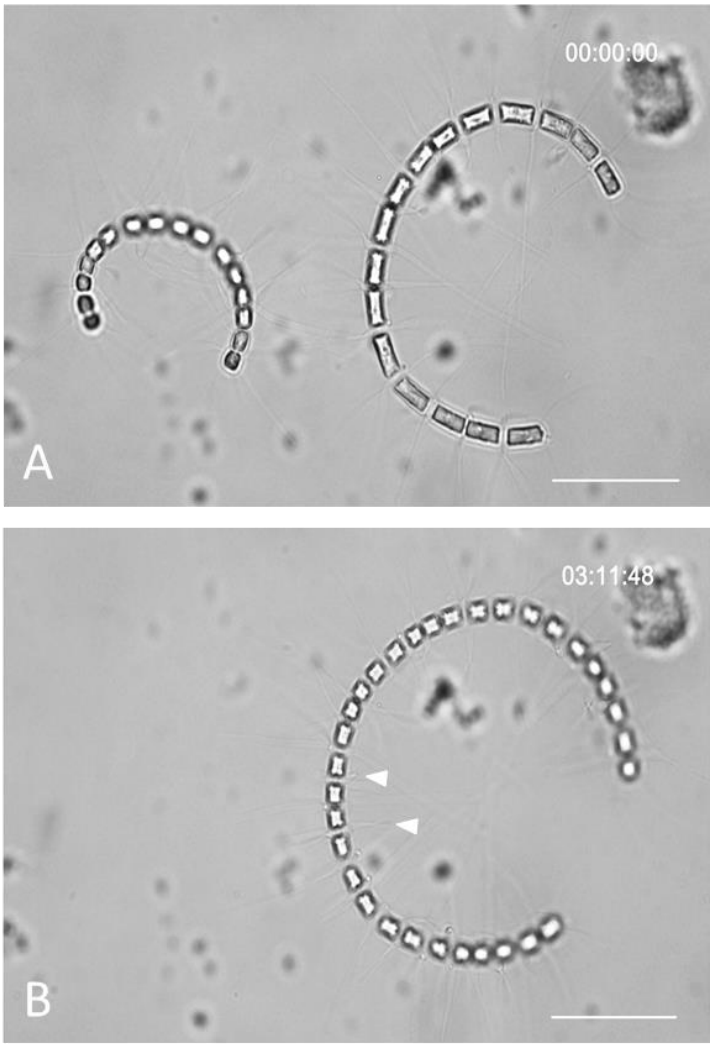

Figure 2.3: Time-lapse frames of vegetative divisions. Two colonies of strain APC2 at time 0 (the colony on the left moved away during the recording period) (A). Colony after 3 hours of observation (B). All cells in the chain duplicated and there are visible also short setae in elongation (arrowheads). Scale bars = 50 µm.

During the 24 hours of incubation with PDMPO, cells were dividing at high rate and, when observed in CLSM, I could see several cells with newly stained setae, synthesized following cell division, and many newly formed valves (Fig. 2.4). Different phases of cell division were visible in the same colony; nuclear duplication was followed by cytokinesis, then the valves of the daughter cells were synthesized in

synchrony and, finally, the setae were produced. Cells with both valves stained by PDMPO were also detected, indicating that daughter cells underwent a second division over the observation period (Fig. 2.5).

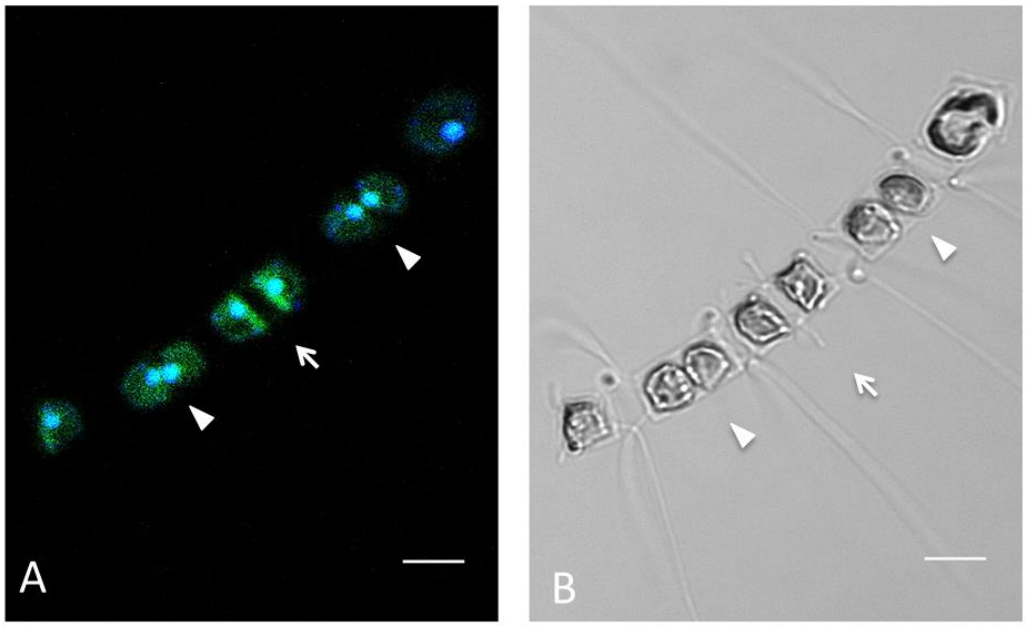

Figure 2.4: CLSM images of strain APC2 stained with PDMPO and SYBER Green (A) and in transmitted light (B). A chain of vegetative cells in division with nuclei stained with SYBER Green (in blue) and newly synthesized frustules stained with PDMPO (in green). The neo-synthesized valves after mitotic division are arrowed Arrowheads mark two cells in which cytokinesis just occurred but the daughter valves were not formed yet. Scale bars = 10 µm.

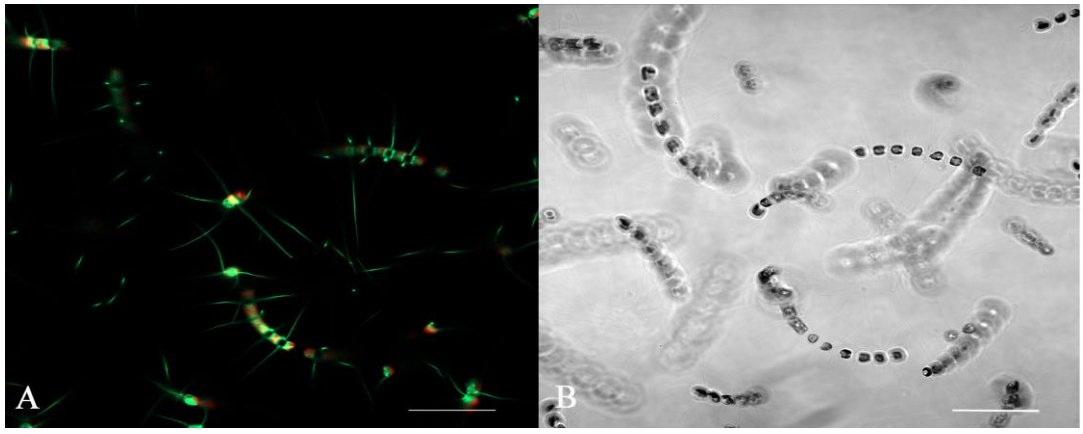

Figure 2.5: CLSM images of strain APC2 stained with PDMPO (A) and in transmitted light (B). In figure A are visible vegetative cells whose newly synthesized valves and setae are stained in green; chloroplasts are red; the overlapping of the different staining can result in a yellow coloration. Scale bars = 50 µm.

Spore formation

Despite several attempts, I was not able to record spore formation in PDMPO-stained cells observed in CLSM with a time-lapse set up. Cells died after about 4 hours probably due to the long exposure to the laser. However, two movies were produced in time-lapse that showed the complete process of spore formation in transmitted light. The early phase did not differ from a normal vegetative division and the formation of the spore became evident during the deposition of the new heteromorphic daughter valve, i.e. the primary valve of the spore. In the first movie, seven spores were formed at the end of the recording time (11h): six adjacent cells and one at the left side of the colony (far from the others) (Fig. 2.6A arrows). At time 0 (when recording started), four cells started to elongate. An intense cytoplasmic activity took place in rapid sequence, first in the four elongated cells and subsequently in the other three cells (Fig. 2.6B). Then, the cytoplasm concentrated on one side of the cells, where the primary spore valve was later formed. No vegetative division was observed in cells with the primary spore valve. The other cells in the chain that did not form spores also showed cytoplasmic movements but then underwent vegetative division.

The process including cell elongation, re-organization of cellular content and the formation of the two spore valves lasted approximately 8 hours (Fig. 2.6F). For the first 3-4 hours there was re-arrangement of cytoplasm and the increase of cell length (Fig. 2.6B) and at the end of this period the new primary spore valve became clearly visible. This heteromorphic phase (i.e. one thick valve and one thin parental one) lasted for about 3.5 hours (Fig. 2.6C). The formation of the secondary spore valve started from the border of the primary valve and it was faster on one side (Fig. 2.6D, arrowhead). The deposition of the thick valve then continued on both sides, towards the distal side of the spore (Fig. 2.6E arrowhead) until completion of the hypovalve (Fig. 2.6F).

In the second time lapse, the formation of two spores in cells that were not close to each other was recorded (Fig 2.7). During the recording time, one cell formed directly a spore whereas the other completed first a vegetative division in about 15 minutes (Fig. 2.7A, arrowhead). Only one of the daughter cells formed a spore while the other divided again forming two small vegetative cells (Fig. 2.7C arrowhead). The formation of the first spore took about 13 hrs: after 4 hours from the beginning of time lapse, the primary valve was completed and after 9 hrs. the secondary valve. (Fig. 2.7 B arrow on the bottom). The second spore completed the formation of the primary valve after 7 hours; and the formation of the secondary valve after 10 hours (Fig. 2.7D).

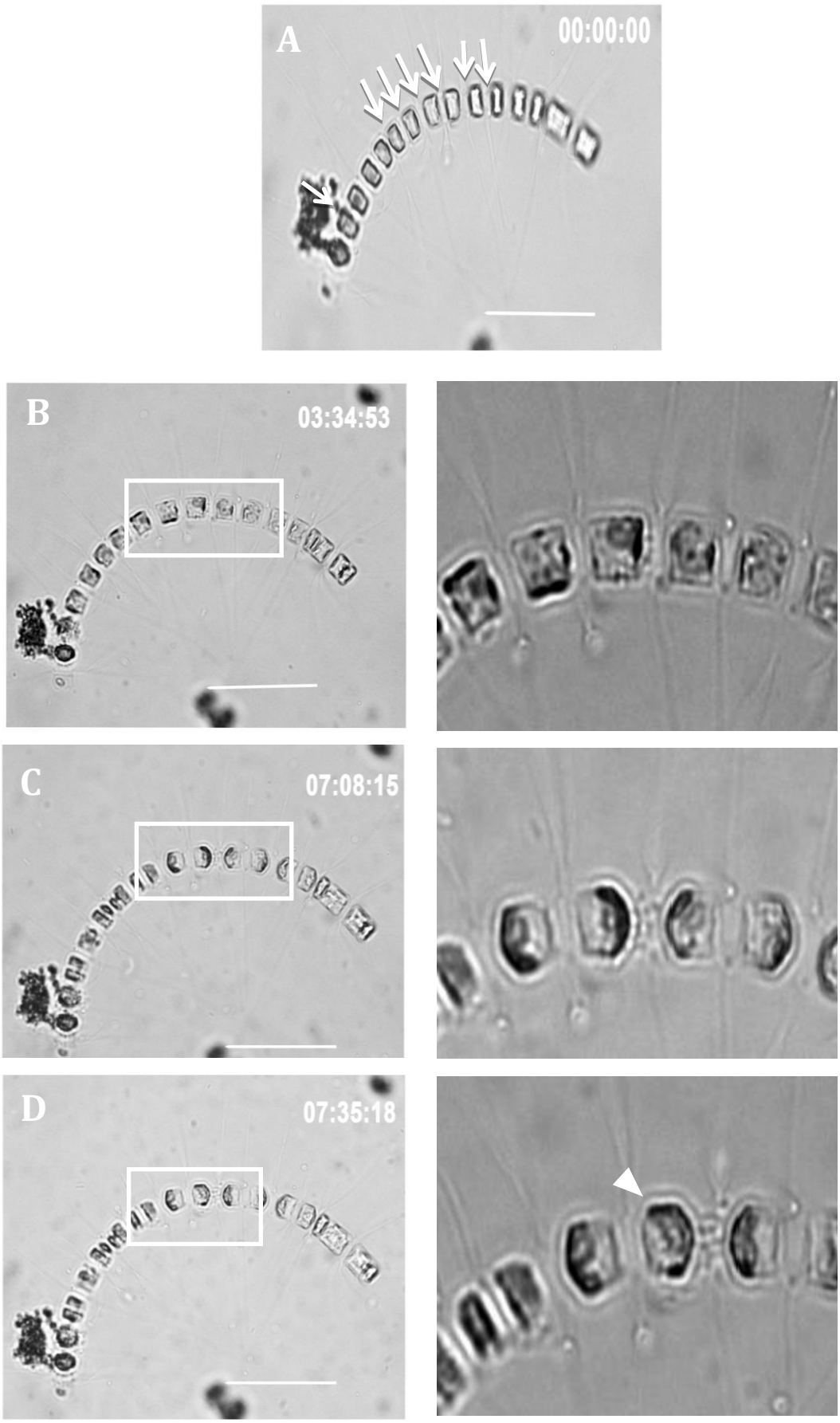

Figure 2.6: Frames extracted from the first time-lapse showing the formation of four spores in strain APC12. See next page for description.

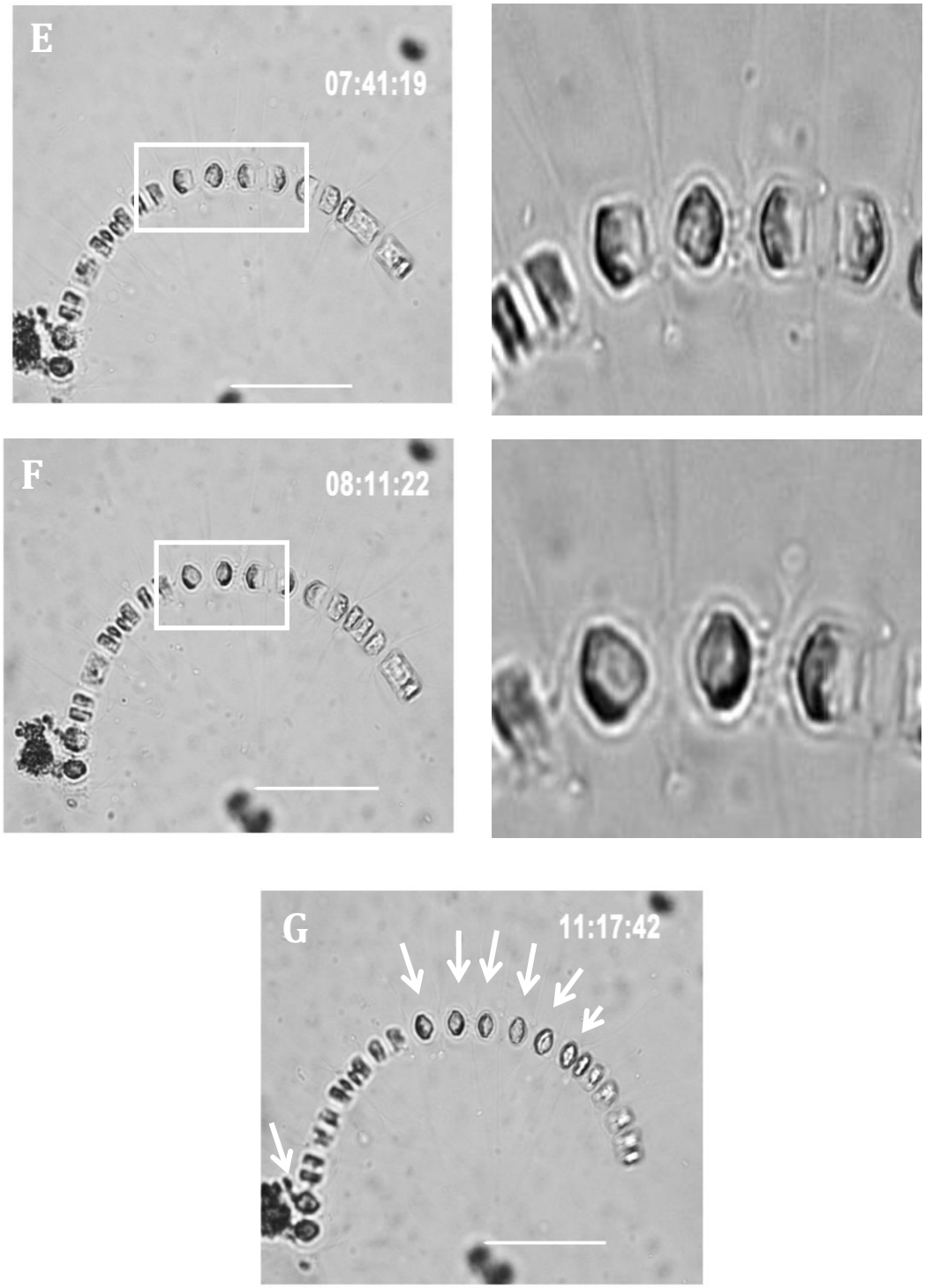

Figure 2.6: Frames extracted from the first time-lapse showing the formation of four spores in strain APC12. On the top-right time: hours, minutes, seconds. The cells that turned into spores are marked with arrows (A). Frames showing several steps of spore formation (see text for details) (B-F). On the left the entire chain and on the right magnification of the first two spores formed. Frame at the end of recording with all seven spores marked with arrows (G). Scale bars = 50 µm.

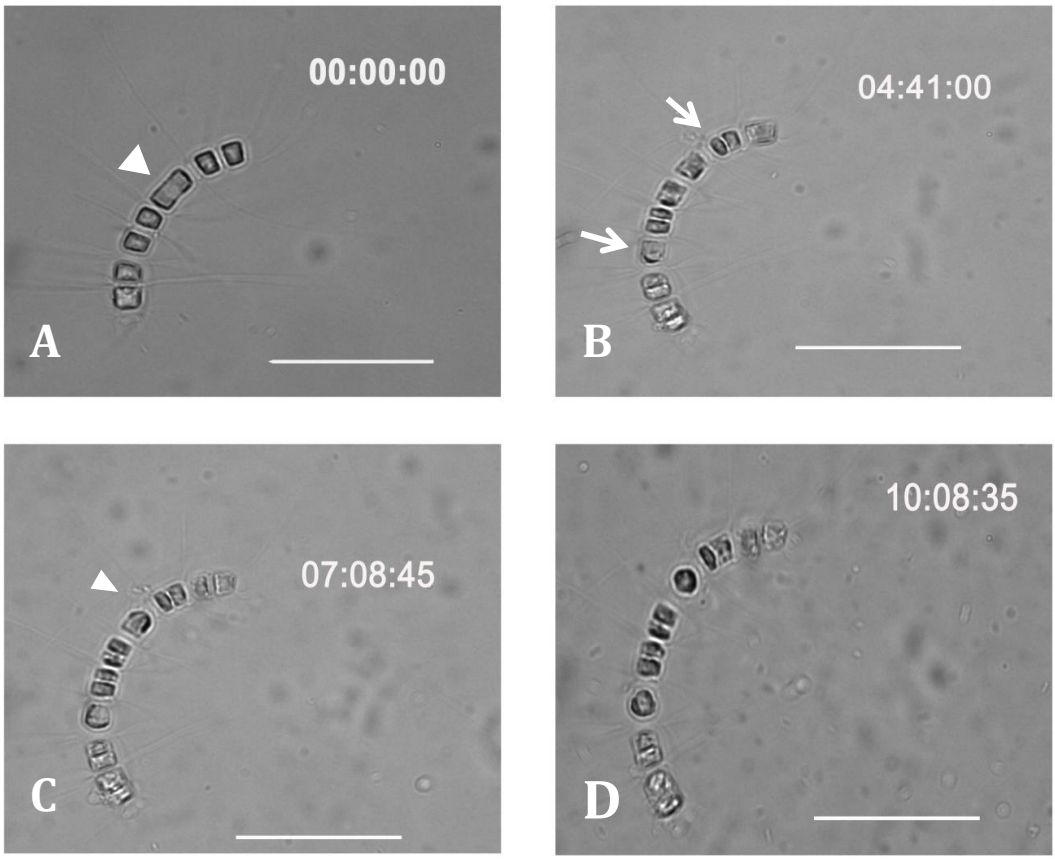

Figure 2.7: Frame extracted from the second time-lapse showing the formation of two spores in strain APC2. Colony at time zero with a cell undergoing vegetative division (arrowhead) (A). The two cells that are transforming into spores (arrows). The one on the bottom is already forming the primary spore valve (B). Spore formation in one of the daughter cells (arrowhead) (C). Spores completely formed (D); Scale bars = 50 µm.

Observations in CLSM were carried out in a culture after 24 hours of incubation with PDMPO. Some cells were healthy and forming colonies, others were senescent, and there were also spores completely formed and in formation, i.e., with only one valve (Figs 2.8 and 2.9).

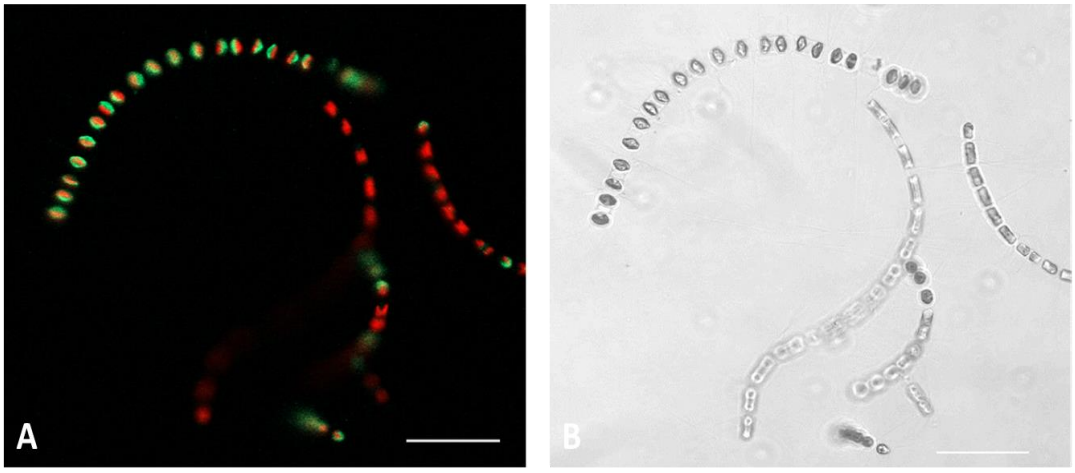

Figure 2.8: CLSM images of strain APC2 stained with PDMPO (A) and in transmitted light (B). In figure A spores and vegetative cells with neo-synthesized valves stained in green are visible. Chloroplast auto fluorescence is in red. Scale bars = 50 µm.

Another observation in CLSM was carried out on a culture induced to form spores and stained both with PDMPO and with the nuclear stain SYBER Green. Nuclei could be visualized in vegetative cells and in spores with only one valve. I could see the nucleus only in a few completely formed spores in which the secondary valve was probably recently synthesized and thus still permeable to the stain (Fig. 2.9). I could obtain proof that the mitotic division is associated to the formation of the secondary spore valve: it has been possible to detect two nuclei in a few spores in which the primary valve was already deposited and the secondary valve was in formation (Fig. 2.10). The observation of two nuclei in a spore where the formation of both valves was already completed and where one nucleus was smaller than the other, is an indication that one of the two nuclei was going to degenerate (Fig. 2.11).

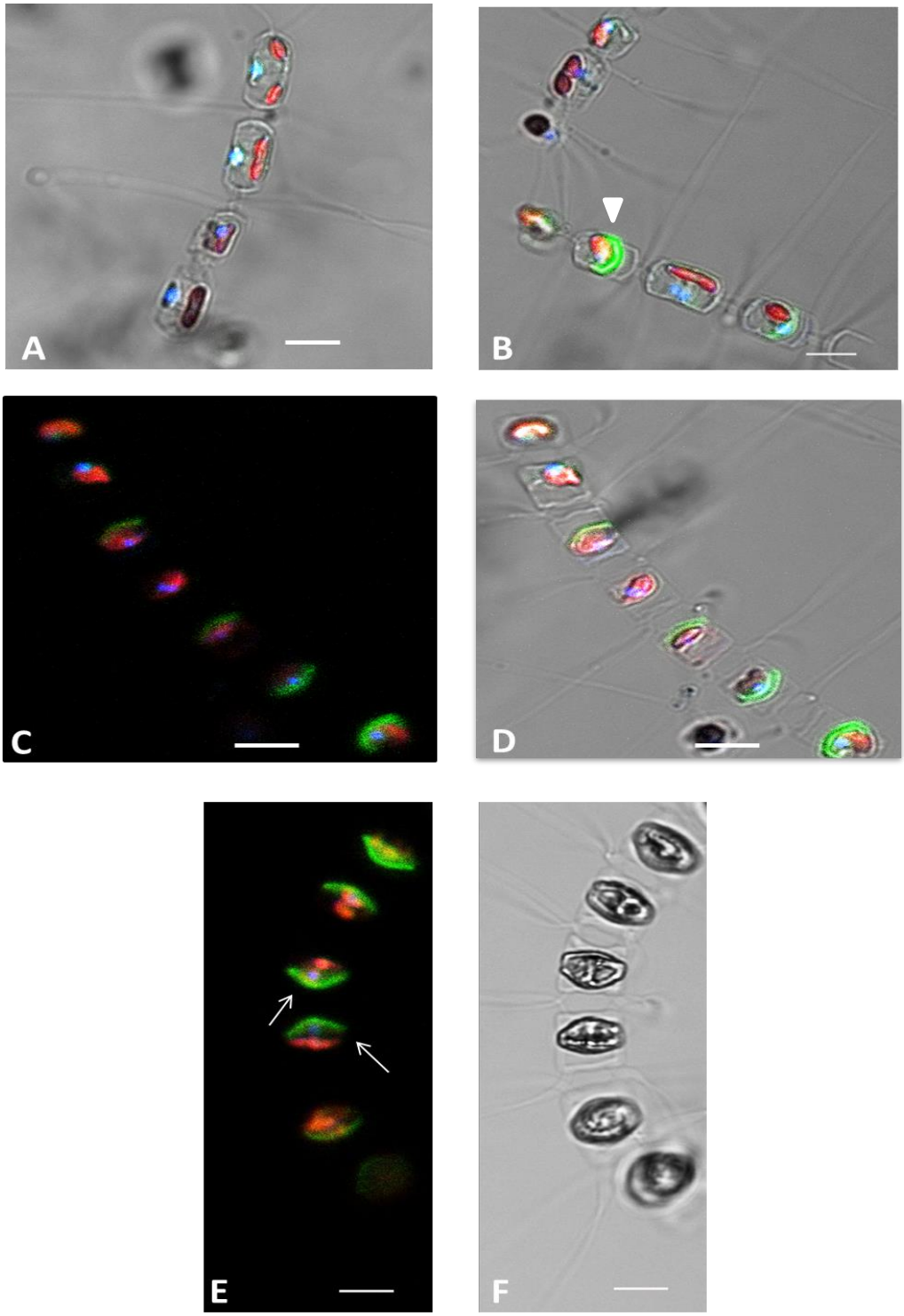

Figure 2.9: CLSM images of strain APC12. Vegetative cells stained with the nuclear stain SYBER Green (A). The primary valve of a spore stained with PDMPO (arrowed) close to a vegetative cell in which the two SYBER green-stained nuclei just completed mitosis (B). Vegetative cells and spores in formation stained with PDMPO and SYBER Green (C) and transmitted light (D). Chain of spores stained with PDMPO and SYBER Green; the secondary valve of each spore is visible but the nucleus is visible in only two spores (arrows) (E). The same image in transmitted light (F). Scale bars = 10 µm.

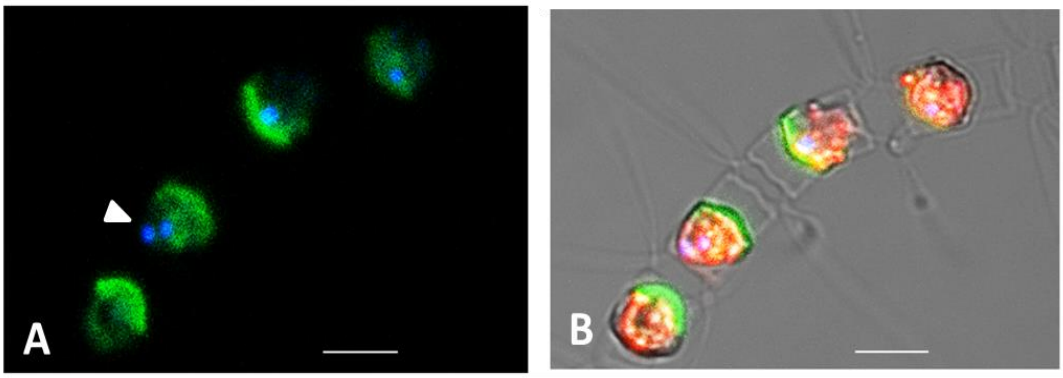

Figure 2.10: CLSM images of strain APC12. Spores stained with SYBER Green (blue) and PDMPO (green); two nuclei are visible in the second spore in formation (arrowhead) (A). The same image in which also chloroplasts (red) have been visualized (B). Scale bars = 10 µm.

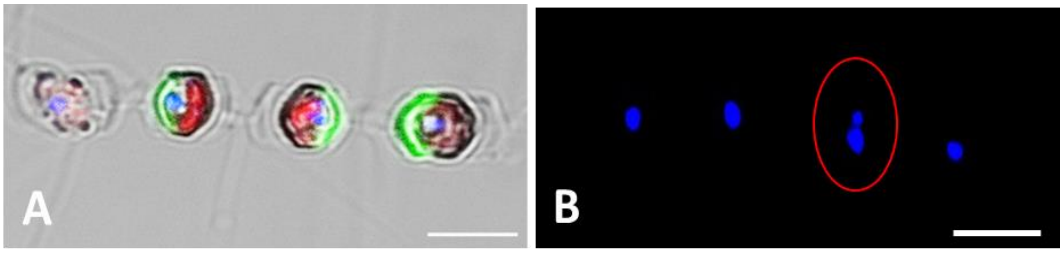

Figure 2.11: CLSM images of strain APC12 showing a chain of spores. Spores stained with SYBER Green (blue) and PDMPO (green); chloroplasts (red) (A). The same image in which only the nuclei are visualized; the red circle marks two nuclei in the same spore (B). Scale bars = 10 µm.

The observation of several cells in CLSM allowed demonstrating that formation of the spores is endogenous, i.e. it occurs inside the frustule of the vegetative cell that keeps the connection with the other cells in a chain. This process is not perfectly simultaneous in the different cells of a colony, although often spores are formed within the same time window (Fig. 2.12).

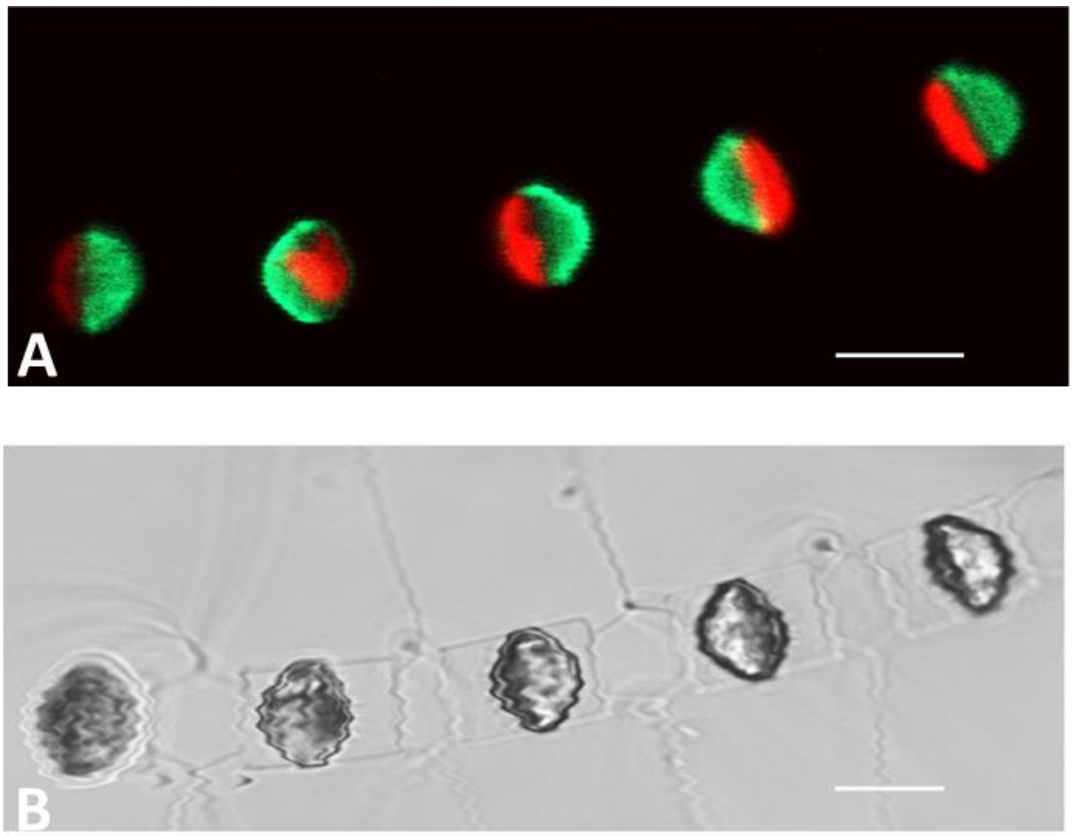

Figure 2.12: CLSM images of strain APC2 showing a chain of spores in which are visible the newly synthesized secondary valve and the chloroplast. A) Spores stained with PDMPO and B) in transmitted light. Scale bars =10 µm.

Spore germination

Spore germination could only be followed in time-lapse microscopy with bright-field illumination. The process started few minutes after the beginning of recording and involved only one spore in the chain (Fig. 2.13A). A marked cytoplasmic rearrangement, accompanied by the elongation of the central part of the spore, was visible. The cytoplasm moved on one side of the spore (Fig. 2.13B) and the new valve of the vegetative cell was formed on the other side (Fig. 2.13C). This process required approximately two hours. The cytoplasm then moved towards the newly deposited vegetative valve (Fig. 2.13C) and, after two more hours, the second vegetative valve was formed. The two spore's valves eventually detached from the new vegetative cell (Fig. 2.13 D). The whole germination process required 4.30 hours.

I recorded also the first vegetative division of the new cell (Fig. 2.14). Although the details of this process were not clearly visible I observed the formation of a new

daughter cell after 2.5 hours from its emersion from the spore (Fig. 2.14A, B) with the formation of new setae (arrowed in Fig. 2.14C).

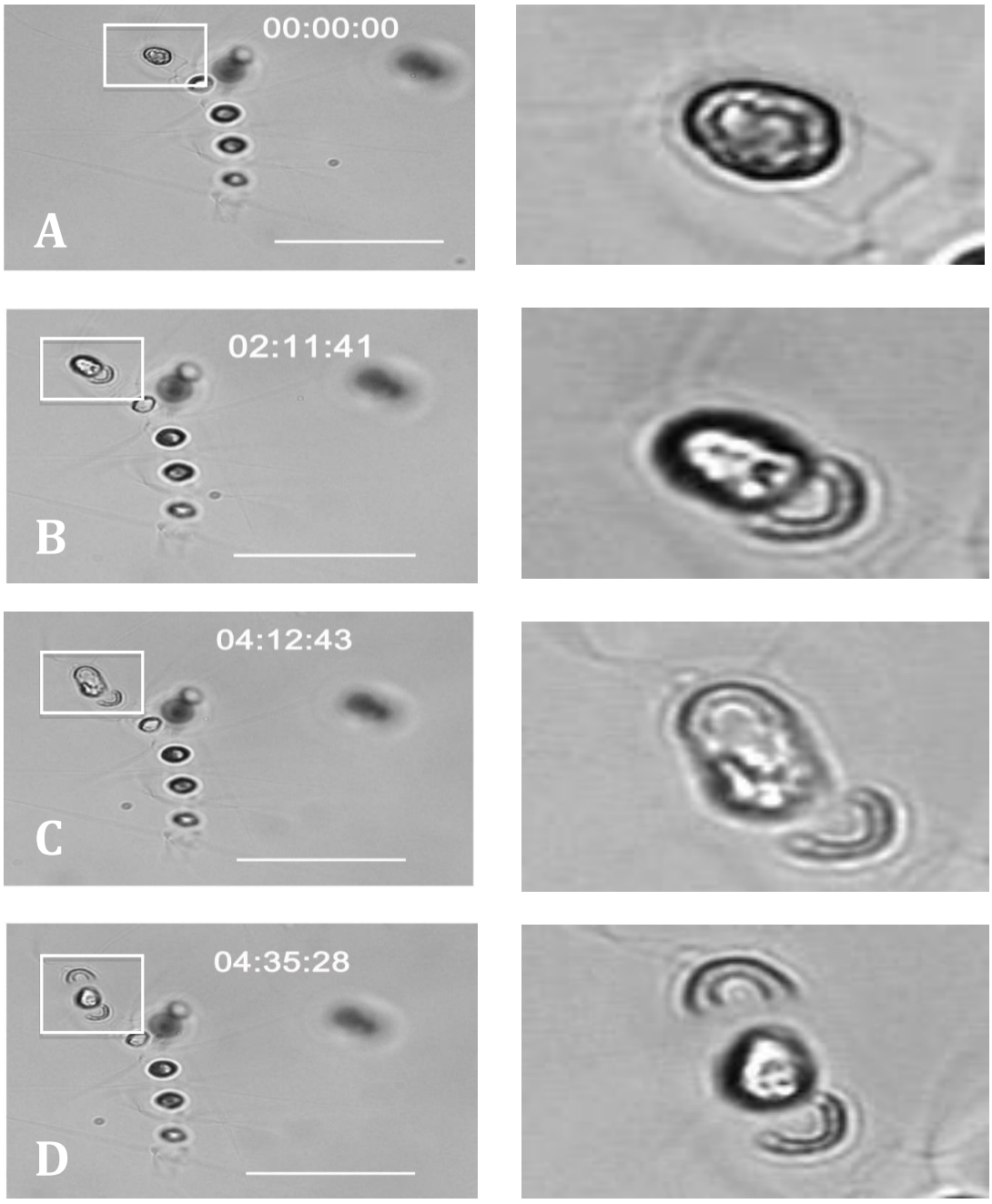

Figure 2.13: Frames extracted from time-lapse that show the germination of a spore. On the left frames time is reported: hours, minutes, seconds (on the top-right). The white box is the portion expanded on the pictures on the right. Beginning of time-lapse (A). The cytoplasm movement and the formation of the first vegetative valve (B). Beginning of the second vegetative valve formation (C). Detachment of the spore valves (D). Scale bars = 50 µm.

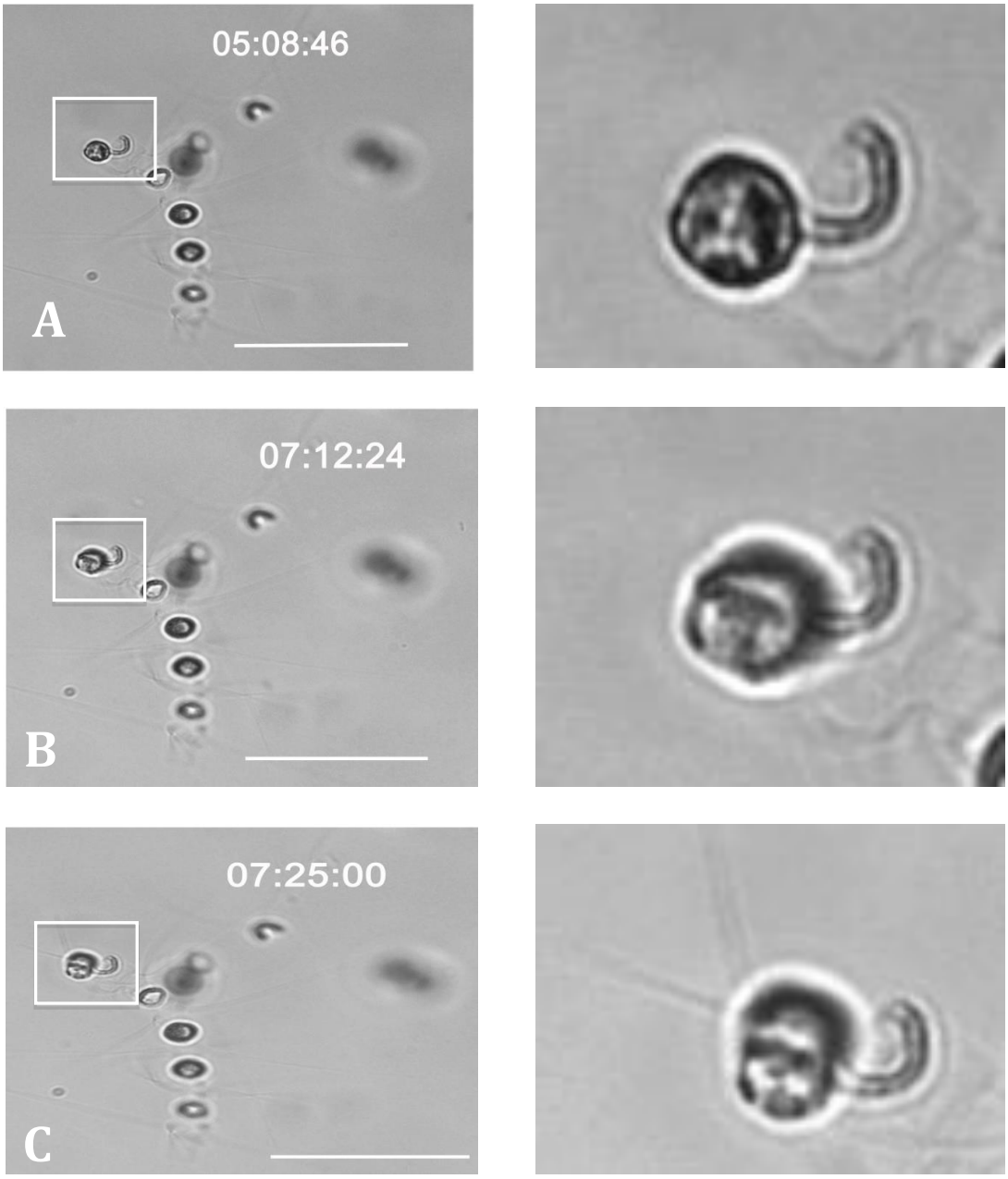

Figure 2.14: Frames extracted from time-lapse that show cellular division of a of a freshly germinated cell with hours, minutes, and seconds on the top-right. The white box marks the portion expanded on the pictures on the right. Free vegetative cell (A). End of cellular division (B). Elongation of setae (C). Scale bars = 50 µm.

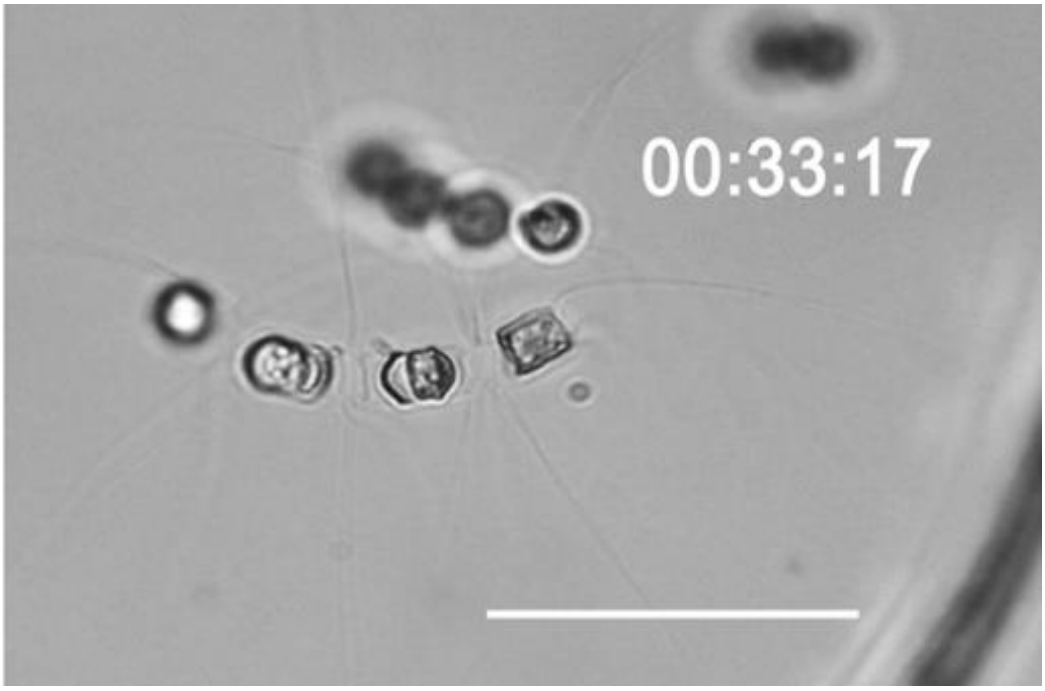

Figure 2.15: Frame of second experiment showing the first vegetative epivalve formation. Scale bar = 50 µm.

Discussion

This is the first time the three important phases of the life cycle of *C. socialis* were observed and recorded in time-lapse. Relative few studies investigated these processes in other *Chaetoceros* species (Pickett-Heaps, 1998; von Stosch *et al*., 1973) but never used flourochromes that allow describing the details of spore formation. With recordings in time lapse, I obtained information about the time required for spore formation and germination. The use of PDMPO allowed to visualize cells undergoing vegetative division and others forming spores and to see the modality through which endogenous spores are produced. Using SYBER Green I could follow the fate of the nuclei, which cannot be seen in transmitted light because of the relatively small size of the cells. I found some difficulty in staining mature spores with SYBER Green probably due the thickness of their frustule that does not allow the penetration of the stain. Similarly, the thick cyst wall of the dinoflagellate *Alexandrium pseudogonyaulax* did not allow staining the cyst nucleus with the nuclear stain Hoechst (Montresor, 1995). Cellular division of vegetative cells was the faster process, whereas both formation and germination of spores were slower probably because of the dramatic physiological and morphological changes that these two processes require.

Vegetative division

In some colonial species of *Chaetoceros* the terminal cells of the chain are charaterzied by the presence of terminal setae with a differrent orientation as compared to the intercalary ones (Hasle *et al.*, 1996). This is not the case of *C. socialis*. Cell in division were obseved in any position of the chain suggesting that there is no polarization and that all of them have the same capability to replicate. Moreover, since cells within the chain have identical morphology, it has been impossible to understand the mechanisms by which a chain breaks, originating two or more shorter chains. In *C. socialis* chains can break at any point and two or more 'fan-shaped' chains were produced. In other *Chaetoceros* species, such as *C. decipiens*, the breaking point is determined by the formation of cells with distinctive terminal setae; the chain breaks in correspondance to these cells (Pickett-Heaps, 1998; Dell'aquila *et al.*, 2017). This suggests that there is no specialization of cells within the colony and that the length of the chains and the subsequent formation of colonies with a sphaerical tertiaty shape may be determined by microscale physical dynamics.

Spore formation

Spores of *C. socialis* in culture and in natural samples can be surrounded by the frustule of the parental cell, when present in a chain of cells, or be completely free. These spores were defined as endogenous by many authors (Syvertsen, 1979) but the mechanism of their formation was never described. Hargraves (1979) observed spores in pair within a chain and suggested that from two vegetative cells two spores were produced simultaneously. However, the time-lapse recording demonstrated that one vegetative cell gives rise to only one spore and this does not influence the fate of the neighbour cell, which can undergo vegetative division.

I have observed the presence of two nuclei in cells that already had the primary spore valve and one of the nuclei was smaller, most probably undergoing pyknosis. This supports the general rule that the deposition of a valve in diatoms is always associated with nuclear division (von Stosch & Kowallik, 1969). In this specific case, nuclear division is not followed by cytokinesis; one of the two nuclei degenerates and the secondary spore valve is synthesized. It was however not possible to demonstrate that a similar process occurs when the primary spore valve is produced. Vegetative cells with two nuclei have been observed but unfortunately it was not possible to record the formation of spores in samples stained with SYBER green in time lapse using CLSM. The presence of two nuclei is an indication that the cell approaches mitotic division, but

there were no distinctive morphological features that could help to distinguish a cell that undergoes vegetative division from the one that will turn into spore.

In the tested experimental conditions, *C. socialis* formed spores in about 8-17 hrs. In *C. dydimus*, resting spore formation needed from 6 to 48 h (von Stosch *et al.*, 1973). It is reasonable to assume that also in nature this process is relatively fast once the cells perceive the environmental cue. The experiments aimed at testing the role of possible cues to induce spore formation will be illustrated in Chapter 3 and 4 of this thesis. It is interesting to point out that only a fraction of the cells respond to the external cues, showing that not all cells in the population have the same threshold for perceiving the cue/s that determine the shift between the vegetative stage to the resting stage. It is, indeed, necessary to consider that the simultaneity probably depends on the strength of the stimuli that cue their perception; it in turn influences the initiation by any single cell of the population. Von Stosch (1973) suggested that cells of *Chaetoceros* species are physiologically determined to become spores already from the mitotic division that precedes the formation of the spore. I cannot exclude von Stosch's hypothesis, but my observations did not provide peculiar morphological characteristics that can allow identifying the vegetative cells that later turned into spores.

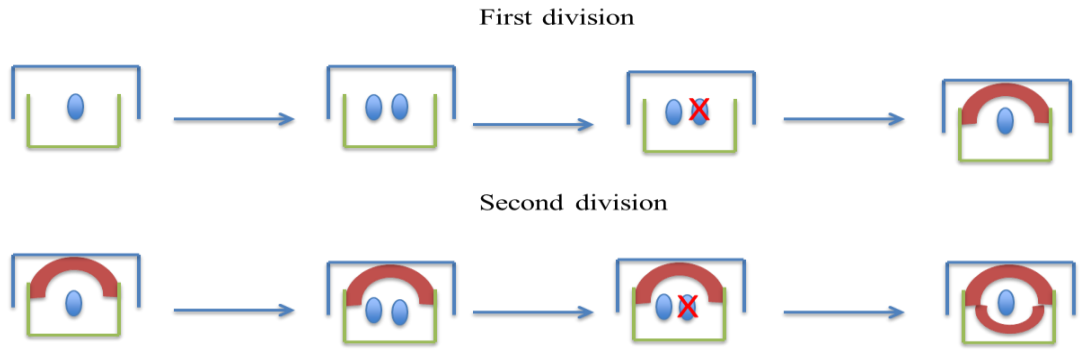

Figure 2.16: Schematic drawings of the formation of endogenous spores in C. *socialis*. A mitotic division with the degeneration of one nucleus precedes the formation of both spore's valves.

In *C. socialis* spores are formed inside the maternal cells (Fig. 2.16). The second nuclear division were supported by the observation of bi-nucleate spores in formation (Figs 2.10 and 2.12). In Fig. 2.12 there is the proof that one nucleus was degenerating. The marked re-organization of cellular content of spores reminds what has been observed during the formation of akinetes in cyanobacteria (Kaplan-Levy *et al.*, 2010). Both are colonial microorganisms and resting stages are formed in response to environmental stresses. Akinetes are tick-walled, morphologically different from vegetative cells, with reduced metabolic activity and are formed within the vegetative

mother cell as in *Chaetoceros socialis*. Both in diatoms and in cyanobacteria these resting stages are not enclosed in lager structure (as happens, for example, in myxobacteria or fungi) and all vegetative cells have the potential to become dormant (Kaplan-Levy *et al.,* 2010). During the formation of akinetes, there is an increase of storage compounds (mainly glycogen and cyanophycin) used then when they are mature; an increase of carbon content took place also during the formation of spores in *C. socialis* (see Chapter 3). Contrasting evidences are instead present on the DNA content: in *Nostoc* PCC 7524 it is the same in vegetative cells and resting cells (Sutherland *et al.,* 1979) whereas in *Anabaena cylindrica*'s akinetes have a double DNA content (Simon, 1977).

Spore germination

The valves of the vegetative cell are formed within the spore. I could not follow nuclear behaviour since cells are extremely small, the nuclear stain does not penetrate into the spores and it was not possible to carry out time lapse on stained cells with CLSM. In the larger species *C. dydimus* two acytokinetic mitosis were observed (von Stosch *et al.,* 1973) and the data presented in this Chapter suggest that a similar process also occurs in *C. socialis*.

The cells produced after germination performed a vegetative cell division at the tested experimental conditions (nutrients and light were available) demonstrating that they are immediately ready to duplicate. The elongation of spore's frustule was the only morphological feature that indicates that a spore was starting to germinate. This can be the only character that can be used in the future to choose single cells to analyse with a single cell approach for, e.g. transcriptomic studies.

Spore germination at the tested experimental conditions took about 4 hrs; however, it is not clear how long time is required from the perception of external stimuli to the beginning of the germination process. It seems that the perception of light is the cue that induces spore germination (e.g., Shikata *et al.,* 2011). Experiments, in which the molecular mechanisms at action during this life cycle transition , will hopefully shed light on the capability of diatoms to perceive environmental stimuli and react to them.

Chapter 3

Factors inducing spore formation: nitrogen limitation and cell density

Introduction

As illustrated in Chapter 1, nutrient limitation – mostly nitrogen – has been shown to be effective in inducing the formation of resting stages in several diatom species. One of the aims of this chapter is to describe experiments made to test if a growth medium deprived in nitrogen is an effective cue also for *Chaetoceros socialis*. Although similar experiments have been carried out with other *Chaetoceros* species, experimental set ups did not include all parameters and/or they were not exhaustively described. At times, control conditions in which strains were grown with full strength medium were not included (e.g. (Kuwata *et al.*, 1993), the concentration of dissolved inorganic nutrients was not monitored during the experiment (e.g., (French & Hargraves, 1980), and only in a few experiments (Kuwata *et al.*, 1993); (Oku & Kamatani, 1995) the concentration of the internal pool of nutrients was included (for a summary, see Table 1 in Chapter 1). The experimental set up used in this thesis included the assessment of all these factors in order to obtain a clear picture of the physiological changes occurring in *C. socialis* when grown in a nitrogen-limited culture medium.

A second set of experiments was carried out to test the role of cell concentration for the induction of spore formation in *C. socialis*. This question arose from the results of the previous experiment, where spores – although with lower percentages - were produced also in cultures grown in full strength medium, when concentrations of all the major inorganic nutrients were not limiting. To answer this question, spore formation was investigated using a semi-continuous culture set up, in which three different cell concentrations and two growth media (the control full-strength medium and a medium without nitrogen sources) were used. The semi-continuous culture set up offers the advantage to keep the tested experimental conditions within a relatively narrow range of variation in nutrient concentration and thus physiological status of the cells, over time. The role of cell density in various aspects of the organism biology (physiology, formation or germination of resting stages, production of biofilms) has been studied in bacteria. *Quorum sensing* represents a well-known mechanism by which unicellular organisms can perceive their population's density and react accordingly. This mechanism has been mainly studied in bacteria, social amoebae and fungi. *Quorum sensing* consists in the production of specific signalling molecules, their release in the environment and their perception by conspecifics. In bacteria, the crosstalk between cells is mediated by trans-membrane proteins that induce intracellular changes (Lennon & Jones, 2011). A well-studied model organism is a soil bacterium, *Bacillus subtilis*, in which spore formation depends both on cell density (*quorum sensing*) as well as on

environmental cues signalling the onset of adverse conditions. The shift from vegetative cells to spore is primary dependent from the activation of the transcription factor Spo0A. This factor is activated by environmental cues such as nitrogen and carbon starvation and by chemical signals implicated in quorum sensing that are excreted in the medium. These molecules accumulate and thereby the higher the cell concentration, the higher is the activation Spo0a and the higher is the number of cells that transform into spores (van Gestel *et al.*, 2012).

The results of the experiment run with semi-continuous cultures confirmed that spore formation occurs at high cell density, without nutrient limitation, and this suggested the presence of a chemical signal. This hypothesis was tested in two additional experiments in which cells were grown with the medium produced by high-density cultures.

Materials and Methods

Experiments were performed using strains APC1, APC2 and APC12 following the procedures for culture isolation, genetic characterization and maintenance described in Chapter 2.

Experiment 1: nitrogen limitation as a factor for the induction of spore formation

The experiment was carried out in batch cultures using two strains of *C. socialis*, APC1 and APC2, which were acclimated for several generations (more than five) at the experimental conditions selected for the experiment. The cultures were grown in a modified full strength f/2 medium (control) (Guillard, 1975) and in a N-limited f/2 medium (treatment) (Table 3.1). The control medium had a lower N concentration than f/2 so to obtain a N/P ratio close to the Redfield ratio, and higher Si concentration to avoid possible Si limitation that may negatively influence spore formation. The N-limited medium had the same nutrients concentration as the control with the exception of nitrate, which was much lower. Culture media were prepared with artificial seawater at salinity of 36 (Sea salts, Sigma-Aldrich St. Louis, USA). The experiment was carried

out in culture chamber with controlled temperature and light conditions. Light and temperature were monitored for the entire duration of experiment with a HOBO Pendant® Temperature/Light Data Logger. To mimic the natural condition to which this species is exposed when blooming in the Gulf of Naples, temperature was set at 18 ± 2 °C and a sinusoidal illumination system was used with a maximum irradiance of 180 µmol photons·m^{-2}·sec^{-1} and 12:12 h light:dark cycle.

Three replicates for treatment and three for the control condition were prepared by inoculating cells in exponential growth phase in 750 mL flasks with cap vent, filled with 500 mL of culture medium at a final cell concentration of about 3,000 cells·mL^{-1}. The parameters measured were: cell concentration, spore concentration, intracellular nitrogen and carbon content and dissolved inorganic nutrients (SiO_2, PO_4, and NO_3). Cell and spore concentration was determined every day, while particulate and dissolved nutrients were measured at the beginning, exponential, early stationary and late stationary growth phase corresponding to days 0, 2, 4, and 7, respectively.

In order to estimate cell and spore concentration, 4 mL from each flask were fixed with 40% neutral formaldehyde solution (final concentration 10:1 v:v) and counted with a Sedgwick-Rafter chamber on a Zeiss Axiophot microscope (ZEISS, Oberkochen, Germany) at 40x magnification. More than 200 cells were counted when possible. The growth rate µ, expressed as specific growth rate· (day^{-1}), was calculated following (Wood *et al.*, 2005).

To measure intracellular carbon and nitrogen at the different time points, three samples were collected from each bottle as technical replicates. The volume collected for each culture (15 or 20 mL) was different because of variation of cell density during the growth curve. Samples were filtered using pre-combusted (450 °C, 4 h) glass-fiber filters (Whatman GF/F) with 1.2 µm pore size and immediately stored at -20 °C. The analyses were performed with a Thermo Scientific FlashEA 1112 automatic elemental analyser (Thermo Fisher Scientific, Waltham, MA, USA) following the procedure described by Hedges and Stern (1984). Cyclohexanone-2,4- dinitrophenylhydrazone was used as standard.

To evaluate the concentration of dissolved inorganic nutrients, 50 mL of sample were collected from each flask. Samples were filtered using Whatman® Celluose Acetate Membranes with a pore size of 0.45 µm in two high-density polyethylene vials (20 mL each) and immediately stored at -20 °C until analysis. The analyses were carried

out using FlowSys Systea Autoanalyzer equipped with three continuous flux channels. The analyses were performed following Hansen and Grasshoff (1983).

For intracellular carbon and nitrogen (Fig. 3.7) and their ratio (Fig. 3.8) comparisons were made between treatment and control for each time point. Two-tailed unpaired t-test assuming unequal variance was performed. Same test was performed on uptake rates of nitrate silicate and phosphate. Statistical analyses were made using GraphPad Prism version 6.0 and values were defined significantly different when $p < 0.05$.

Table 3.1: Concentration of the main nutrients in the Low N medium (treatment) and High N medium (control) used in Experiment 1.

Nutrients	- N (treatment)	+ N (control)
$NaNO_3$	23 µM	580 µM
K_2HPO_4	29 µM	29 µM
$NaSiO_3$	300 µM	300 µM

Experiment 2: cell density as a factor for the induction of spore formation

Experiments were carried out using strain APC12. Three different cell densities were tested:

High: $3*10^4$ cells·mL^{-1} Medium: $3*10^3$ cells·mL^{-1} Low: $3*10^2$ cells·mL^{-1}

For each cell density condition, two culture media were tested (Table 3.2): the modified f/2 medium as a control and a treatment that differed from that used in the previous experiment for the fact that the nitrogen source was not added. In order to avoid silica limitation, the amount of SiO_3 has been slightly increased in both media at a concentration of 360 µM.

Strain APC12 was inoculated in a 250 mL culture flask filled with 100 mL of control medium. The culture was acclimated at the experimental conditions using a semi-continuous set up (7 days) and high cellular concentration. Aliquots of this culture were then used to inoculate the flasks at different cell densities: High (30,000 cells mL^{-1}), Medium (3,000 cells mL^{-1}), Low (300 cells mL^{-1}) in both nitrogen limited and full

strength medium (Fig. 3.1). The experiment was carried out at the same temperature and irradiance conditions used in Experiment 1. Every day, a 3-mL subsample to assess cell and spore concentration was collected from each bottle; every two days, cell concentration was brought back at the initial density eliminating the required amount of culture and adding new medium. The concentration of vegetative cells and spores was assessed as illustrated above.

The pH was measured in the high-density set-up with a pH meter Corning 240 (Missouri City, USA) before refreshing each cultures with the appropriate medium.

The statistical analysis of growth rates at different density conditions and growth media were performed using a two-way ANOVA followed by a Tukey's multiple comparisons test. Statistical analyses were made using GraphPad Prism version 6.0 and values were defined significantly different when $p < 0.05$.

Table 3.2: Concentration of nutrients in the two media used in Experiment 2.

Nutrients	- N (treatment)	+ N (control)
$NaNO_3$	0 µM	580 µM
K_2HPO_4	29 µM	29 µM
$NaSiO_3$	360 µM	360 µM

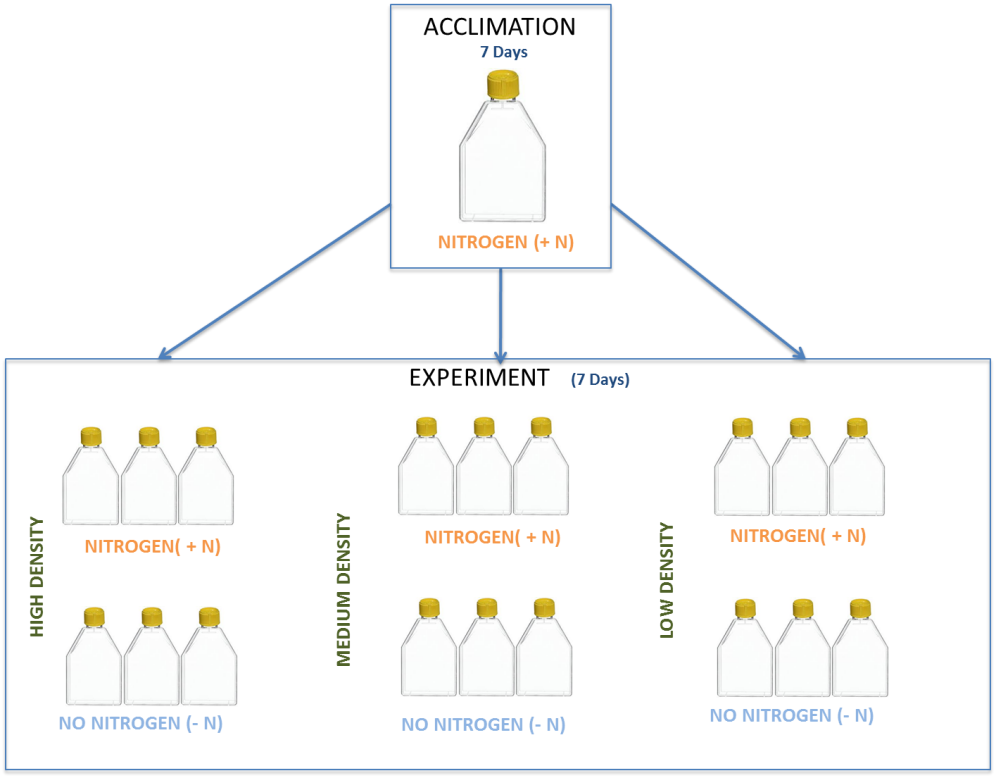

Figure 3.1: Schematic representation of the experimental set up for Experiment 2.

Experiment 3: spore formation in high-cell-density conditioned medium

Strain APC12 was grown at high cell density in full strength medium (+N) under semi-continuous conditions for a week. This culture was used to inoculate three 750 mL flasks with cap vent, filled with 600 mL at high-density conditions (initial cell concentration of $3 \cdot 10^4$ cells·mL^{-1}). After two days, 4 mL were collected from each bottle and fixed to assess cell concentration as illustrated for the previous experiments. The content of the three flasks was pooled together and immediately filtered on a 1.2 µm pore size membrane in order eliminate all cells and obtain a stock of medium 'conditioned' by the growth of cells at high density. The conditioned medium was used to fill three 250 mL flasks used then to perform Experiment 3 with a semi-continuous set up. Flasks were inoculated with an exponentially growing culture to reach low-density conditions, i.e., $3 \cdot 10^2$ cells mL^{-1}, and incubated at the same temperature and light conditions used for Experiments 1 and 2 (Fig. 3.2). The concentration of vegetative cells and spores was monitored daily for 8 days.

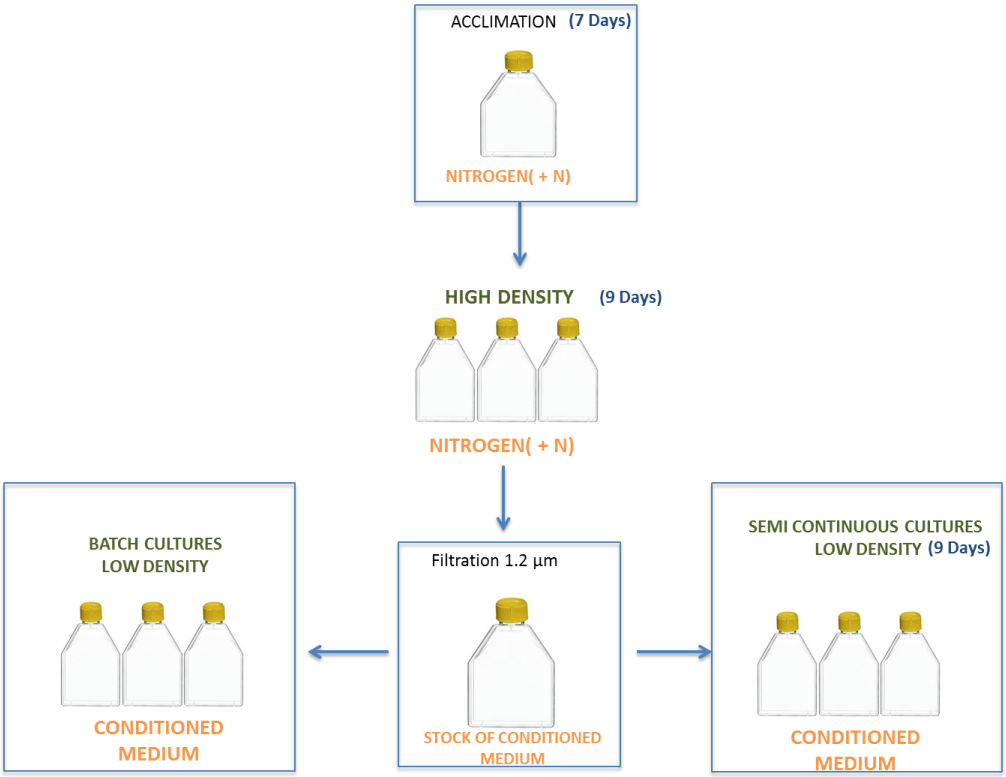

Figure 3.2: Schematic representation of the experimental set up used for Experiment 3.

The cultures used to obtain the 'high-density' conditioned medium used for Experiment 3 grew at the same rate, and reached similar cell concentration, as the high-density cultures of Experiment 2 (Fig. 3.3).

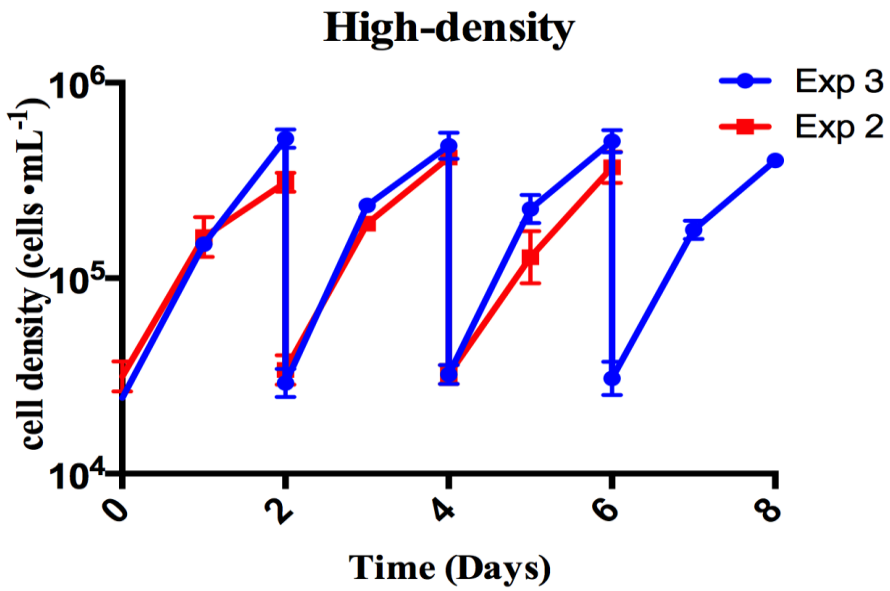

Figure 3.3: Total cell concentration of strain APC12 in semi-continuous growth, at high cell density with full strength medium (+N) in Experiment 2 (red) and during the semi-

continuous acclimation growth of the cultures used to prepare the high-cell-density conditioned medium (blue). Data represent average values ± S.D. (n=3).

Spore percentage in conditioned medium was compared to the percentage obtained in Exp 2 at low density in both media. A Two-tailed unpaired t-test assuming unequal variance was performed using GraphPad Prism version 6.0 and values were defined significantly different when $p < 0.05$.

Experiment 4a and 4b: short-term experiment with high-cell-density conditioned medium

Two short term (2-days) experiments were carried out to test spore formation in cultures inoculated in:

Exp. 4a: treatment 1: high-cell-density medium obtained by filtration on a 1.2 µm pore sized filter; treatment 2: high-cell-density medium obtained by sonicating the culture and then filtering it on a 1.2 µm pore sized filter; control with full strength culture medium.

Exp. 4b: treatment 1: high-cell-density medium obtained by filtration on a 1.2 µm pore sized filter; treatment 2: high-cell-density medium obtained by filtration on a 1.2 µm pore sized filter and adding an aliquot of nutrients (final concentration equal to f/20) to rule completely out nutrient limitation; treatment 3: high-cell-density medium obtained by sonicating the culture and then filtering it on a 1.2 µm pore sized filter; treatment 4: high-cell-density medium obtained by sonicating the culture, filtering it on a 1.2 µm pore sized filter, and adding an aliquot of nutrients (final concentration equal to f/20) to rule completely out nutrient limitation; control with full strength culture medium.

To set up both experiments, strain APC12 was grown at high cell density in full strength medium (+N) under semi-continuous conditions for one week and used to inoculate triplicate flasks (containing 30 mL of culture medium each) for all treatments and control at initial cell concentration of 300 cells mL^{-1} (Experiment 4a) and 1,000 cells mL^{-1} (Experiment 4b).

The cultures were sonicated with a Branson Sonifier 250 (Branson Ultrasonics Corporation, Danbury, USA) three times for 30 seconds min.

Every day a 3-mL subsample was collected, fixed and used to enumerate cell and spore concentration as illustrated above.

Results

Experiment 1: nitrogen limitation as a factor for the induction of spore formation

The aim of this experiment was to test the dynamics of spore formation in batch cultures of *C. socialis* where the treatment was a culture medium deprived of nitrogen source and the control a full-strength medium. In control condition, both strains grew exponentially for the first two days and reached more than 10^6 cells mL^{-1} at the end of the exponential growth phase (Fig. 3.4). In cultures grown in nitrogen depleted medium, cell concentration reached an average maximum value of $\approx 2 \times 10^5$ cells mL^{-1}, although strains showed a growth rate similar to that recorded in the control condition in the first two days. From the third day onwards, cells continued to grow only in nitrogen replete medium (Figs 3.4 and 3.6 C, D). In the treatment, more than 90% of cells were present as spores in both strains from day 4 (strain APC1) or day 3 (strain APC2) (Fig. 3.6 A, C) and the remaining cells appeared senescent, i.e. with degraded cytoplasmic content, at the end of the experiment. However, spores were recorded also in the controls, with average maximum percentages of 44% in APC1 and 27% in APC2 (Fig. 3.5 B, D).

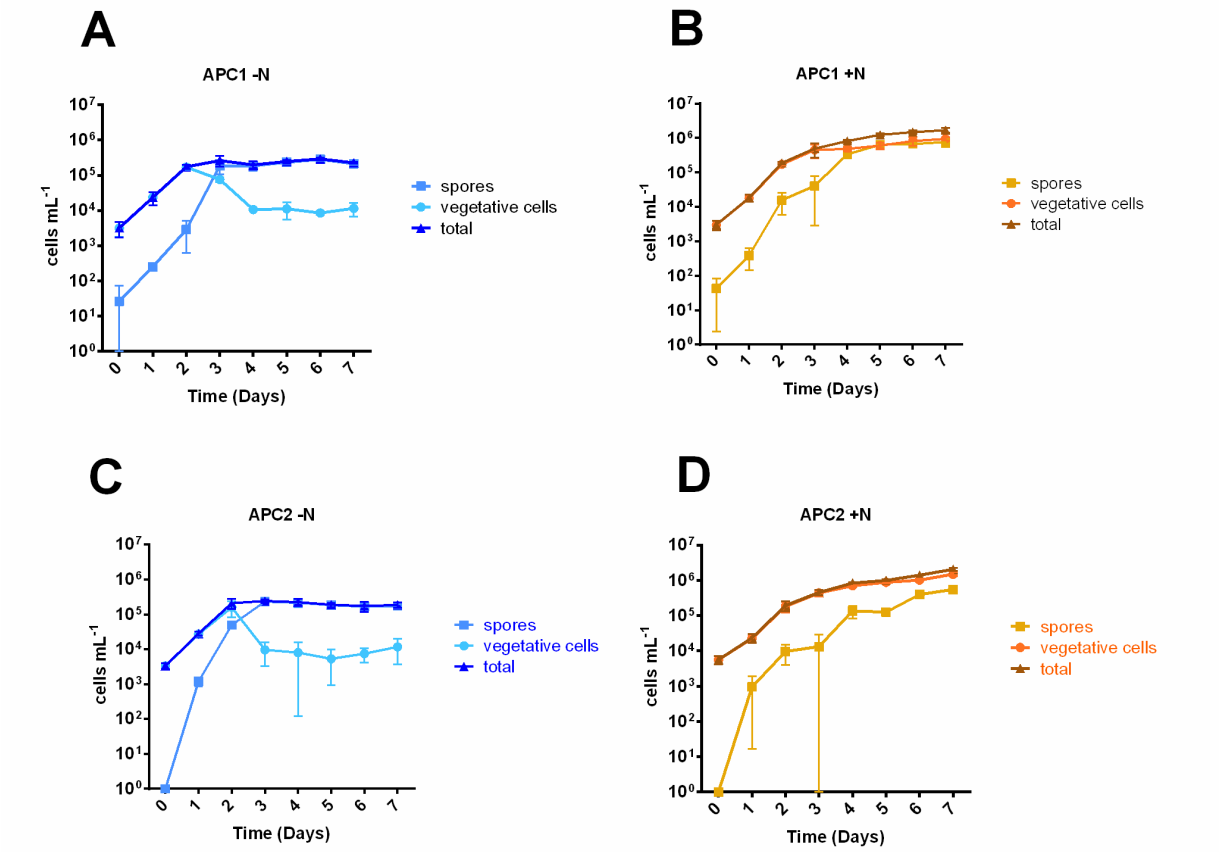

Figure 3.4: Growth curves of strain APC1 (A, B) and APC2 (C, D) in low nitrogen medium (A, C; blue) and in high nitrogen medium (B, D; orange). Data shown as average ± S.D. (n=3).

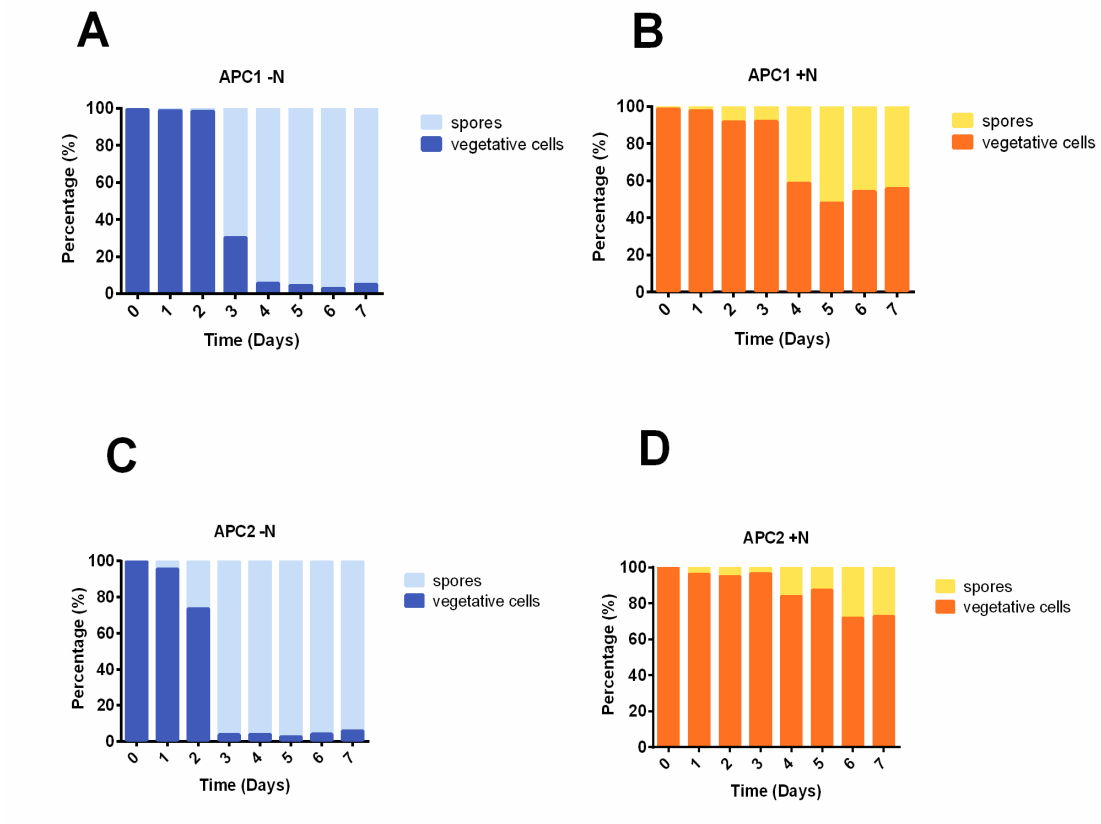

Figure 3.5: Average percentages (n=3) of spores and vegetative cells in strains APC1 (A, B) and APC2 (C, D) grown in low nitrogen medium (A, C; blue) and in high nitrogen medium (B, D; orange).

In the treatment condition, nitrate concentration reached almost undetectable values on day 4 in strain APC1 and already on day 2 in strain APC2 (Fig. 3.7 A, B). In control conditions, average nitrate concentration of 279 ± 4 and 248 ± 15 µmol L^{-1} were still present at the end of experiment in strain APC1 and APC2, respectively (Fig. 3.7 A, B). Silicates reached almost undetectable levels in both strains at the end of the experiment (day 7) in control conditions, while their average concentrations on day 7 in the treatment was 172 ± 15 and 139 ± 22 µmol L^{-1} for strain APC1 and APC2, respectively (Fig. 3.6 C, D). Orthophosphates never reached limiting concentrations in strains grown both in high and in low nitrogen medium. The consumption of orthophosphates, however, increased drastically in the control condition, while it was gradual in the treatment (Fig. 3.7 E, F).

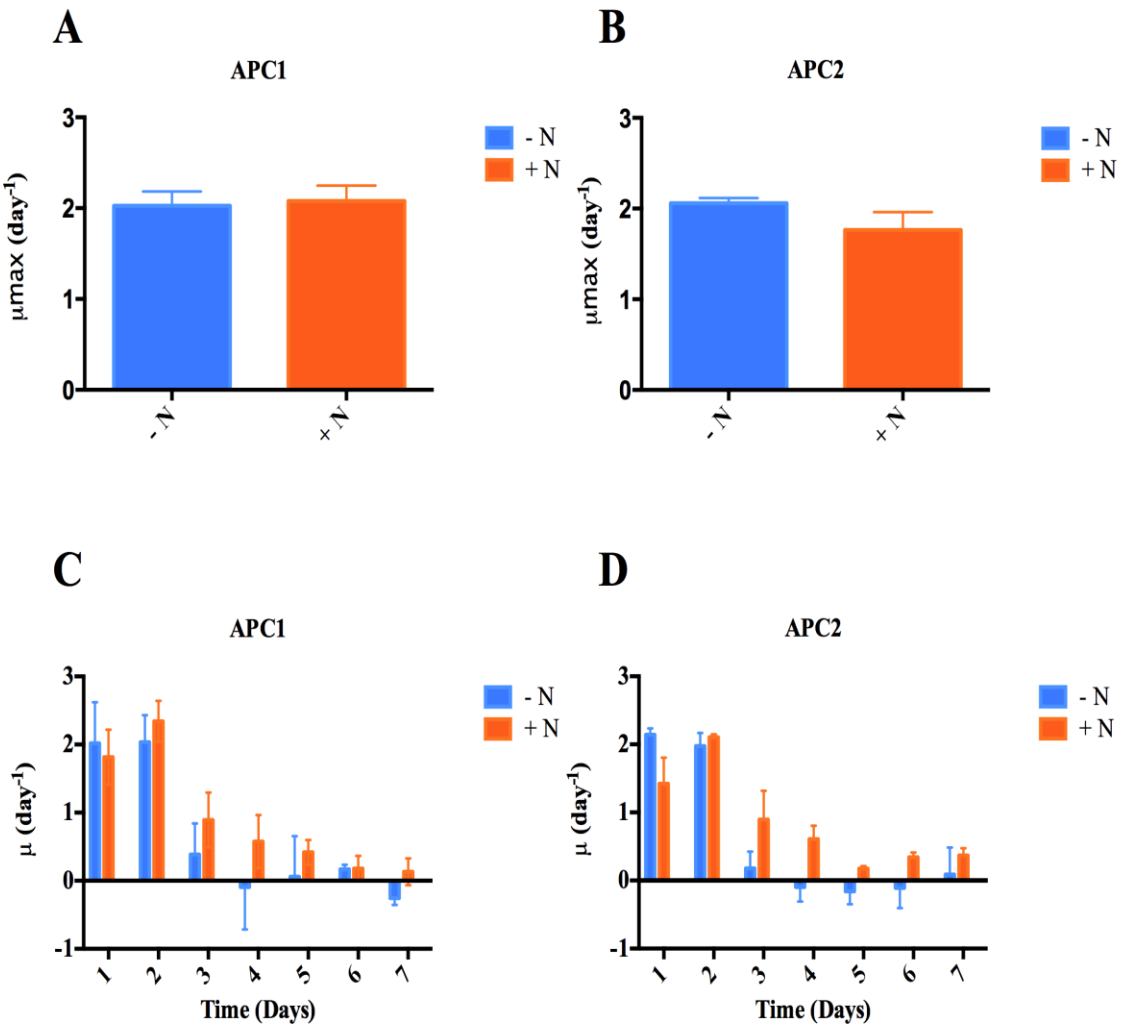

Figure 3.6: Maximum exponential growth rate of the two strains, APC1 (A) and APC2 (B), grown in low-nitrogen medium (blue bars) and high-nitrogen medium (orange bars); the exponential phase lasted two days. Data shown as average ± S.D. (n=3). Daily growth rate of the two strains APC1 (C) and APC2 (D) grown in low-nitrogen medium (blue bars) and high-nitrogen medium (orange bars) during the entire experiment. Values on the x axis show the time interval over which growth rate was measured, i.e. 1= growth rate between day 0 and day 1. Data shown as average ± S.D. (n=3).

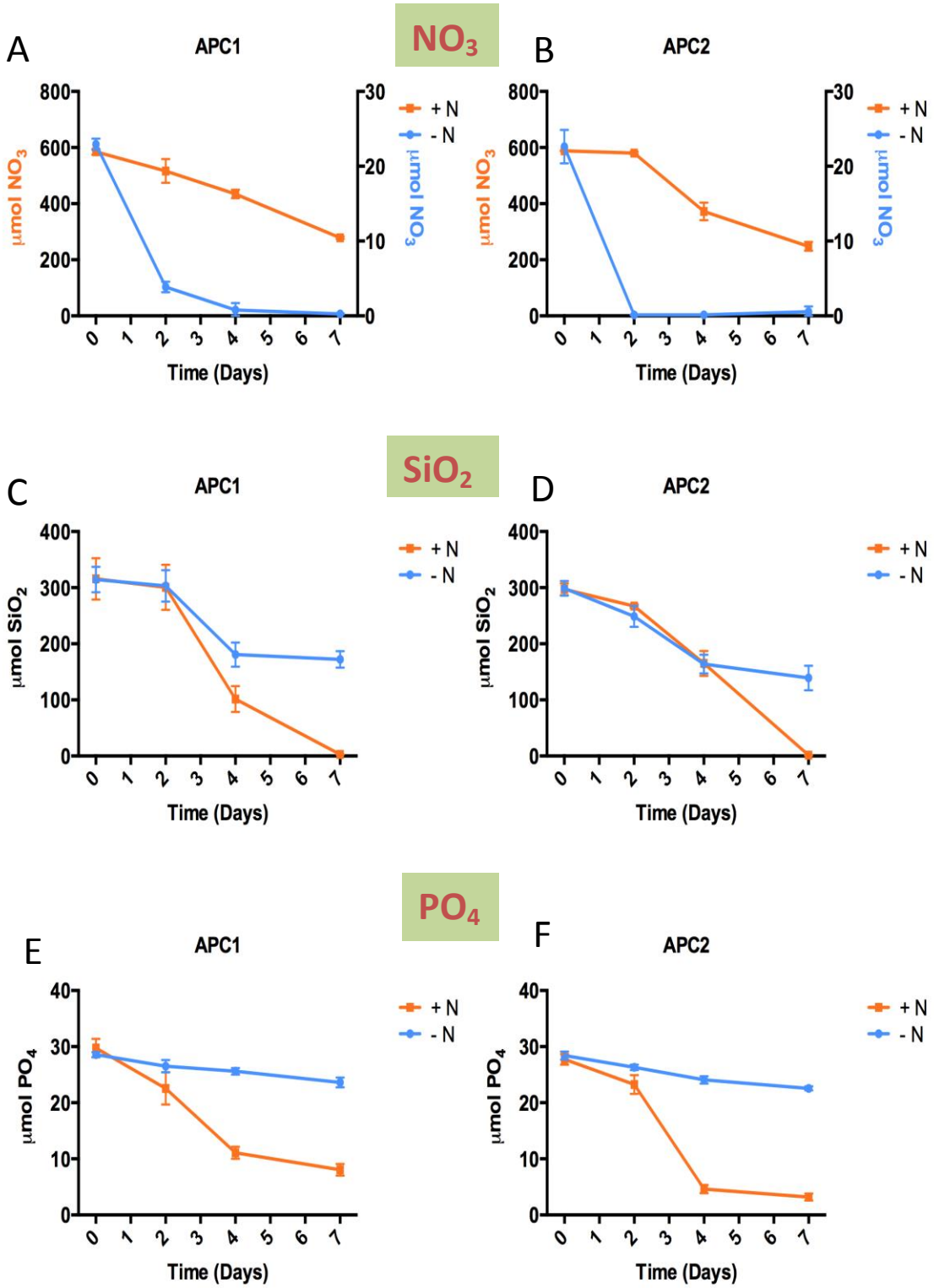

Figure 3.7: Concentration of: nitrates (NO_3; A, B), silicates (SiO_2; C, D) and orthophosphates (PO_4; E, F) in strains APC1 (A, C, E) and APC2 (B, D, and F) grown in low nitrogen medium (blue) and in high nitrogen medium (orange). Data shown as average ± S.D. (n=3). Note that NO_3 concentration for the low nitrogen condition is represented on the right axis.

The intracellular content of nitrogen and carbon estimated at each time point were not statistically different (non-parametric t-test) between control and treatment for both strains (Fig. 3.8). However, when comparing all the intracellular nitrogen data collected over the time course of the experiment, the treatment was significantly different from the control (p=0.015 for APC1 and p= 0.001 for APC2). Differences in carbon content between treatment and control were instead significant only for APC2 (p=0.036). Looking at the cellular pools of carbon and nitrogen, I could observe that, starting from day 2, values of intracellular nitrogen were slightly higher in control conditions for both strains (Fig. 3.8 A, B), while intracellular carbon content was comparable (Fig. 3.8 C, D). Nitrogen content kept increasing in cultures grown with full strength medium (Fig. 3.8 A, B) at higher rate than carbon content (Fig. 3.8 C, D) at the onset of the stationary phase (day 4). Carbon content was instead considerably higher in cultures grown in nitrogen-depleted medium till the end of the experiment.

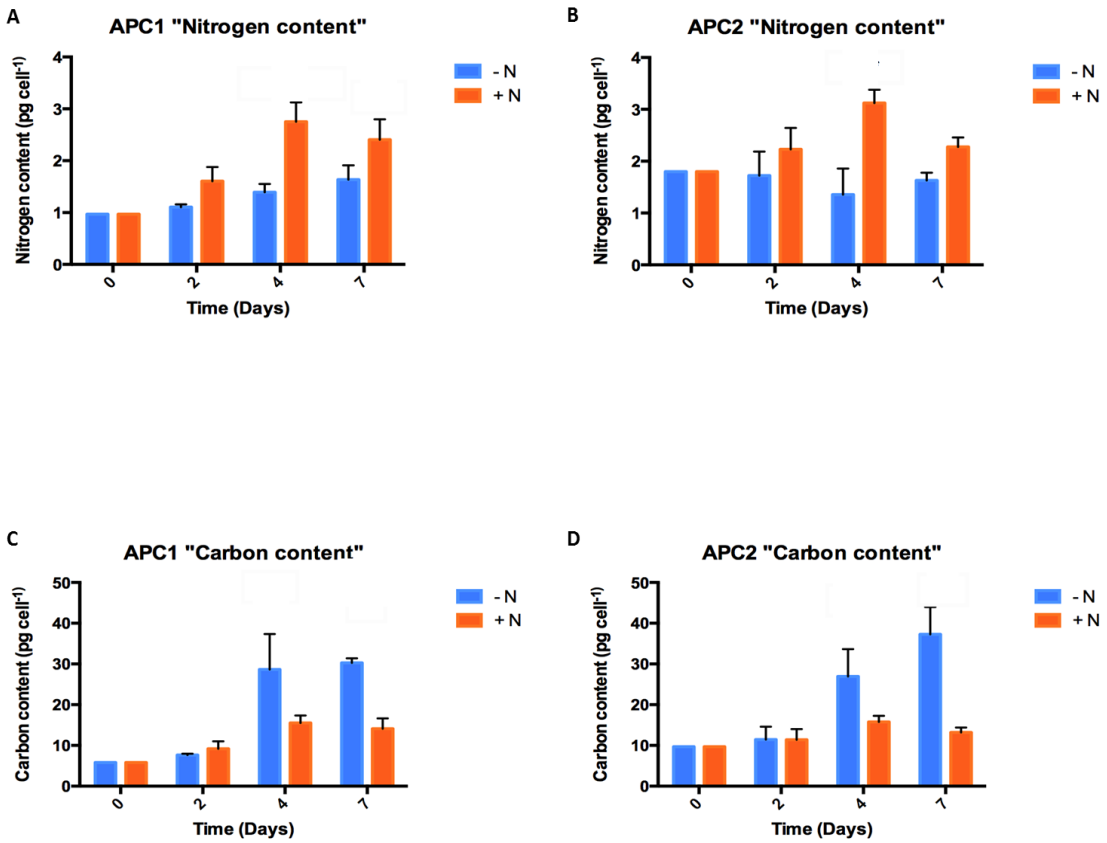

Figure 3.8: Intracellular nitrogen content (A, B), carbon content (C, D) in strain APC1 (A, C) and APC2 (B, D) grown in low nitrogen medium (blue) and in high nitrogen medium (orange). Data shown as average ± S.D. (n=3). Treatment and control values for each sampling time have been compared with a t-test.

The C:N ratios clearly illustrate the changes in intracellular nutrient pools at the beginning and during the stationary phase, i.e. day 4 and 7 (Fig. 3.9 A, B), in the treatment condition. The difference between control and treatment condition was significant (APC1 $p < 0.0001$; APC2 $p = 0.0002$). Along the growth curve, this C:N ratio increased until it became four times higher in the stationary phase of the treatment, when massive spore formation occurred, while it remained constant in the strains grown in nitrogen replete medium. This constant difference was mostly due to an increase in carbon content in both strains grown in low-nitrogen condition.

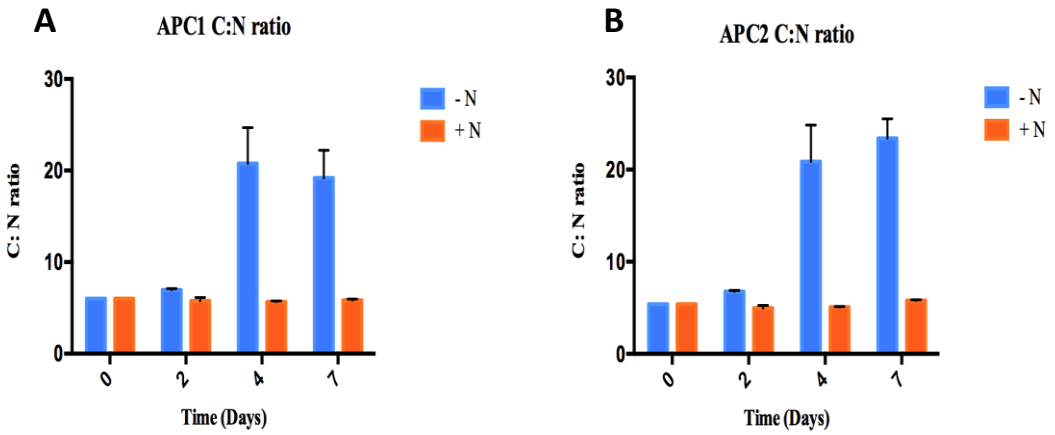

Figure 3.9: C:N ratio in strain APC1 (A,) and APC2 (B,) grown in low nitrogen medium (blue) and high nitrogen medium (orange). Data shown as average ± S.D. (n=3).

On the base of the variation in concentration of the dissolved nutrients in the medium (Fig. 3.7), I have calculated the nutrient uptake rates for both strains. Calculations were made dividing the variation of concentration of each nutrient in the medium by the variation of cell density in the same time interval. The nutrient uptake rates were calculated during the exponential growth phase (from day 0 to day 2, i.e. two days), when cells showed the maximum growth rates. The applied formula was:

$$\text{Nutrient uptake rate} = \left(\frac{C2 - C0}{(n_2 - n_0)}\right)/2$$

where c_2 and c_0 were the concentration of nutrients at day 2 and day 0, respectively, and n_2 and n_0 was the total cell number per litre at day 2 and day 0, respectively.

The uptake rates of major nutrients were not significantly different between treatment and control during the exponential growth phase due to the high variability between replicates of each condition. During the exponential growth phase, cells of APC2 took up three times more silica than APC1 when grown in nitrogen-depleted medium. This may be explained by the fact that in this strain spore formation started already in the second day and it may have stimulated a higher uptake rate. The uptake of phosphate was considerably higher in both strains grown in control condition as compared to the ones grown in the nitrogen depleted medium even tough not statistically different, as assessed by t-test (Fig. 3.10 E). The higher uptake in full strength medium can be explained by the luxury phosphorus uptake of cells.

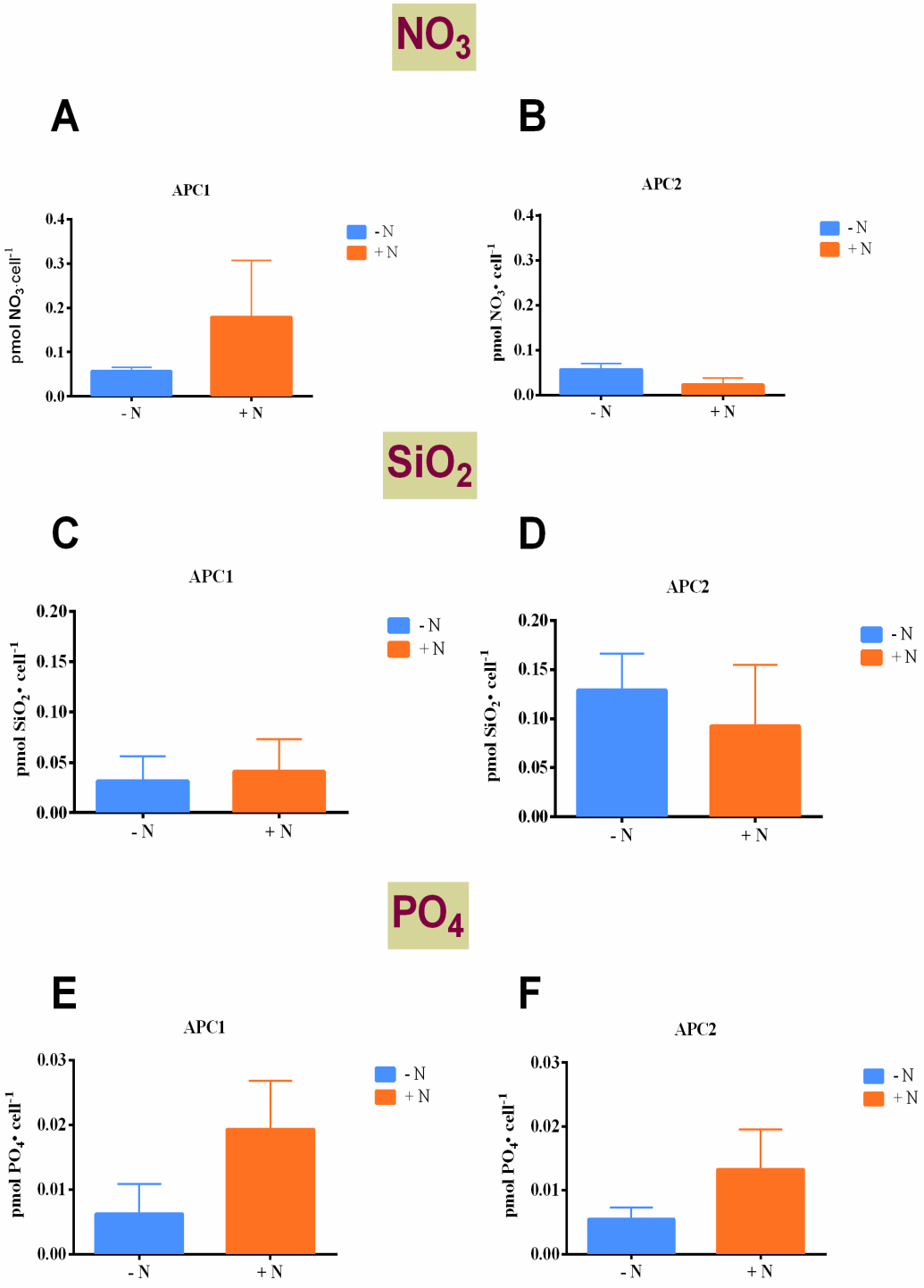

Figure 3.10: Nitrogen (A, B) silicate (C, D) and phosphate (E, F) uptake rate per day, during the exponential growth phase, in strains APC1 and APC2 (right) grown in depleted (blue) and full strength (orange) medium. Data shown as average ± S.D. (n=3).

Experiment 2: cell density as a factor for the induction of spore formation

One unexpected result of Experiment 1 was that spore formation was detected also in control conditions when cell concentration was relatively high (> 10^5 cells ml^{-1}), but the concentration of nitrogen and the other nutrients was not at all limiting. I thus planned to measure spore formation using a semi-continuous culture set up that allows keeping nutrient concentration within a narrow range of variation. I planned to test three cell concentrations where treatment condition was the culture medium deprived of nitrogen source (-N) and the controls the full-strength medium (+N). Based on the results of Experiment 1, I formulated the following hypotheses (Table 3.2): i) if nitrogen depletion is an environmental factor that induces the formation of spores, I expect to find them independently of cell density; ii) if cell density plays also a role in inducing spore formation, they should be recorded only in cultures kept at high-density in full-strength medium or, possibly, also at medium cell density but with lower percentages.

Table 3.3: Hypotheses at the base of experiment #2.

Cell density	**-N**	**+N**
Low	Yes	No
Medium	Yes	No?
High	Yes	Yes

The results of Experiment 2 are shown in Figures 3.11, 3.12 and 3.13. In control conditions, the dilution of the cultures every second day with fresh medium (+N) allowed them to grow with rather similar average growth rates, comprised between 1.9 and 1.2 day^{-1} (Fig. 3.11; Table 3.4), independently from cell concentration.

In the treatments with -N medium, lower growth rates were recorded in high- and medium-density cultures, which stopped to grow after one (high density) or two transfers (medium density) (Fig. 3.11). Growth rates of these cultures were significantly lower, compared with all other conditions, with average values of $0.9 \cdot day^{-1}$ after the first dilution for high cell density and even negative values ($-0.5 \cdot day^{-1}$) on day 4 after the second dilution for medium cell density (Table.3.4). The cultures at low cell density

maintained instead average growth rates comprised between 1.7 and 1.2 day^{-1} for the three subsequent transfers.

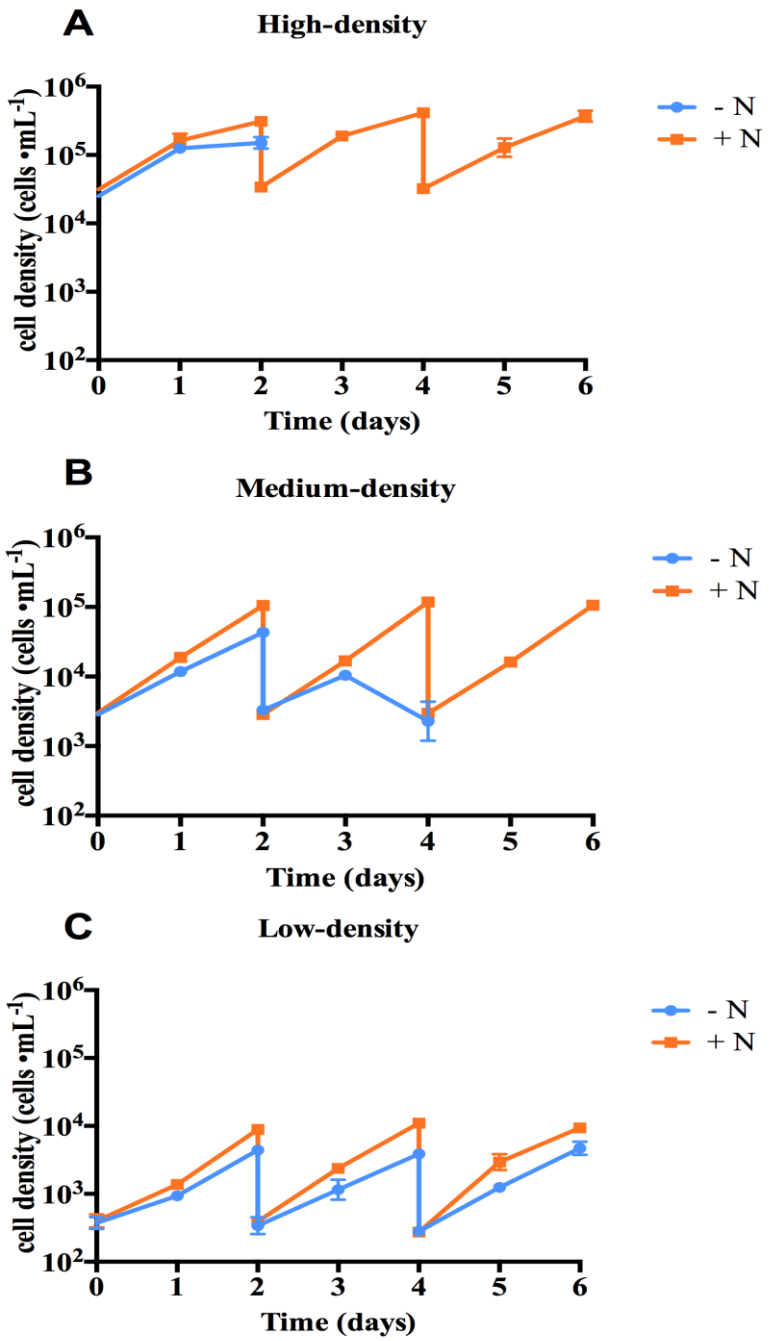

Figure 3.11: Total cell concentration (vegetative cells and spores) of strain APC12 in semi-continuous growth with full strength medium (orange) and medium depleted in nitrogen (blue), at three different cell densities (high, A; medium, B; low, C). Data represent average values ± S.D. (n=3); the error bars is not visible in most time points because it was lower than the symbol.

The pH of the cultures grown at high density in '+N' medium was measured every second day, before diluting the cultures, and it was comprised between 8.39 on day 0 and 8.62 on day 4 (Table 3.5).

Table 3.4: Growth rates (specific absolute growth rate· (day^{-1}) estimated over the time interval between two subsequent dilutions (two days) for each cell density and media treatment. Values shown as average ± S.D. (n=3). * Data statistically different to all other conditions ($P<0.005$).

Day	-N			+N		
	High-density	**Medium-density**	**Low-density**	**High-density**	**Medium-density**	**Low-density**
0-2	0.9 ± 0.1*	1.4 ± 0.1	1.2 ± 0. 2	1.2 ± 0.2	1.8 ± 0.1	1.6 ± 0.2
2-4		-0.5 ±1.0*	1.2 ± 0.1	1.3 ± 0.1	1.9 ± 0.1	1.7 ± 0.1
4-6			1.4 ± 0.1	1.2 ± 0.1	1.8 ± 0.1	1.8 ± 0.1

Table 3.5: pH values at different time points in the cultures grown at high density in '+N' medium. Values shown as average ± S.D. (n=3).

Day	pH
0	8.39 ± 0.01
2	8.62 ± 0.01
4	8.49 ± 0.02
6	8.50 ±0.02

In the cultures incubated with nitrogen depleted medium, spore formation was detected with markedly different percentages amongst the three cell density treatments. In high-density cultures, 64 % of cells became spores already at the end of the first dilution (Fig. 3.12 A, 3.13 A). Cultures at intermediate density showed higher variability between replicates and an average 86% of the cells were spores after the second dilution (Fig. 3.12 C, 3.13 C). The experiment at low cell density could be conducted for three consecutive dilutions and only few spores were detected (Fig. 3.12 E, 3.13 E).

In the experiments carried out in nutrient replete "+N" medium, spores were detected in all dilution steps only in high-density cultures, where average percentages were comprised between 2% and 9% before diluting the cultures (Fig. 3.12 B and 3.13 B), suggesting that cell density may play a role in inducing the formation of spores. Spores were detected at much lower percentages as compared to what observed in the treatments without nitrogen and their percentages slightly increased in subsequent dilutions (Fig.3.13). We have to consider that when diluting cultures a fraction of spores was eliminated, but new spores were produced in the two-days intervals after each dilution. In the medium- and low-density treatments few spores were found until the end of experiment, with percentages lower than 1% (Fig 3.12 B,C; Fig. 3.13 C, F).

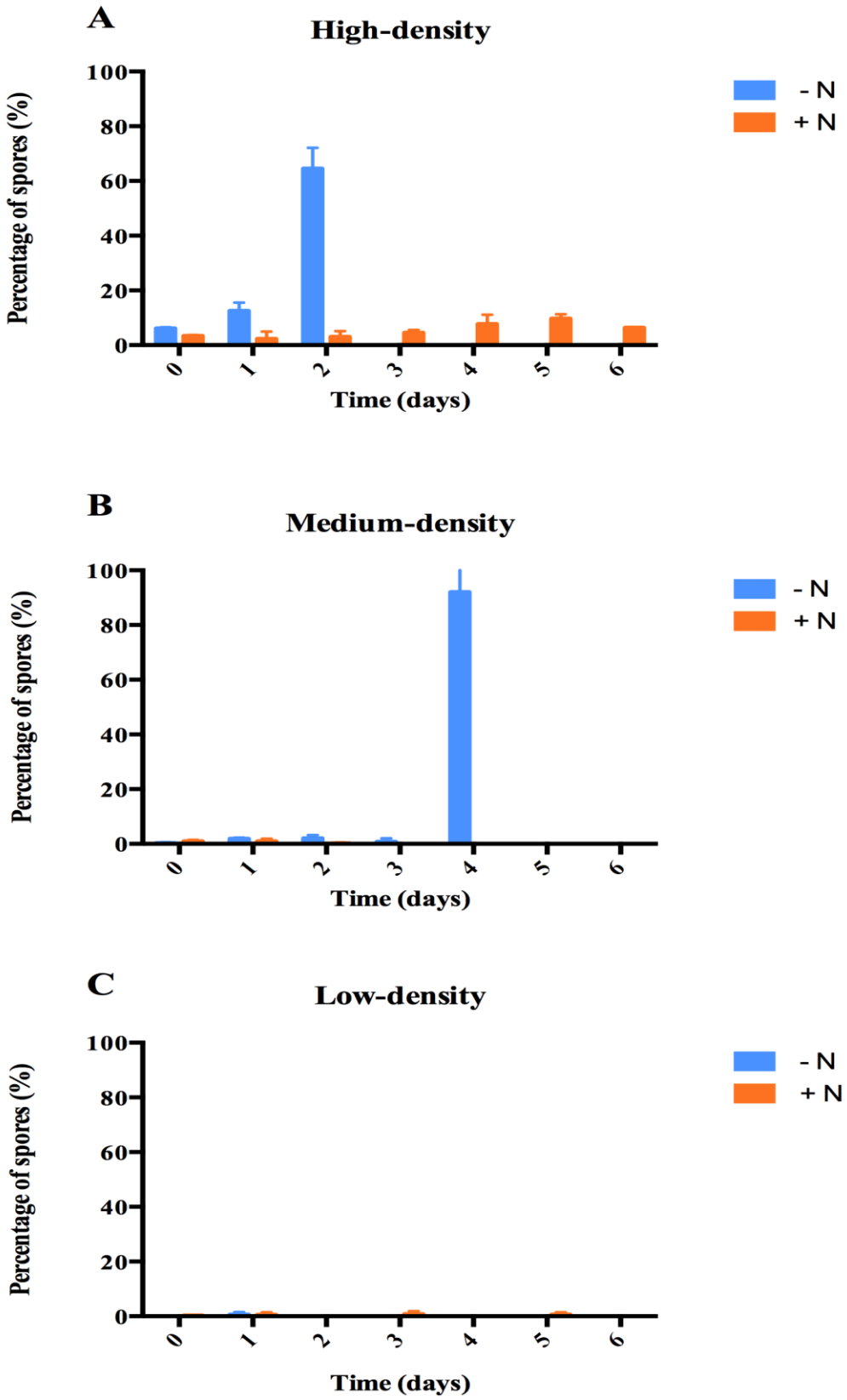

Figure 3.12: Spore percentage of strain APC12 in semi-continuous growth with full strength medium (orange) and medium depleted in nitrogen (blue), at three different cell densities (high, A; medium, B; low, C). Data represent average values ± S.D. (n=3).

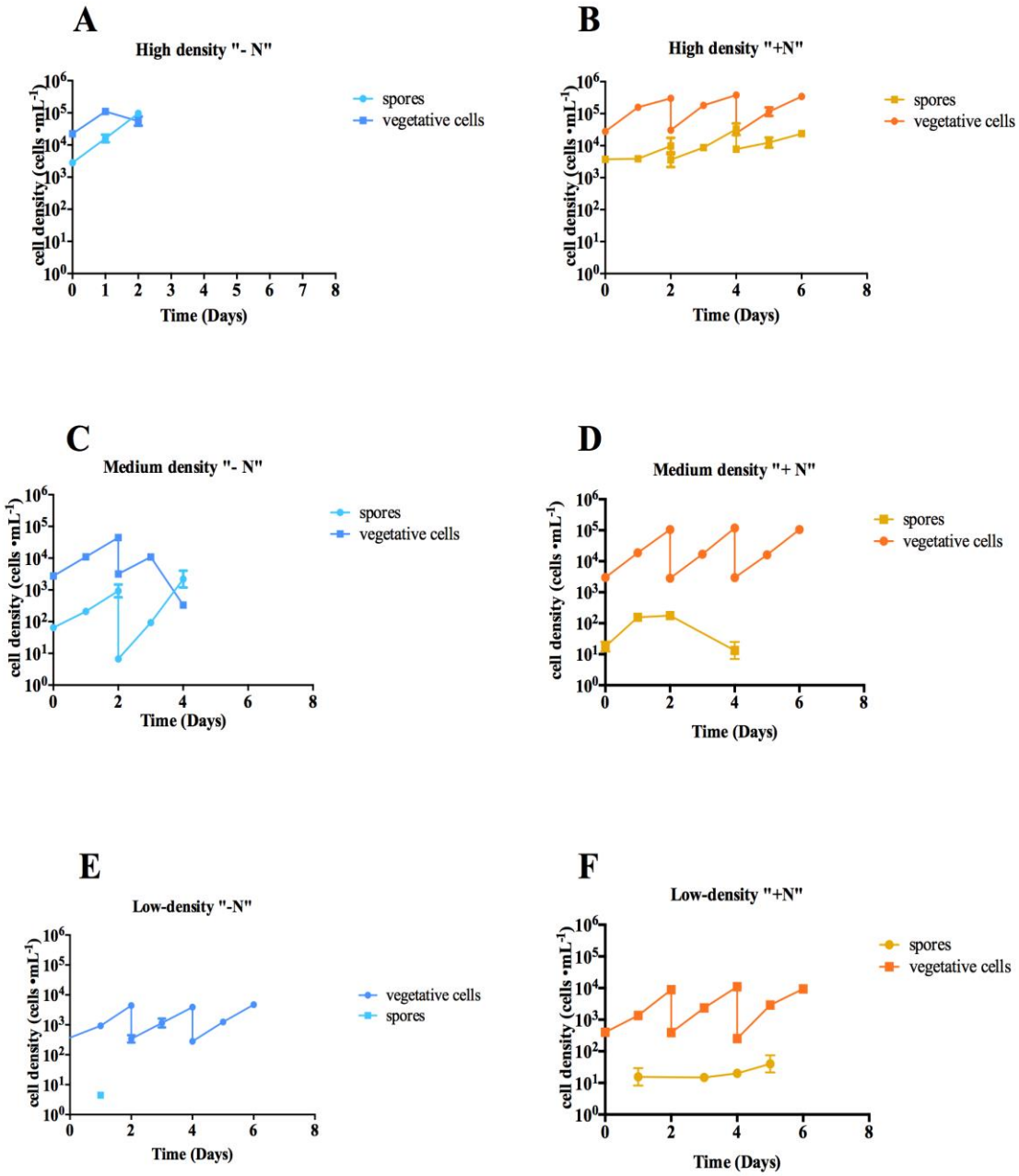

Figure 3.13: Growth curves of high (A, B) medium (C, D) and low (E, F) density in low nitrogen medium (A, C, E; blue) and in high nitrogen medium (B, D, F; orange). Data shown as average ± S.D. (n=3). Note that in panels D and F values equal to zero are missing.

Experiment 3: spore formation in high cell density conditioned medium

The results of Experiment 2 showed that, over the short 2-days intervals between subsequent dilutions, spores were constantly produced only at high cell concentration. This suggests that cell density may play a role in the induction of spore formation. To further test this hypothesis, I performed Experiment 3 in which low cell concentration of strain APC12 was inoculated in culture medium conditioned by high cell concentration. If this medium contains a chemical factor that induces the formation of spores, it should be active also in a culture at low cell concentration.

In Fig. 3.14 it is represented the total concentration of cells and spores measured in Experiment 3 (blue line) and in Experiment 2 (red line) carried out at low cell density and with nutrient-replete medium. Growth curves were similar in the second and third dilution steps but not in the first growth interval (between day 0 and day 2) where cells grown in high-cell-density conditioned medium experienced a lag phase. In Experiment 3 the total number of spores and their percentage was low, but a slight increase was observed during the first, second and fourth dilution interval, but not in the third one, when only a few spores were recorded (Fig. 3.15). The percentages of spores in conditioned medium was significantly different from that obtained in Exp 2 at low density in +N ($p= 0.01$) and –N ($p=0.0002$)

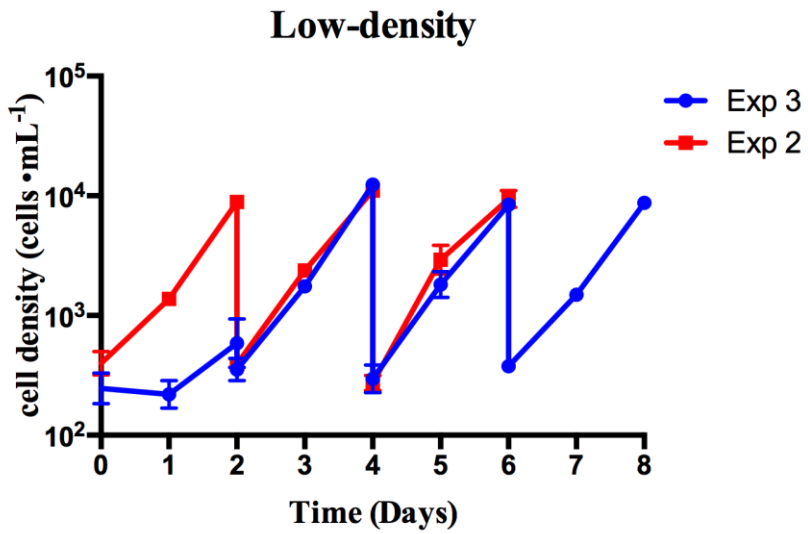

Figure 3.14: Total cell concentration (vegetative cells and spores) of strain APC12 in semi-continuous growth, at low cell density with full strength medium in Experiment 2 (red) and with the high-cell-concentration conditioned medium in Experiment 3 (blue). Data represent average values ± S.D. (n=3).

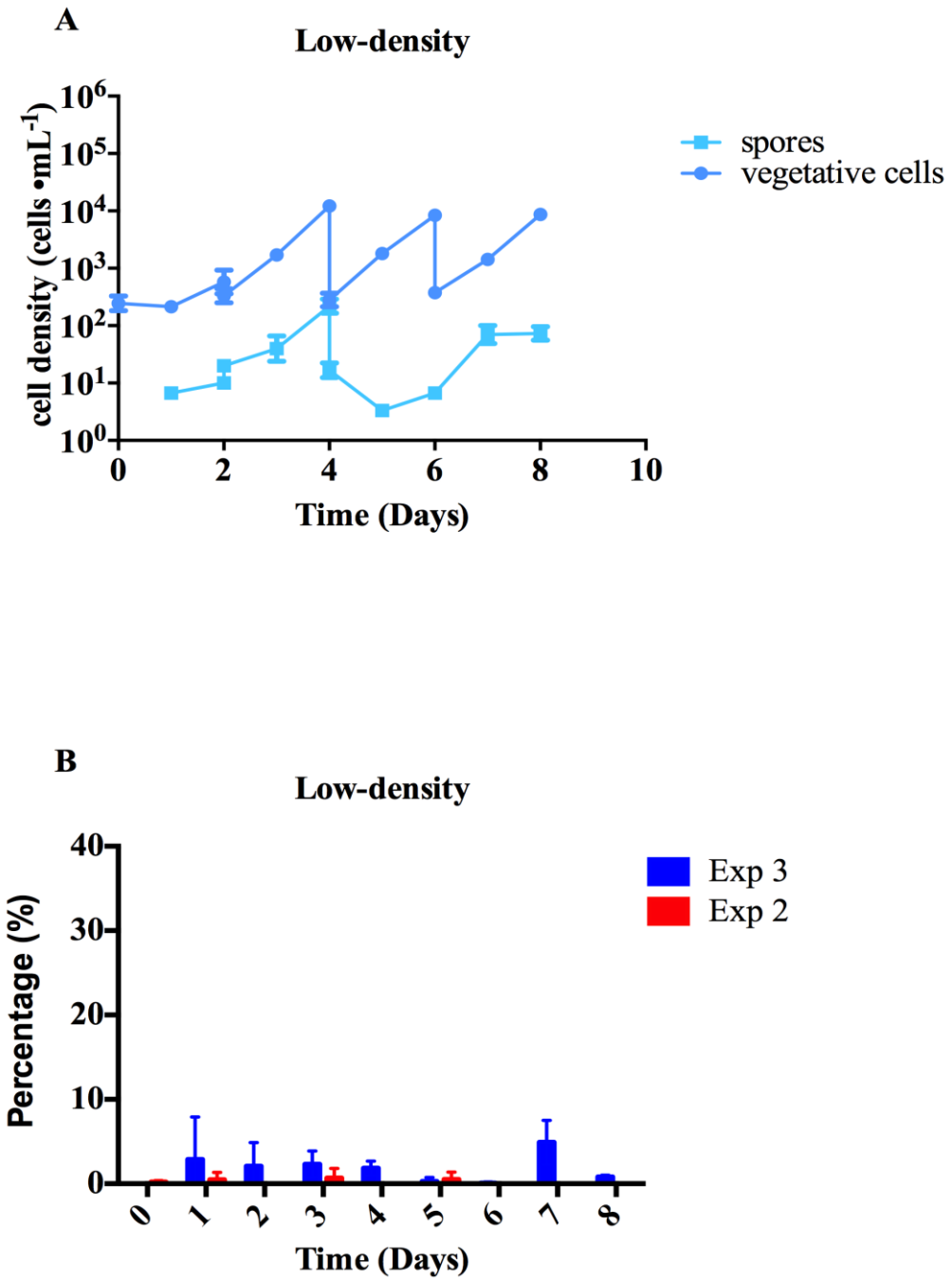

Figure 3.15: Concentration of vegetative cells and spores in Experiment 3 where cultures were inoculated in high-cell-density conditioned medium (A). Percentage of spores in Experiment 3 (blue) and in Experiment 2 at low cell density with full strength medium (red). Data represent average values ± S.D. (n=3).). Note that in panel A equal to zero are missing.

Experiment 4a and 4b: short-term experiment with high-cell-density conditioned medium

The results of Experiment 3 provided some support for the presence of a factor related to cell density that could induce spore formation. However, few spores were produced and their number and percentage was variable in subsequent dilutions. With the hypothesis that the chemical cue could be degraded with time, I planned to run short term experiments. I also tested the hypothesis that spore formation could be induced by a cue deriving from senescent/dying cells. To test this hypothesis, besides using a filtered high-cell-density medium, I sonicated the high-cell-density culture to break the cells and induce the possible release of an active chemical. In Experiment 4b, I have added two additional control conditions in which nutrient were added to both the filtered and sonicated conditioned culture medium; this should completely rule out any effect of nutrient limitation.

In Experiment 4a, total cell concentration increased in control conditions and when using the filtered medium, although with lower growth rate. Total cell concentration instead decreased when using the sonicated medium (Fig. 3.16 A). Spores were not produced in the control (Fig. 3.16 B, C), while they were produced when strain APC12 was inoculated in filtered conditioned medium, reaching concentration of 157 ± 15 cells·mL^{-1}on day 2 (Fig. 3.16 D). In the set-up with the sonicated medium the concentration of alive cells dramatically decreased already on day 1 and spores were produced (Fig. 3.16 E). Spore percentage was considerably significantly high in both treatments when compared to control condition ($p=0.02$ filtered, $p=0.007$ sonicated) (Fig. 3.16 B); in the case of sonicated medium one should consider that the number of vegetative cells was extremely low in this set up (Fig. 3.16 E).

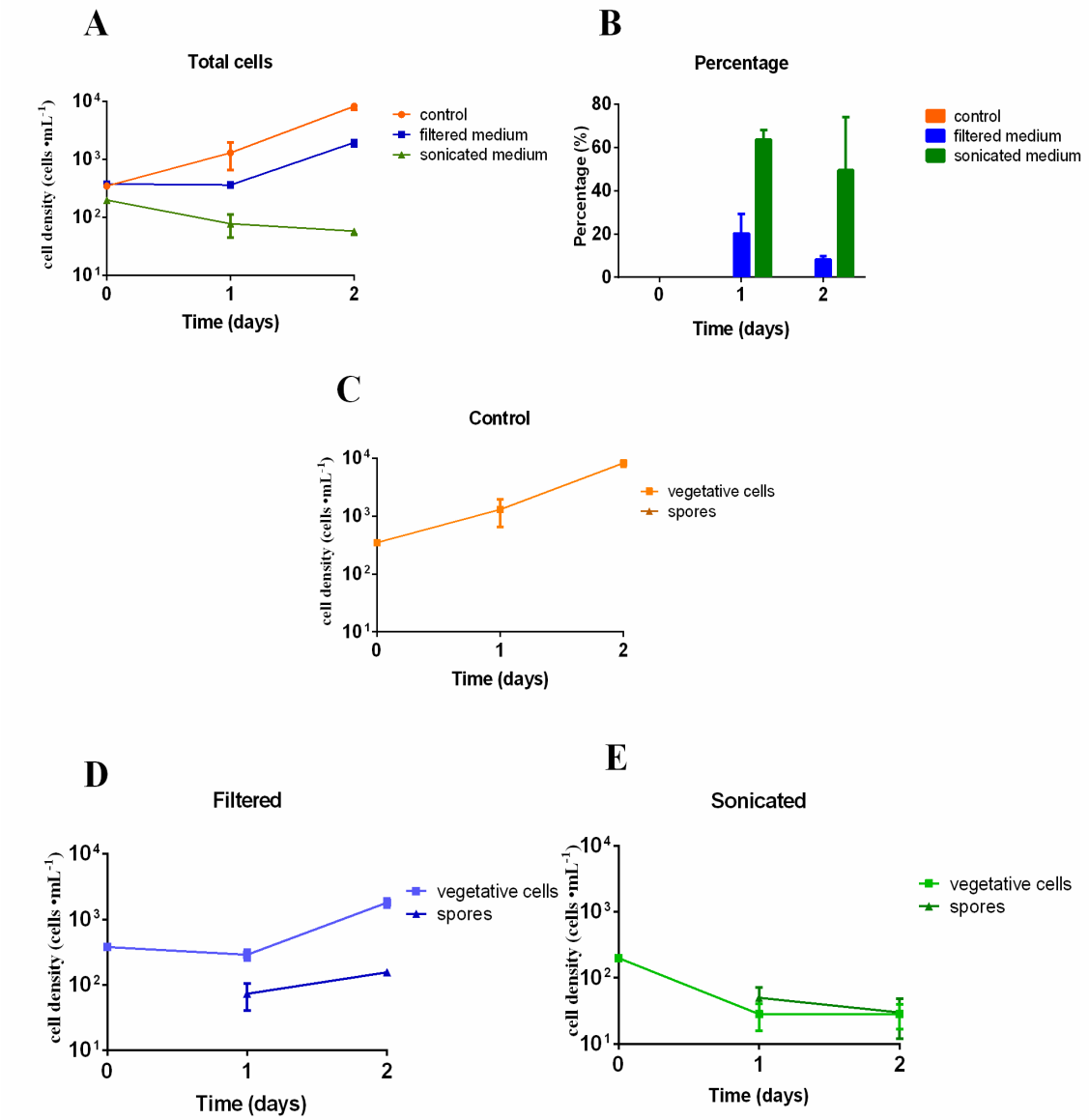

Figure 3.16: Results of Experiment 4a in which strain APC12 was inoculated in high-cell-density conditioned medium obtained by filtration (filtered medium) and by sonication and filtration (sonicated medium) and in the control (full strength f/2 medium). Total cell concentration (A), percentage of spore (B) in the treatments and control, concentration of vegetative cells and spores in control (C), filtered medium (D) and sonicated medium (E). Data are shown as average ± S.D. (N=3).

Experiment 4b, besides including the two additional controls with the addition of nutrients, was started with a higher inoculum of strain APC12 (1,000 cells mL^{-1}). The total cell number increased in the control already at day1 (Fig. 3.17 A), it remained constant on day 1 and increased only on day 2 in the set up with filtered conditioned medium, and remained almost constant in the sonicated conditioned medium. Spores were not produced in the control (Fig 3.17 C). Spores were detected on day1 – average concentration around 100 spores mL^{-1} - in all the experimental set ups with both filtered and sonicated medium (Fig. 3.17, D filtered, E filtered+Nut., F sonicated, G sonicated + Nut). Spore concentration increased on day 2 only when using filtered medium, reaching average concentration of 257± 146 cells·mL^{-1} in the filtered medium and of 730 ± 135 cell·mL^{-1} in the filtered medium amended with nutrients (Fig. 3.17 D and E), which corresponded to average percentages of 9% ± 3 and 18% ±1, respectively (Fig. 3.17 B). In the sonicated medium spore concentration did not change significantly on day2 (Fig. 3.17 F and G), and average percentages were 12% ±1 and 8% ± 1 in the set ups without and with amended nutrients, respectively (Fig. 3.17 B).

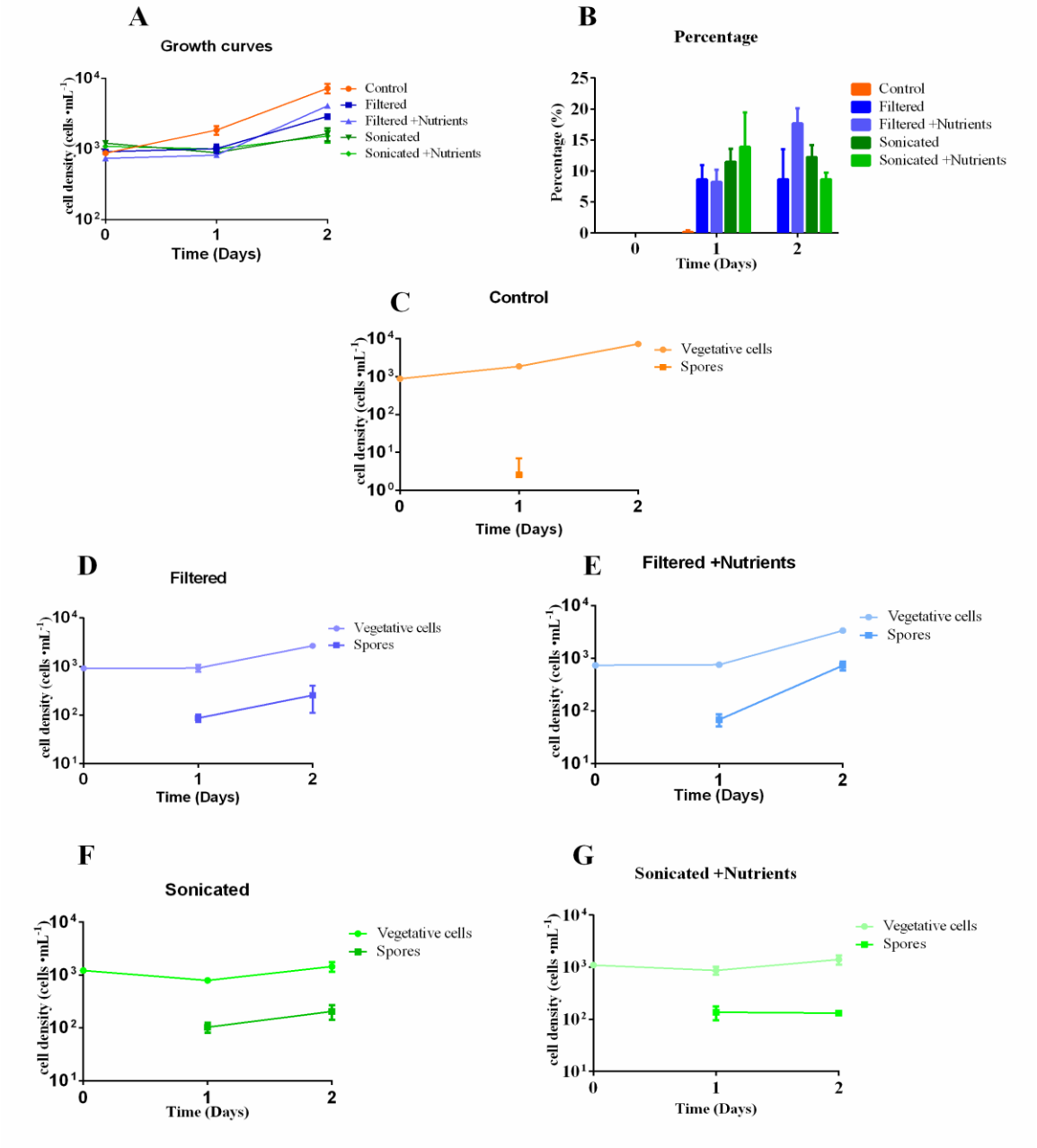

Figure 3.17: Results of Experiment 4b in which strain APC12 was inoculated in high-cell-density conditioned medium obtained by filtration (filtered medium), by filtration with the addition of nutrients (filtered medium+ nutr.), by sonication and filtration (sonicated medium), by sonication and filtration with the addition of nutrients (sonicated medium+ Nutr.) and in the control (full strength f/2 medium). Total cell concentration (A), percentage of spore formation in the treatments and control (B), concentration of vegetative cells and spores in control (C), filtered medium (D), filtered medium + Nutr. (E), sonicated medium (F), sonicated medium + nutr (G).Data are shown as average ± S.D. (N=3).

Discussion

The results of the experiments illustrated in this chapter i) confirmed that nitrogen limitation is a strong trigger of spore formation in *C. socialis* (Experiment 1), ii) showed that spores were formed, although at low percentages also in nutrient-rich control conditions (Experiment 1), iii) confirmed this finding when testing different cell concentrations with a semi-continuous experimental set up (Experiment 2), iv) provided evidence that the growth medium conditioned by high density cultures is effective in inducing spore formation as compared to the control growing in normal full strength medium (Experiments 3 and 4), and v) showed that, when using a conditioned growth medium in which cells were previously damaged by sonication, cell growth was affected (Experiment 3 and 4).

Nitrogen-limitation as a factor inducing spore formation

The fact that depriving or limiting nitrogen sources in the cultures was an effective way to induce the formation of resting spores became evident since the first studies carried out in controlled conditions in the laboratory (e.g (French & Hargraves, 1980)). Nevertheless, most of these studies did not include a complete experimental set up and, when designing Experiment 1, I considered all relevant parameters such as external nutrients, internal pools of carbon and nitrogen in both control and treatment conditions. I wanted to have a reliable experimental set up for the transcriptomic experiment illustrated in Chapter 5.

Spores started to be produced in the treatment (-N) when nitrate was consumed. The internal pool of N and C became unbalanced in the treatment as compared to the control conditions after 4 days from the inoculum. The ratio of C:N content in exponentially growing cultures grown in nutrient replete conditions should be close to the Redfield ratio, i.e. around 6.6, although a certain level of variation due to clonal diversity is expected (Geider & La Roche, 2002). The C:N ratio was relatively constant, around 5.8 in strain APC1 and 5.3 in APC2, at all sampling points in the full strength medium, while it became much higher (ca. 20 ± 3.3 in APC1 and 22 ± 3.2 in APC2) in the treatment when the cultures were dominated by spores. These results confirmed observations by Kuwata *et al.* (1993) who estimated an increase of 4 times in nitrogen-limited cultures of *C. pseudocurvisetus* that contained extremely high percentages of spores. The increase of C:N ratio was due to an accumulation of carbon that is used for

storage of carbohydrates and neutral lipids.

The possible role of density in inducing spore formation

The most intriguing question raised by the result of Experiment 1 was to understand what triggers spore formation when nutrients are not limiting. Evidence for spores formed in nutrient replete conditions was provided by other studies carried out in the laboratory (e.g. (Doucette & Fryxell, 1983)for *Thalassiosira weissflogii*; (Oku & Kamatani, 1995) for *Chaetoceros pseudocurvisetus*) and also by studies carried out in the natural environment where phytoplankton populations were dominated by *Chaetoceros* species (e.g., (Garrison, 1981; Pitcher, 1986). One hypothesis is that spores in these conditions are formed as an effect of high cell density. I tested this hypothesis testing cultures at three cell concentrations (differing one order of magnitude) and applying a semi-continuous set up (Experiment 2). The semi-continuous growth set up, with dilution steps every two days, offers the advantage of keeping the cultures within a rather constant condition and of avoiding the large changes in the external or internal nutrient pools and the possible accumulation of waste products or secondary metabolites that occur in a batch culture. The results of Experiment 2 confirmed my hypotheses. In the treatment with full strength medium, an average 5% of cells turned into spores within all dilution steps only in the high-density cultures. At the same time, Experiment 2 further confirmed the role of nitrogen limitation as a factor that can induce massive spore formation in laboratory experiments. When high- and medium-density cultures were diluted with nitrogen-deprived medium, a large percentage of cells turned into spores within the first dilution steps. In the experiment carried out with low cell concentration almost no spores were detected, probably because the very low cell concentrations could not consume the nitrogen present in the inoculum volume.

I planned to test nutrient concentration in Experiment 2 as well but, unfortunately, due to a de-freezing problem, I have lost the samples. I tested that nutrients were not limiting in the treatments (dilutions with full strength medium) using the average data on daily assimilation rates obtained in Experiment 1 (Fig. 3.18) to obtain a conservative estimate of the maximum nutrient uptake of cells in exponential growth. In this way I could estimate the amount of silicates, phosphates and nitrates consumed over the dilution interval (two days) in the experiments carried out at different cell densities. In Fig. 3.18 is represented the estimated concentration of the three nutrients in the medium at the end of each dilution interval.

These calculations showed that the concentration of nitrates in high-density cultures diluted with '-N' medium dropped to zero at day 4, in medium–density cultures on day 6 and never became limiting in low-density cultures (Fig. 3.18 A blue lines). This scenario matched what happened in nitrogen-depleted medium in Experiment 1. On the contrary, all cultures grown in "+N" medium never experienced nutrient limitation (Fig. 3.18 B, C, D orange lines.). The fact that spores were observed again in high-density cultures not limited by nitrogen supported the conclusion that cell density may represent an additional factor in inducing the formation of spores in *C. socialis.*

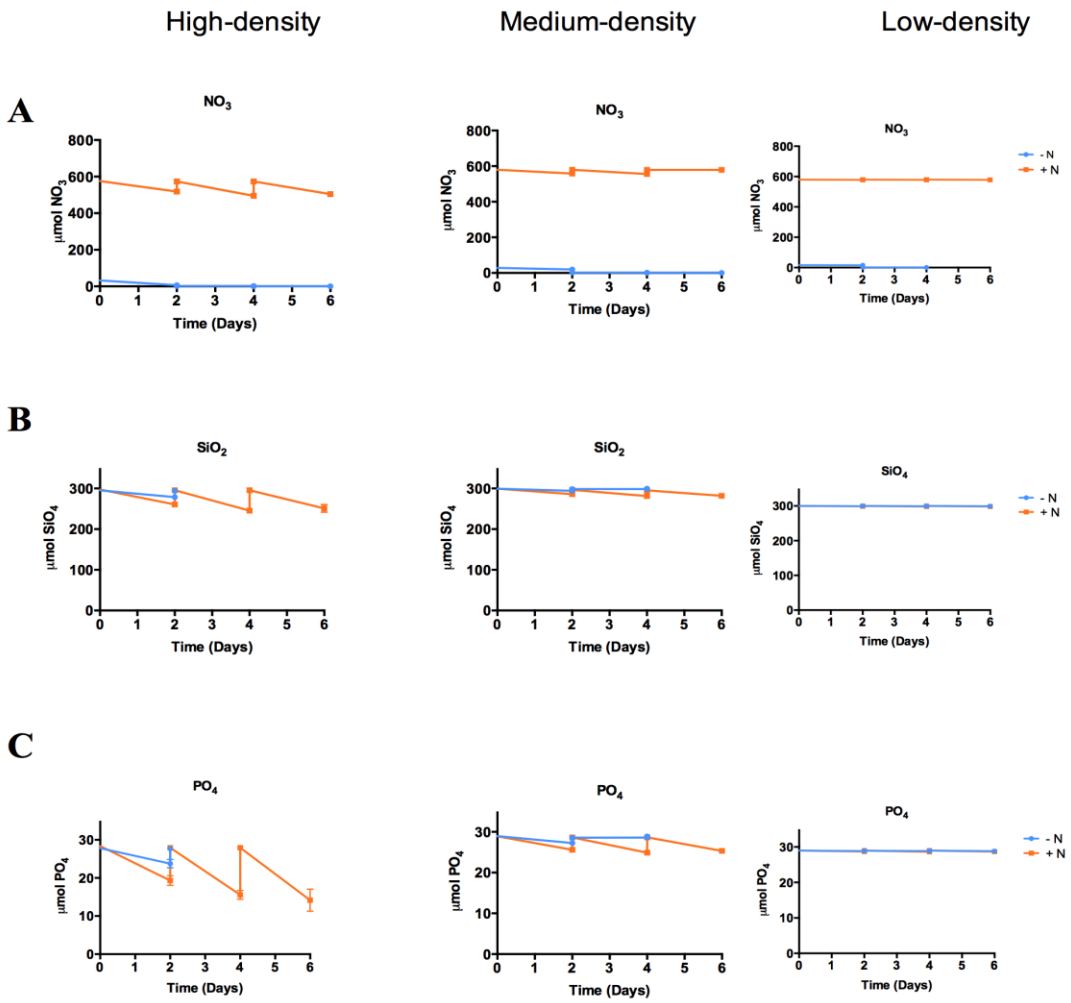

Fig 3.18: Estimates of nitrates (A), phosphates (B) and silicates (C) concentration in the medium of cultures growth at the three cell densities in nitrogen depleted (blue) and full strength medium (orange). Data represent average values ± S.D. (n=3).

Also the comparison between the growth rates within the dilution intervals (2 days) of the cultures grown in full medium (Table 3.3) showed very similar values, which were in turn similar to the values recorded during the exponential phase in Experiment 1. All these considerations support the fact that high-density cultures, where spores were formed in Experiment 2, were not limited by nutrients.

One factor that can change with cell density is pH. The formation of spores in control conditions, i.e. in cultures grown with full-strength f/2 medium was reported by Oku & Kamatani, (1995), who hypothesized that an increase in pH due to the high-density of cultures could have explained their results. In fact it is known that variation in this parameter can have considerable effects on algal growth (Hansen, 2002). When the change in pH is relatively low, it can cause variations in the chemistry of seawater, for example in the availability of trace metals and carbon dioxide species that in turn affects phytoplankton growth. Instead when the pH increase is extreme, it can induce physiological damages due to high intracellular concentration of reactive species and then the death of the culture. It has been shown that during a natural bloom of the dinoflagellate *Peridinium gatunense* pH arose at values higher than 9 resulting in CO_2 limitation (Vardi *et al.,* 1999). This stimulated the formation of reactive oxygen species (ROS) and consequent cell death. The pH values recorded in the experiments carried out at high cell density spanned from 8.39 (day 0) to8.62 and were higher than those usually recorded in seawater. These values were much lower than those reported for the dinoflagellate. However, I cannot exclude that high pH values might have contributed to induced stress conditions responsible for spore formation.

Cell density can play a role in regulating cell-cell communication in several organisms, but this parameter has been investigated mostly in bacteria (Miller & Bassler, 2001). Nevertheless, there are examples also among unicellular eukaryotes where transitions between different life stages may be related to cell density. An example is the chrysophycean *Synura petersenii* where the formation of cysts seemed to be induced in high density cultures (Sandgren & Flanagin, 1986). Another example is sexual reproduction of heterothallic pennate diatoms, where the formation of gametes and their conjugation occurs only when a threshold cell concentration is reached (Scalco *et al.*, 2014). However, cell density is only the first evidence and an indication that cells are capable of producing and sensing specific chemical compounds that act as signals. Information on the molecular mechanisms in action has been gained for bacteria, but little is known for unicellular microalgae. In heterothallic diatoms it has been shown that the requirement for cell density thresholds is due to the production of sexual pheromones that signal the presence of opposite mating types and mediate the attraction of gametangia (Gillard *et al.*, 2013; Basu *et al.*, 2017).

Spore formation mediated by a chemical signal?

The results obtained in Experiment 3 and especially those obtained in Experiments 4a and 4b, seem to support the presence of a chemical signal related to high cell concentration that induces the formation of spores. In fact, the use of a culture medium conditioned by high cell concentration, but not limited by nutrients, induced the formation of spores. Here we should distinguish between the results obtained with filtered high-cell-density medium and those obtained with the same medium in which cells were sonicated – and thus damaged – before the filtration step. The first medium induced the formation of spores, while the second also negatively affected cell viability or growth capability.

There are several examples of chemically-mediated communication in unicellular organisms where specific molecules affect the physiology of conspecific cells. In diatoms intra- and inter-specific cellular communication has been been related to the production of compounds belonging the large family of oxylipins. Their occurrence in photoautotrophs is widespread, in marine and freshwater environments, indicating their important ecological role (Ianora *et al.*, 2015). The major class of oxylipins produced by diatoms are polyunsaturated aldehydes (PUAs) and non-volatile oxylipins (NVOs) that are synthesized during stationary growth phase thanks to the oxygenation of fatty acids. The PUAs were implicated in the same mechanisms detected in plants, i.e. antibacterial activity (Ribalet *et al.*, 2008) and defence from grazing (Ianora *et al.*, 2004; Ianora *et al.*, 2011). The latter implies that the PUA produced by diatoms have teratogenic effects of copepod nauplii, which are the major grazers of diatoms. PUA were also implicated in bloom termination (Ribalet *et al.*, 2014) allelopathy (Casotti *et al.*, 2005) and cell-to-to cell communication (Vardi *et al.*, 2006). In *Phaeodactylum tricornutum* and *Thalassiosira weissflogii* the exposure to PUAs had a double effect: cells died when exposed directly to a high concentration of PUAs, but acclimation mechanisms were induced when cells were pre-treated with sub-lethal doses allowing the population to increase its survival (Vardi *et al.*, 2006). Less is known about the role of NVOs; it has been assessed their negative effect on copepods reproduction, the same effect already known for PUAs (Ianora *et al.*, 2015). Interestingly, the production of non-volatile oxylipins has been reported also in *C. socialis* (Fontana *et al.*, 2007) although their role has not been elucidated.

The results of the experiments in which the high-density culture was sonicated before filtration to produce the conditioned medium (Experiments 4a and 4b), seem to

support the hypothesis that an oxylipin compound may be released by senescent or damaged cells and negatively impact *C. socialis* cells, besides inducing the formation of spores. However, cells were apparently not harmed – and even higher abundances of spores were produced - when inoculating cultures in filtered conditioned medium in which cells were not damaged. This suggests that a different compound may be involved that can signal high density and induce the shift from resting cells to spores.

Conclusion

While nitrogen-deprived media induces the formation of spores in the laboratory, there is limited evidence that this mechanism operates also in the natural environment. Spore formation in various *Chaetoceros* species has been found when external nutrients were not limiting (Garrison, 1981; Pitcher, 1986). A massive production of spores of *C. cf. affinis* was recorded in sediment traps deployed in the north Atlantic, but inorganic nitrogen concentration was always above 8 µM in surface waters (Rynearson *et al.*, 2013). *Chaetoceros socialis* can reach considerable cell abundances at the LTER-MC station in the Gulf of Naples (Ribera d'Alcalà *et al.,* 2004) and spores are at times recorded in the surface samples routinely examined on a weekly basis. High percentages of spores were recorded only on two occasions (2.11.2005 and 23.03.2007) but the major inorganic nutrient were not limiting on those occasions (Diana Sarno and Francesca Margiotta, pers. comm.). Nevertheless, spores of *C. socialis* are amongst the major contributors of spore assemblage at LTER-MC (Montresor *et al.*, 2013; Piredda *et al.*, 2017). It is thus reasonable to assume that spore formation is 'triggered' in the surface layer but actually is completed during the sinking process towards the deeper layers of the water column, as hypothesized also by Rynearson *et al.*, (2013).

The results presented in this chapter suggest that mechanisms related to high cell density can play a role in inducing the shift between vegetative cells to resting spores in *C. socialis.* The evidence was provided by short-term responses of spore production when using growth medium from cultures at high cell concentration. Results supporting the hypothesis were further confirmed by Experiment 4b in which an additional supply of nutrients was added, thus definitively ruling out any limiting nutrient. It should be also remembered that the conditioned medium was always obtained by cultures kept in semi-continuous, thus in good physiological state. Both scenarios, i.e. i) an effect of high cell concentration during the bloom or ii) an effect of senescent cells towards the end of the bloom occur in nature and the preliminary results obtained in this chapter should be further investigated to understand the nature of the chemical signal and the mechanisms involved.

Chapter 4

Effect of viral infection on spore formation

Introduction

Ecological role of virus-phytoplankton interactions

Despite studies on the effect of environmental factors (nutrients, temperature, light, and salinity) on the formation of resting stages in diatoms (see Introduction), little information is available on the effects of biotic interactions such as predation, competition and viral infection. Studies testing the relationships between resting stages and their predators, for example, were focused on the grazing rates of copepods fed with diatom vegetative cells, resting cells and spores and on the viability of spores after the passage through copepod gut (Kuwata & Tsuda, 2005). Copepods grazed preferentially on vegetative cells and the spores that were eaten could germinate, thus suggesting that they can also represent a defence stage towards grazing pressure. There are no studies on the possible role of viruses as cues for inducing formation of resting stages. This is probably due also to the lack of knowledge about the possible role that viruses play in the termination of diatom blooms.

Viruses are the most numerically abundant organisms with an estimated concentration of 10^7 viral particles per millilitre of surface seawater (Breitbart, 2012) and with a total biomass second only to the total biomass of prokaryotes (Suttle, 2005). Viruses can be subdivided in four categories on the base of the kind and organization of their nucleic acids: double and single-stranded DNA or double and single-stranded RNA viruses. It is generally accepted that in the marine environment the majority of viruses are double–stranded DNA (dsDNA) included in three families: Podoviridae, Myoviridae, and Siphoviridae (Wommack & Colwell 2000; Weinbauer 2004).

Viruses transform a quarter of the carbon fixed by the phytoplankton into dissolved organic matter trough the lysis of their host cells in a process known as “viral shunt” (Wilhelm & Suttle, 1999). It has been estimated that the carbon released at the global level by this process is up to 10^9 tons per day (Suttle, 2007).

Moreover, viruses shape the diversity and the community dynamics in different ways:

- Viruses kill only a part of the population (the sensitive individuals) and in this way

they create new niches and favour the growth of the virus-resistant species with the nutrients released by the species that are killed by viruses (Middelboe & Lyck, 2002).

- At least in prokaryotes, the mechanism by which viruses spread is density-dependent and follows the ecological rule "kill the winner" by which the winner is the most competitive and most abundant species (Winter *et al.*, 2010).
- Viruses change the host's metabolism interfering with its genes, i.e., activating or inhibiting expressions of specific genes.
- Viruses mediate horizontal gene transfer through different mechanisms, such as i) inducing the release in the environment of genetic material of the host which can thus be incorporated by other organisms (Jiang & Paul, 1995), ii) being directly responsible for the DNA transduction in host cells (Jiang & Paul, 1998) and iii) being responsible of the transfer of randomly selected genomic fragments through virus-like particles named Gene Transfer Agents, GTAs (Lang & Beatty, 2007).

Once inside the cell, viruses replicate themselves and are released in the environment through the breakage of the host cell in a 'lytic cycle'. Viruses can also form 'prophages', i.e. the viral genes that are inserted in the host genome can remain dormant and be inherited by the progeny following a 'lysogenic cycle'. In seawater the majority of viruses are proposed to be lytic even though a latent period as prophages inside the host may be present. At the moment, however, it is largely unknown what controls the switch from a lysogenic phase to a lytic one (Breitbart, 2012). In general, the induction of a lytic process occurs when the host reaches high abundance and high growth rates, whereas lysogeny seems to be more frequent during adverse environmental conditions (Paul, 2008).

This is in agreement with several observations made in the field, where the termination of blooms of different phytoplankton species (*Heterosigma akashiwo, Heterocapsa circularisquama, Phaeocystis globosa* and *Emiliania huxleyi*) due to a viral infection has been documented (Nagasaki *et al.*, 1994; Tarutani *et al.*, 2000; Tomaru *et al.*, 2004; Baudoux *et al.*, 2006).

The prymnesiophycean *Emiliania huxleyi* is the unicellular microalga for which there is most information on the mechanisms of viral infection, derived both from laboratory studies as well as investigations in the natural environment (Bratbak *et al.*, 1993, 1996;

Brussaard *et al.*, 1996; Jacquet *et al.*, 2002; Wilson *et al.*, 2002; Vardi *et al.*, 2012; Sharoni *et al.*, 2015).

Diatom viruses

In 2004 Nagasaki *et al.* discovered the first ssRNA infecting the diatom *Rhizosolenia setigera* followed one year later by the first marine single stranded DNA (ssDNA) virus in the bloom-forming diatom C*haetoceros salsugineum* (Nagasaki *et al.*, 2005).

Thereafter, eleven other viruses with icosahedral shape and small size (22 to 38 nm in diameter) were discovered and two new families were established: Bacillariodnaviridae and Bacillariornaviridae. In most cases they are species-specific viruses and were shown to infect species belonging to the genus *Chaetoceros*, including *C. socialis* (Tomaru *et al.*, 2009). The only exception is the CtenRNAV type II virus, isolated from *C. tenuissimus* and capable to infect also other diatom species, such as *C. socialis* and *C. setoenis* (Kimura and Tomaru, 2015).

In the papers characterising these viruses, the presence of spores was reported in cultures of *C. cf. gracilis*, *C. debilis*, *C. socialis* f. *radians* and *C. lorenzianus* (Bettarel *et al*. 2005, Tomaru *et al.*, 2008; Tomaru *et al.*, 2009; Tomaru *et al.*, 2011). The authors speculated about the possibility that spores where produced as a defence strategy against the infection but none of them tested this hypothesis.

The aim of this chapter is to elucidate the possible role of viruses in inducing spore formation in a diatom host population. If spores percentage increases during viral infection as compared to control conditions it can be hypothesized that sporulation may serve as a defence strategy to avoid or to limit viral infections in the population. This information has deep implications for our understanding of the mechanism of diatom sporulation, viral infection and the ecological impact.

Material and Methods

Algal and virus isolation and maintenance

Two strains of *Chaetoceros socialis* were used: APC12 and DA. The former has been isolated from sediments collected in the Gulf of Napoli and was genetically characterised (see Chapter 2), whereas the second has been provided by dr. Kay Bidle (Rutgers University, USA) together with the virus (CsfrRNAV) that is known to infect strain DA. This strain was isolated from surface seawater of Hiroshima Bay, Japan, in 2005 (Tomaru *et al.*, 2009). Also this strain has been genetically characterized following the protocol described in Chapter 2 and resulted to belong to *Chaetoceros socialis sensu stricto* (Gaonkar *et al.*, 2017)

Both *C. socialis* strains were acclimated for more than five generations to the same conditions (light, temparature and medium) used as control during the experiment. The experiments on viral infection were carried out using the same medium and environmental conditions used in the experiments illustrated in Chapter 3 as control (see Table 2.1 +N column for details) were used.

The virus CsfrRNAV, with an infection-specificity for *C. socialis*, belongs to Bacillariornaviridae and was isolated in Itsukaichi fishing port (Japan) in 2005 (Tomaru *et al.* 2009). It is a single- stranded RNA virus and its genome has been sequenced. The lysates were maintained at 4 °C in the dark until use during the experiment.

Experimental set-up

The same experimental set up was used in two experiments Exp#001 and Exp#002. Six 50 mL plastic flasks (Corning Inc., NY, USA) and six glass tubes were filled with 30 mL and 10 mL, respectively, of exponentially growing culture of strain DA containing 3,000 cells·mL^{-1}. The same cell concentration was used to prepare six plastic flasks and six glass tubes of the Neapolitan strain APC12. During the second experiment, an additional flask was prepared for this strain and was used for TEM (transmission electron microscopy) micrographs of an infected sample (see below). All bottles and tubes were incubated in a culture chamber with controlled environmental conditions (temperature 18 °C, irradiance 180 µmol m^{-2} sec^{-1}, photoperiod 12:12). On day 2, when cultures were in the middle of

exponential growth phase, three flasks and three tubes for each strain were infected with the viral lysate whereas the others were used as control. I used a ratio of 1:0.1 (v:v) between the algal culture and the original viral lysate to infect both strains as suggested by dr. Kay Bidle (personal communication) .

The growth of cultures was assessed daily at the same time measuring chlorophyll fluorescence with a Turner Designs fluorometer (model 10-005R. Turner Designs, INC. Sunnyvale, CA, USA). The concentration of cells and spores has been quantified daily as described in Chapter 3.

At the end of Exp#002, all infected cultures were filtered through a 0.22 Sterivex GV filter unit (Millipore) and stored at -80 °C. The filtrates were used for viral titration and to visualize viruses with a Transmission Electron Microscope.

Calibration to assess cell viability

During Exp#001 cells appeared stressed and damaged because of the viral infection; therefore calibration with a vital stain was performed to be able to discriminate between vital and dying cells. Samples of infected cells were collected at different time points and incubated with the nucleic acid staining dye SYTOX® Green (excitation, 504 nm; emission, 523 nm; Thermo Fisher Scientific) at a final concentration of 0.5 μM for 20-30 minutes in the dark. The live cells with intact plasma membranes cannot be penetrated by SYTOX® Green stain, but enters dead cells and stains the nucleus green (Roth *et al.*, 1997). In phytoplankton studies this stain is used mostly in flow cytometry allowing the discrimination of vital cells (Peperzak & Brussaard 2011); Since *C. socialis* is a chain-forming species the flow cytometer cannot not be used for this purpose and samples were counted using a Zeiss Axiophot microscope with epifluorescence illumination at 40x magnification. In optical field, cells were enumerated first using a blue filter (Blue 450 = BP 450-490; FT 510; LP 520) and then with transmitted light in order to avoid the bleaching of the fluorochrome. This stain was especially useful in the late phase of infection when the distinction between live and dead cells was not obvious.

Sample preparation for Transmission Electron Microscopy

Transmission Electron Microscopy was used to assess the presence of viruses inside cells and spores of strain APC12 and in the lysate produced at the end of the experiment. The culture was fixed with 2% glutaraldehyde overnight and concentrated by centrifugation at 4,000 rpm for 10 minutes. The pellet was then washed three times with the same medium used during the experiment and post-fixed with 1% osmium tetroxide in filtered seawater for 3 h. Samples were then washed three more times for 10 minutes and dehydrated in a graded ethanol series (30%, 50%, 70%, 90% and three times in 100%). Samples were maintained for 30 minutes in each percentage; dehydration was then continued with propylene oxide for 20 minutes. Samples were treated then with 3 mixtures of Epon 812: propylene oxide (1:2, 1:1 and 2:1) and finally embedded in Epon 812. The polymerization was made at 62 °C for 48 h and then ultra-thin sections were cut with a Laica Ultracut ultramicrotome. Sections were settled on grids (200 mesh) and stained with Ems uranyl acetate replacement stain for 30 minutes, washed ones with MilliQ: methanol (1:1) and twice with pure MilliQ. Dry samples were stained with 1% lead citrate and washed again three times with MilliQ. Several dried sections were examined with a Zeiss Leo 912 AB transmission electron microscope (Karl Zeiss, Oberkochen, Germany).

Direct TEM preparations were made with the viral lysate: chloroform (1:50 v:v) was added to 1.5 ml of the lysate and maintained for 10 minutes at 37 °C in the shaker. The solution was then centrifuged at 13,000 rpm for 20 minutes to eliminate the cellular debris. The resulting supernatant was then mixed with the same volume of a solution of Polyethylene glycol (PEG) 8000 20% (w:v) in NaCl 2.5 M and incubated overnight at 4°C. This solution was then centrifuged (13,000 rpm for 30 minutes) and the pellet was resuspended in 10 µL of SM solution. This suspension containing viruses was mounted on a Formvar-Carbon coated grid (200 mesh) for 30 seconds and the excess of solution dried with blotting paper. The sample was stained for 10 seconds with 10 µL of 2% phosphotungstic acid. After the removal of excess dye, the grid was dried under a chemical hood for 2 days and examined with transmitted electron microscopy (TEM) Zeiss LEO 912 AB (Zeiss, Oberkochen, Germany).

Viral genome extraction, primer design and preparation of the standard curve

Viral RNA was extracted from the following samples: 1) the lysate obtained from one replicate at the end of Exp#001 2) the original lysate used to infect the cultures and 3) the lysate obtained at the end of Exp#2 (triplicate samples of Exp#2).

1/50 (v:v) of chloroform was added to the de-frozen samples and maintained for 10 minutes in the shaker; then it was centrifuged for 20 minutes at 13,000 rpm. The supernatant containing the viral particles was transfer into a new Eppendorf tube. To avoid contamination of nucleic acids from host cells, 1 µg/mL RNAase and DNAase were added and incubated for 30 minutes at 37 °C. At this point, the same volume of polyethylene glycol (PEG) 8000 20% (w:v) in NaCl 2.5 M solution was added and incubated overnight at 4°C. The sample was centrifuged at 10,600 rpm for 30 minutes and the supernatant removed. The obtained pellet was re-suspended in 0.5 mL of TRIzol® Reagent (Thermo Fisher Scientific) for the extraction of genomic RNA. After 10 minutes in a thermo-shaker at 60 °C with glass beads, samples was centrifuged for 1 minute and the supernatant was transferred into a new Eppendorf vial. The samples, after the incubation at room temperature (RT) for 15 min with chloroform 1:5 (v:v), were then centrifuged for 15 minutes. Of the three-layer solution obtained, only the uppermost was transferred into a new Eppendorf tube with an equal volume of isopropanol and incubated 10 minutes at RT. This solution was then centrifuged for 10 minutes to allow the precipitation of RNA molecules. The pellet formed was washed with 1 mL of 75% ethanol that was removed after centrifugation for 10 minutes. The resulting RNA sample was further purified on Qiagen columns (74104, RNeasy Mini Kit) following the manufacturers' protocol and quantified with NanoDrop ND-1000 Spectrophotometer (Nanodrop Tecnologies Inc., Wilmington, USA). These samples were used to synthesize cDNA trough qScript™ XLT cDNA SuperMix (Quanta BioScience, Inc) following the manufacturers' protocol. The template obtained by Exp#001 was employed to check the primers quality with a PCR and to obtain the standard curves for the virus titration. Primer sequences (Table 4.1) were designed using the gene encoding non-structural polyprotein CSfrRV_gp1 available on the NCBI website (https://www.ncbi.nlm.nih.gov/gene/7559143) and the Prime3Plus version 2.4.2 (Untergasser *et al.*, 2012) as a reference for the quantification of viral abundance through qPCR (as described below).

PCR was performed using the following reagents: 0.4 µM of forward and reverse primers, 2 µL of template, 5x XtraWhite buffer solution (GeneSpin, Milano, Italy) a 0.2 mM of dNTPs, 1,12 U of XtraTaq Pol (GeneSpin, Milano, Italy) and water to a final volume of 20 µL. The thermal cycling conditions were: 2 min at 95°C followed by 35 cycles of 15 sec at 95°C and 30 sec at 58°C, 30 sec at 72 °C and 7min at 72°C.

A serial dilution of this reverse transcript sample was employed to construct the standard curve.

Table 4.1: Primer sequences used to prepare the standard curve and qPCR.

Primer	Target	Sequence (5'-3')
1: CSfrRV_gp1_F1	non-structural polyprotein (ID: 7559143, NCBI)	TCGACAAGAACCAAGCACAG
1: CSfrRV_gp1_R1	non-structural polyprotein (ID: 7559143, NCBI)	GTCCCCAAAGTGGTTGAGAA
2: CSfrRV_gp1_F2	non-structural polyprotein (ID: 7559143, NCBI)	TTGGCATTGGGATTTCTTTC
2: CSfrRV_gp1_R2	non-structural polyprotein (ID: 7559143, NCBI)	AATCCATCATCCGTGACCAT

qPCR assay conditions and total viral genome copy number enumeration

Real Time qPCR was performed on the original lysate used to infect both the strains, and the lysates obtained at the end of Exp#002 from each biological replicate. The aim of this analysis was to obtain the number of copies of viral particles per millilitre of sample. The reagents used were: 5 µL of 2× Power SYBR Green Master Mix (containing buffer, dNTPs, SYBR Green I, AmpliTaq Gold DNA Polymerase LD and Passive Reference;

Thermo Fisher Scientific) forward and reverse primers at a final concentration of 0.4 µM each; 1 µL of template cDNA; and RNAse-free water to a final volume of 10 µL. The analysis was performed on the ViiA™ 7 Real-Time PCR System with 384-Well Block and the thermal cycling condition were set at 10 min at 95 °C followed by 40 cycles of 15 s at 95 °C and 1 min at 60 °C, with the addition of a melting curve to assess the potential amplification of non-specific products. Fluorescence was detected at the end of each cycle with the automatic determination of C_T. The viral copy number was calculated with the empiric formulas described by Tomaru & Kimura (2016):

$$Y = Vn \times 340/ Ac \quad (1)$$

$$Vc = Vr / Y \quad (2)$$

where, in equation (1) Y is the weight of viral genome (gr), Vn its length (the length of CsfrRNAV) that is 9467 nucleotides (Tomaru *et al.*, 2009), Ac is Avogadro's constant (6.02×10^{23}). By using the viral genome concentration Vr (g/µL) and the values of Y obtained by (1) the viral copy number Vc, as number of copies μL^{-1}, was calculated following equation (2).

Most Probable Number (MPN) assay

The MPN assay establishes the number of infectious virus units and depends not only on the quality of lysate in terms of active viruses present, but also on the susceptibility of the host culture. Since the Exp#001 showed that mortality induced by the same viral solution was different for the two strains, the initial lysate used to infect cultures during Exp#002 was tested using both strains.

Following the protocols suggested by Dr. Thamatrakoln (Fig. 4.1), exponentially growing cultures of the Neapolitan strain APC12 and the Japanese DA strains at a cell concentration of 3.26×10^5 and 3.98×10^5 cells·mL^{-1}, respectively, were used to evaluate the viral infectious units of the original lysate and the ones produced at the end of experiment. A 96-well plate was filled with 240 µl of the host culture using a multichannel pipette. In the meantime a total of 10 serial 10-fold dilutions were prepared with each lysate and an aliquot of 10 µl for which dilution was transferred into a column of 8 wells containing the

host culture. As control, a column of wells was inoculated with only medium. Plates were incubated in a growth chamber at the standard environmental conditions and checked daily for 12 days until controls appeared discoloured. Scores were defined positive when samples were discoloured and EPA-MPN Calculator 2.0 determined the final quantification of infectious viral units·mL-1.

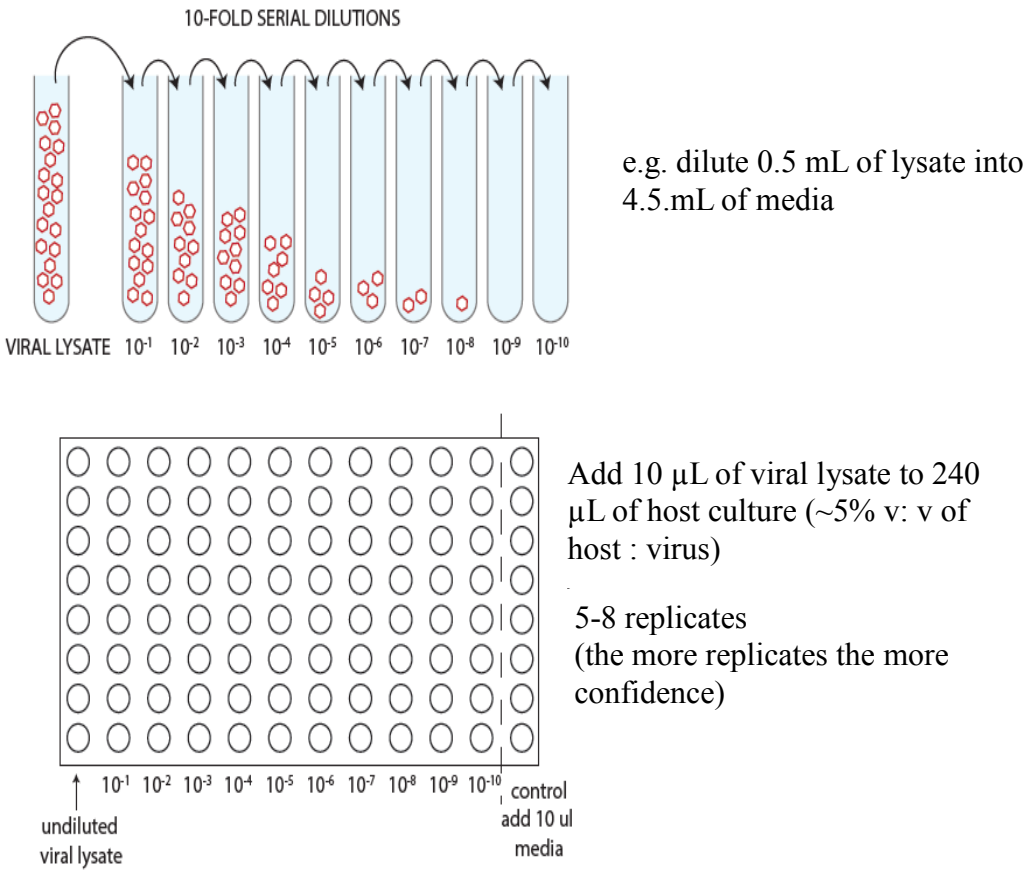

Figure 4.1: Schematic drawing of 10-fold serial diluitions of the viral lysate and MPN assay. Drawing provided by K. Thamatrakoln.

The total amount of spores produced by the two strains in infected cultures was compared to that of control condition. A Two-tailed unpaired t-test assuming unequal variance was performed using GraphPad Prism version 6.0 and values were defined significantly different when $p < 0.05$. Same test was used to compare the variation of viral concentration.

Results

Effect of viral infection on cell concentration and spore formation

In Exp#001 the growth of both strains was measured by fluorescence (Fig. 4.2), quantifying the total cell number (Fig. 4.3) and the composition of spores and vegetative cells (Fig. 4.4). Cultures were infected when cell concentration was $\approx 7\times10^4$ cells·mL^{-1} in the Neapolitan strain (APC12) and $\approx 5\times10^4$ cells·mL^{-1} in the Japanese (DA). The effect of viral infection was visible at the end of the experiment in both strains as shown by a decrease of both fluorescence and total cell number (Fig. 4.2 and 4.3). In the case of Neapolitan strain, fluorescence decreased the third day after the viral infection (Fig. 4.2 A) whereas in the Japanese already from day 2 (Fig. 4.2 B).

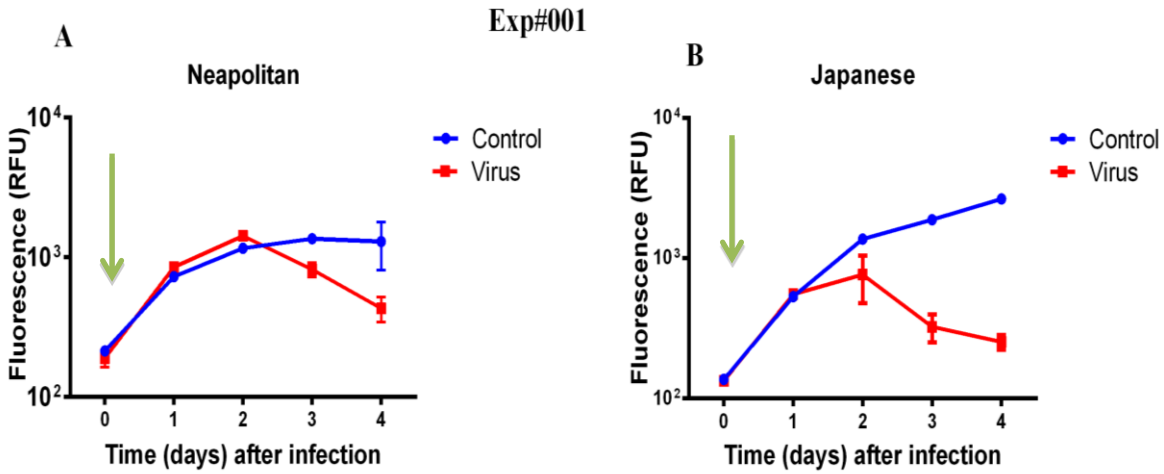

Figure 4.2: Fluorescence curves of control cultures (blue) and cultures infected by viruses (red) for the Neapolitan (A) and Japanese (B) strains during four days after the infection in Exp#001. Green arrows show the day of infection. Data shown as average ± SD (n=3).

Trends observed with fluorescence were comparable to those detected by the enumeration of total cell numbers (Fig. 4.3), and the effect of viral infection in the Japanese strain was less evident looking at cell density as compared to fluorescence (Fig. 4.3 B).

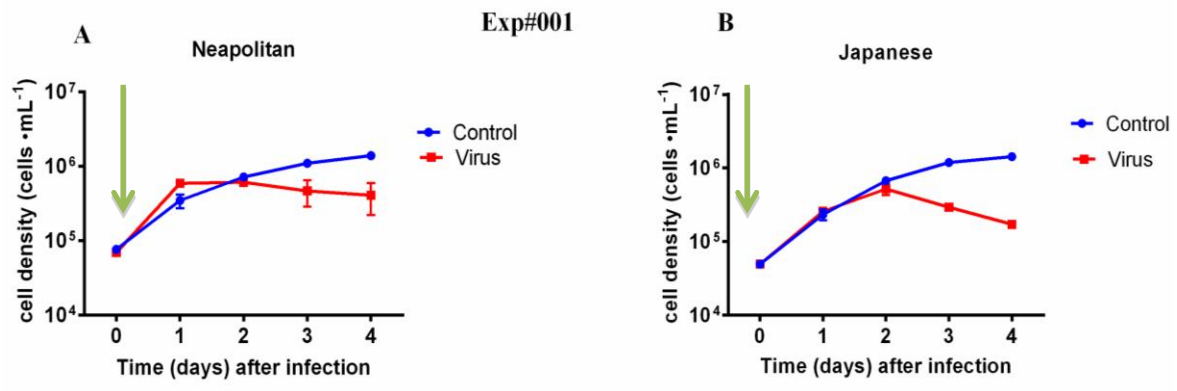

Figure 4.3: Cell densities (cells ml-1) of control cultures (blue) and cultures infected by viruses (red) for the Neapolitan (A) and Japanese (B) strains during four days after the infection in Exp#001. Green arrows show the day of infection. Data shown as average ± SD (n=3).

In the Neapolitan strain an increase of spores was detected in both the control and the infected cultures in spite of their absence the day after infection (Fig 4.4 A, B red lines). In Japanese strain, few spores were counted the last two days after infection, and none in the control conditions (Fig. 4.4 C, D).

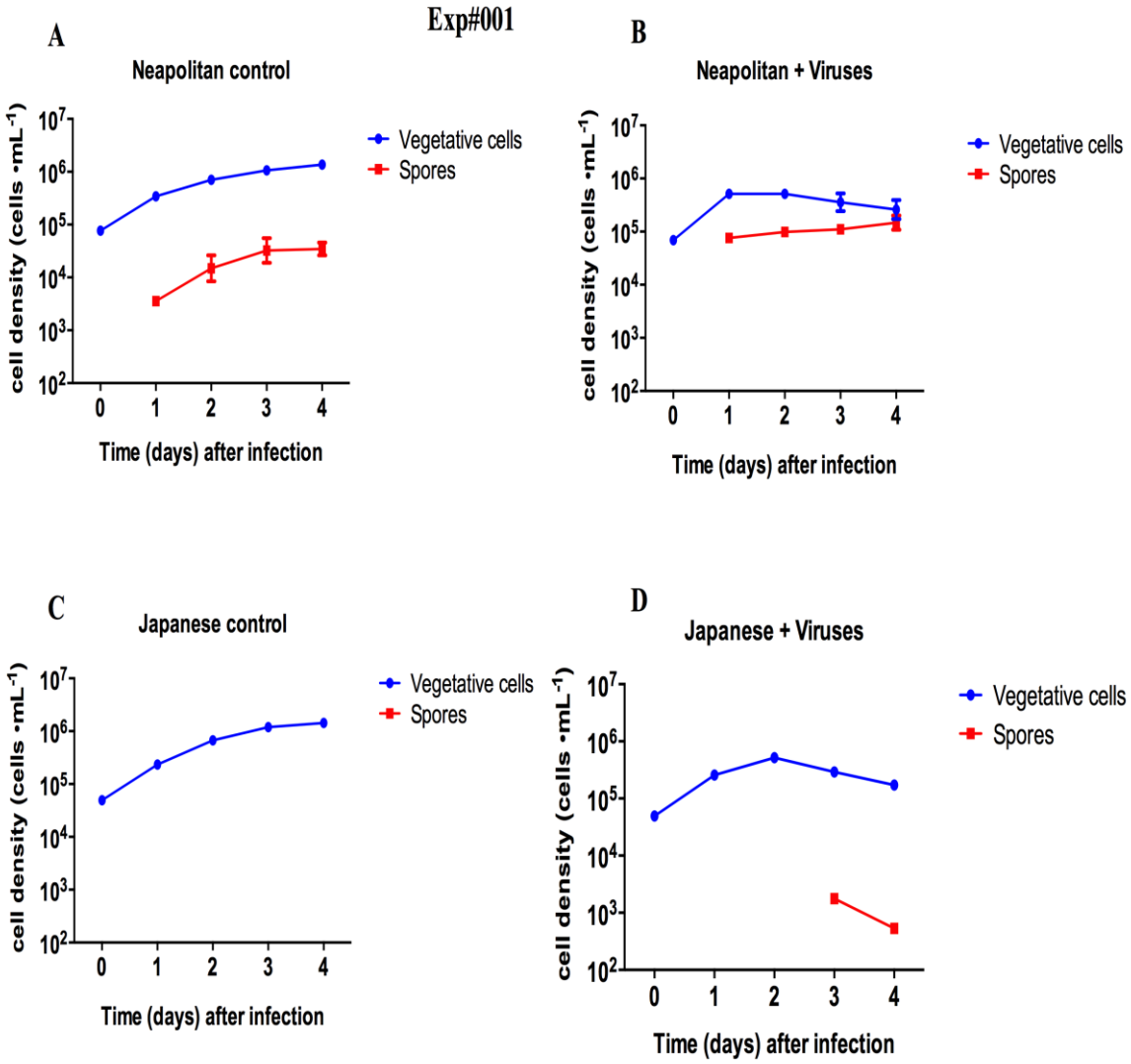

Figure 4.4: Vegetative cells (blue) and spores (red) concentration in Neapolitan (A, B) and Japanese (bottom, D) strains in control (A, C) and infected (B, D) cultures in Exp#001. Data shown as average ± S.D. (n=3).

In Exp#002, the cell concentrations in the Neapolitan and Japanese strains on the day when cells were infected were 6 $\times 10^4$ and 5 $x10^4$ cells·mL^{-1}, respectively. In this experiment, the number of alive vegetative cells was estimated in samples stained with SYTOX green that allowed a more precise enumeration, i.e. only non-stained cells were enumerated. Also, in this experiment the host density trends estimated with fluorescence (Fig. 4.5) were comparable to those obtained by cell counting (Fig. 4.6). The effect of viruses on the Neapolitan strain was less pronounced and became visible only the last day (Fig. 4.5 A and Fig. 4.6 A), while on the Japanese strain the effects were comparable to

what was observed in Exp#001 (Fig. 4.5 B and 4.6 B). As in the previous experiment, the effect of viral infection on host cell density in the Japanese strain was more pronounced in the fluorescence measurement as compared to cell counts.

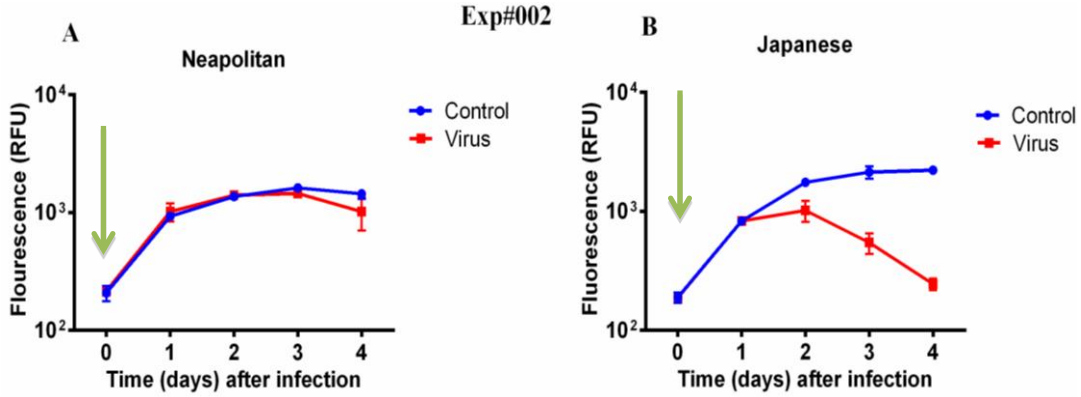

Figure 4.5: Fluorescence measurements in control cultures (blue) and in cultures infected by viruses (red) for the Neapolitan (A) and the Japanese (B) strains during four days after the infection in Exp#002. Green arrows show the day of infection. Data shown as average ± SD (n=3).

Control Neapolitan cultures were in stationary phase two days after infection while Japanese cultures were still growing. Also, in this experiment the decline in the population due to the viral infection was more evident in the Japanese strain than in the Neapolitan one.

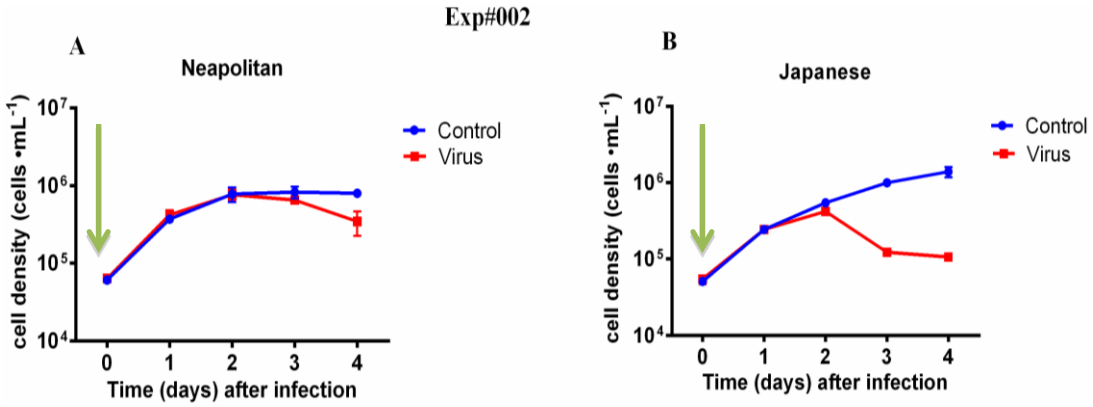

Figure 4.6: Total cell numbers in control cultures (blue) and in cultures infected by viruses (red) for the Neapolitan (A) and Japanese (B) strain during four days after the infection in Exp#002. Green arrows show the day of infection. Data shown as average ± S.D. (n=3).

In the Neapolitan strain, a few spores were present in control conditions already before the infection and their concentration reached $3.5 \pm 1.1 \times 10^4$ cells·mL^{-1} on day 4 (Fig. 4.7 A). Spore concentration was however much higher in infected cultures where spore concentration reached $1.5 \pm 0.5 \times 10^5$ cells·mL^{-1} at the end of the experiment (Fig. 4.7 B).

As in Exp#001, in the Japanese strain spore formation (up to $5.3 \pm 9.2 \times 10^2$ cells·mL^{-1} on day 4) was detected only in the infected cultures. (Fig. 4.7 D).

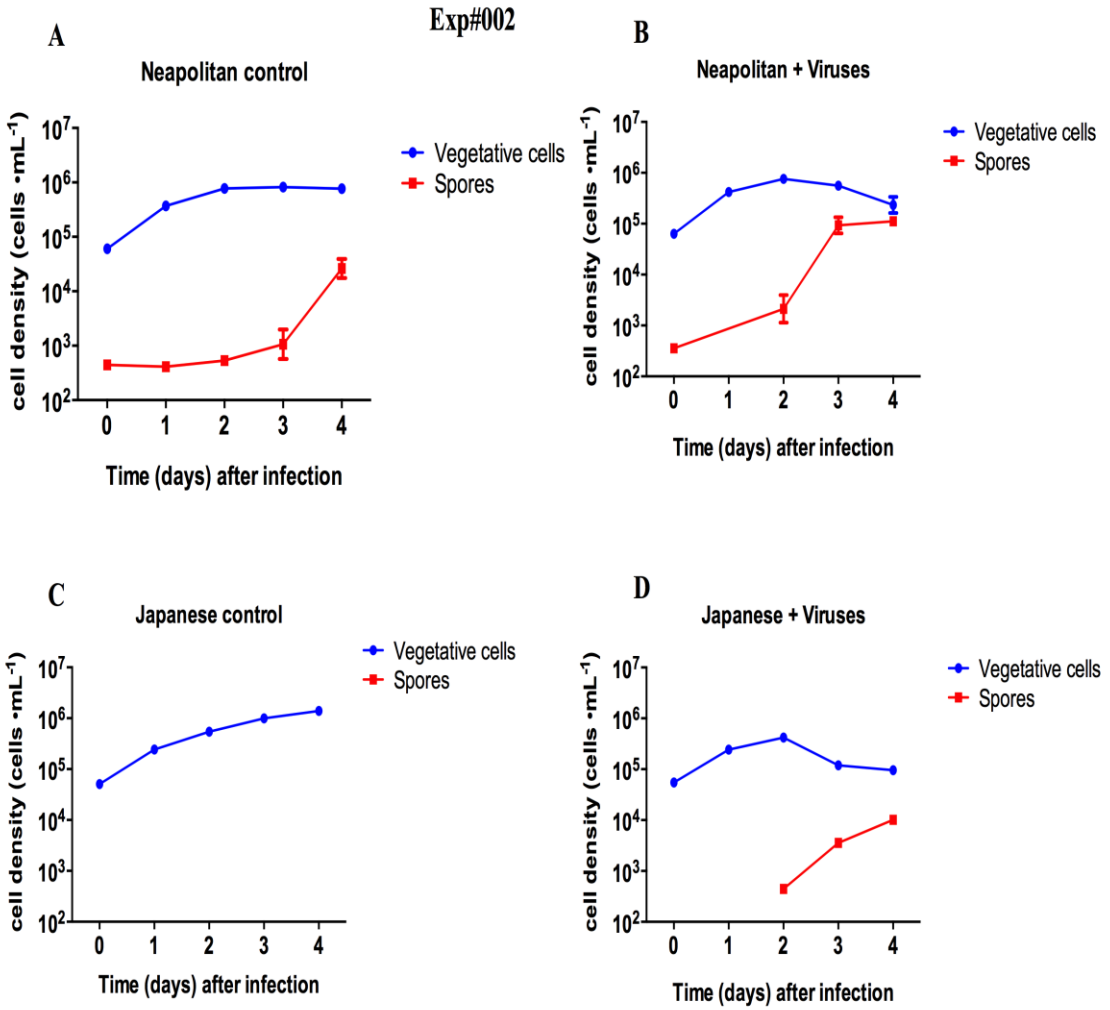

Figure 4.7: Vegetative cells (blue) and spores (red) concentration Neapolitan (A, B) and Japanese (C, D) strains in control (A, C) and infected (B, D) cultures in Exp#002. Data shown as average ± S.D. (n=3).

In both experiments the proportion of spores was higher in cultures treated with viruses (Fig. 4.8). These values were for the Neapolitan strain significantly higher in Exp#001 (p = 0.0007) experiments whereas only in Exp#002 for the Japanese (p=0.0241).

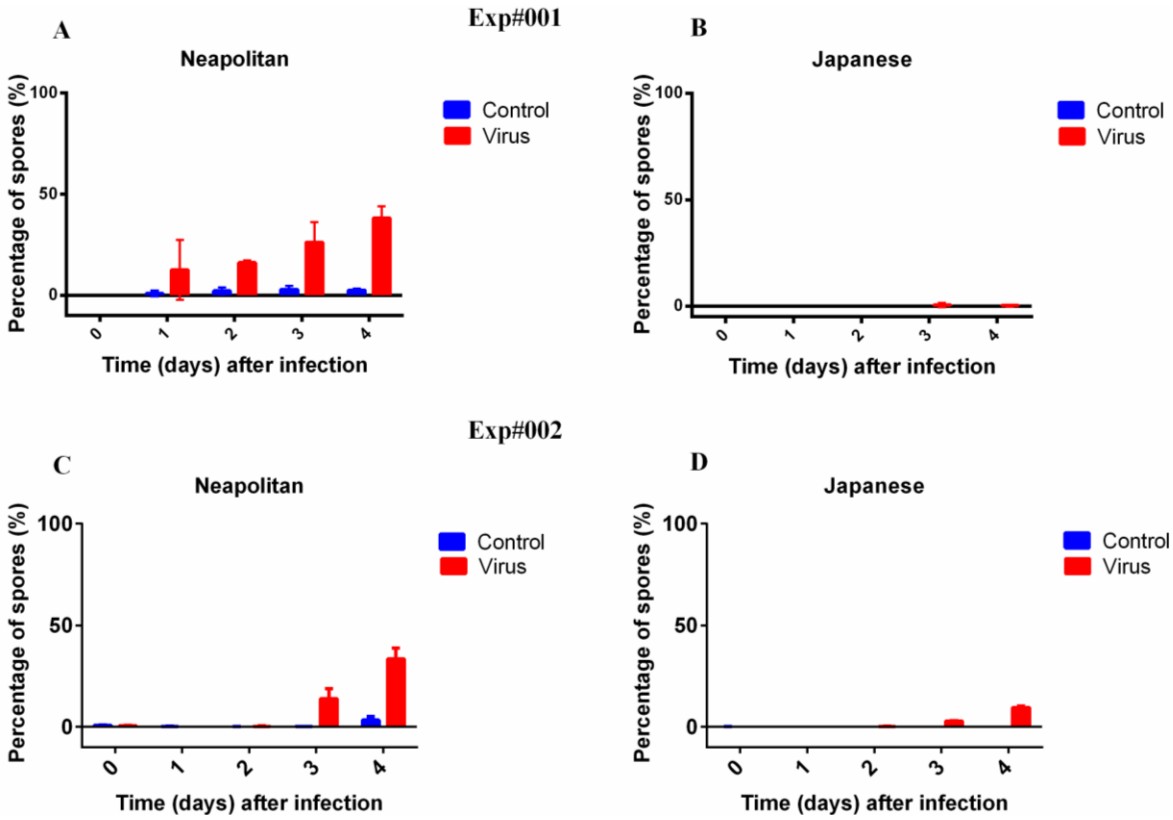

Figure 4.8: Spore percentage (number of spores of total number of alive cells + spores) in control condition (blue) and infected (red) cultures of the Neapolitan strain (A, C) and Japanese strain (B, D) in Exp#001 (A, B) and in Exp#002 (C, D). Data shown as average ± S.D. (n=3).Statistical analysis performed considering values over time.

Evidence for the presence of viruses: TEM preparations

I used TEM preparations to prove the presence of viral particles in the cells of the Neapolitan strain APC12. Micrographs of vegetative cells demonstrated that viruses successfully completed their cycle infecting the cultures. Particles with the same size of the virus CsfrRNAV were detected in the vegetative cells (Fig. 4.9 A, B arrowed).

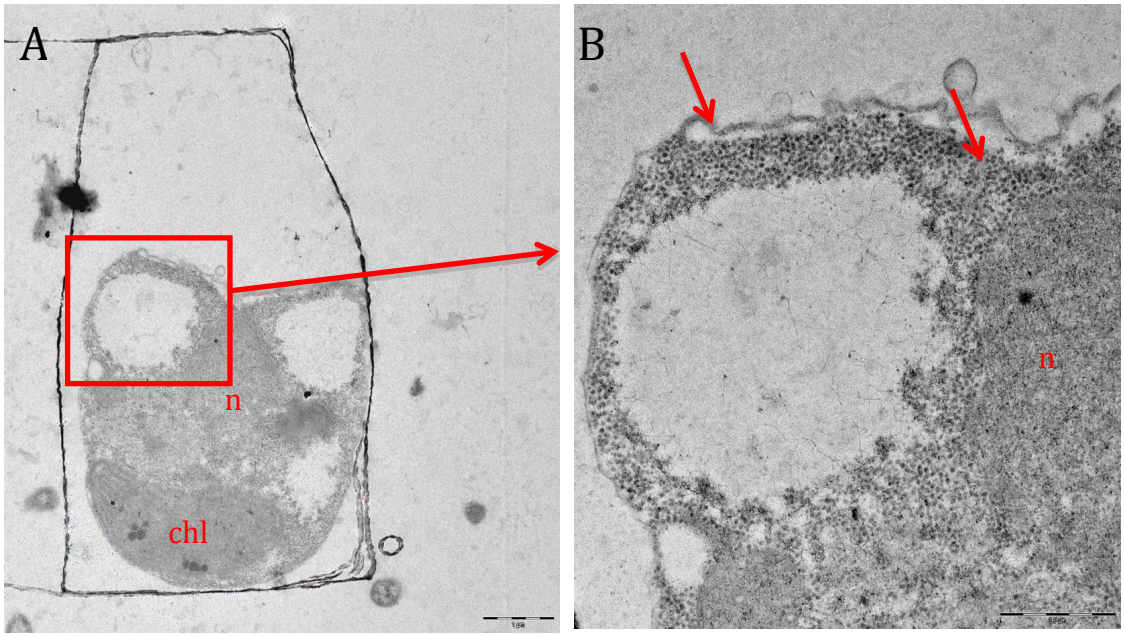

Figure 4.9: TEM micrograph of infected vegetative cell of strain APC12 with degraded cytoplasm (A). Detail of (A) with arrows indicating viral particles (B). n=nucleus, chl= chloroplast. Scale bars = 1 (A) and 0.5 μm (B).

Also spores were successfully sectioned (Fig 4.10) but in this case viral particles were not detected. Viruses were visualised also in the lysate produced by the filtration of the infected Neapolitan culture at the end of the experiment (Fig. 4.11). Individual viral particles could be visualized on the grid.

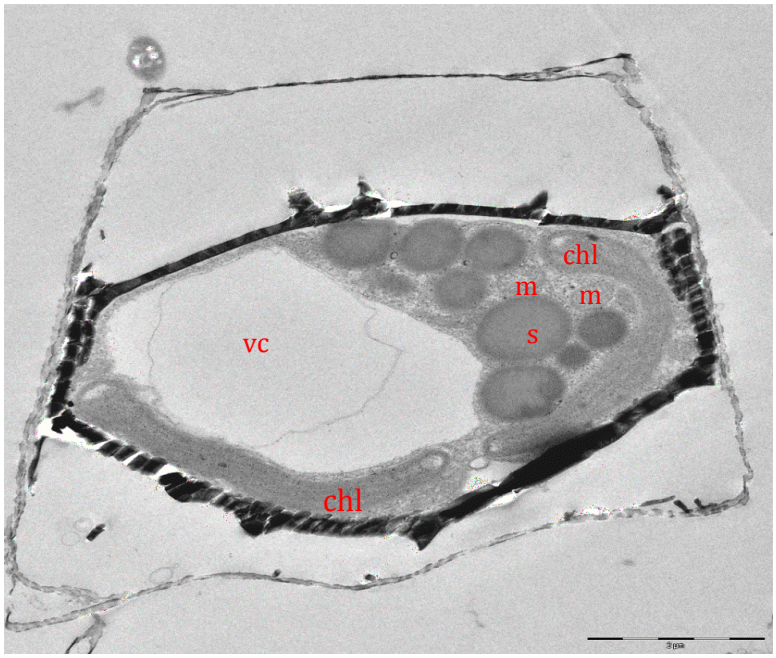

Figure 4.10: Micrograph of TEM ultrathin-section of a spore of the Neapolitan strain APC12. Vc= vacuole chl=chloroplast, m=mitochondria, s= storage compounds. Scale bar = 3 µm.

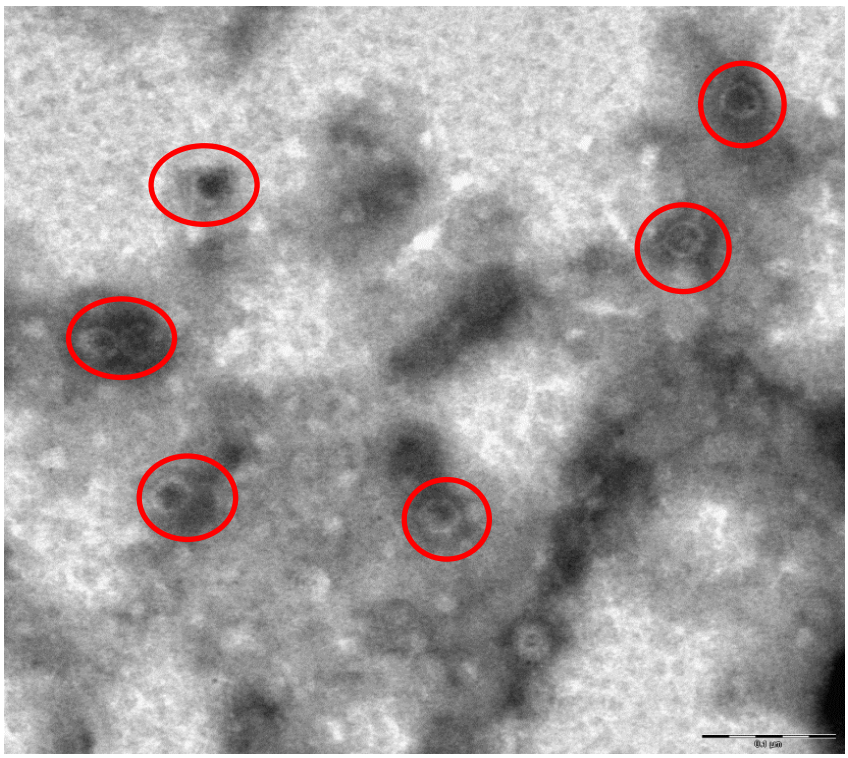

Figure 4.11: TEM micrograph of viral lysate produced by filtration of an infected culture of strain APC12. Viral particles are encircled in red. Scale bar = 0.1 µm.

Viral concentration assessed by qPCR

The standard PCR confirmed that both designed primer-pairs were working with the extracted genomic RNA and could be used to obtain the standard curve and in turn the quantification with qPCR (Fig 4.12). The construction of the standard curve was visualized taking into account the C_T obtained for each dilution and the number of viral copies per mL was retrieved following the formula describe above. I used the cDNA obtained from the final lysate of Exp#001 and the first couple of primers designed (CSfrRV_gp1_F1 and R1). All values obtained by the technical replicates were consistent and were used to calculate the slope of the curve (R^2 = 0.993; Fig.4.13).

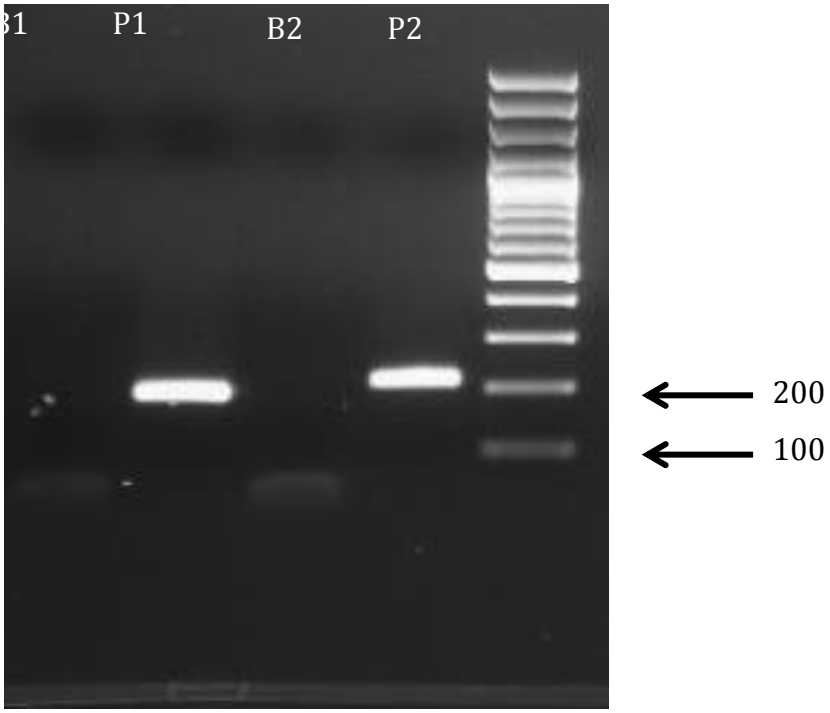

Figure 4.12: Gel of the PCR to test the two primers with viral genomic RNA. B1: blank for the first primer-pair, P1: primer1, B2: blank for the second primer-pair, P2: primer2 and the ladder where the values for 100 and 200 bp are indicated.

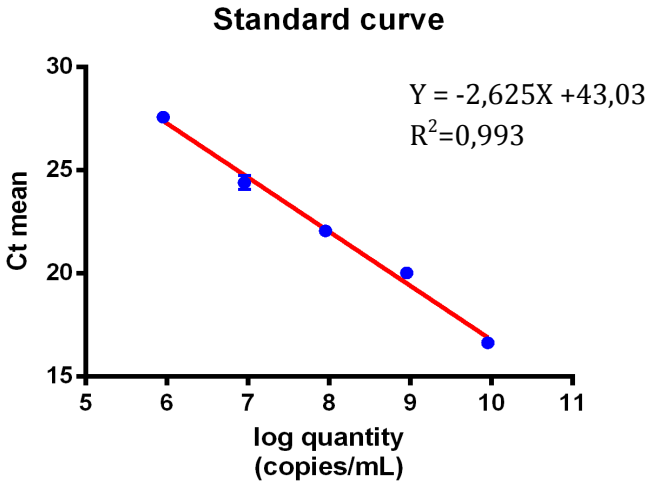

Figure 4.13: Standard curve used for the direct quantification of initial lysate used for the infection and final lysate of the Neapolitan and Japanese strains. It represents is the Ct values of three technical replicates. Data shown as average ± S.D (n=3).

The Real Time PCR indicated that the initial lysate contained $7.6 \cdot 10^4$ copies of viruses·mL^{-1} and the final, after 4 days from the infection, contained ≈ 38 $\times 10^9$ and ≈ 1.4 × 10^9 copies·mL^{-1} in the Neapolitan and Japanese strains, respectively (Fig. 4.14). These results demonstrated that viruses completed their lytic cycle successfully infecting both strains. The variability among replicates was higher in the Neapolitan strain.

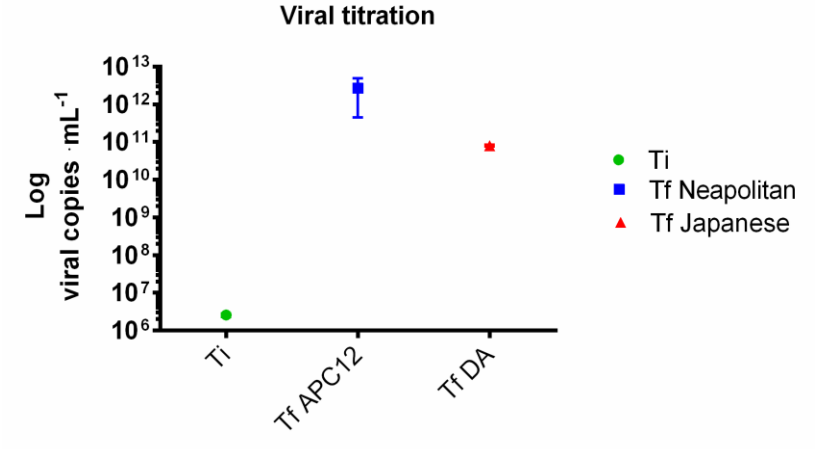

Figure 4.14: Quantification by qPCR of viral copy number·mL-1of initial lysate (green), final lysate of the Neapolitan (blue) and Japanese (red) strains. The latter two values are the average of the triplicate samples and are shown as average ± SD.

Viral concentration assessed by MPN

The MPN assay showed that the number of viral infection units in the initial lysate was of the same order of magnitude as the estimate by qPCR (Fig. 4.15). The MPN estimate in the final lysate showed there was an increase in viruses of about 2-3 orders of magnitude in both strains and also this estimate provided slightly higher values for the Neapolitan strain. The absolute concentration of viruses in the final lysates resulted to be several orders of magnitude lower than that measured with the Real Time PCR.

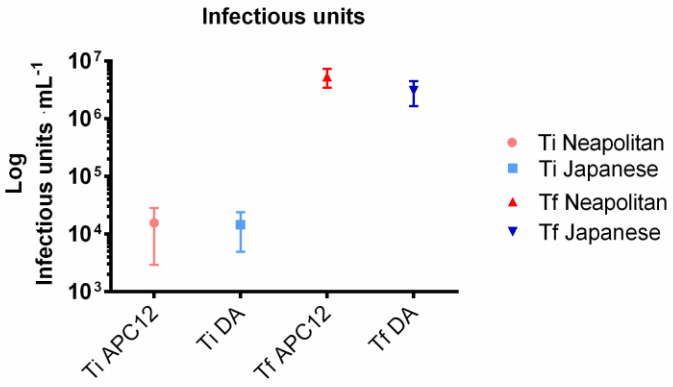

Figure 4.15: Infectious units calculated with MPN assay; initial lysate (Ti) in Neapolitan (light red) and Japanese (light blue) strains and final lysates (Tf) in Neapolitan (red) and (blue). Average data ± SD (n=3).

Discussion

The experiments illustrated in this chapter were aimed to evaluate the capability of the virus CsfrRNAV to infect the Neapolitan and Japanese strains of *C. socialis* and to test if viral infection could induce a significantly higher spore formation as compared to the uninfected controls. This is the first time that the effect of viruses on the formation of spore has been followed and quantified. I provided evidence that the infection with a *Chaetoceros socialis*-specific virus induces an increase in the number of spores in cultures. This has been proved for two strains belonging to geographically distant populations, one from the Gulf of Naples and the other one from Japan.

Without any doubt viruses have been able to complete their lytic cycle in both strains. The number of copies of viral particles showed an increase in the experiment carried out with both strains. These numbers were similar in the two strains at the end of the experiment.

However, some differences were observed in the viral infection dynamics between the two strains. Both experiments showed that the viruses affected the Japanese strain faster as shown by the viral-induced mortality of the population. In fact, the decrease in fluorescence and cell number started earlier in the Japanese strain. Moreover, the Neapolitan strain seemed to be less sensitive to viral infection because the final cell concentration was higher.

The differences observed between the two strains may be explained by different factors: the geographic provenance of the virus, the age of the strains, i.e. the time spent in laboratory conditions or the strain-specific sensitivity. Since the virus was isolated from *C. socialis* originating in Japanese waters (Tomaru *et al.,* 2009) it is possible that its infective capability is higher towards *C. socialis* strains from the same geographic area. The second hypothesis is the effect of long-term maintenance of spore-forming strains in laboratory conditions. It is known that evolution is a continuous process not only in nature but also in laboratory cultures. This means that older cultures may depart more from the natural environment "original" state (Lakeman *et al*., 2009). Contrary to the Neapolitan strain, which has been isolated about 1 year before the experiments, the Japanese was isolated more than 10 years ago and the long-term maintenance in the laboratory can have selected for cells with low capability to form spores since this life cycle trait may not be necessary in constant conditions. Unfortunately, no data are available on spore production performance of the Japanese strain at the time of isolation.

However, it is possible that this variability of responses to the viral infection by the two *C. socialis* strains is due to strain-specific sensitivity. This has been demonstrated in other phytoplanktonic species such as the prasinophyte *Micromonas pusilla* (Zingone *et al.,* 2006) and the pennate diatom *Pseudo-nitzschia* (Carlson *et al.,* 2016). In the first case, authors carried out infection experiments with 11 strains of *M. pusilla* from the Gulf of Naples and other geographic areas and two different viruses isolated from the Gulf of Naples. The sensitivity of the host strains to both viruses was quite different and could not be explained by the geographic origin of the strains nor their phylogenetic diversity. In the

second case, authors obtained similar results using several natural viral communities to infect *Pseudo-nitzschia* cultures that had the same ITS profiles and were isolated from the same sites of the viruses. Infections were carried out in all possible combinations. Higher infectivity was observed in diatom cultures isolated from the same area as the virus; this suggests that viruses can perceive a finer level of genetic differences in the diatoms.

The Japanese strain did not produce spores when infected by the virus in experiment #1 and produced a very low number of spores in experiment #2. Nevertheless, the Japanese and the Neapolitan strains shared exactly the same LSU and thus belong to the same species. During the characterization of species-specific viruses of *C. lorenzianus*, the authors noted that it did not form spores when infected with its virus (Tomaru *et al.*, 2011). In that paper however, there was no information on spore production performance of the strain in other conditions, and also the host was not genetically characterized. As *C. socialis*, *C. lorenzianus* is known to be a species-complex, including genetically distinct species (Li *et al*., 2017). It may be that the *C. lorenzianus* from which the virus was isolated was not capable of producing spores.

The absence of viral particles inside the spores, as appeared in the TEM preparations, cannot prove the immunity of the spores to viral infection. Although several micrographs were taken, they represent just a tiny part of the population and do not allow any assertion. On one side, it can reasonably be hypothesized that the transition from vegetative cells to spores is only possible in healthy cells with proper physiological conditions. The spores have to be formed before the extreme viral duplication. However, it is also possible that a few viral particles may have been incorporated in the host genome and remains a latent phase. This possibility raises another question: are viruses direct inducers of this life cycle transition or are spore produced indirectly, i.e. responding to a chemical cue produced by virus-infected cells?

The well-studied *Emiliania huxleyi* is the only other species in which viruses have been observed to induce a shift in life cycle (Frada *et al.*, 2008), and it became a model species in studies of host-viral dynamics. *E. huxleyi* is characterized by a haplo-diplontic life cycle

and the shift between one diploid phase, covered by coccoliths, to a naked haploid seems to be triggered by viral infection. The interesting fact is that the haploid phase is immune to viral infections. The replication machinery used by viruses in this species is related to an increase of ROS in the host cell, as well as the expression of metacaspases and PCD pathways. ROS are known to kill cells, but important also in inducing the arrest of the cell cycle (Nedelcu & Michod, 2003), and the formation of resting stages as observed in the amoeba *Dictyostelium discoideum* (Ameisen, 2002). What induces the shift to the haploid virus-resistant phase of *E. huxleyi*, however, is still not completely understood but it seems to be linked to the physiological state of virus-infected cells (Frada *et al.*, 2008).

On the other hand, C. *socialis* has been observed forming spores during adverse conditions, when nitrogen was severely limited. In other diatoms, this condition leads to the activation of PCD pathways (Berges & Falkowski, 1998). It cannot be excluded that the pathways at the base of spore formation in nitrogen depletion and as a reaction to viral attack are closely related.

In conclusion, I could answer to the first question: viral infection induces spores formation but the possibility that spores represent life stages immune to viruses needs to be better studied. These results increase the information on the potential ecological role of spores in population dynamics of this species but also in understanding the relationships between diatoms and their natural enemies in the sea. Studies on *Cheatoceros* specie-specific viruses were never performed in the Gulf of Naples so we do not know if *C. socialis* or other species of this genus experience viral infection in nature.

Chapter 5

Differential gene expression analysis during spore formation

Introduction

New insights on marine microbial communities have been reached in the last decades thanks to genomic-based studies. The *de novo* sequencing of genomes provides information of the genomic repertoire that rules metabolic pathways, the capacity of the organisms to sense the environment and react to external stimuli as well as information on the structure and evolution of the genomes (Armbrust *et al.*, 2004; Derelle *et al.*, 2006; Read *et al.*, 2013). Genes are annotated in the genomes based on the homology with genes whose function is known in other organisms. The interest of experimental biologists and ecologists is in understanding the mechanisms in action under specific experimental conditions or in different environments. Transcriptomic studies allow following the gene expression changes occurring in a cell transitioning from one condition to another. For these studies, the RNA of the target organism is extracted, retrotranscribed to cDNA and sequenced with high-throughput sequencing (HTS) technologies to obtain the transcripts up- and down-regulated at the different experimental conditions. To study the genes active in the whole community, metatranscriptomic approaches are carried out in which all RNA transcripts present in the microorganisms of the community are sequenced.

When these approaches started to be applied to marine organisms, only a few eukaryotic genomes were sequenced; they belonged to multicellular animals, plants or parasites of biomedical and biotechnological interest, while those of free-living and ecologically important unicellular organisms remained scanty (Keeling *et al.*, 2014). Ecological field studies based on molecular approaches, such as metagenomics and metatranscriptomics, necessitate reference sequences that are currently limited. Since the sequencing and assembling of nuclear genomes of eukaryotes remains difficult, a first attempt to cope with the requirement of taxonomically and functionally annotated genes was the production of a gene expression database: the Marine Microbial Eukaryote Transcriptome Project (MMETSP). The large-scale sequencing of genes expressed by an organism under different environmental conditions gives a clear idea of how the organism responds without the challenges posed to the interpretation of meta-data deriving from, e.g., presence of introns, intergenic regions ad repetitive DNA. MMETSP included 680 transcriptomes obtained in different conditions of taxonomically-identified cultures representing the most abundant ad ecologically important microbial eukaryotes in the oceans (Keeling *et al.,* 2014). It provided information on how microbes react to competition, predation, symbiotic interactions

and especially to environmental cues. This increased both the number of protists lineages studied with a genomic approach and the amount of genes expressed from free-living organisms (Caron *et al.*, 2017). The availability of a large number of transcriptomes from organisms spanning a broad range of phylogenetic diversity allowed, for instance, the identification of genes under selection that are expanding or contracting, the evaluation of mechanism such as horizontal gene transfer and also to study the genetic variation between strains of the same species (Caron *et al.,* 2017). Furthermore, the transcriptomic approach allowed carrying out comparative studies that are needed to decipher the genetic bases of the adaptations to different environments and gain knowledge on important biological processes. Examples are studies on the genes expressed during sexual reproduction of pennate diatoms (Moeys *et al.*, 2016; Basu *et al.*, 2017) and on the transcriptomic response of diatoms to turbulent conditions (Amato *et al.*, 2017). Another example is the work on nitrogen transporters in diatoms that illustrated how diverse and articulate the assimilation of nitrogen is in microalgae (Rogato *et al.*, 2015).

In this context, a growing number of differential gene expression studies, in some cases also supported by proteomic and lipidomic approaches, were focused on the capability of diatoms to change their physiological state in response to nutrient availability (Abida *et al.*, 2015; Jian *et al.*, 2017). Particular attention was given to variation in gene expression at low concentration of nitrogen, phosphorous, silicon and iron as compared to control conditions. These nutrients were selected because they are the main factors accounting for the variation of growth of microalgae. These studies demonstrated that diatoms perceive nutrient availability and adapt their cellular state with nutrient-specific physiological responses, indicating also a high plasticity in their responsiveness (Bender *et al.*, 2014; Lin *et al.*, 2017). As an example, the pennate diatom *Phaeodactylum tricornutum* is capable to reduce the expression of genes of iron-containing pathways when grown in iron-depleted conditions (Allen *et al.*, 2008). However, the reaction to iron starvation was different from that of the centric *Thalassiosira pseudonana* with which *P. tricornutum* shared only 16% of homologous genes (Thamatrakoln *et al.*, 2013). In this study the authors demonstrated also the implication of death-related genes in the acclimation to oxidative stress induced by iron absence that might allow the survival of diatoms in Fe-limited region of Northeast Pacific Ocean.

Nitrogen limitation

The formation of a considerable number of spores was obtained by inoculating the exponentially growing culture of *C. socialis* in nitrogen deprive culture medium (Chapter 3). Several transcriptomic studies were carried out to test physiological responses to nitrogen limitation since physiological experiments of past years lead to suppose that its concentration is the principal driver of phytoplankton abundance in marine environment (Falkowski *et al.*, 1998).

The general response of diatoms to nitrogen limitation includes the recycle of nitrogenous compounds with the breakdown of proteins, the down-regulation of genes related to photosynthetic processes and the rearrangement of carbon allocation in triacylglycerides (Alipanah *et al.*, 2015). The complex molecular diversity of diatoms was highlighted by comparisons made between different diatom species and with other autotrophs (cyanobacteria, green algae and plants). For example, two pennate diatoms, *Fragilariopsis cylindrus* and *Pseudo-niztschia multiseries,* reacted to nitrogen depletion by recycling nitrogen compounds, decreasing carbon fixation and activating fatty acids and carbohydrates metabolisms but they shared only 5% of the genes differentially expressed when compared to the centric *Thalassiosira pseudonana* (Bender *et al.*, 2014). Although the overall response was similar, the pennates and the centric diatom are phylogenetically distant and *F. cylindrus* is a species adapted to cold waters while the other two species are from temperate environments and this may explain the fact that they evolved distinct metabolic pathways to respond to similar nutrient forcing. When compared to the molecular response to nitrogen starvation of distantly related species, *T. pseudonana* had a physiological rearrangement of nitrogen and carbon metabolisms that reminded more those of the cyanobacterium *Prochlorococcus marinus* than that of the eukaryotic *Chlamydomonas reinhardtii* and the higher plant *Arabidospis thaliana* (Hockin *et al.*, 2012).

Table 5.1: Overview of papers in which molecular responses to nitrogen starvation were examined in diatoms.

Reference and approach	Species	Remarks
Mock *et al.,* 2008 (N, P, Si, Fe –limitation, alkaline pH, low temperature)	*Thalassiosira pseudonana*	Transcripts induced by nitrogen limitation displayed different profile from those in Si limitation and a majority

Whole-genome oligonucleotide tiling arrays		encoded proteins had a predicted function.
Bender *et al*., 2014 (N-limitation) Transcriprome	*Thalassiosira pseudonana*, *Fragilariopsis cylindrus* and *Pseudo-nitzschia multiseries*	Diatoms share pathway-level responses although only the 5% of genes were common to the three species. Increase in nitrogen recycling pathways and general decrease of cellular metabolism such photosynthesis and carbon-related pathways.
Levitan *et al*., 2015 (N-limitation) Transcriptome, lipids analysis	*Phaeodactylum tricornutum*	Recycle of nitrogen compounds through the degradation of proteins. Genes related to TCA, urea cycle and nitrogen assimilation were up-regulated. The most down- regulated genes were related to chlorophyll biosynthesis and fucoxanthin chlorophyll *a/c* binding proteins. Lipid biosynthesis genes were down regulated, including acetyl-CoA carboxylase.
Alipanah *et al*., 2015 (N –limitation) Microarray	*Phaeodactylum tricornutum.*	Down regulated: protein biosynthesis, ribosomal assembly, translation, photosynthesis, light harvesting and nitrogen metabolism. Upregulated: signal transduction and ubiquitination.
Hockin *et al*., 2012 (N-limitation) Proteome	*Thalassiosira pseudonana, Chlamydomonas reinhardtii,*	Nitrogen starvation induced the repression of proteins involved in the metabolism of nitrogen, amino acids, proteins,

	Prochlorococcus marinus and *Arabidospis thaliana.*	carbohydrates, photosynthesis and chlorophyll biosynthesis. Changes in carbon metabolism were closer to those of *Prochlorococcus marinun* than to the other eukaryotes.
Lin *et al*., 2017 (N and P -limitation) Proteome	*Thalassiosira pseudonana*	Under N- and P-limited conditions genes in response to oxidative stress were up regulated.

The aim of this Chapter is to show insights provided from a first exploration of the genes up- and down-regulated during the process of spore formation in *C. socialis*. I first looked to those transcripts involved in the formation of resting stages in other organisms and related to observation made during the microscopical investigation described in Chapter 2. Then, due to the fact that nitrogen starvation was used as a trigger, I tested the expression pattern of genes related to this specific physiological state (Table 5.1). Other pathways, not strictly related with nitrogen metabolism and possibly involved in spore formation were also taken in account. Finally I considered the 20 most up-regulated genes in the comparisons of treatments to control conditions, in order to evaluate which they were and if shared by all sampling points.

Materials and methods

Experimental set up and transcriptome sequencing

The experiment was carried out using a newly established clonal strain of *C. socialis,* APC12, which was genotyped by sequencing the LSU rDNA region. A non-axenic culture was maintained in a culture chamber at 18 ± 2 °C in batch cultures under sinusoidal illumination (12 h light with a maximum irradiance of 180 µmol photons m^{-2} s^{-1}). Cultures were maintained in a slightly modified f/2 medium made with artificial seawater at salinity of 36 psu and 580µM of $NaNO_3$, 300 µM Na_2SiO_3 and 29 µM

NaH_2PO_4. The acclimated culture was transferred during the exponential growth phase into three 5 L glass flasks filled with nutrient-replete medium (the same nutrient concentration listed above) and three flasks filled with low nitrate medium (23 µM of $NaNO_3$, 300 µM Na_2SiO_3, 29 µM NaH_2PO_4) both prepared with artificial seawater at salinity of 36 psu. Flasks were filled with 3 L of culture medium and the initial cell density was about 3×10^3 cells·mL^{-1}. Temperature and light conditions were monitored during the experiment with a HOBO Pendant® Temperature/Light Data Logger. To estimate cell concentration, 4 mL of sample were collected every day, fixed with 40% formaldehyde solution and vegetative cells and spores were enumerated using a Sedgwick-Rafter chamber on a Zeiss Axiophot (ZEISS, Oberkochen, Germany) microscope at 40x magnification. With the exception of the first day, more than 200 cells were counted.

RNA extraction

Total RNA was extracted from each replicate in mid-exponential growth phase in cultures grown in high nitrogen medium (control, T2C) and in three consecutive days in low nitrogen cultures: before the formation of spores (T2T), when spore formation started (22% of spores, T3T), and when they reached 72% of the total cell number (T4T). A total cell number of ~2.4×10^7 was harvested from each replicate by filtration onto 1.2 µm pore size filters (RAWP04700 Millipore). Filters were cut in two halves, placed in two different Eppendorf vials filled with 1.5 mL of TRIzol® Reagent (Thermo Fisher Scientific) and immediately frozen in liquid nitrogen and stored at -80° C until the extraction. Before proceeding to the total RNA extraction, samples were defrosted at room temperature (RT) and cells were disrupted with glass beads (G1277, Sigma-Aldrich) on an Eppendorf Thermomixer R (Eppendorf) at 60 °C for 10 minutes at maximum rpm. Samples were centrifuged for 1 minute and the supernatant transferred into a new Eppendorf vial. Each sample, after the incubation with chloroform 1:5 (v:v) at RT for 15 min, was then centrifuged for 15 minutes. Of the three-layer solution obtained, only the uppermost was transferred in a new Eppendorf with an equal volume of isopropanol and incubated 10 minutes at RT. This solution was then centrifuged for 10 minutes to allow the precipitation of RNA molecules. The pellet was washed with 1 mL of 75% ethanol then removed after centrifugation for 10 minutes. The RNA samples were further purified on Qiagen columns (74104, RNeasy Mini Kit) following the manufacturers' protocol. All samples were quantified with

Qubit® 2.0 Fluorometer (Invitrogen) and the quality was checked with an Agilent2100 bioanalyzer. Contaminations were tested with NanoDrop ND-1000 Spectrophotometer (Nanodrop Tecnologies Inc., Wilmington, USA). Samples were pooled in equal concentration of 100 $ng \cdot \mu l^{-1}$ and sequenced at the Molecular Service of Stazione Zoologica. Sequencing was conducted using the Ion P1 sequencing Kit v2 on a Ion Proton™ (Life Technologies, Carlsbad, USA) sequencer using four Ion P1 Chip Kit v3 chips (Thermo Fisher Scientific).

De novo transcriptome assembly, functional annotation and differential gene expression analysis

The bioinformatics analyses were performed by Laura Entrabasaguas Monsell at Stazione Zoologica. Summary control of raw reads quality was done with FastQC (v0.11.5) software (Andrews, 2010). Raw reads were subjected to a cleaning procedure using the Fastx-toolkit v0.0.14 (http://hannonlab.cshl.edu/fastx_toolkit/). Low quality extreme nucleotides were trimmed from the ends (first 10 bases and reads were additionally cropped to a maximum length of 100 bp), and only reads with a quality score ≥20 and a minimum length of 50 bp were retained. In order to filter out any remaining post-sequencing ribosomal RNA, the local sequence alignment tool SortMeRna 2.1 (Kopylova *et al*., 2012) was applied against different databases (Rfam 5.8S;Rfam 5S; Silva 16S archaeal, bacterial; Silva 18S eukaryote; Silva 23S archaeal, bacterial; Silva 28S eukaryote) with an E-value cut-off of 1e−20. A final FastQC runwas performed on the filtered data to ensure the validity of preprocessing steps.

Cleaned reads were assembled into a transcriptome using Trinity v.2.0.6 (Haas *et al.,* 2013) with in silico read normalization and --min_kmer_cov 2. The annotation of the transcriptome was performed by Annocript v1.1.3 with default settings (Musacchia *et al.*, 2015).

Reads from each biological replicate were individually mapped to the assembled transcriptome and expression of each gene was quantified using the Expectation Maximization method (RSEM). Before differential expression analysis, very lowly expressed genes were removed keeping those genes that have at least a cpm (read/count per million per million) of 1 or greater for at least three samples (the size of the smallest group of replicates) and subsequently, data was normalized to scale the raw library sizes. Differentially expressed genes were determined using the edgeR package

(Robinson *et al.,* 2010). The method for testing differentially expressed genes was the quasi-likelihood F-test under the glm framework, which is more conservative and rigorous, type I error rate control. Differential expression comparisons have been performed between:

1. t2treatment vs t2control (T2T_T2C)
2. t3treatment vs t2control (T3T_T2C)
3. t4treatment vs t2control (T4T_T2C)
4. t3treatment vs t2treatment (T3T_T2T)
5. t4treatment vs t2treatment (T4T_T2T)
6. t4treatment vs t3treatment (T4T_T3T)

Genes that were more than twofold differentially expressed at a significance of a false discovery rate (FDR) threshold corrected P value < 0.05 were considered as differentially expressed.Principal component analysis (PCA) was conducted using the "prcomp" function within R environment v. 3.2.2 (R Core Team, 2015) and scatter plot of PCA results was generated using the ggplot2 package (Wickham, 2009).In situations in which a given gene contained multiple isoforms, the longest isoform was defined as the gene functional annotation.

Gene ontology (GO) enrichment analyses of differentially expressed genes were conducted by using the R prop.test function (Newcombe, 1998) through a R plugging of the Annocript software. Results obtained on biological processes were presented here, while those on cellular compartments and molecular functions are presented as appendix at the end of thesis.

Genes related to specific processes

Genes involved in the main metabolic pathways were manually searched across the differentially expressed genes. As some transcripts were found to be significantly differentially expressed at different sampling point, the average of their differential expression was computed while those present redundant were counted as a single gene. The original file of differentially expressed genes and those used in this study are consultable in the attached CD-ROM.

Results and discussion

Spore formation in the experiment for transcriptomic analysis

The total cell density of cultures maintained in nitrogen-limited media reached lower cell concentration at the end of the experiment as compared to the control conditions (Fig 5.1 A, B). The lower number of cells in nitrogen-depleted conditions was due to the fact that cells stop dividing due to nutrient limitation. Moreover, in the treatment conditions, a large fraction of cells transformed into spores as demonstrated by the experiments illustrated in Chapter 3.

Indeed, after 3 days of exponential growth, cells in low nitrogen condition entered in stationary phase; vegetative cells progressively turned into spores starting from day 2. The highest percentage of spores was ~75% on day 4 (Fig. 5.1 A, C). However, as in the experiments described in Chapter 3, spores were present also in control condition but with a lower percentage (15%) at the end of experiment (Fig. 5.1 B, D).

In order to evaluate the molecular mechanisms involved in spore formation, samples from three subsequent timing points (T2T, T3T and T4T) were collected from treatment cultures (red circles in Fig. 5.2 A). A further sample was obtained on day 2 from cultures in control conditions (T2C), when no spores were present and cells were in exponential growth (red circle in Fig. 5.2 B). The resulting transcriptomes were then compared with each other.

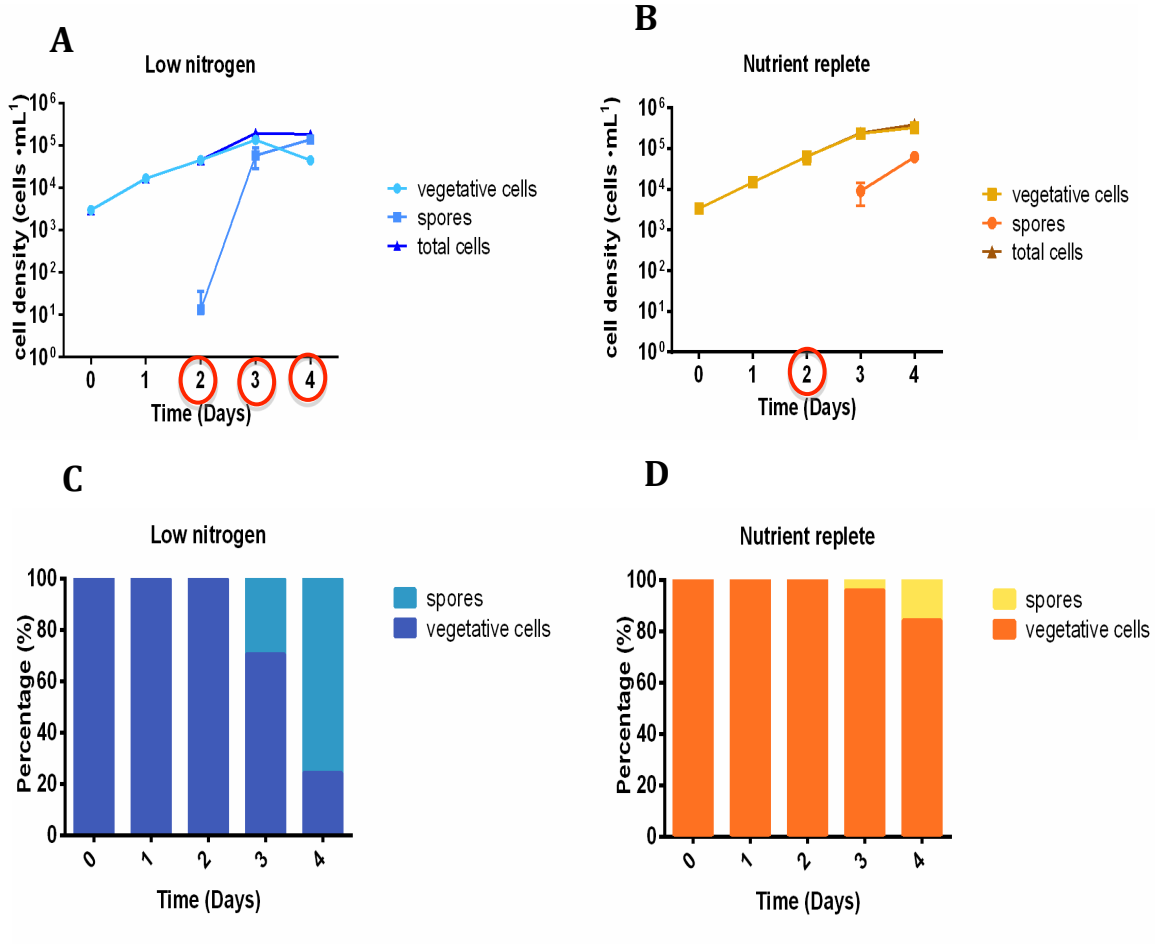

Figure 5.1: Cell density (A, B) and percentage (C, D) of vegetative cells and spores in cultures grown in low nitrogen (treatment, A, C) and nutrient replete (control, B, D) medium. Red circles indicate sampling points for the differential gene expression analysis. Data in panels A and B are shown as average ± S.D. (n=3).

Differential gene expression and Gene Ontology enrichment analysis

The main features of the transcriptome of *C. socialis* are illustrated in Table 5.2. The mean quality value of base pairs in the first 100 bp was around 24 ("reasonable quality"), decreasing towards the end of the read. A total number of 89,300 sequences were assembled with a minimum conting length of 224 bp and a maximum of 8,150. At least the 50 % of the assembled bases were found in contigs that are 887 bases long (N50). The three biological replicates of each sampling point clustered together in the output of the PCA analysis (Fig. 5.2); for this reason all replicates have been taken in account during the analysis of differentially expressed genes.

Table 5.2: Basic statistics of the de novo transcriptome of *C. socialis*

Number of transcripts	89,279
Number of Trinity 'genes'	52,945
GC	45.51
N50	887
Mean (bp)	622.31
Median (bp)	383
Minimum contig length (bp)	224
Maximum contig length (bp)	8,150

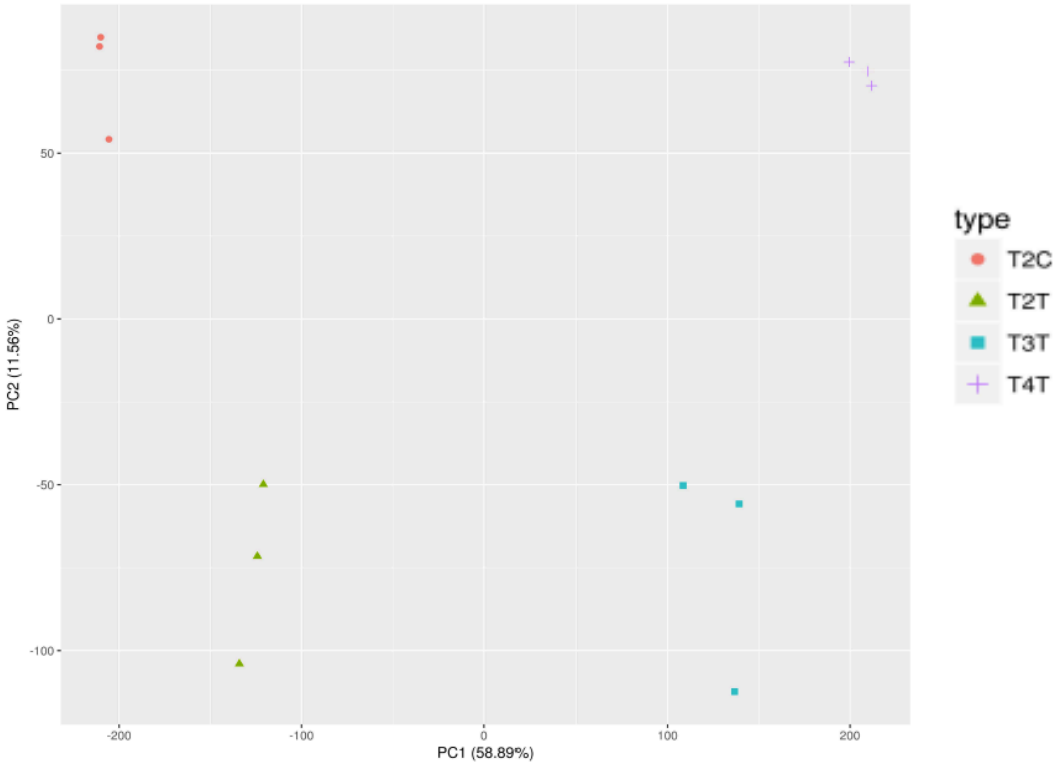

Figure 5.2: Dimensional plot of PCA components 1 and 2 (x and y axis, respectively) of expression values of C. *socialis*.

A very high number of genes were differentially expressed during the formation of spores as shown by the results of the analysis of the four sampling points (Fig. 5.3, Table 5.3).The number of up-regulated genes was lower in the comparison between T2T and control T2C (4221 genes), while it increased considerably in the comparison between T3T and control and T4T and control when 11,135 and 12,870 differentially expressed genes were recorded, respectively. The number of down-regulated genes was in general lower than that of up-regulated ones, but still considerable. The lowest number of down-regulated genes was detected in the comparison between T2T and control with only 273 genes down-regulated genes, whereas the highest was recorded between T4T and the control (4,150).

High numbers of differentially expressed genes were recorded also when comparing the three days of treatment with each other (Fig. 5.3, Table 5.3). As predictable, in these comparisons the T4T had the highest number of up-regulated (9,166) and down-regulated (2,421) genes when compared to T2T, whereas the lowest number of differentially expressed genes was detected in the comparison between T4T and T3T.

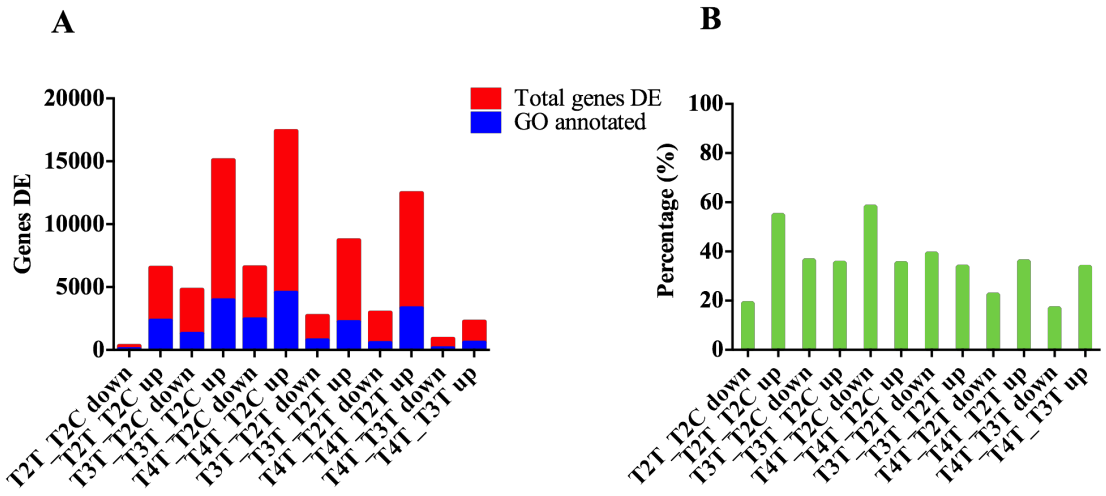

Figure 5.3: A) Number of differentially expressed genes (red) and those annotated with at least one GO term (blue); B) Percentages of differentially expressed genes annotated with GO terms.

Unfortunately, only a minority of these transcripts was already annotated and this

limited the description of gene expression through Gene Ontology (GO) in the different comparisons. Indeed, only an average of 35% of differentially expressed genes was annotated with GO terms (Fig. 5.3). Only in two cases the percentage of annotated genes was > 50%: the up-regulated genes in the comparison of T2T to the control (55%) and the down regulated genes of the comparison between T4T and the control (58%). On the contrary, less than 20% of GO terms were annotated among the down-regulated genes of the comparison of T2T to the control (19%) and between T4T and T3T (17%).

Table 5.3: Number of differentially expressed (DE) genes in the comparisons between the control (T2C) and the treatments at three time points (T2T, T3T, T4T) and between pairs of treatments. For each comparison, the number of DEGs, the number of the individual GO terms (BP= biological processes; MF= molecular functions; CC= cellular compartments),in common between categories (BP_MF _CC, MF_CC, BP_CC, BF_MF); the number and percentage of annotated GO terms are listed for both up- and down-regulated genes and functions (GO annotated).

DE	GO annotated	Comparisons	BP	MF	CC	BP_MF _CC	MF_CC	BP_CC	BP_MF
273	52 (19%)	T2T_T2C down	1	12	7	12	6	8	6
4,221	2,317 (55%)	T2T_T2C up	156	662	764	0	0	0	735
3,514	1,282 (36%)	T3T_T2C down	24	266	171	409	111	73	228
11,135	3,949 (35%)	T3T_T2C up	97	1,128	489	922	401	269	643
4,150	2,419 (58%)	T4T_T2C down	218	1,524	336	3	0	337	1

12,870	4,540 (35%)	T4T_T2C up	112	1,300	572	1,046	448	300	762
1,949	764 (39%)	T3T_T2T down	15	135	91	293	58	29	143
6,514	2,205 (34%)	T3T_T2T up	206	782	471	0	0	0	746
2,421	546 (23%)	T4T_T2T down	13	107	92	135	72	23	104
9,166	3,301 (36%)	T4T_T2T up	275	1,329	665	0	1,032	0	0
759	129 (17%)	T4T_T3T down	5	21	28	29	22	5	19
1,686	570 (34%)	T4T_T3T up	166	91	117	0	0	196	0

Although growth rate and cell concentration of control and treatment cultures were very similar on day 2 (Fig 5.1), the analysis of differentially expressed genes between T2T and T2C showed that cells in T2T were preparing differently (Fig 5.4 for biological processes and Appendix 5.1. for cellular compartment and molecular function). Up-regulated genes in the treatments were related to the assembly of ribosomal subunits, indicating an increase of protein biosynthesis. A different trend was shown by the carbon metabolism, since both gluconeogenesis and pentose phosphate shunt were repressed in T2T. The genes belonging to same biological function were also up-regulated in T3T and T4T. Several binding factors increased in T2T, T3T and T4T compared to the control, and the main molecular function was rRNA processing (Fig. 5.4). This was also the only molecular function under expressed between T4T and T3T, indicating that probably there was a decrease of transcriptional activity in the already formed spores (Fig 5.5).

Following the spore formation process in the treatments, the translation decreased in T3T and T4T as compared to T2T while silica mobilization and DNA replication increased in the last two time points (Fig. 5.5). The comparison between T4T and T3T provides information on biological functions that characterize the spores (Fig 5.5). Here an important role is played by pyruvate-related metabolism and the gluconeogenesis. This latter metabolism however, even though the expression remained lower than in vegetative cells (shown by T4T *vs* T2C). In T4T as compared to T3T there was an increase also in the purine guanosine-5 triphosphate (GTP) biosynthesis that might be used as energetic molecule during translation, gluconeogenesis or be converted in ATP. The translational activity that was over expressed during the formation of spores (comparison between T3T and T2T) was still on going at the last sampling point as shown by the comparison between T4T and T3T. Furthermore, the same comparison showed also the increase of methylation activity that characterized spores already formed. Another interesting biological process that was detected comparing T3T to the control was the biosynthesis of spermidine, known to be a phyto-hormone in higher plants. It was up-regulated also in T4T when compared to T2T but not in the comparison between T4T and T3T. In *Arabidopsis thaliana* it is responsible for the normal embryo development (Imai *et al.*, 2004). Mutants in which the two genes encoding spermidine synthesis were silenced presented abnormal size and arrested the germination in the middle of embryogenesis.

Other important changes that took place during spore formation were related to

the chloroplast thylakoid membranes and the ribosomes, as shown by the comparison of T3T and T4T *versus* control and *versus* T2T (Fig 5.4 and 5.5). Indeed the translation, the photosynthesis with the light harvesting complex and the protein-chromophore linkage were under expressed when spore formation was active (T3T and T4T). Instead when spores were mature (T4 vs T3) the actin mediated cytoskeleton organization was the main biological processes down-regulated, together with the shutdown of transporter activity (included urea transmembrane transporters) and the histone methyltransferases.

T2T_T2C

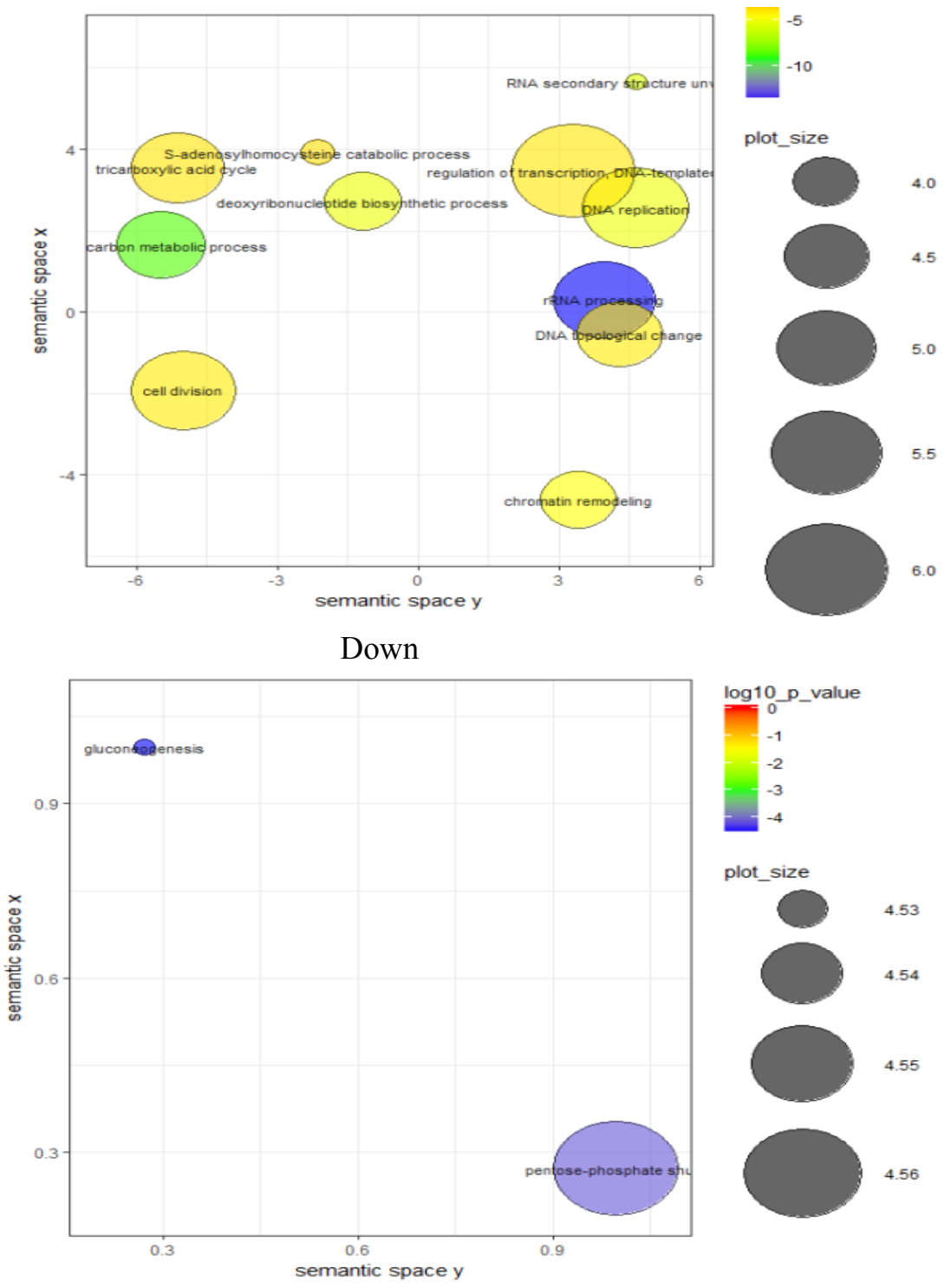

Figure 5.4: Biological processes up (upper panel) and down (lower panel) regulated in T2, T3 and T4 versus control (T2C). The size of the grey circles on the right side of each panel represent the frequency of the GO term in the underlying GO databases (more general terms have larger circles) and the colour code represents the level of statistical significance (log 10 p value). The plots representing the comparisons between T3/T4 and the control are in the next two pages.

T3T_T2C

Up

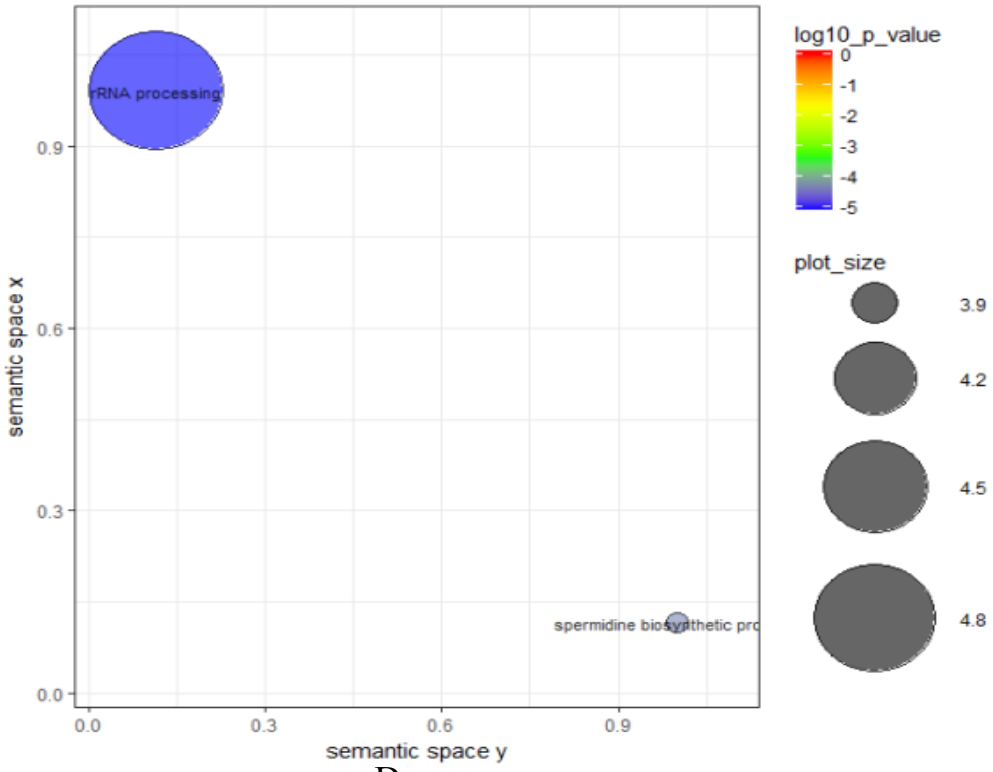

Down

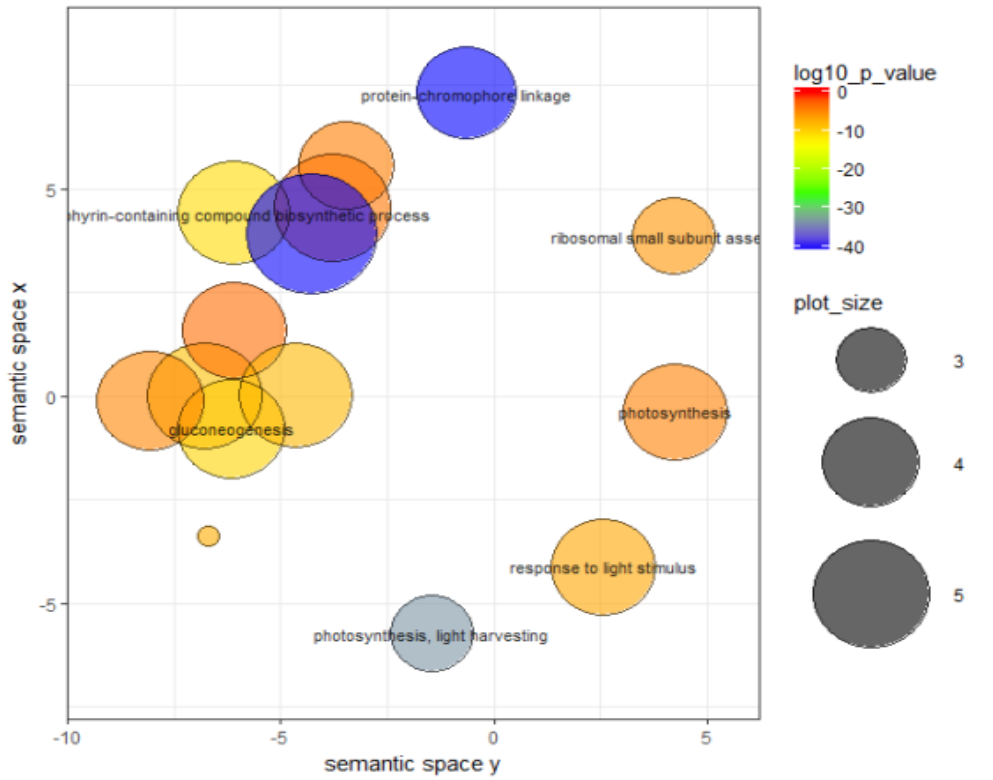

T4T_T2C

Up

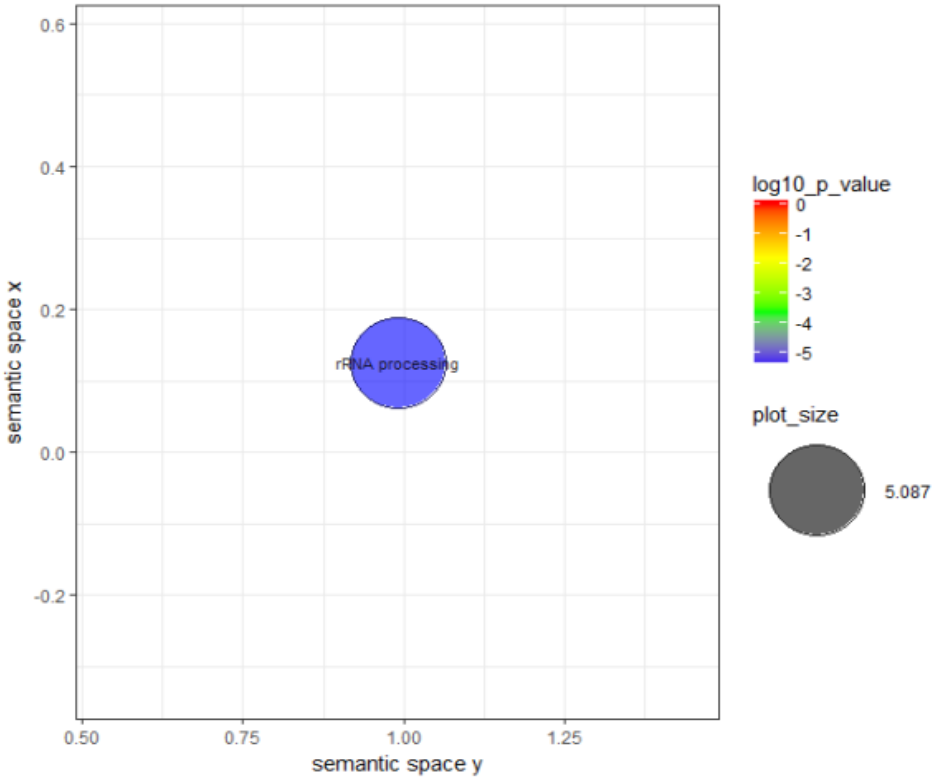

Down

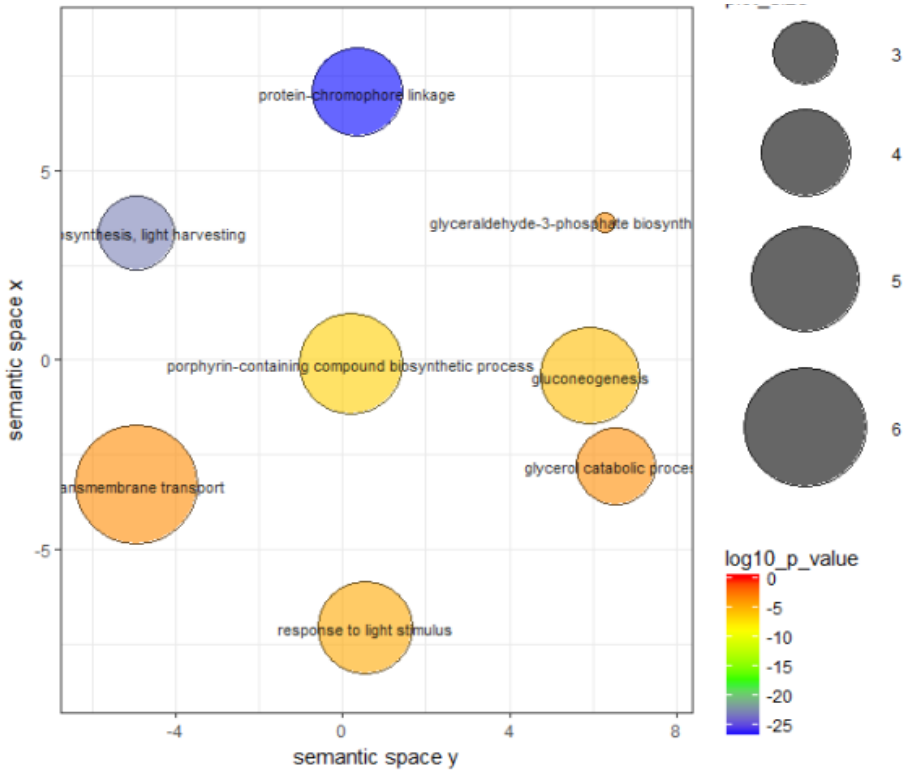

T3T_T2T

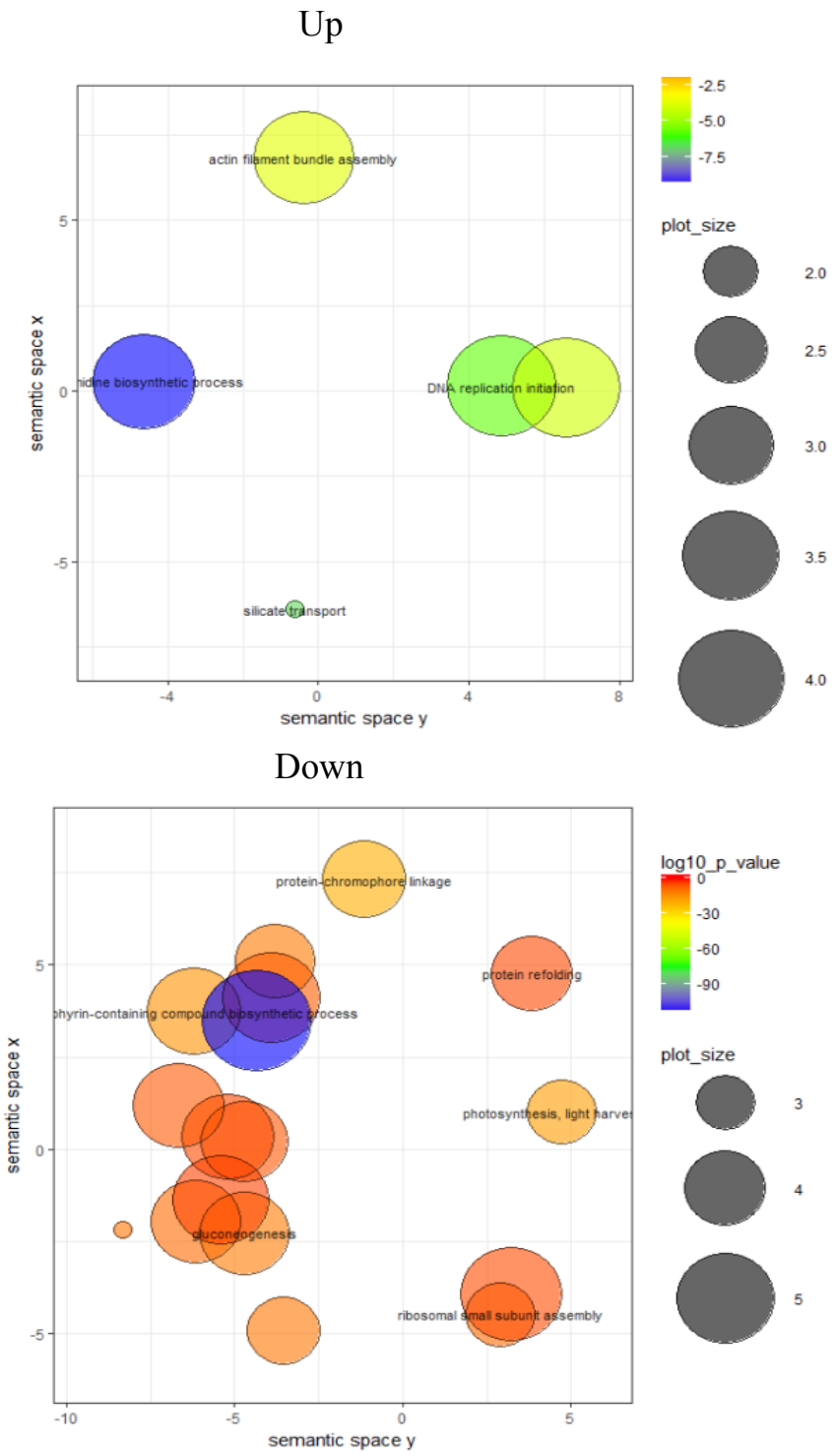

Figure 5.5: Biological processes down (upper panel) and up (lower panel) regulated in T3 and T4 versus treatment (T2T) and each other. The size of the grey circles on the right side of each panel represent size indicates the frequency of the GO term in the underlying GO databases (general terms have larger circles) and the colour code represents the level of statistical significance (log 10 p value). The plots representing the comparisons between T4 and T2/T3 are in next two pages.

T4T_T2T

Up

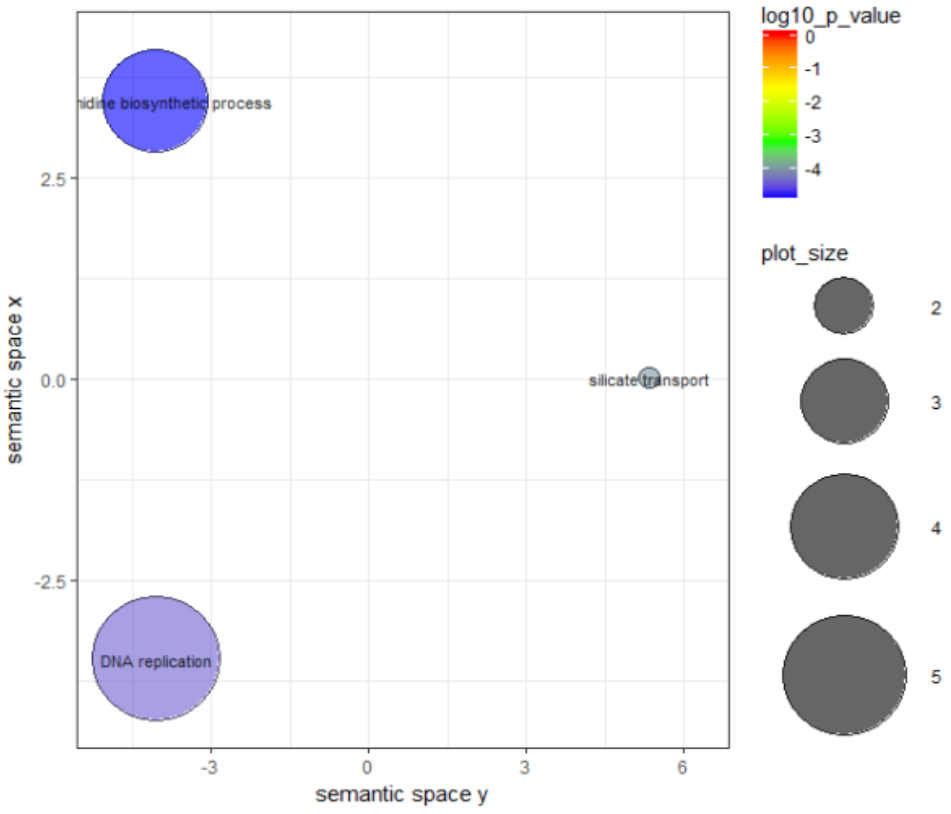

Down

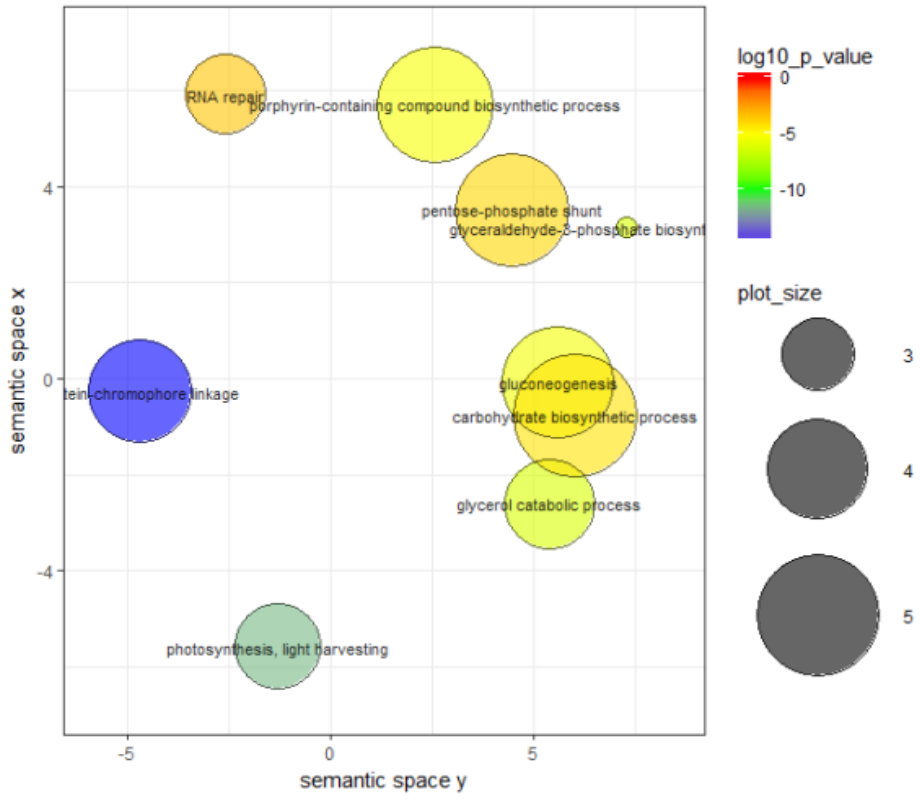

T4T_T3T

Up

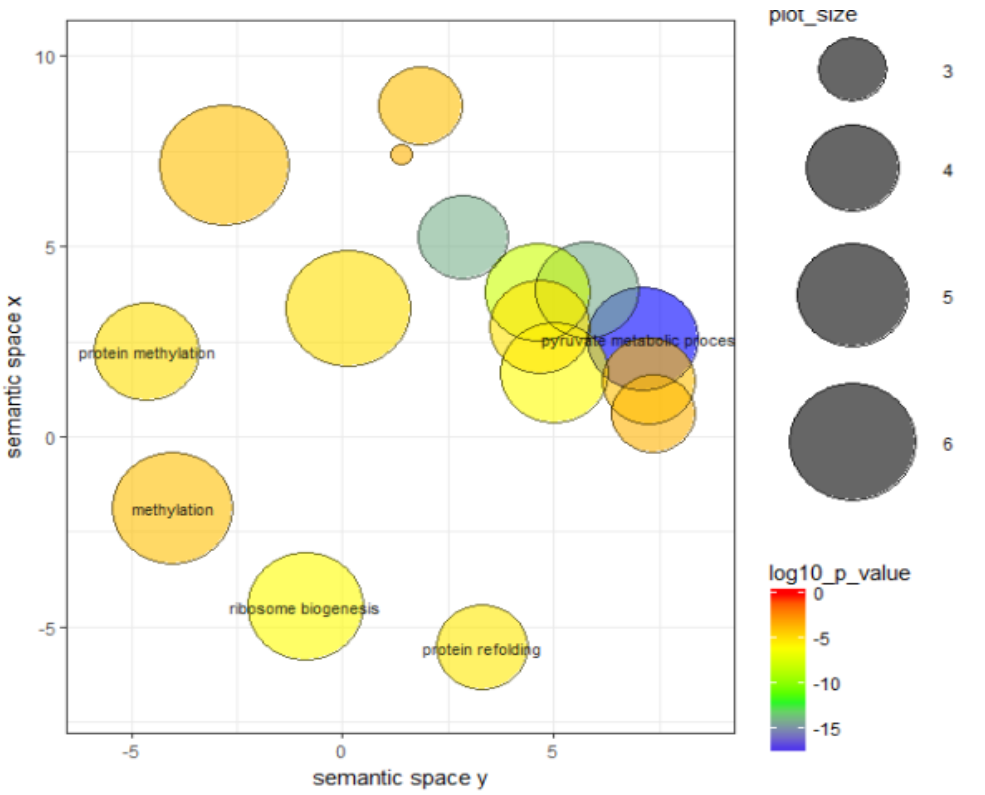

Down

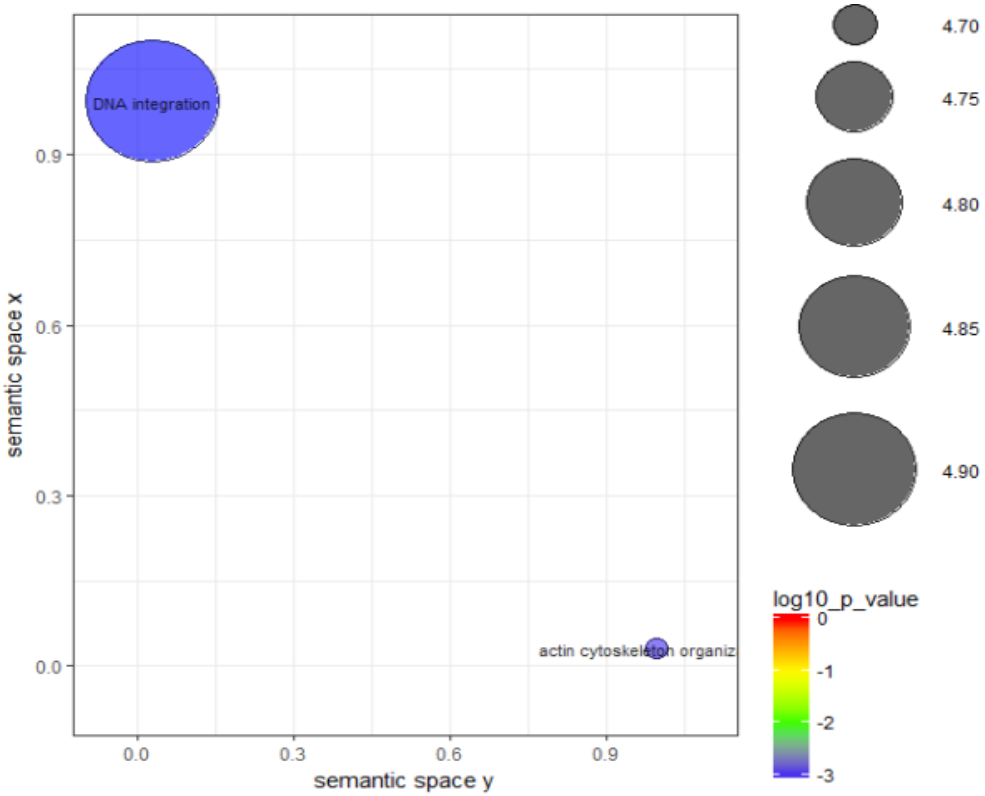

Common and unique transcripts

Additional information was obtained comparing the DEGs common and unique in the comparisons between treatments (T3T and T4T) and the control (T2C) (Fig. 5.6). This approach reduced drastically the number of candidate genes involved in the different steps of spore formation. As expected, the number of up-regulated genes was higher as compared to the down-regulated ones in the comparison of the treatments with the control (Fig. 5.6). The majority of up-regulated genes (10,977) resulted to be shared between T3T and T4T, while 728 genes were uniquely expressed in T3T and 1,939 in T4T (Fig. 5.6.A). A total of 2,567 of down-regulated genes were shared between the two treatments, while the number of unique transcripts was 955 in T3T and 1,592 in T4T (Fig. 5.6 B).

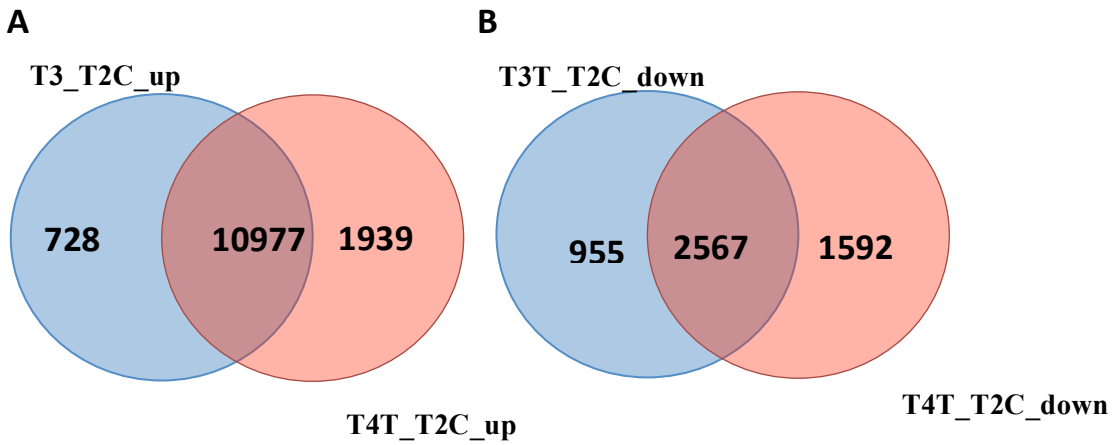

Figure 5.6: Number of up (A) and down-regulated (B) genes common and unique in T3T and T4T compared to the control condition (T2C).

Expression patterns of genes related to specific processes

I mainly focused on the differential expression of genes common in T3T and T4T, when spores were produced, as compared to the control condition. However, describing the pathways analysed I will mention also those genes expressed uniquely in one of these points and or present before spore formation.

I used nitrogen starvation as a cue to induce spore formation in *C. socialis* and one of the first steps of analysis of transcriptomic data was to look at the expression pattern of genes reported in studies on the pennate diatom *Pheaodactylum tricornutum* and the centric *Thalassiosira pseudonana* grown in nitrogen depleted conditions mentioned in

the introduction (Table 5.1). I looked at several pathways searching manually for DE genes and I found several of them partially overlapping with genes differentially expressed in those studies. I also looked at genes related to programmed cell death found in *T. pseudonana* with a transcriptomic approach during Fe-starvation (Thamatrakoln *et al.*, 2013), and at genes induced by nitrogen and phosphorus limitation detected with a proteomic approach (Lin *et al.*, 2017b). Even though the gene expression profile does not always exactly match with the proteins and different stressors were used, several genes were included in both these papers, making them good candidates to be considered in *C. socialis*.

A. *Genes related to spore formation*

In accordance to microscopical observations (see Chapter 2), spore formation requires a mitotic division prior to the deposition of each of the two thicker siliceous thecae. The transcriptome confirmed those observations: many genes related to DNA duplication, such as DNA polymerase and DNA ligases, and silicon transporters were expressed with fold changes from 2 to 8 in all treatments. The same trend was recorded for several ribonucleotides-diphosphate reductases (Supplementary, Table A). The genomic material was not only duplicated but also rearranged to allow the correct transcription of genes involved in spore formation, as suggested by the up regulation of several histone methyltransferases especially in T3T and T4T. Besides genes directly related to DNA replication, high up-regulation both at T3T and T4T was detected for cell cycle control proteins and AAA family cell division control-like proteins, that are genes involved specifically in cell division (Supplementary, Table A).

The rearrangement of cells that were transformed into spores required the activation of a number of genes related to cytoskeleton organization, and tubulin and kinesin-like protein, were highly over-expressed in both T3T and T4T (Supplementary, Table A). At these time points active cytoplasmatic movements characterized cells that were transforming into spores and this is in agreement with the finding of overexpressed genes linked to the synthesis of microtubules.

I could also find three genes that might be specifically involved in the early stage of spore formation (Table 5.4). Two of them are related to the biosynthesis of spore coat polysaccharide layer in two *Bacillus* species, while the third is a well-known protease involved in the germination of seeds in higher plants. The first two genes were

expressed with high fold changes in all treatments as compared to the control (Table 5.4). The formation of spores in *Bacillus* species is related to an asymmetric cell division; at the end of process a resting cell with a different phenotype is formed inside the original mother cell (McKenney *et al.*, 2013). As in diatoms, this stage can cope with harsh environmental conditions and quickly germinate when optimal conditions are restored (McKenney & Eichenberger, 2012; Plomp *et al.*, 2014). It is a multilayer envelope that involves more than 70 different proteins; specifically the transcripts detected in *C. socialis* are required for the correct development of the inner membrane (McKenney *et al.,* 2013) .

The transcript homologous to a protease involved in the germination of seeds in higher plants was weakly over-expressed only in T4T and it could be related to the germination of some mature spores that could have occurred in T4T.

Table 5.4: Differential expression of genes related to resting stage formation; log fold change in the different time point comparisons.

Transcript ID	**Gene**	**Log fold change**					
		T2T_T2C	**T3T_T2C**	**T3T_T2T**	**T4T_T2C**	**T4T_T2T**	**T4T_T3T**
TR24164|c0_g2_i1	Spore coat polysaccharide biosynthesis protein SpsC	4.702	6.370	-	6.081	-	-
TR29215|c0_g6_i1	Spore coat assembly protein ExsA (Fragment)	6.109	11.521	5.412	12.654	6.545	-
TR6310|c0_g3_i1	Germination-specific cysteine protease 1	-	-	-	2.501	2.526	2.030

B. Nitrogen uptake

Diatoms usually use inorganic nitrate taken from the environment that is then reduced to ammonium by nitrate and nitrite reductases. In higher plants, based on the

external concentration of nitrate, root cells can use three types of transporters: i) when the external concentration of nitrate is close to 0.2 mM, diatoms use the constitutive high affinity nitrate transporters (cHATS); ii) when the external concentration is below this value, diatoms are capable to induce another family of high affinity transporters (iHATS); iii) when values are higher than 1 mM they use low affinity transporters (Rogato *et al*., 2015). In this experiment only the constitutive high affinity nitrate transporters (cHATS) were differentially expressed in the treatments (Fig. 5.7). The transcription level of all nitrate transporters was strongly down regulated in T3T and T4T but not in T2T (Fig. 5.7). Although nitrate is the main stock of nitrogen in the ocean, its concentration may be variable and diatoms evolved the capability to take up also ammonium, urea and small nitrogenous molecules. Out of the five ammonium transporters found in *C. socialis,* two were up-regulated in T3T, two only in T4T and one at both time points. One urea-proton symporter DUR3 decreased while the other three were highly expressed during the formation of spores (both T3T and T4T) (Fig. 5.7) suggesting that nitrogen was consumed under reduced forms. Usually when nitrogen is limiting, diatoms increase the expression of nitrate transporters (Bender *et al*., 2014; Alipanah *et al.*, 2015; Levitan *et al.*, 2015b); the only case in which they were found down regulated was when the sole external source of nitrogen was urea or ammonium (Allen *et al.*, 2011).

C. Nitrogen assimilation

The only copy of nitrate reductase in *C. socialis* was down regulated, but with a lower folds change compared to nitrate transporters. A similar decrease in T3T and T4T was detected for one chloroplastic nitrite reductase, while two nitrite reductases (NADH) increased T2T and then weakly decreased in T3T and T4T (Fig. 5.7).

Despite the repression of enzymes involved in nitrate reduction, nitrogen assimilation did not decrease. High levels of expression were observed for the four glutamine synthases type III and the two NAD-dependent ones in T3T and T4T; other two glutamine synthases (one of which type III) were down regulated in T3T. They are implied in glutamate synthesis and one of them showed also a higher fold change in T2T when compared to control. In addition, very high levels of expression were found at both sampling points for four different glutamate dehydrogenases that can catalyse the reversible conversion of 2-oxoglutarate in glutamate. Since the uptake of oxidative nitrogen was limited in the treatments in N-depleted medium, the recycling of nitrogen

from other sources has been probably the most important way to cope with the cell requirements (Fig. 5.7). In *P. tricornutum*, the up-regulation of two of the glutamyl-tRNA amidotransferase and three acemidase/formamidases have been associated to the uptake of nitrogen from other organic compounds (Alipanah *et al.*, 2015). In *C. socialis*, there was the increase of only different subunits of the glutamyl- tRNA amidotransferase, some of them unique of T4T, when spores dominated the sample (Supplementary, Table B).

As reported in other studies (Armbrust *et al*., 2004; Allen *et al.*, 2006; Allen *et al.*, 2011) the urea cycle is one of the main pathways activated in diatoms in nitrogen starvation verifies their capability to take up nitrogen from alternative resources. This capability was confirmed for *C. socialis*. An increase of a single urease, responsible for the production of CO_2 and NH_4^+, was already visible at T2T before spore formation and maintained at high level during all sampling points (Fig. 5.7) even though three urease accessory proteins, were slightly down regulad during spore formation (T3T and T4T compared to control); Highly expressed were three of four amino acid/polyamine transporters (Supplementary, Table B).

Figure 5.7: Differential expression of genes involved in nitrogen metabolism and TCA (Tricarboxyilic Acid) cycle pathway in nitrogen-stressed cultures vs control condition at T2T, T3T and T4T.

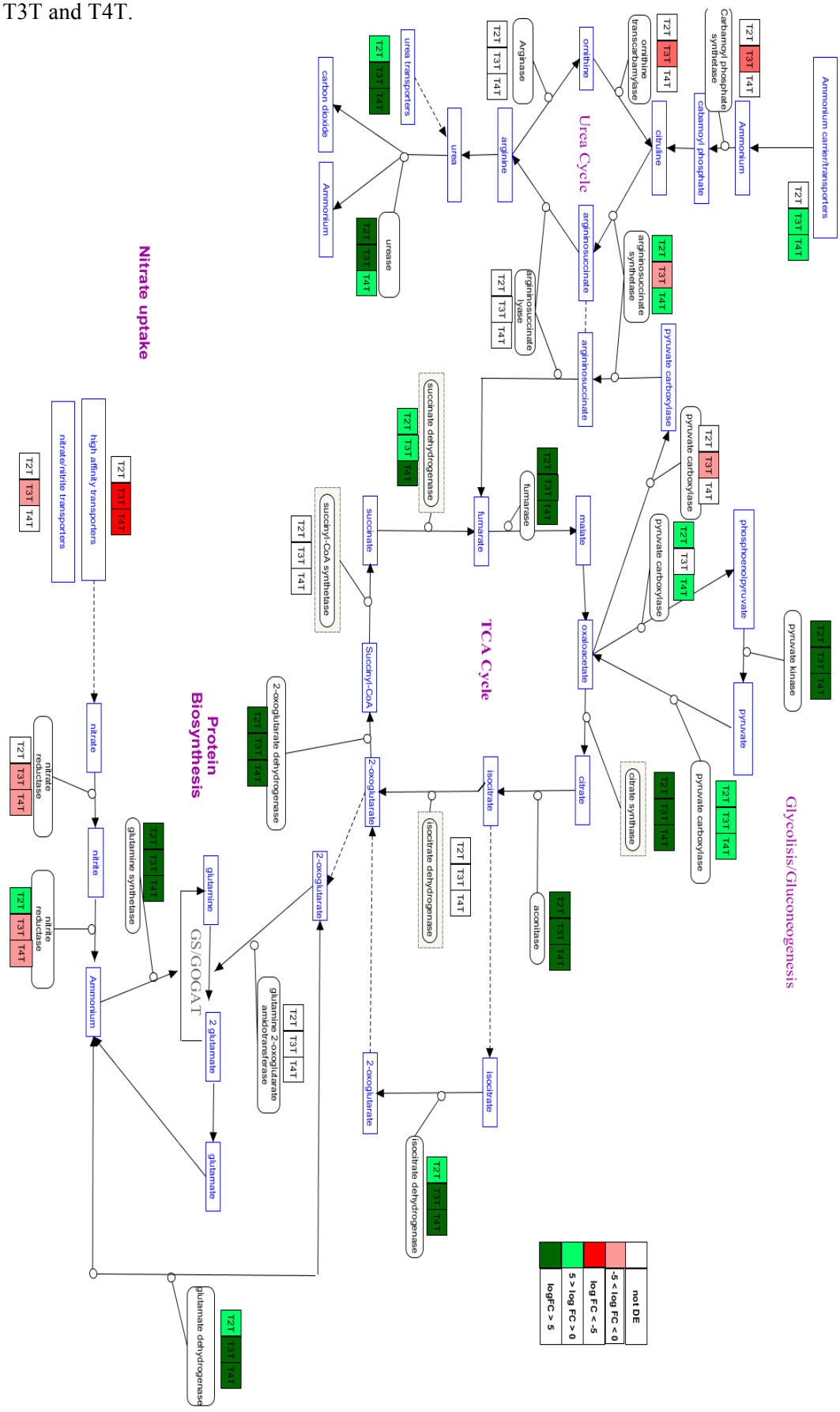

The key enzyme that directs NH_4^+ into the urea cycle, the carbamoyl phosphate synthase, was down-regulated in T3T and not in the other sampling points. This enzyme, as the others involved in the urea cycle, was not differentially expressed compared to control condition but showed an increase in T4T when compared to T3T, suggesting that the urea cycle might increase during spore formation (Supplementary Table B). This is in accordance to the fact that in diatoms, up regulation of the urea cycle was observed only during the recovery from nitrogen starvation (Allen *et al.*, 2011) and never during starvation itself (Mock *et al.*, 2008). In *C. socialis,* as in *Thalassiosira pseudonana,* two members of ornithine biosynthesis included in the urea cycle were differentially expressed: the N -acetyl-g –glutamylphosphate reductase and the N-acetylornithine aminotransferase that showed a slight increase in T4T *vs* control and *vs* T3T, i.e. when spores were already formed (Supplementary Table B). It has been hypothesised that these enzymes may favour the accumulation of reduced forms of nitrogen (Hockin *et al.*, 2012) and this might be particularly useful in the case of resting spores.

The repression of protein biosynthesis observed for N-limited cultures of *Thalassiosira pseudonana* (Mock *et al.,* 2008) was not evident in *C. socialis*: only two aminoacyl-tRNA synthases - that bind amino acids in a peptide - were weakly down regulated one in T3T and the other in T4T (Supplementary, Table B). On the contrary, numerous transcription elongation factors, transcription initiation factors ribosomal subunits and several tRNA synthetases were up regulated in T3T and T4T, and some also in T2T. Simultaneously also the amino acid biosynthesis increased; indeed, the strongest down regulated transcripts found in *T. pseudonana*- homoserine dehydrogenase and l'N- acetylglutamate kinase were only weakly repressed compared to those transcripts related to amino acid biosynthesis. This indicates that protein biosynthesis increased notwithstanding nitrogen limitation. While species that do not form spores can simply stop protein synthesis, those that form spores might keep synthesizing the ones that are needed to produce the spore. They thus need nitrogen and this is why N recycling is particularly important in *C. socialis*.

However, protein biosynthesis was always accompanied by the degradation of cellular material. The overexpression of several aminopeptidases, two carboxypeptidases, and several proteases and aminotransferases at T3T and T4T suggests the presence of protein degradation. As reported for other diatoms grown in N-limited conditions (Alipanah *et al*., 2015), many peptidylpropyl isomerases, involved in

protein folding were strongly down regulated at all time points (Supplementary, Table B). More important was the catabolic process operating on proteins and amino acids that involved different endopeptidases that were highly over expressed in both T3T and T4T. High expression values of proteasome subunits (a complex of proteins that are involved in the same process) and their activators were found in treatment conditions and were accompanied by high expression values of ubiquitins, small proteins that tag the ones that should be degraded. The up-regulation of all this enzymes responsible for the breakdown of specific substrates may be a way to respond to nitrogen starvation and obtain the macromolecules necessary for the formation of spores. In accordance to this, several autophagy-related proteins were up-regulated at all sampling points (Table 5.6.). It has been shown that these proteins, involved in the degradation of long-lived proteins, help the recycle of macromolecules in conditions of nutrient limitation (Onodera & Ohsumi, 2004).

Besides proteins, nitrogen is also involved in the formation of nucleobases: several uracil/xanthine permease and adenine/guanine permeases – involved both in biosynthesis and degradation of purines and pyrimidines - were weakly up-regulated (Supplementary, Table B).

Table. 5.6: Differential expression of genes related to autophagy; log fold change in the different time point comparisons.

Transcript ID	**Gene**	**Log fold change**					
		T2T_T2C	**T3T_T2C**	**T3T_T2T**	**T4T_T2C**	**T4T_T2T**	**T4T_T3T**
TR182|c0_g1_i1	Autophagy-related protein 9	-	-	-	3.974	3.634	2.275
TR7823|c0_g4_i1	Autophagy protein 5	2.410	3.690	-	3.916	-	-
TR6650|c0_g3_i1	Autophagy-related protein 18a	-	3.283	-	3.617	2.293	-
TR27967|c0_g1_i1	Autophagy-related protein 9	2.124	-	-	3.072	-	-
TR4098|c0_g2_i1	Activating molecule in BECN1-regulated	-	2.060	-	2.141	-	-

	autophagy protein 1						

While the nitrogen derived from the degradation of amino acids and proteins might be recycled, the carbon skeletons activated the Tricarboxylic Acid Cycle (TCA cycle also known as Kreb's cycle) as shown in Fig 5.7.

D. Carbon metabolism

In this section the major pathways involved in carbon skeleton and reduction power production are illustrated. Some of them are necessary for the cell survival, such as those relative to carbon fixation and glycolysis. Since CO_2 is volatile, photoautotrophs evolved mechanisms for its concentration within cells that implicate the use of carbonic anhydrases. Those mechanisms were active during the entire experiment. Of the ten differentially expressed genes carbonic anhydrases detected in *C. socialis*, six were up-regulated in T2T, T3T and T4T whereas the others were slightly down regulated only in T3T and T4T (Supplementary, Table C). Additionally, two sodium bicarbonate co-transporters were found up-regulated in T2T and T4T and in T3T and T4T, respectively. Several pathways related to carbon metabolism were differentially expressed during the experiment.

Enzymes responsible for carbon fixation showed contradictory trends: the ribulose bisphosphate carboxylase, were repressed both in T3T and T4T while several phosphoglycerate kinases increased in T2T (Supplementary Table C).

Increased expression of genes related to the pyruvate metabolism was observed, as already shown by GO terms, during spore formation. For example, pyruvate phosphate dikinases, responsible for the conversion of pyruvate to phophoenolpyruvate without the consumption of ATP, were up-regulated in all treatments (Supplementary Table C).

Genes in common between gluconeogenesis and glycolysis were over-expressed during spore formation (T3T and T4T). Some intermediates of glycolysis were down regulated during spore formation, although the key enzymes were overexpressed in T3T and especially in T4T (Supplementary Table C). Examples were the differential expression of several glyceraldehyde-3 phosphate dehydrogenases at T4T and the up regulation of pyruvate kinases; out of nine of these enzymes, three were up regulated at

all sampling points (T2T, T3T and T4T) compared to the control, while the others only during spore formation, at T3T and T4T.

The pyruvate produced with these pathways may enter in TCA cycle thanks to the pyruvate dehydrogenase. Also the increase of short chain acyl- coenzyme A dehydrogenases and the long-chain fatty acid CoA ligases, suggest the central role of TCA cycle; through the β-oxidation of fatty acids these enzymes produce the main substrate Acetyl-CoA and reduction power (NADH and $FADH_2$) (Supplementary Table D). The activity of these transcripts increased proportionally to the increase of spores.

The majority of TCA cycle enzymes were in fact always highly expressed during the experiment, especially in T3T and T4T (Fig. 5.7).

Another induced pathway was the pentose phosphate pathway (PPP) that produces reducing power (NADPH), 5-carbon sugars and ribose 5-phosphate, the precursors of nucleotides used for both replication and transcription (Fig. 5.8). In *P. tricornutum,* only the enzymes of the oxidative phase responsible of the formation of NADPH were up-regulated (Alipanah *et al*., 2015), while in *C. socialis* also the enzymes involved in the formation of sugars were significantly upregulated during spore formation. This was expected, since cells in this phase are undergoing to DNA replication and also translation.

In accordance with those observed in *Phaeodactylum tricornutum* (Levitan *et al.*, 2015) most transcripts related to the fatty acid biosynthetic pathway were down regulated; the production of energy from their oxidation seemed to be important, as shown by the significant up regulation of carnitine acetyl transferase (Supplementary, Table D).

The production of the reserve compound crysolaminarin trough the 1, 3 ß-glucan synthase was also detected during spore formation. This compound was also consumed during all sampling points as shown by the up-regulation of several exo 1, 3 ß glucosidases (Table 5.7).

Since the fatty acid biosynthesis seemed to be repressed during spore formation, it is possible that the pathway used by spores to synthesize storage lipid compounds was the conversion of carbohydrates into lipids as shown by the high fold change values of

glycerol 3 phosphate dehydrogenases (Supplementary Table D).

Table 5.7: Differential expression of genes related to the metabolism of crysolaminarin; log fold change in the different time point comparisons.

Transcript ID	Gene	Log fold change					
		T2T_T2C	T3T_T2C	T3T_T2T	T2T_T2C	T4T_ T2T	T4T_ T3T
Crysolaminar biosynthesis							
TR3717|c0_g1_i1	1 3-beta-glucan synthase	5.511	7.853	2.342	8.527	3.016	-
TR21832|c0_g1_i1	Putative callose synthase 8	6.212	7.474	-	8.203	-	-
TR20125|c0_g4_i1	Transketolase	-	-4.745	-3.259	-3.924	-2.438	-
Crysolaminarin degradation							
TR1706|c0_g3_i1	Exo-1 3-beta-glucosidase	-	2.4698	-	-	-	-
TR22778|c0_g1_i2	Exo-1 3-beta-glucanase	-	2.236	2.374	-	-	3.237
TR23747|c0_g3_i1	Exo-1 3-beta-glucanase	2.469	7.223	4.754	7.828	5.358	-
TR27055|c0_g3_i7	Endo-1 3-beta-glucanase	-	2.401	-	3.506	2.741	-

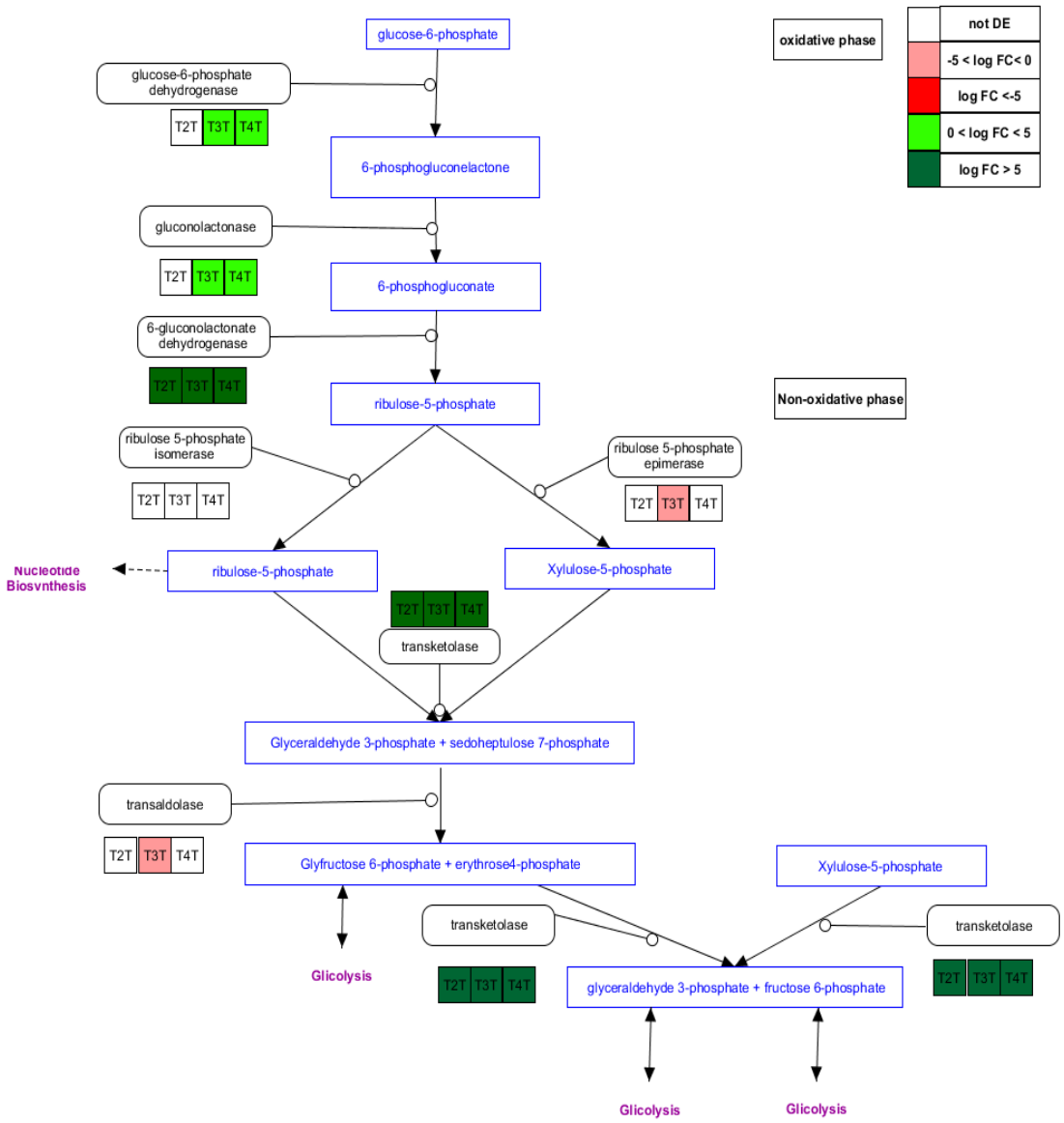

Figure 5.8: Differential expression level of genes involved in Pentose Phosphate Pathway in nitrogen-limited cultures vs control condition during at T2T, T3T and T4T.

A common consequence to nitrogen starvation is the accumulation of neutral lipids (triacylglycerols, TAG) through the *de novo* biosynthesis from the glycerol-3-phosphate (Alipanah *et al.*, 2015). This is in accordance with the expression profile of several related enzymes, especially at T3T and T4T as, for example, glycerol-3-phosphate dehydrogenase (Fig. 5.9). Alternative pathways involved in the accumulation of TAG were the breakdown of glycerophospholipids and sphingolipids, as shown by the up-regulation of several phospholipases and ceramidases that started already before spore formation and the use of an acyl-CoA-independent mechanism that involve phospholipid:diacylglycerol acyltransferase (Fig. 5.9); their activity increased over time,

starting with a weakly up regulation before spore formation. These mechanisms seem to be common to diatoms under nitrogen starvation as observed in *P. tricornutum* (Alipanah et *al.,* 2015).

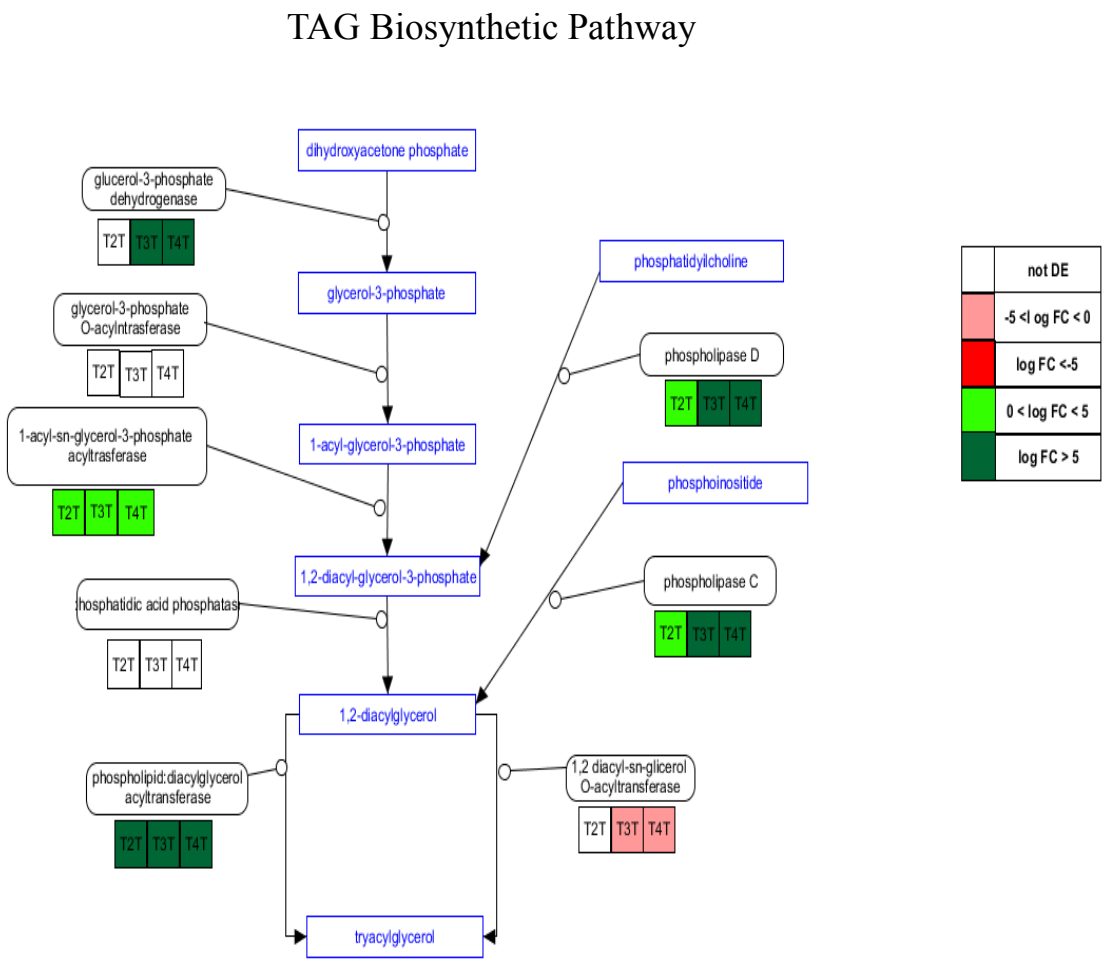

Figure 5.9: Differential expression level of genes involved in TAG biosynthesis in nitrogen-stressed cultures vs control condition during at T2T, T3T and T4T.

E. Photosynthesis

The reduction of nitrogen uptake can cause decrease in the transcripts involved in photosynthetic pathway for two reasons: the first is related to the nature of chlorophylls (they are molecules containing nitrogen), the second to the protection against reactive oxygen species that are produced by the electron flow through the photosynthetic apparatus when they cannot be dissipated when carbon skeleton are scanty. Indeed, the chlorosis (yellowish colour due to the lack or degradation of chlorophyll) of a culture and the decrease in the photosynthetic yield are general features of nitrogen starvation) (Hockin *et al*., 2012; Bender *et al*., 2014). The same process has been observed in this study, as shown by the strong down regulation of protein D1 of the photosystem II in

T3T and T4T (Supplementary Table E). The same trend was observed for many other transcripts related to both chlorophyll and fucoxanthin biosynthesises and for mRNAs associated to photosystem II and I (Supplementary Table E). However, high expression level (more than 6 log fold change) was found for two 12 kDa extrinsic proteins of photosystem II, a photosystem II reaction center PSB28 protein and some fucoxanthin chlorophyll *a/c* proteins that were all highly expressed at the same time points. These proteins are usually involved in the light-induced turnover of D1 in the PSII damage–repair cycle (Bondarava *et al.*, 2005). Also three differentially expressed geranylgeranyl reductases were up-regulated in all treatments (T2, T3 and T4); these enzymes, crucial for the biosynthesis of chlorophyll in higher plants, were usually found down regulated both in *P. tricornutum* and *T. pseudonana* (Hockin *et al*., 2012; Alipanah *et al*., 2015). The energy derived by light was then probably converted to reduced equivalent (NADPH) thanks to chloroplastic ferredoxin-NADP reductase root type that was highly expressed before and during spore formation.

At T3T and T4T, protection of the cell from oxidative stress was conferred by the xanthophyll cycle as demonstrated by the down regulation of zeaxanthin epoxidase and the concomitant up regulation of two violaxanthin de-epoxidases (Supplementary Table E); these enzymes allow the dissipation of the excess energy as heat in the process known as non-photochemical quenching. It was already observed that in spores of *Chaetoceros pseudocurvisetus* exposed to different light regimes, the xanthophyll cycle increased compared to vegetative cells and it was particularly high at high irradiance conditions (Oku & Kamatani, 1999). The activation of the xanthophyll cycle avoids the production of triplet and singlet oxygen that may destroy the chloroplast membranes and induce the death of cells.

Another process that was induced by spore formation is the activation of photoreceptors that will be further discussed in Chapter 6. Several cryptochromes were up regulated specifically in T3T and T4T, while a single aureochrome was already up regulated before spore formation, i.e. at T2T (Table 5.8). Both are stimulated by the blue light, but have different functions: cryptochromes might be involved in the repair of DNA damages (Jaubert *et al.*, 2017) while the aureochrome is a transcription factor and may be involved in the gene network related to spore formation.

Table 5.8: Differential expression of photoreceptors; log fold change in the different time point comparisons.

Transcript ID	Gene	Log fold change					
		T2T_T2C	T3T_T2C	T3T_T2T	T4T_T2C	T4T_T2T	T4T_T3T
TR28590|c0_g1_i1	Cryptochrome-2	-	5.013	5.013	5.933	5.933	-
TR14554|c0_g1_i1	Cryptochrome-2	-	3.676	6.901	3.899	7.122	-
TR3562|c0_g1_i1	Cryptochrome-1	-	5.406	-	6.369	2.822	-
TR15325|c0_g1_i1	Cryptochrome DASH chloroplastic/mitochondrial	-	2.736	-	2.369	-	-
TR31632|c0_g1_i1	Cryptochrome/photolyase-like protein	-	3.185	2.422	3.813	3.050	-
TR8582|c0_g1_i1	Blue-light-activated protein	3.761	3.854	-	4.479	-	-

F. Fermentation /Anaerobic respiration

One of the feature of resting stages is their capability to survive also in anoxic conditions for very long times (Härnström *et al.*, 2011). It has been hypothesized that this capability is related to use nitrate as donor of electrons for the respiration. This metabolism is well known in bacteria and fungi while very little information are present for diatoms (Catalanotti *et al.*, 2013). It has been shown that the internal nitrate pool is used by the benthic diatom *Amphora coffaeformis,* through a dissimilatory pathway to ammonium, to respire in dark and anoxic condition (Kamp *et al.*, 2011). During conditions of strict anoxia the ammonia fermentation (Fig. 5.10) uses the reductant (NADH) produced by the oxidation of ethanol to acetate to reduce nitrate to ammonia with the production of ATP. In case of hypoxic conditions the oxidation of ethanol to acetate is used to reduce nitrite in N_2O that is then excreted. Many aldehyde

dehydrogenases and an acetate kinase were up-regulated when spore formation was going on (in T3T and T4T). However in this case spores were in oxygenic conditions and both nitrate reductase and nitrite reductase were down-regulated. While it is possible that spores of C. socialis use the fermentation both in aerobic and anaerobic conditions the role of nitrogen might be active only when spores are in the sediments.

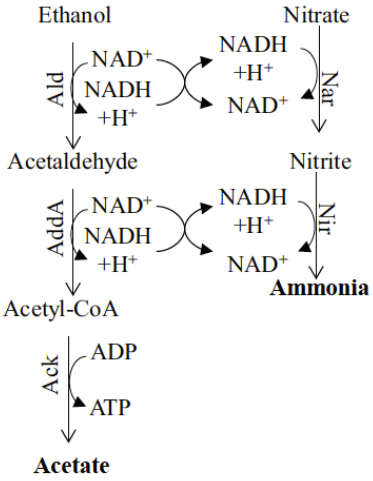

Figure 5.10: Ammonia fermentation pathway. Image taken from Catalanotti et al., 2013. Ald: alcohol dehydrogenase; AddaA: acetaldehyde dehydrogenase; Ack: acetate kinase.

G. Oxidative stress and programmed cell death

Cell differentiation has been related to the responses to the oxidative stress in many organisms (reviewed by (Aguirre *et al.*, 2005). This kind of stress induced by nitrogen starvation has been investigated with a proteomic approach in *Thalassiosira pseudonana* and compared to that produced in phosphorus-limited cultures (Lin *et al.,* 2017). I used the results obtained by these authors to evaluate the reaction of *C. socialis* under the same stress.

A high expression of transcripts coding for antioxidant molecules that most probably represent a reaction to the production of reactive oxygen species (ROS) was detected during spore formation in *C. socialis* without a specific trend. Peroxiredoxin was found up-regulated only at T3T, while the superoxide dismutase was slightly up-regulated in T4. One catalase and one mitochondrial glutathione peroxidase slightly increased both in T3 and T4, similarly to what was observed in N-starved *T. pseudonana*. High values of a putative ascorbate peroxidase and an L-ascorbate were

found at the same sampling points. These enzymes were already found up-regulated in Fe- and Si-limited cultures of *P. tricornutum* (Mock *et al*., 2008; Thamatrakoln *et al.*, 2013).

Although many proteins related to photosystem II and I were down regulated, important enzymes for the dissipation of electron flow were maintained high. For example, several ferredoxin NADP-reductases that are the last acceptors of the photosynthetic electron transport were differentially expressed: six of them increased before spore formation, and two of them were maintained up-regulated also at T3 and T4. However, at these time points, the oxidative stress was reduced increasing extrinsic proteins of photosystem II as in *T. pseudonana* (Alipanh *et al.,* 2015).

Another source of ROS production may be mitochondrial respiration but no specific antioxidant mechanism was found while many different proteins responsible for the repair of DNA were highly up regulated at all treatment sampling points (Supplementary Table F). Particular importance in signal transduction has been related to nitric oxide. It can be produced by nitrate reductase during nitrogen assimilation or by nitric oxide synthase (NOS). It regulates hormonal and defence responses in higher plants but also the development of fruiting bodies in fungi (Aguirre *et al.,* 2005). In *C. socialis* this enzyme was only weakly upregulated when spores were formed (T4),

The oxidative stress leads the activation of programmed cell death. Ten different metacaspases were differentially expressed in *C. socialis*. They did not show the same trends: six of them were up-regulated at T3T and T4T with log fold changes higher than 5, and two were also highly expressed at T2T (Table 5.9). The upregulation of several caspases together with the increase of other apoptosis markers such the histone 4 and the calmodulin in all treatments points leads to the idea that the expression of apoptosis markers is connected to the formation of spores. A support to this idea is the fact that many heat shock transcription factors were highly expressed in T3 and especially in T4 (Supplementary Table F). The number and expression level of these factors was high as compared to what was recorded for other diatoms in nitrogen limitation studies. In addition, other proteins related to programmed cell death, especially metacaspases, were also found upregulated both at T3 and T4, the time points at which spores were produced. The upregulation of metacaspases was already found in other phytoplanktonic species experiencing nitrogen starvation (reviewed by Bidle, 2015 and Lin *et al*., 2017). However, none of those species were spore formers. It is thus possible that sophisticated machineries that include both genes related to cell death and oxidative

stress act as signalling mechanisms to induce spore formation sending the message: 'form a spore or die'.

Table 5.9: Differential expression of metacaspases; log fold change in the different time point comparisons.

Transcript ID	Gene	Log fold change					
		T2T_T2C	T3T_T2C	T3T_T2T	T4T_T2C	T4T_T2T	T4T_T3T
TR19162|c0_g6_i1	Metacaspase-1	2.077	4.715	2.638	5.0362	2.959	-
TR10482|c0_g4_i1	Metacaspase-1	-	10.508	6.006	12.631	8.129	2.123
TR19162|c0_g5_i1	Metacaspase	4.837	8.170	3.332	10.060	5.223	-
TR19162|c0_g8_i1	Metacaspase	-2.111	-	-	-4.322	-2.211	-2.762
TR27105|c0_g1_i1	Metacaspase-1B	-	-2.014	-	-3.921	-2.859	-
TR26562|c0_g1_i2	Metacaspase-1A	-	-	-	-3.185	-	-2.612
TR27105|c0_g2_i1	Metacaspase-1	-	-	-2.366	-	-	-
TR26562|c0_g2_i1	Metacaspase-1	-	7.172	5.549	9.073	7.450	-
TR19162|c0_g6_i1	Metacaspase-1	-	6.720	4.643	8.762	6.684	2.041

H. Genes related to sexual reproduction

One of the opportunities of using a transcriptomic approach is the possibility to look for biological processes otherwise difficult to find. In diatoms, for example, a potentially underestimated and understudied process, both in cultures and in the natural environment, is sexual reproduction that is crucial for the restoration of their cell size. The main two reasons are the very low frequency by which this event happens and the low number of cells in the population that undergo meiotic division producing gametes. This makes very difficult to recognise sexual stages with a classical microscopical approach. Fortunately, in the last years transcriptomic approaches allowed the

identification of molecular markers that can be used to track meiosis and gametes formation (Patil *et al.*, 2015; Nanjappa *et al.*, 2017). In centric diatoms like *C. socialis,* the only flagellate stages are the male gametes (Montresor *et al.*, 2016). The intraflagellar transports (ITF) proteins are related to the development of flagella. These genes usually are subdivided in three classes: ITF-A, ITF-B and BBSome. While all diatoms have lost the last class, the presence of ITF-A genes was confirmed for the centric diatom *Leptocylindrus danicus* undergoing sexual reproduction (Nanjappa *et al.*, 2017). Genes involved in meiosis have been searched in the available diatom genomes and are illustrated in Patil *et al.* (2015). I tested the presence of flagellar and meiotic genes in *C. socialis*; I do not have evidence for the presence of flagella or auxospores in my experiments but, due to the very small size of *C. socialis* and their possible low abundance, these stages might have been easily overlooked. Moreover, in centric diatoms sexual reproduction is related to a wide range of environmental cues, including nitrogen depletion (Montresor *et al*., 2016) and this is another motivation to search for the possible expression of these genes.

Several transcripts indicate that this process was ongoing. Four distinct transcripts related to ITF-A, common to T3 and T4 were found up-regulated, three of which with high fold change (Table 5.10). Furthermore, 56 genes related to the meiotic process were also up regulated (Supplemetary, Table G), of which three known to have a function exclusively during meiosis (Table 5.10).

Table 5.10: Differential expression of genes related to synthesis of flagella and meiosis; log fold change in the different time point comparisons.

Transcript ID	**Gene**	**Log fold change**					
		T2T_T2C	**T3T_T2C**	**T23T_T2T**	**T4T_T2C**	**T4T_T2T**	**T4T_T3T**
Flagellar genes							
TR9976|c0_g1_i1	Intraflagellar transport protein 122 homolog	-	6.685	6.685	9.710	9.710	3.024
TR5554|c0_g1_i1	Intraflagellar transport protein 122 homolog	-	6.665	6.665	9.372	9.372	2.707
TR13529|c0_	Intraflagellar transport	-	3.806	3.823	4.517	4.534	-

g1_i1	protein 140 homolog						
TR13529|c0_g2_i1	Intraflagellar transport protein 140 homolog	-	2.471	-	3.251	2.584	-
Meiotic genes							
TR26915|c0_g3_i1	Mer3 meiotic cross-over helicase	-	5.510	5.510	5.666	5.666	-
TR24097|c0_g1_i1	Mer3 meiotic cross-over helicase	-	3.040	-	3.217	2.877	-
TR8458|c0_g2_i6	Mnd1 meiotic DNA recombination/cross-over promotion	-	2.882	2.776	3,902	3.797	-
TR21047|c0_g1_i19	DNA mismatch repair protein MSH4	-	4.001	2.100	4.595	2.694	-

Top 20 genes

I looked to the top 20 genes up regulated genes in the comparison between T2T, T3T and T4T to control condition. Out of the initial 60 genes obtained for all the three comparisons, all transcripts of T2T *vs* T2C were common to the other comparisons of treatments to control condition, but usually the fold change increased from T2T to T3T while remained constant from T3T to T4T (Appendix 5.2). Only six were not identified in T2T and one was unique of T3T. The number of gene annotated was extremely low, since only seven had a known function: five of them belong to different pathways, i.e. transcription, TCA cycle, chlorophyll biosynthesis and nitrogen assimilation and antioxidant response that were treated in the previous sections. The other two transcripts were the UPF0187 protein alr2987, a multipass membrane protein with unknown function and a heat shock protein involved in the actin polymerization (Table 5.4). This latter protein has been found over expressed during the formation of resistant cells in *Dictyostelium discoideum* (Serafimidis *et al.,* 2007) and is responsible of their resistance to the antibiotics; It might important also in the formation of resting spore in *C. socialis.* Although these genes represented the main pathways involved during the

metabolic rearrangement of a cell undergoing spore formation, they highlight how scanty is the molecular information relative to this biological process.

Conclusions

The formation of spores in diatoms, as that of resting stages in bacteria and seeds in plants, is a very articulate process that involves the entire cell metabolism and molecular machinery.

In *C. socialis,* nitrogen starvation induced modifications of metabolic pathways similar to those recorded in other diatoms in similar conditions. However, some processes were clearly related to the formation of spores, such as the over-expression of genes involved in DNA duplication (mitotic divisions precede the deposition of spore thecae) and of silicon transporters that are usually not expressed in other N-depleted diatoms. During the formation of spores, the main nitrogen source was ammonium, while the uptake of oxidized nitrogen forms, as nitrate and nitrite, was down regulated. This response is in accordance with what was seen in N-limited *Emiliania huxleyii* (Bruhn *et al.*, 2010), while it is different from the response in the other diatoms, either due to the specificity of the process of spore formation or to variability among different diatom groups. The expression of enzymes responsible for the degradation of different organic compounds containing nitrogen might give *C. socialis* the possibility to access additional sources of this element needed for DNA replication and the synthesis of spore-specific proteins.

The degradation of membrane lipids and their conversion to TAG may allow for survival in dark condition since they represent a form of energy storage. Noteworthy is the activation of fermentation pathway that could be the metabolic process allowing their survival over time in anaerobic conditions and that needs further investigations.

However, certain processes remain poorly delineated, probably due to the fact that not all cells were turning into spores at the same time and in the samples collected at T3T, but also at T4T, there were both spores and vegetative cells. This, for example, is the case of the crysolaminarin metabolism that showed enzymes related to both its synthesis and degradation. Notably, there was not any metabolism that was completely

down regulated making it more difficult to decipher what characterized cells forming spores from those that were still in a vegetative stage, probably senescent.

Spore formation in *C. socialis* involved the transcription of many genes related to the response to oxidative stress and the up-regulation of several genes related to apoptosis. It is common also in bacteria to produce resting stages in harsh environmental conditions (Lennon & Jones, 2011). A common response to different environmental stresses is the production of reactive oxygen species (ROS) within the cell that can be fatal or can induce cell differentiation. For example, reactive species of oxygen and nitrogen increase during spore formation in fungi (Aguirre *et al*. 2005). Among algae, ROS production following environmental stress (temperature increase) induced sexual differentiation in *Volvox carteri* (Nedelcu *et al.*, 2004) and high pH values induced cyst formation in *Peridimium gatunense* (Vardi *et al.*, 1999). In this study many genes and transcription factors related to antioxidant and DNA repair mechanisms were expressed and furthermore investigations are needed.

The aim of this chapter was to present an overall picture of the pathways and genes that were modified during the formation of spores. The transcriptome of *C. socialis* during spore formation represents a large data-set full of opportunities to answer to many questions on genes function. For example genes related to post-transcriptional methylation can be used to track epigenetic mechanisms in diatoms, for which very limited information is available. This data set can be used to understand if genes related to meiotic division or flagella production are specific of sexual reproduction or have also other functions. However, more effort is needed to investigate genes specific for spore formation looking, for example, at the most up-regulated genes that have very high expression values in the samples containing spores but are still unknown. The information provided in this chapter is the starting point to uncover the mechanisms at action during this important life cycle transition.

Chapter 6

Spore germination

Introduction

A general introduction on the studies that have been carried out on the factors influencing germination of marine diatom resting stages has been provided in the introduction. Relatively few studies were carried out mainly addressing the success of spore germination at different photoperiods, irradiance and wavelength composition. Light availability seems the key factor that induces germination of diatom resting stages, which do not have mandatory dormancy. However, there is one study that shows germination occurring also in darkness (Jewson *et al.*, 2008). Apparently very low levels of irradiance are sufficient in inducing germination (Hollibaugh *et al.*, 1981; Shikata *et al.*, 2011), while the studies addressing the effect of photoperiod provided contrasting results (Eilertsen *et al.*, 1995; McQuoid *et al.*, 2002; Montresor *et al.*, 2013). This is due to the experimental approach used, where germination was assessed measuring the abundance of vegetative cells after sediment samples were incubated for several days at different photoperiods. In this way it is not possible to discriminate the germination success from differential growth rates of the various species. Only two experiments tested the effect on spore germination of different wavelengths and reported that the blue and red components were effective (Shikata *et al.*, 2009; Shikata *et al.*, 2011).

Spectral modification of light

Light has a pivotal role for ecosystem functioning both in marine and in terrestrial environments since it is necessary for all photoautotrophs. The major wavelengths that compose light are the blue (B: 400–450 nm), green (G: 500–550 nm), red (R: 630–680 nm) and far red (700–750 nm) and their quantity, as well the ratio between them, change over time and space in all environments becoming a message for the entire community. This is especially noteworthy in aquatic systems, where the quantitative and qualitative variation is much higher than on land. First of all, the intensity of light in seawater is one or two order lower than in terrestrial environments and more factors can change its composition and quantity than in the atmosphere (Ragni & Ribera D'Alcalà, 2004; Depauw *et al.*, 2012). The incident solar radiation depends on the latitude and period of the year, which determine the duration of twilight and the

maximal irradiance, while the angle of sun during the day impacts also the spectral composition. For instance, an increase of the ratio B:G and of the amount of far red light occur at dusk and dawn. In addition, scattering and absorption processes due to water and particles present in the water affect the depth at which different wavelength can arrive.

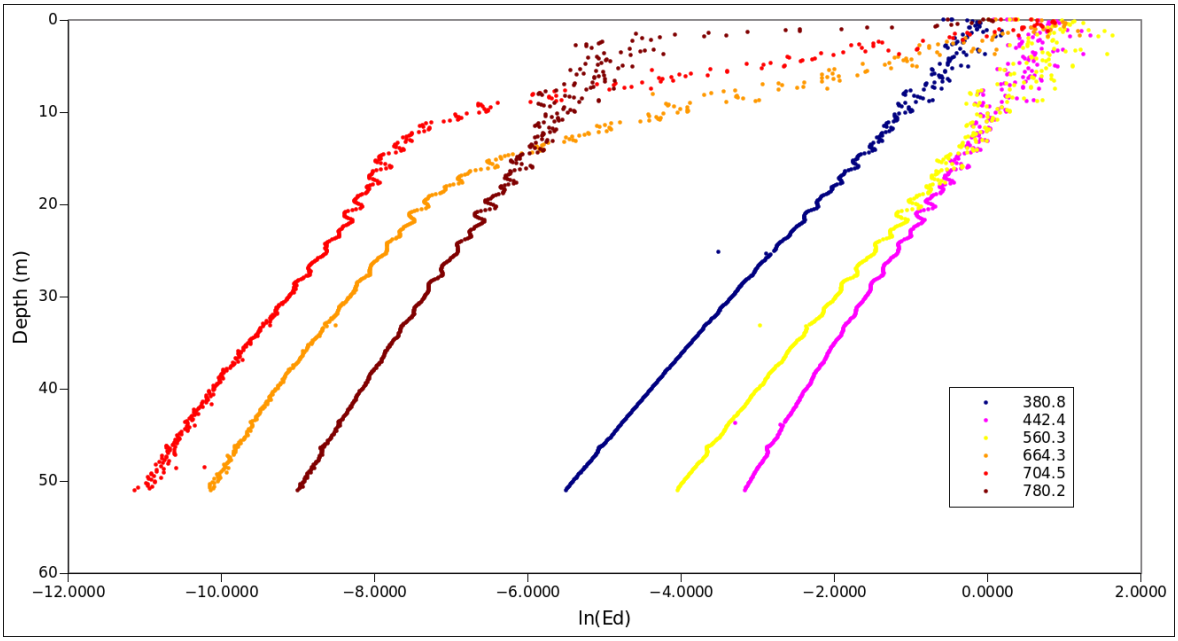

Figure 6.1: Underwater profile of different light wavelengths. Profile provided by dr. Maurizio Ribera d'Alcalà.

The variation of light along the water column is particularly high in terms of quantity and especially of composition since *per se* water absorbs red and far red wavelengths in the first 10-15 m (Fig. 6.1) shifting the light spectrum composition towards blue-green light very soon (Fig. 6.1). In addition, the far red component is subjected to a higher attenuation than the red one in the first meters due to the variation of the far red along the day that induces important variations also in their ratio. Different attenuation coefficients of blue and green light are responsible for the increase of the ratio B:R and G:R of various orders of magnitude along the water column. Furthermore, variability is also related to dissolved and particulate matter concentration and especially phytoplankton presence. Light penetration in the water column can be quite different in bloom or post bloom conditions because the absorption by chlorophyll *a* that decreases significantly (at scales of meters) the G:R and B:R ratios but not the

R:FR one. All these variations are important signals for the phototrophs living both on land and in water that developed adequate mechanisms to perceive them and react to their signals.

Light perception

All phototrophs have on one hand to maximise the capture of photons necessary for photosynthesis and, on the other, to avoid the damage that excessive irradiation can cause. In general the perception of high irradiances induces a rapid photoprotection response that involves changes in gene expression only if the exposure is prolonged. On the other hand when exposed to low irradiance, cells increase their pigment content and/or photosynthetic units in order to capture more efficiently photons. In this contest it is evident that the perception of light intensity and its spectral variation in the water column could be very important for their survival. Red light has, for instance, a double message: it is related to the proximity to the surface where the damages due to high irradiance are more probable or be the signal of more favourable conditions when cells are far from the surface. This information, indeed, can then be translated/induce in modifications of the chloroplast orientation as in green algae (Kraml & Herrman, 1991; Sineshchekov *et al.*, 2000) or in positive or negative phototaxis. In addition to the information carried by the single wavelengths also the ratio between different wavelengths can carry information that is perceived by the activation of more than one light sensor protein. These proteins, known also as photoreceptors, have been found in different phytoplankton groups, cyanobacteria included, and allow the perception of a wide chromatic range (red-far red, UV-blue and green). They are modular in structure, with one or more protein domains linked to a non-protein component called chromophore that is capable to perceive and chemically react to specific wavelengths. When excited by light, the chromophore undergoes structural changes that stimulate a signal cascade within the cell (van der Horst & Hellingwerf, 2004). On the base of their chemical features and the action spectrum, photoreceptors are classified in at least six different types that were identified in unicellular and pluricellular organisms. In diatoms, the analysis of genomes and transcriptomes lead to the discovery of cryptopchromes, LOV-type aureochrome, and several phytochromes. However, information on their function and molecular structure are still limited (Jaubert *et al.*, 2017).

The blue light sensors that include several members of the aureochrome and cryptochrome families are the only blue photoreceptors presents in diatoms. In diatoms,

indication of the functional properties of cryptochromes came from *Pheodactylum tricornutum* where the potential role as circadian clock repressors and as repair system of DNA due to UV-A exposure has been demonstrated (Jaubert *et al.*, 2017).

Aureochromes are exclusive of stramenopiles and act as transcription factors, although the cascade implicated is completely unknown. Information for diatoms derived also in this case from *P. tricornutum;* aureochromes participate to the cell-cycle since the concomitant expression with another transcription factor (bZIP10) induces the initiation of cell division through the activation of a cyclin known to work also at low irradiances. Also the photoacclimation to high irradiances is related to both blue light receptors: *P. tricornutum* exposed to blue, white and red light at low and medium intensity showed the induction of photoprotection mechanisms, such those relative to non-photochemical quenching, as well as the increase of the xanthophyll cycle and changes in the chloroplast membrane proteome only when exposed to blue light (Jaubert *et al.*, 2017).

In diatoms the perception of red/far-red light is done by phytochromes, which are different from those of other organisms to form a separate clade (Depauw *et al.*, 2012). At least in prasinophytes and diatoms it has been demonstrated that a phosphorylation initiates the signal cascade after light perception but the downstream steps remain unknown. Red and far red light may carry very different messages: for example, the R:FR ratio informs higher plant on the beginning and the end of the day (Smith, 2000). In addition it is used to avoid the proximity to the surface layer where damage due to the high irradiation can occur.

In this chapter I will illustrate the experiments relative to two main questions: i) if germination can occur also at very low irradiance comparable to that recorded at the limit of the photic zone (~100 m depth) and ii) if germination differs at different wavelengths. To gain information on wavelengths could be tested for germination experiments I determined the absorption spectrum of spores.

Material and methods

Absorption spectra

Cultures of *C. socialis* strain APC12 were prepared to quantify the absorption spectrum of i) vegetative cells, ii) freshly produced spores and iii) mature spores maintained in the dark at cooler temperature for 3 months before the experiment. Two flasks, one containing 200 mL of f/2 medium (to obtain vegetative cells) and the other with 200 mL of f/2 without nitrogen addition (to obtain spores) were inoculated with 3,000 cell·mL^{-1}. Cultures were grown at a photoperiod of 12:12h light:dark, an irradiance of 180 µmol photons·m^{-2}·sec^{-1}, and a temperature of 18 °C. Vegetative cells were collected for the absorption spectra analysis after two days from the inoculum; a sub-sample of the culture was fixed with formaldehyde 0.4 % (v:v) to assess cell concentration. After nine days from the inoculum, the culture grown in –N medium was split into two bottles. The content of one bottle was filtered for the analysis of the absorption spectra of fresh spores, while the other bottle was stored in the dark and at the cooler temperature (9°C) for 3 months before the analysis. From each bottle, a subsample was collected before filtration, fixed with neutralized formaldehyde 0.4 % (v:v), and spore concentration was estimated. No vegetative cells were found in the culture grown in –N nor spores in the one grown in +N. Three filters were measured from each culture. A volume of 20 mL for each culture was filtered with a peristaltic pump on glass-fibre filters (Whatman GF/F) with 1.2 µm pore size and immediately stored at -20 °C until the analysis. Filters were placed on a wet paper with ASW for one hour to be gradually defrosted and the samples were analysed with a an Agilent 8453 UV-Visible spectrophotometer (Agilent, Santa Clara, CA, USA) equipped with a Labsphere RSA-HP-8453integrating sphere (Labsphere, North Sutton, NH, USA). After quantification, all filters were treated with an equal quantity of sodium hypochlorite (0.1 %) in order to oxidize all pigments and were analysed again. The spectra obtained in the second analysis were then subtracted from the previous absorption spectra in order to have the absorption spectra of the pigments without the absorption of the cellular cell wall and cytoplasm. In parallel, an untreated filter was processed in the same way and its absorption was also removed to eliminate also the absorption due to the filter material and thus obtain the net absorption spectra of each cellular type. Calculations were made following Tassan & Ferrari (1995, 1999). Spectra of vegetative cells and fresh spores were normalised using the total number of cells/spores, while this was not possible with old spores that formed agglomerates impossible to count (see Results).

Spore germination at different irradiances and wavelengths

The role of light as message carrier in inducing spore germination was evaluated exposing spores to a very low irradiance (~ 1.2 µmol photons·m^{-2}·sec^{-1}) of different wavelengths (blue, red and white light). The white light was also tested at irradiance values of 20 µmol photons·m^{-2}·sec^{-1}. All samples were incubated at a 12:12 h L:D photoperiod and a temperature of 18 °C under LED lights Heliospectra E60 (Heliospectra AB, Goteborg, Sweden) for 7 days.

Spores were obtained as described in the previous section and were then transferred in dark conditions at the same temperature for one week before the experiments (1 bottle with 100 ml of culture). This period in the dark was applied to allow the complete maturation of spores and, at the same time, to induce death of the few vegetative cells present in the culture. Before incubation, an aliquot of each culture was sampled, fixed with neutralized formaldehyde 0.4% (v:v) and used to assess the concentration of spores and vegetative cells. For each tested light condition, twelve 35 mm glass bottom chambers (Ibidi, Martinsried, Gerrmany) were used. Each chamber was filled with 1 mL of f/2 medium and 1 mL of culture.

Six chambers were exposed to the light, while the other six were kept in the dark in the same dark room at a temperature of 18°C. Dark chamber were positioned far from the lamp and covered with several aluminium foils. Six chambers (three in the light and three in the dark) were collected after 3 (t3) days and other six after 7 (t7) days and immediately fixed with neutralized formaldehyde 0.4 % (v:v). All steps were performed in completely dark condition until samples fixation during the dark phase of the photoperiod. A total of 200 cells were counted in each sample using a Zeiss Axiophot microscope (ZEISS, Oberkochen, Germany) at 40x magnification. Three cell types were enumerated: spores, spore valves and vegetative cells. With the term ‘spore valves’ I defined the two valves that are released after germination. The values recorded at t3 and t7 were expressed as positive (in case of increase) and negative (in case of decrease) percentage variation as compared to the values recorded at t0. One-way Anova was used to compare the values of percentage variation of spores in all light and dark conditions at time t3 and t7. Statistical analyses were performed using the free software Past (Hammer *et al.*, 2001).

Results

Absorption spectra

The absorption spectra of vegetative cells and fresh spores (expressed as absorption·cell^{-1}) showed several differences. Vegetative cells absorbed more light than spores showing the two typical peaks of chlorophyll *a* in the blue and red part of the spectrum (Fig. 6.2 A, B). The peak in the blue was not so evident for fresh spores (Fig. 6.2 B). In both cases the peak in the blue region showed a lot of scatter. It was not possible to calculate absorption per cell^{-1} for the 3-months-old spores because of the formation of aggregates that made impossible to assess spore concentration. To obtain an estimate of the absorption properties of old spores, I calculated the difference between absorption spectra of the old spores and that of the new ones, based on the assumption that the number of spores remained the same after the dark storage period (Fig 6.3 C). If the absorption spectrum was exactly the same, I would expect values = 0 and negative values for the absorption values recorded in the new spores but not in the old ones that in meanwhile could decrease the pigment content. The obtained values were only slightly below zero all along the PAR spectrum with a negative peak in correspondence to the red and blue portions of absorbance (Fig 6.2 C). This indicated that spores were still capable of absorbing light after three months of storage in the dark, although slightly less than fresh spores and that the decay in absorbance was especially in the red and blue portion of the spectrum.

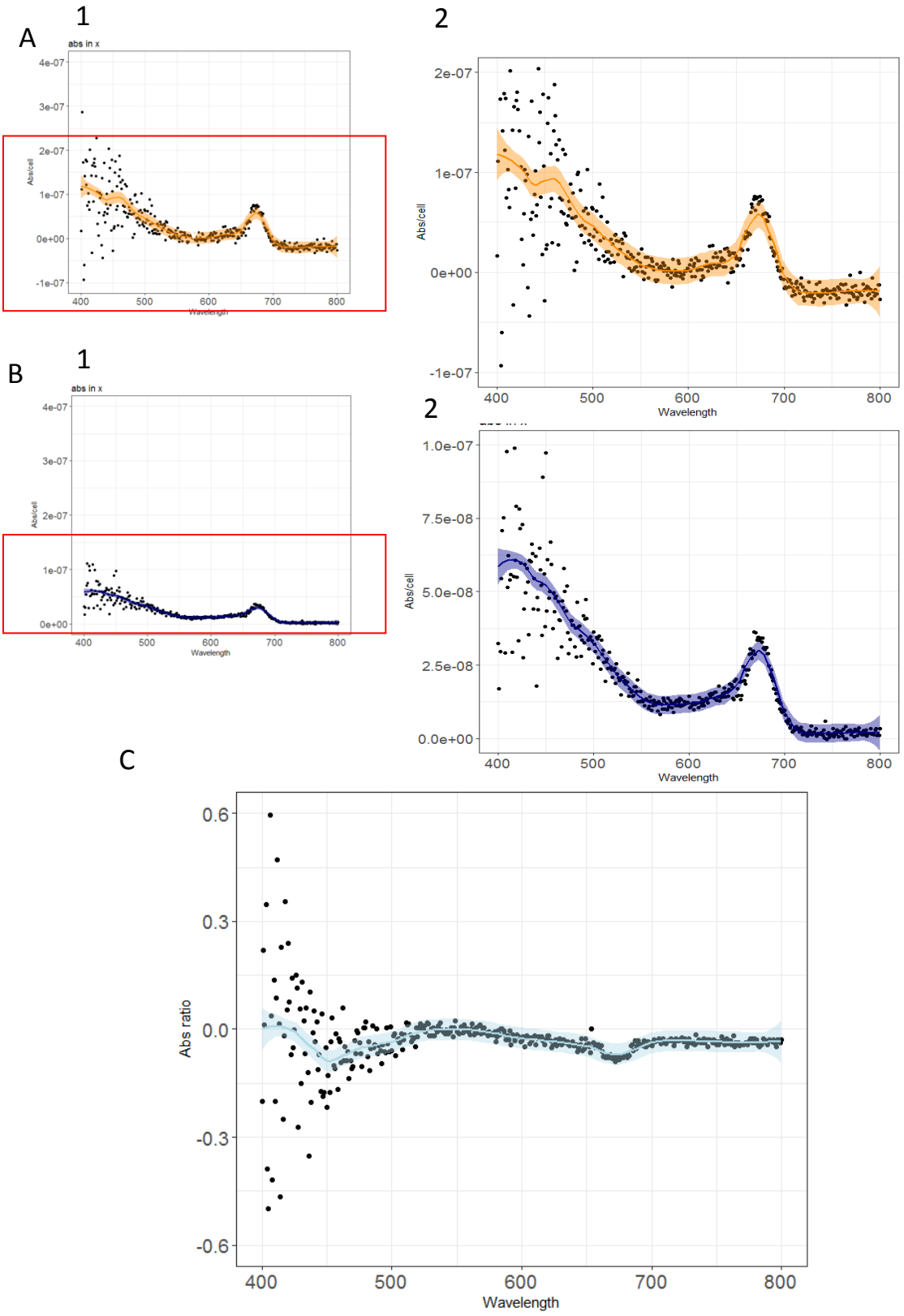

Figure 6.2: Absorption spectra of vegetative cells (A 1, 2), fresh spores (B 1, 2) expressed as absorption·cell[1]; the old-fresh spores ratio of absorption spectra (C). Panels on the right side are enlargements of the portion marked in red of the panels on the left. Lines represent loess fitted curves and halos the standard error (n=3).

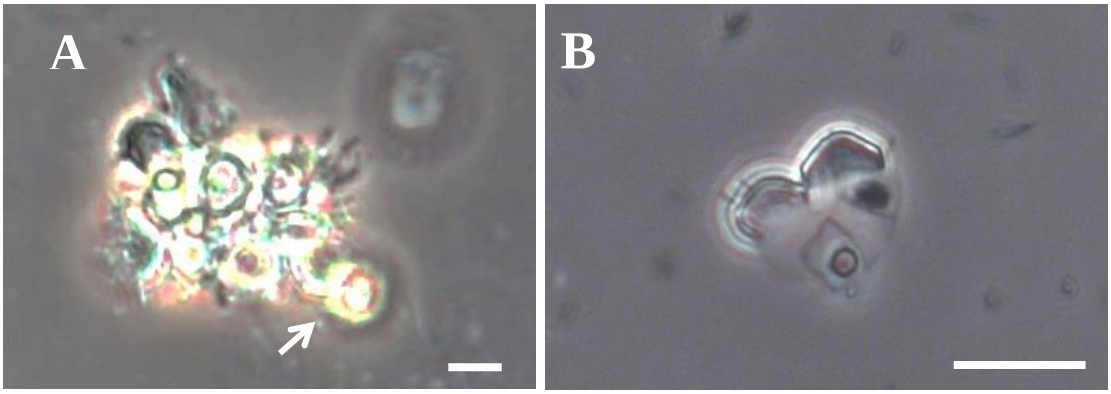

Figure 6.3: Agglomerates found in cultures maintained in the dark for three months, spores and spore valves are marked with arrows (A); two valves and two dead vegetative cells found in one sample kept in the dark (C). Scale bars: 10 µm.

Spore germination at different irradiances and wavelengths

The experiment aimed at assessing germination of spores exposed to low irradiance (1.2 µmol photons·m^{-2}·sec^{-1}) obtained with white, blue and red wavelengths showed that the most effective one for germination was the blue light (Fig. 6.4). In these conditions, the number of spores decreased by ≈ 20 % at t3 as compared to t0. The decrease in spore concentration roughly corresponded to the increase of vegetative cells, suggesting that the 'missing' spores germinated after 3 days and produced vegetative cells (Fig. 6.4). The number of 'missing' spores should have matched the number of spore valve pairs, but this latter value was instead considerably lower. Value of germinated spores in blue light, as inferred by their negative percentage variation, was higher at t3 as compared to t7.

The other experimental set up that provided a relatively good percentage of germinated spores was the one carried out at an irradiance of 20 µmol photons·m^{-2}·sec^{-1} of white light (Fig.6.4). Also in this experiment, the percentage of germinated spores (≈ 40%) roughly corresponded to the increased percentage of vegetative cells, but not with the number of pairs of spore valves. In this experiment the percentage of spore germination increased from t3 to t7. The variation of spore percentage detected at low blue light and at white 20 µmol light were the ones showing significantly different values when compared to the other tested conditions (red and while low light) after 3 days of exposure. Values recorded at low white light and low red light did not show consistently significant differences both after 3 and after 7 days of exposure (Tables 6.1 and 6.2). One noticeable result was the absence of significant differences in germination

percentages between the treatments at the different wavelength conditions and their values in the respective controls in the dark. The only exceptions were the values at white 20 μmol light after both 3 and 7 days (Tables 6.1 and 6.2).

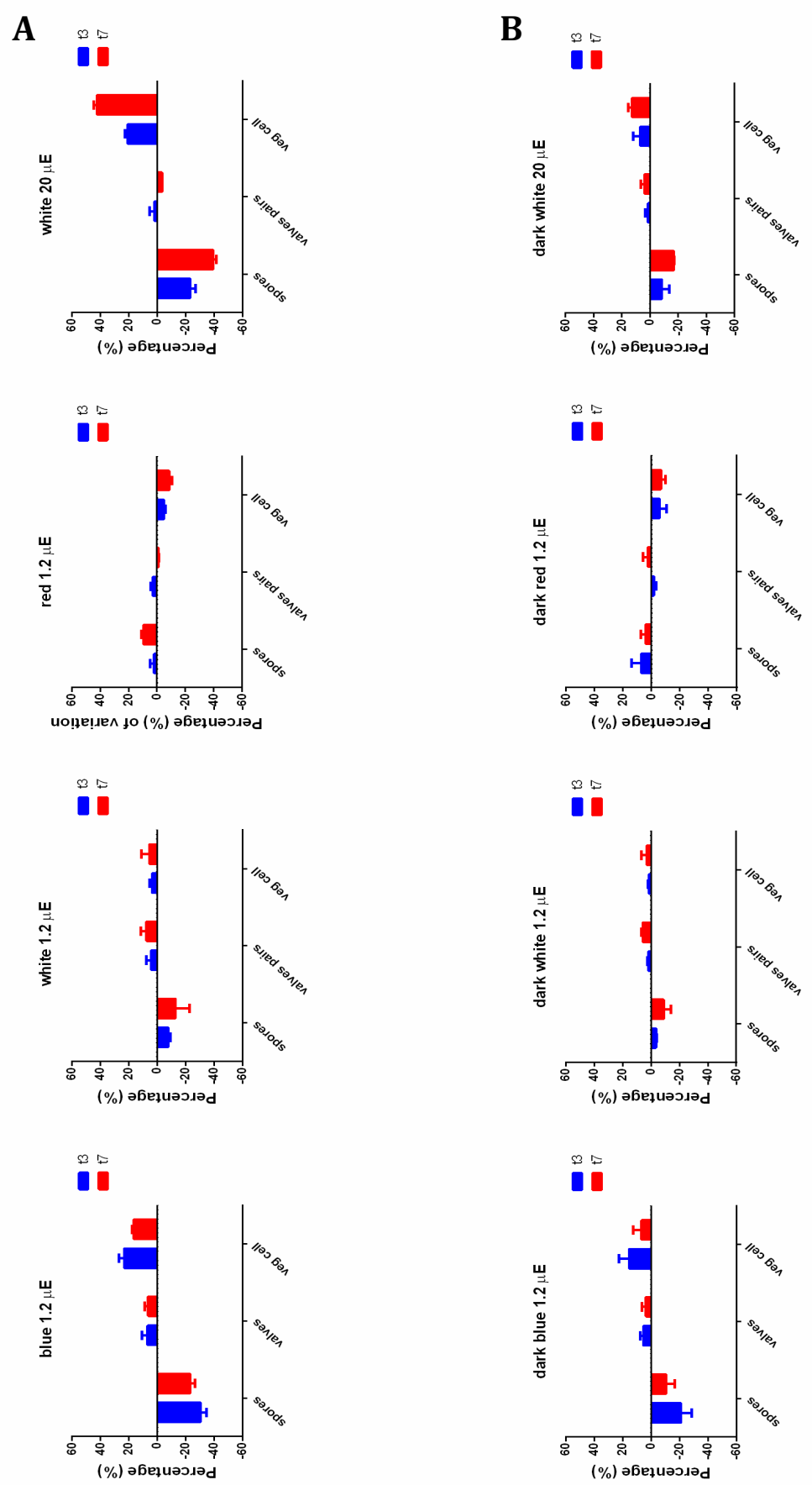

Figure 6.4: Percentage variation of the increase or decrease of full spores, valve pairs and vegetative cells in the different experimental conditions as compared to the values recorded at t0 after 3 (blue) and 7 (red) days. In the upper row cultures incubated at different wavelengths (A)

in the lower row, the respective control in the dark (B). Data represent average values ± S.D. (n=3).

Table 6.1: One-way Anova performed on the variation of spore percentages in samples collected at day t_3. Values significantly different (P value < 0.05) are reported in red.

	White 20	**Dark (White 20)**	**White 1.2**	**Dark (White 1.2)**	**Blue**	**Dark (Blue)**	**Red**	**Dark (Red)**
White 20	-	0.0306	0.0220	0.0026	0.5666	0.9997	0.0004	0.0002
Dark (White 20)	-	-	1	0.8907	0.0012	0.0734	0.1974	0.0187
White1.2	-	-	-	0.9442	0.0007	0.05335	0.2587	0.0261
Dark (White 1.2)	-	-	-	-	0.0002	0.0063	0.8471	0.1946
Blue	-	-	-	-	-	0.3163	0.0002	0.0002
Dark (Blue)	-	-	-	-	-	-	0.0007	0.0002
Red	-	-	-	-	-	-	-	0.8874
Dark (Red)	-	-	-	-	-	-	-	-

Table 6.2: One-way Anova performed on the variation of spores in samples collected at day t_7. Values significantly different (P value < 0.05) are reported in red.

	White 20	**Dark (White 20)**	**White 1.2**	**Dark (White 1.2)**	**Blue**	**Dark (Blue)**	**Red**	**Dark (Red)**
White 20	-	0.0031	0.0007	0.0003	0.0431	0.0004	0.0002	0.0002
Dark (White 20)	-	-	0.9881	0.6642	0.8513	0.8512	0.0007	0.0059

White1.2	-	-	-	0.9812	0.3901	0.999	0.0030	0.0293
Dark (White 1.2)	-	-	-	-	0.0928	1	0.0166	0.1522
Blue	-	-	-	-	-	0.1703	0.0002	0.0006
Dark (Blue)	-	-	-	-	-	-	0.0084	0.0823
Red	-	-	-	-	-	-	-	0.9204
Dark (Red)	-	-	-	-	-	-	-	-

Discussion

The results obtained in this experiment showed that the exposure of *Chaetoceros socialis* spores at 20 µmol photons·m^{-2}·sec^{-1} of white light (white20 from here onwards) and at very low levels (1.2 µmol photons·m^{-2}·sec^{-1}) of blue light (blue1.2 from here onwards) was effective in inducing spore germination. Nevertheless, spore germination was detected also in the corresponding controls in the dark; the only significant difference between values in the light and those in the dark was observed for samples incubated at white20.

Experiments were designed to maximize the precision in estimating germination: it included the assessment of the number of full spores, the number of vegetative cells (I expected it to be equal or higher than the number of germinated spores) and the number of pairs of spore valves, which should equal the number of germinated spores. Moreover, the stock sample dominated by freshly-produced spores used for the experiments was kept in the dark for one week before running the tests to induce the death of vegetative cells. Last but not least all the steps carried out from this point onwards were conducted in complete darkness.

While in most tests the percentage of germinated spores roughly matched that of vegetative cells produced after three or seven days (exception was the test carried out in red light), I could not find a match between the percentage of germinated spores and that of valve pairs that were always rather low. This can be explained either by the difficulty of identifying the half valves in the samples or by the fact that the organic part of empty diatom frustules can be very rapidly degraded by bacteria (Bidle *et al.*,1999).

The results of the experiments suggest that germination occurs also in the dark. Indeed this was already reported for other microalgae. Anderson *et al*. (1987) tested the capability of natural populations of cysts of several dinoflagellates collected in a pond along the US east coast to germinate in the dark. Aliquots of sediment were stored in the dark and germination was assessed after a variable number of days as the difference between the concentration of full cysts in the sediments immediately after collection and the cyst concentration estimated at the different time points. The empty cysts recorded were considered as evidence for germination in the dark. Similar experiments were conducted also with *Ligulodinium polyedrum* cysts produced in laboratory. This latter species required light to germinate while *Gonyaulax tamarensis, Scrippsiella* sp., and *Gonyaulax verior* germinated faster in the light than in the dark and one species (*Gonyaulax rugosum*) germinated at a similar rate in the light and in the dark (Anderson *et al.,* 1987). However, cysts collected from natural samples may have been already exposed to some light in the sediments or during the collection procedure, which may have induced the subsequent germination in the dark. A similar approach was used to test the germination success of natural populations of *Alexandrium* spp. cysts collected in Puget Sound, and also in this case cyst germination was detected also in the dark although at lower rates (Moore *et al.,* 2015).

For the experiments with *C. socialis*, I used freshly-produced spores that were immediately stored in the dark. This procedure should have mimicked the sinking of spores in the sediment. The germination of diatom spores using culture material was studied by Shikata *et al.,* (2011) using the centric diatom *Leptocylindrus danicus*, which is the only diatom known so far in which spores are produced following sexual reproduction. The authors i) induced spore formation in the culture using N depleted medium, ii) stored them in the dark for 2 days, iii) exposed them to the treatments (different wavelengths, see below) and a control in the dark for two days, iv) than back to the dark for two additional days and then fixed them to enumerate the germinated cells. The germinated cells were larger than the normal vegetative cells, since they were

produced from a spore that was the product of sexual reproduction. The principle of this experiment was that the exposure to the light for two days should have provided the cells the 'signal' to germinate. Shikata *et al* (2011) state '*At 3 µmol* m^2 s^1*, all wavelengths produced germination rates (Li') that did not differ significantly from the rates for the dark control*'. Germination rates were very low, but this means that also *L. danicus* was able to germinate at low rates in the dark.

The absorption spectra of freshly produced spores of *C. socialis* showed a peak at 450 nm (blue peak) and a peak at 680 (red peak); these peaks of absorbance were similar also in 'old' spores, i.e. spores that were stored in the dark for 3 months, although peaks were lower. Germination was detected at blue1.2 although the percentage variation of spores was not significantly different from the values measured in the dark control, but there was almost no germination with low levels of red light. One explanation is that these very low irradiance values were not sufficient to induce germination significantly higher than that occurring in the dark. I selected extremely low values of irradiance (1.2 µmol photons$\cdot m^{-2} \cdot sec^{-1}$) of blue and red light to test if these values, below those required for photosynthesis (Geider *et al.,* 2008), could be perceived by cryptochromes and aureochromes (blue) and phytochromes (red) and induce the germination of spores. Cryptochromes and one aureochrome were detected in the transcriptome of *C. socialis* (see Chapter 5) but the results of my experiment were not providing evidence for their response to these extremely low irradiance values.

Germination in the dark and at low irradiance values was extremely low, however a few spores were apparently capable to germinate and produce alive cells. This raises two additional questions: i) which is the destiny of the vegetative cells that may germinate in very deep waters, where there is no light at all or values below the threshold for photosynthesis? ii) Why only a few cells can germinate and the others not? For what concerns the first question, I have to consider that diatoms are not motile and cannot actively swim towards a source of light as can do, e.g., phototrophic dinoflagellates. It thus seems that the spores that germinate in the deep sea are 'lost', unless they are transported to shallower waters by, e.g. upwelling events or deep waves and currents. The second question shows that there is a considerable level of variability also within a clonal culture that is considered genetically identical. Apparently the physiological state of the cells is very different and some cells require longer exposure to the light before being able to germinate. This seems to be the case of the cells

exposed at white20 where germination percentages increased from day 3 (about ≈20%) to day 7 (about ≈40%).

Conclusions and perspectives

My PhD project aimed to define ecologically relevant factors that induce the shift between a vegetative cell to a resting spore and from the resting spore back to the vegetative stage in the marine planktonic diatom *Chaetoceros socialis*. The results obtained in this study showed that spore formation is induced by different factors, including i) external nitrogen concentration, ii) density-dependent factors related to high cell concentration, iii) factors related to the presence of senescent/dying cells, and iv) the effect of viral infections. As discussed below, some of these factors may be related, i.e., spore formation may occur as a response to stress conditions that can induce death in some cells of the population and the formation of spores in other cells. Besides nitrogen starvation that has been extensively tested in several diatom species, all the other possible inducers were never considered before. This study had also the aim to bring novel information on the molecular pathways in action during the formation of spores through a transcriptomic approach; this is also an aspect that has never been addressed before. With the aim of understanding the role of light in inducing the germination of spores, I tested the possible effect of different wavelengths at irradiance values below the threshold required for photosynthesis to see if there was evidence of spore germination. In these experiments however, the low levels of spore germination were not significantly different from those recorded in dark conditions. These results on one side may suggest that spore germination can occur also in the dark, but also show the experimental difficulties of study the response to different light conditions in very small unicellular microalgae.

I started my PhD project gradually, from the basic questions of investigating the modality of spore formation at the cellular level and the time required to complete spore formation and germination (Chapter 2). This first part of my project allowed me to 'familiarize' with the species and gain basic information on the life cycle processes I wanted to study. The use of time lapse microscopy and confocal laser scanning microscopy coupled with two fluorescent dyes - PDMPO for newly deposited silica and SYBR green to stain the nuclei – allowed i) to prove that *C. socialis* spores are formed within the maternal cell (endogenous spores), ii) to see that the formation of spores takes 10-13 hours at the tested experimental conditions, iii) to visualize the nuclear division preceding the deposition of spore valves, and iv) to visualize the intense cytoplasmic trafficking during both spore formation and germination. When I started microscopical observations, I was hoping to find possible morphological features that could allow to localize cells undergoing spore formation at the very beginning of the process (e.g., see if all cells in a colony form spores, perhaps in a progressive way). This

could be useful to perform targeted single-cell studies (e.g., single cell transcriptomic). Unfortunately, cells undergoing the transformation into spores became clearly recognizable only after the deposition of the first spore valve, i.e. when the cytological transformation was already in action and cells that transform in colonies are randomly distributed in a colony. Nevertheless, the basic cytological information acquired in the first part of my study found support of the transcriptomic data (Chapter 5), which showed that DNA duplication was still very active during spore formation, confirming the presence of acytokinetic mitotic divisions, or the upregulation of actin- and tubulin-related genes that supports the active cytoplasmic rearrangement. Knowing that spore formation can occur in less than 24 hours is also relevant for possible studies carried out in the environment, where the bloom of a spore-forming species should be followed with a very tight sampling, possibly along the water column to follow the sinking of the bloom. All that is very difficult, especially in coastal areas due to currents and advection processes and perhaps the use of mesocosms may represent a possible approach for these studies.

As shown in the general introduction of this thesis contrasting results were obtained by laboratory and field studies for what concerns the role of nitrogen limitation in inducing the formation of spores. It was reported as the major trigger in culture conditions but its role in natural environment remained elusive. I thus decided to start the experimental investigations on spore formation with the 'standard' approach, i.e. checking the role of nitrogen starvation in *C. socialis* with a controlled experimental design in which external macronutrients together with the internal pools of organic carbon and nitrogen were monitored in both treatment and control conditions. The role of nitrogen deprivation as cue for spore formation in the lab was proved, but there were two more interesting results: i) the intra-cellular nitrogen pool did not decrease in the nitrogen depleted treatment, suggesting that the trigger of the process was not nitrogen limitation inside the cell; ii) that spores were produced also in nutrient-replete conditions. A considerable percentage of cells turned into spores with this experimental set up, which was selected for the transcriptomic study where I should have had a strong signal to interpret the pattern of up- and down-regulated genes as compared to the control (see Chapter 5). I would like to add here that the dynamic of spore formation under nitrogen limitation was almost identical when testing genetically distinct strains of *C. socialis* isolated from the Gulf of Naples. This can be seen by the results of the experiments in Chapter 3 where three strains were tested (APC1, APC2 and APC12),

but also by additional experiments carried out within a Master Thesis during the same year (Maria Elisabetta Santelia, unpublished data).

The results of the first 'standard' experiment illustrated in Chapter 3 prompted me to test spore formation at three different cell densities – comparable to those recorded in the environment during non-bloom and bloom conditions - with and without nitrogen limitation and to run other experiments with a growth medium 'conditioned' by the growth of high cell densities. Performing these experiments it is not an easy task and several factors should be taken into account, such as the way in which conditioned medium is produced, the initial cell inoculum to obtain the clearest results, the length of the experiment, etc. The results of these experiments provided support for my hypothesis that the formation of spores can also be induced by a chemical cue produced by vegetative cells. In fact spores were produced i) in semi-continuous culture only in the treatment with high cell concentration and ii) the high-cell-concentration conditioned medium was effective in inducing the formation of spores, with a clear response in short-term experiments. Additional information provided by the experiments illustrated in Chapter 3 was the positive effect on spore formation also of a high-cell-concentration conditioned medium produced after the disruption of cells by sonication. These results can provide a framework to interpret spore formation in the natural environment: cell concentration increases during the bloom and the 'message' that induces the transition from vegetative cells to spores can be produced by the high cell concentration and/or by presence of senescent cells. As discussed later, further work is required to understand if the chemical message is a single compound or two distinct ones.

This is the first time that cell-density has been taken in account to explain the formation of resting spore in diatoms, although it has been shown to induce the formation of resting stages in other microrganisms such as bacteria and fungi (Miller & Bassler. 2001, Brown *et al.,* 2008). In bacteria, this mechanism works through passive or active excretion of molecules - infochemicals or autoinducers - that are dispersed in the environment and perceived by other cells. When the concentration of the signalling molecules exceeds a certain threshold, it can trigger the shift of the vegetative cell into a resting stage (Miller & Bassler. 2001). Similar mechanisms can be hypothesized also in diatoms. The results reported in Chapter 3 highlighted the fact that shifts between life cycle stages are not only driven by bottom up (nutrients) factors but may be regulated also by cell to cell communication. When cell concentration is too high, or when other

stressful conditions are present, cells can send a signal that induces the transformation of a fraction of the population into resting stages that will survive in a different environment (the sediments or deep layers of the water column).

Spore formation was induced both by the medium obtained by sonicated high-density-cells and in cultures of *C. socialis* infected by a species specific virus (Chapter 4). The viral infection has been proven by different quantification methods as well as by thin sections in transmission electron microscopy. Infected cells of the Neapolitan strain APC12 were growing in full strength medium and percentages of spores varying from 33% to 38% were produced in these conditions. It has to be considered that viruses cause the lysis of the cell: are we in a condition similar to the effect of sonicated high-density-cells? In other words: is there a compound that is produced by broken cells and acts as a stressor determining the production of spores?

The information on cell-to-cell communication in diatoms is related mainly to the intraspecific effect of volatile oxylipins. It has been shown that these compounds are released by broken diatom cells produced by grazers and can interfere with the reproduction success of copepods and other invertebrates (Caldwell *et al.*, 2002; Ianora & Miralto, 2010; Ianora *et al*., 2015). It has been also proposed that these volatile oxylipins can have a role as signals in bloom termination, by starting progressive death of the cells of other species (Casotti *et al.*, 2005; Ribalet *et al*., 2008). *C. socialis* produces a stereospecific non-volatile oxylipin derived from the oxidation of eicosapentaenoic acids (a fatty acid) by a lipoxygenase and seems to have toxic effects on copepods, inducing malformation that block larval development (Fontana *et al.*, 2007). This could be an explanation for the formation of spores in the treatments with medium from sonicated cells and in the experiments with viral infection. In order to gain information on the production of oxylipins in *C. socialis* I looked for the expression of lipoxygenases in the transcriptome, but I could not find them.

To summarize: spore formation may be induced by a compound released by conspecific cells both when they are healthy and/or when they are damaged (viral infection, damaged by sonication). How do these result reconcile with the strong effect of nitrogen deprivation that can induce the very rapid shift to spores in a few days? The most plausible explanation is that a strong and brisk nitrogen deprivation – something that never occurs in the natural environment – induces a strong stress in the cells that respond shifting their genetic program to the production of spores. Since the intracellular nitrogen did not change during the formation of spores, it is not an

intracellular threshold that acts as a cue (Chapter 3). Comparing the results obtained by the transcriptomic approach during nitrogen starvation with those obtained for other non-spore forming diatoms subjected to the same stress, I was expecting to find some differences (Chapter 5). The overall behaviour in *C. socialis* resulted in the recycling of internal pools of nitrogen, as detected in other diatoms, where the intracellular ammonium derived from the degradation of nitrogen-containing molecules. There were differences on the nitrogen uptake as shown by the down-regulation of high-affinity nitrate transporters and the up-regulation of ammonium and urea transporters during spore formation. Nitrogen deprivation in the treatment caused also changes in many different pathways, spanning from carbon re-allocation to the production of antioxidants. It was thus complicate to find specific candidate genes that could be specific for the shift from vegetative cells to spores. On the other hand, some suggestions came from other organisms in which the formation of resting stages is related to the production of antioxidants that can defend the cell from reactive oxygen species produced by external stressors (Aguirre *et al.,* 2005). Actually, there are commonalities between the pathways activated by different stressors (nitrogen starvation, crowding and viral infection): all of them lead to an increase of oxidative stress, with the activation of the redoxome, i.e. the redox sensitive network that can vary in the chemical oxygen species produced and in their localization. In plants there are evidences that this network not only prevents the death of cells but also acts as a signal for their development and defence against pathogens and herbivores (Laloi *et al.,* 2004). The exposure to a sub-lethal concentration of reactive oxygen species modifies a broad range of cellular processes, activating or inhibiting transcription factors, membrane channels etc., and acting thus as second messenger for various physiological processes aimed to increase cell survival (Winterbourn & Hampton, 2008). Depending on the duration of stress conditions, the reaction can include protein modification, which allows a rapid response to the stress, and a reprogramming of the transcriptome as can be in the case of spore formation. Few years ago, it has been demonstrated the close connection between nitrogen limitation and specific redox responses in the cell (Rosenwasser *et al*., 2014). Authors found a high number of redox-sensitive proteins associated to specific organelles (high oxidation in chloroplasts and mitochondria but not in the nucleus). This redox network has the potential to be the common link that I was looking for, since it could explain why some cells die and others form spores. Oxidative stress has been related to another important process in phytoplankton, the programmed cell death (PCD). Although it is not clear if PCD has the same function than in the other organisms, i.e., to induce the death of specific cells, the expression of

several enzymes related to PCD has been demonstrated in different occasions: during nutrient starvation (Thamatraklon *et al.*, 2005; Lin *et al.*, 2017), when diatom cells were treated with oxylipins (Vardi *et al.*, 2006) or infected by viruses (Bidle *et al.*, 2007). The results of the transcriptomic analysis illustrated in Chapter 5 now demonstrate that these enzymes are also expressed during spore formation.

In the experiment carried out to obtain the transcriptome, nitrogen starved cells were harvested at three different sampling points in which a heterogeneous population was present. At T2 there were vegetative cells, but they may have already perceived a signal deriving from nitrogen limitation and/or high cell concentration (on T2 cell concentration was $\sim 5 \cdot 10^4$ cell $\cdot mL^{-1}$), at T3 (one day after) spore formation started and the average spore percentage was 30%, while at T4 (after another day) average spore percentage was 75%. It is reasonable to assume that some of the molecular signals detected in with the transcriptomic analysis were not involved in the metabolic processes that lead to spore formation but in those related to the senescent state of a fraction of the population (in T3 and T4). For example, while it is clear that genes related to DNA replication were upregulated in cells forming spores (remember the mitotic divisions that precede spore valve deposition), it is not so clear if the genes related to programmed cell death were expressed by the senescent cells or by the cells that were turning into spores.

Another intriguing question came from the evidence of spore production during viral infection (Chapter 4). Two aspects, in my opinion, resulted very interesting: the capability of the RNA virus CsfrRNAV to infect strains of *C. socialis* isolated from biogeographically extremely distant populations and the potential role that spores could have as defence strategy. If the signal involved in spore formation comes from cells damaged by viral infection, the formation of spores could be a way to 'secure' a fraction of the population that can escape viral infection and have the opportunity to germinate in another season. This strategy has been observed in *Emiliana huxleyi* (Frada *et al.*, 2008), a coccolithophore with a haplo-diplobiontic life cycle in which only the diploid phase was susceptible to viral attacks, while the haploid phase was immune. The hypothesis illustrated above is valid if spores are not infected by the virus and they can be interpreted as a strategy to avoid the viral attack. On the contrary, if spores are infected, they could represent a way to spread viruses through space and time. This would be an interesting question to address in future studies.

The experiments aimed at investigating the role of light in triggering spore germination resulted more difficult than expected. Light quantity and quality governs the germination of the vast majority of plants in the terrestrial environment (Bentsinka & Koornneef, 2008). The light field changes with depth in the water column, depending on the latitude, seasons, and the abundance of phytoplankton in the water column. The time-lapse records presented in Chapter 2 showed that freshly produced spores can germinate within a few hours after the exposure to the high light intensity under the microscope. However, irradiance is much lower in the deep layers of the water column. For this reason, I focused my experiments testing very low irradiances. The hypothesis was that very low levels of blue or red light – wavelengths that could be absorbed also by freshly produced spores and old ones – could induce the germination of spores. Blue wavelengths are the ones that penetrate deeper (in clean waters also up to 200 m) and can thus act as signals for inducing germination. Red wavelengths are absorbed much faster, but I decided to test them for two reasons: i) these wavelengths are absorbed by the chlorophyll present in the spores and ii) red wavelengths could be emitted by the chlorophyll of cells at depth when excited by the blue light. This very faint red light could also be a signal for the spores in the deeper layers. If successful, these experiments could have provided information on the depth at which light-triggered germination could occur. The results of the experiment I have carried out did not allow discriminating between the germination rates occurring at blue and red low irradiances and the germination in the controls in the dark. Data between treatment and control were not significant. I can conclude that a small fraction of the spores can germinate also in the dark. I took extreme care in running the experiment and I trust these results. However, vegetative cells that germinate in deep layers of the water column face a considerable problem: they need light to photosynthesize. It has been shown that diatoms can be positively buoyant when in an active growth phase (Acuña *et al.*, 2010). This would be a very interesting hypothesis to test, but the set up will not be an easy one to design.

Future perspectives

Although the work carried out within my PhD project provided many valuable information that open new perspectives for investigating and understanding the factors that induce the formation of spores, they also produced new questions.

The analysis of the transcriptome data presented in Chapter 5 represented for me

a precious experience and a very hard work since I had to jump from the observations in light microscopy and the experimental design to the complexity of the chemical pathways and the genes responsible for them. I gained direct experience in searching the dataset and I know that there is still some work to be done to refine the results as, for example, to explore some pathways in more detail, or validate the presence of some interesting genes. The genes related to the redoxome, especially those that are acting as transcription factors, are interesting candidates. It would be very interesting to follow intracellular ROS production during spore formation using the experimental set up implemented in this thesis. A considerable fraction of genes that showed very high up- or down-regulation levels are unfortunately not annotated. The identification of these genes will require the use of advanced molecular approaches such are their silencing or overexpression; when this information will be available one could start interpreting metatranscriptomic data and address questions related to the evolution of genes related to spore formation in diatoms.

Another approach that is worth to carry out is the chemical characterization of the compounds. There is evidence that chemical cues can be involved in the induction of spore formation and a reliable experimental set up has been designed in this thesis. This could be used to test different fractions of conditioned medium to narrow the identification of active compounds.

In my opinion, the most interesting follow-up of this PhD project for me would be to identify the internal switch that regulates the 'choice' of a cell between death and transformation into a spore. Addressing this question will require an integrated approach including, for example, the use of fluorescent probes that give the possibility to track selected processes like the oxidation state within the cells and among the cells in a culture.

In fact, one of the lessons I have learned from this project is the diversity present in a 'clonal' culture. Also in the more extreme condition, such as the batch experiments in nitrogen starvation, not all the cells behaved in the same way: some produced spores, some others not. The experiments and consequently the transcriptomic data always provide information on the mixed population. Single cell approaches will represent the future of these investigations (e.g., Griffiths et *al.*, 2018)

The analysis of the transcriptomic data provided some evidence for the presence of enzymes related to anaerobic respiration, which has been suggested as the mechanism that will allow survival of the spores in the sediments (Kamp *et al.,* 2011). This would be another interesting topic for future research that could open the possibility to find new biological pathways in resting stages that remain viable in the

sediments for up to 100 years (Härnström *et al.*, 2011)

Last but not least, it would be very interesting to study cues for spore formation in the natural environment. Although what happens in the laboratory does not always match with what happens in nature, I think that some of the results emerging from my study (e.g., the role of cell density, or cell senescence due to viral attacks or to the end of a bloom) are ecologically relevant questions that can be tested in nature. I should be lucky to be able to follow at high temporal resolution a bloom of *C. socialis* in the Gulf of Naples. This information would be very important to define and predict when and where spores are produced in natural conditions overcoming the extremely ephemeral nature of this biological process. Metatranscriptomic data collected during the late phase of a bloom of *C. socialis* could represent a precious resource to be integrated and interpreted with the data produced in the transcriptome experiment I ran in the laboratory.

References

Abida, H., Dolch, L. J., Mei, C., Villanova, V., Conte, M., Block, M. A., Finazzi, G., Bastien, O., Tirichine, L., Bowler, C., Rebeille, F., Petroutsos, D., Jouhet, J. & Marechal, E. 2015. Membrane Glycerolipid Remodeling Triggered by Nitrogen and Phosphorus Starvation in *Phaeodactylum tricornutum. Plant Physiology* **167:**118-36.

Acuña, J. L., López-Alvarez, M., Nogueira, E., & González-Taboada, F. 2010. Diatom flotation at the onset of the spring phytoplankton bloom: an in situ experiment. *Marine Ecology Progress Series* **400:** 115-125.

Aguirre, J., Ríos-Momberg, M., Hewitt, D. & Hansberg, W. 2005. Reactive oxygen species and development in microbial eukaryotes. *Trends in microbiology* **13:**111-18.

Alipanah, L., Rohloff, J., Winge, P., Bones, A. M. & Brembu, T. 2015. Whole-cell response to nitrogen deprivation in the diatom *Phaeodactylum tricornutum. Journal of Experimental Botany* **66:**6281-96.

Allen, A. E., Dupont, C. L., Obornik, M., Horak, A., Nunes-Nesi, A., McCrow, J. P., Zheng, H., Johnson, D. A., Hu, H. H., Fernie, A. R. & Bowler, C. 2011. Evolution and metabolic significance of the urea cycle in photosynthetic diatoms. *Nature* **473:**203.

Allen, A. E., Vardi, A. & Bowler, C. 2006. An ecological and evolutionary context for integrated nitrogen metabolism and related signaling pathways in marine diatoms. *Current opinion in plant biology* **9:**264-73.

Allen, J. I., Smyth, T. J., Siddorn, J. R. & Holt, M. 2008. How well can we forecast high biomass algal bloom events in a eutrophic coastal sea? *Harmful Algae* **8:**70-76.

Amato, A., Dell'Aquila, G., Musacchia, F., Annunziata, R., Ugarte, A., Maillet, N., Carbone, A., d'Alcala, M. R., Sanges, R., Iudicone, D. & Ferrante, M. I. 2017. Marine diatoms change their gene expression profile when exposed to microscale turbulence under nutrient replete conditions. *Scientific Reports* **7**.

Ameisen, J. C. 2002. On the origin, evolution, and nature of programmed cell death: a timeline of four billion years. *Cell Death Differentiation* **9:**367-93.

Anderson, D. M., Taylor, C. D. & Armbrust, E. V. 1987. The effects of darkness and anaerobiosis on dinoflagellate cyst germination. *Limnology and Oceanography* **32:**340-51.

Anderson, O. R. 1976. Respiration and photosynthesis during resting cell formation in *Amphora coffaeformis* (Ag.) Kütz. *Limnology and Oceanography* **21:**452-56.

Anderson, T. R. 2005. Plankton functional type modelling: running before we can walk? *Journal of Plankton Research* **27:**1073-81.

Andrews, S., Gilley, J. & Coleman, M. P. 2010. Difference Tracker ImageJ plugins for fully automated analysis of multiple axonal transport parameters. *Journal of Neuroscience Methods* **193:**281-87.

Armbrust, E. V., Berges, J. A., Bowler, C., Green, B. R., Martinez, D., Putnam, N. H., Zhou, S. G., Allen, A. E., Apt, K. E., Bechner, M., Brzezinski, M. A., Chaal, B. K., Chiovitti, A., Davis, A. K., Demarest, M. S., Detter, J. C., Glavina, T., Goodstein, D., Hadi, M. Z., Hellsten, U., Hildebrand, M., Jenkins, B. D., Jurka, J., Kapitonov, V. V., Kroger, N., Lau, W. W. Y., Lane, T. W., Larimer, F. W., Lippmeier, J. C., Lucas, S., Medina, M., Montsant, A., Obornik, M., Parker, M. S., Palenik, B., Pazour, G. J., Richardson, P. M., Rynearson, T. A., Saito, M. A., Schwartz, D. C., Thamatrakoln, K.,

Valentin, K., Vardi, A., Wilkerson, F. P. & Rokhsar, D. S. 2004. The genome of the diatom *Thalassiosira pseudonana*: Ecology, evolution, and metabolism. *Science* **306:**79-86.

Assmy, P. & Smetacek, V. 2009. Algal Blooms. In: Schaechter, M. [Ed.] Encyclopedia of Microbiology. Oxford, Elsevier, pp. 27-41.

Basu, S., Patil, S., Mapleson, D., Russo, M. T., Vitale, L., Fevola, C., Maumus, F., Casotti, R., Mock, T., Caccamo, M., Montresor, M., Sanges, R. & Ferrante, M. I. 2017. Finding a partner in the ocean: molecular and evolutionary bases of the response to sexual cues in a planktonic diatom. *New Phytologist* **215:**140-56.

Baudoux, A.-C., Noordeloos, A. A. M., Veldhuis, M. J. W. & Brussaard, C. P. D. 2006. Virally induced mortality of *Phaeocystis globosa* during two spring blooms in temperate coastal waters. *Aquatic Microbial Ecology* **44:**207–17.

Bender, S. J., Durkin, C. A., Berthiaume, C. T., Morales, R. L. & Armbrust, E. V. 2014. Transcriptional responses of three model diatoms to nitrate limitation of growth. *Frontiers in Marine Sciences* **1**.

Bentsink, L., & Koornneef, M. 2008. Seed dormancy and germination. *The Arabidopsis Book/American Society of Plant Biologists,* **6**.

Berges, J. A. & Falkowski, P. G. 1998. Physiological stress and cell death in marine phytoplankton: induction of proteases in response to nitrogen or light limitation. *Limnology and Oceanography* **43:**129-35.

Bettarel, Y., Kan, J., Wang, K., Williamson, K. E., Cooney, S., Ribblett, S., Chen, F., Wommack, K. E. & Coats, D. W. 2005. Isolation and preliminary characterisation of a small nuclear inclusion virus infecting the diatom *Chaetoceros cf. gracilis*. *Aquatic Microbial Ecology* **40:**103-14.

Bidle, K. D. & Azam, F. 1999. Accelerated dissolution of diatom silica by marine bacterial assemblages. *Nature* **397:**508-12.

Bidle, K. D., Haramaty, L., e Ramos, J. B., & Falkowski, P. 2007. Viral activation and recruitment of metacaspases in the unicellular coccolithophore, Emiliania huxleyi. *Proceedings of the National Academy of Sciences* **104(14):** 6049-6054.

Bidle, K. D. 2015. The molecular ecophysiology of programmed cell death in marine phytoplankton. *Annual review of marine science* **7:** 341-375.

Bondarava, N., Beyer, P. & Krieger-Liszkay, A. 2005. Function of the 23 kDa extrinsic protein of photosystem II as a manganese binding protein and its role in photoactivation. *Biochimica Et Biophysica Acta-Bioenergetics* **1708:**63-70.

Boyd, P. W., Watson, A. J., Law, C. S., Abraham, E. R., Trull, T., Murdoch, R., Bakker, D. C. E., Bowie, A. R., Buesseler, K. O., Chang, H., Charette, M., Croot, P., Downing, K., Frew, R., Gall, M., Hadfield, M., Hall, J., Harvey, M., Jameson, G., LaRoche, J., Liddicoat, M., Ling, R., Maldonado, M. T., McKay, R. M., Nodder, S., Pickmere, S., Pridmore, R., Rintoul, S., Safi, K., Sutton, P., Strzepek, R., Tanneberger, K., Turner, S., Waite, A. & Zeldis, J. 2000. A mesoscale phytoplankton bloom in the polar Southern Ocean stimulated by iron fertilization. *Nature* **407:**695-702.

Bratbak, G., Egge, J. K. & Heldal, M. 1993. Viral mortality of the marine alga *Emiliania huxleyi* (Haptophyceae) and termination of algal blooms. *Marine Ecology Progress Series* **93:**39-48.

Bratbak, G., Heldal, M., Thingstad, T. F. & Tuomi, P. 1996. Dynamics of virus abundance in coastal seawater. *FEMS Microbiology Ecology* **19:**263-69.

Breitbart, M. 2012. Marine Viruses: Truth or Dare. *Annual Review of Marine Science* **4:**425-48.

Bresnan, E., Hay, S., Hughes, S. L., Fraser, S., Rasmussen, J., Webster, L., Slesser, G., Dunn, J. & Heath, M. R. 2009. Seasonal and interannual variation in the phytoplankton community in the north east of Scotland. *Journal of Sea Research* **61:**17-25.

Brown, S. H., Zarnowski, R., Sharpee, W. C., & Keller, N. P. 2008. Morphological transitions governed by density dependence and lipoxygenase activity in Aspergillus flavus. *Applied and environmental microbiology* **74(18):** 5674-5685.

Bruhn, A., LaRoche, J. & Richardson, K. 2010. *Emiliania huxley* (Prymnesiophycea): nitrogen-metabolism genes and their expression in response to external nitrogen source. *Journal of Phycology* **46:**266-77.

Brussaard, C. P. D., Kempers, R. S., Kop, A. J., Riegman, R. & Heldal, M. 1996. Virus-like particles in a summer bloom of *Emiliania huxleyi* in the North Sea. Aquatic Microbial *Ecology* **10:**105-13.

Caldwell, G. S., Olive, P. J., & Bentley, M. G. 2002. Inhibition of embryonic development and fertilization in broadcast spawning marine invertebrates by water soluble diatom extracts and the diatom toxin 2-trans, 4-trans decadienal. *Aquatic Toxicology* **60(1-2):** 123-137.

Carlson, M. C. G., McCary, N. D., Leach, T. S. & Rocap, G. 2016. *Pseudo-nitzschia* Challenged with Co-occurring Viral Communities Display Diverse Infection Phenotypes. *Frontiers in Microbiology* **7**.

Caron, D. A., Alexander, H., Allen, A. E., Archibald, J. M., Armbrust, E. V., Bachy, C., Bell, C. J., Bharti, A., Dyhrman, S. T. & Guida, S. M. 2017. Probing the evolution, ecology and physiology of marine protists using transcriptomics. *Nature Reviews Microbiology* **15:**6.

Casotti, R., Mazza, S., Brunet, C., Vantrepotte, V., Ianora, A. & Miralto, A. 2005. Growth inhibition and toxicity of the diatom aldehyde 2-trans, 4-trans-decadienal on *Thalssiosira weissflogii* (Bacillariophyceae). *Journal of Phycology* **41:**7-20.

Catalanotti, C., Yang, W. Q., Posewitz, M. C. & Grossman, A. R. 2013. Fermentation metabolism and its evolution in algae. *Frontiers in Plant Science* **4**.

Cleve, P. T. 1896. Diatoms from Baffins Bay and Davis Strait: Collected by ME Nilsson and examined by PT Cleve.

Coates, A. R. 2003. Dormancy and Low Growth States in Microbial Disease (Advances in Molecular and Cellular Microbiology). *Cambridge: Cambridge University Press. doi:10.1017/CBO9780511546242*

Cole, J. J. 1999. Aquatic microbiology for ecosystem scientists: New and recycled paradigms in ecological microbiology. *Ecosystems* **2:** 215-25.

Cullings, K. W. & Vogler, D. R. 1998. A 5.8S nuclear ribosomal RNA gene sequence database: applications to ecology and evolution. *Molecular Ecology* **7:** 919-23.

Davis, C. O., Hollibaugh, J. T., Seibert, D. L. R., Thomas, W. H. & Harrison, P. J. 1980. Formation of resting spores by *Leptocylindrus danicus* (Bacillariophyceae) in a controlled experimental ecosystem. *Journal of Phycology* **16:** 296-302.

de Vargas, C., Audic, S., Henry, N., Decelle, J., Mahe, F., Logares, R., Lara, E., Berney, C., Le Bescot, N., Probert, I., Carmichael, M., Poulain, J., Romac, S., Colin, S., Aury, J. M., Bittner, L., Chaffron, S., Dunthorn, M., Engelen, S., Flegontova, O., Guidi, L., Horak, A., Jaillon, O., Lima-Mendez, G., Lukes, J., Malviya, S., Morard, R., Mulot, M., Scalco, E., Siano, R., Vincent, F., Zingone, A., Dimier, C., Picheral, M., Searson, S., Kandels-Lewis, S., Acinas, S. G., Bork, P., Bowler, C., Gorsky, G., Grimsley, N.,

Hingamp, P., Iudicone, D., Not, F., Ogata, H., Pesant, S., Raes, J., Sieracki, M. E., Speich, S., Stemmann, L., Sunagawa, S., Weissenbach, J., Wincker, P., Karsenti, E. & Tara Oceans, C. 2015. Eukaryotic plankton diversity in the sunlit ocean. *Science* **348(6237):** 1261605

Degerlund, M. & Eilertsen, H. 2010. Main Species Characteristics of Phytoplankton Spring Blooms in NE Atlantic and Arctic Waters (68–80° N). *Estuaries and Coasts* **33:** 242-69.

Dell'Aquila, G., Ferrante, M. I., Gherardi, M., Lagomarsino, M. C., d'Alcala, M. R., Iudicone, D. & Amato, A. 2017. Nutrient consumption and chain tuning in diatoms exposed to storm-like turbulence. *Scientific Reports* **7**.

Depauw, F., Rogato, A., Ribera d'Alcala', M. & Falciatore, A. 2012. Exploring the molecular basis of response to light in marine diatoms. *Journal of Experimental Botany* **63:**1575–91.

Derelle, E., Ferraz, C., Rombauts, S., Rouze, P., Worden, A. Z., Robbens, S., Partensky, F., Degroeve, S., Echeynie, S., Cooke, R., Saeys, Y., Wuyts, J., Jabbari, K., Bowler, C., Panaud, O., Piegu, B., Ball, S. G., Ral, J. P., Bouget, F. Y., Piganeau, G., De Baets, B., Picard, A., Delseny, M., Demaille, J., Van de Peer, Y. & Moreau, H. 2006. Genome analysis of the smallest free-living eukaryote *Ostreococcus tauri* unveils many unique features. *Proceedings of the National Academy of Sciences* **103:**11647-52.

Doucette, G. J. & Fryxell, G. A. 1983. *Thalassiosira antarctica*: vegetative and resting stage composition of an ice-related marine diatom. *Marine Biology* **78:**1-6.

Doyle, J. J. & Doyle, J. L. 1987. A rapid DNA isolation procedure for small quantities of fresh leaf tissue. *Bullettin of Phytochemistry* **19:**11-15.

Durbin, E. G. 1978. Aspects of the biology of resting spores of *Thalassiosisra nordenskioeldii* and *Detonula confervacea*. *Marine Biology* **45:**31-37.

Edlund, M. B. & Stoermer, E. F. 1997. Ecological, evolutionary, and systematic significance of diatom life histories. *Journal of Phycology* **33:** 897-918.

Edlund, M. B., Stoermer, E. F. & Taylor, C. M. 1996. *Aulacoseira skvortzowii* sp. nov.(Bacillariophyta), a poorly understood diatom from Lake Baikal, Russia. *Journal of Phycology* **32:**165-75.

Eilertsen, H. C. H. R., Sandberg, S. & Tollefsen, H. 1995. Photoperiodic control of diatom spore growth: a theory to explain the onset of phytoplankton blooms. *Marine Ecology Progress Series* **116:** 303-07.

Ellegaard, M. & Ribeiro, S. 2018. The long-term persistence of phytoplankton resting stages in aquatic 'seed banks'. *Biological Reviews* **93:** 166-83.

Falkowski, P. G., Barber, R. T. & Smetacek, V. 1998. Biogeochemical controls and feedbacks on ocean primary production. *Science* **281:** 200-06.

Ferrari, G. M. & Tassan, S. 1999. A method using chemical oxidation to remove light absorption by phytoplankton pigments. *Journal of Phycology* **35:**1090-98.

Figueroa, R. I., Estrada, M. & Garces, E. 2018. Life histories of microalgal species causing harmful blooms: Haploids, diploids and the relevance of benthic stages. *Harmful Algae* **73:** 44-57.

Finkel, Z. V., Beardall, J., Flynn, K. J., Quigg, A., Rees, T. A. V. & Raven, J. A. 2010. Phytoplankton in a changing world: cell size and elemental stoichiometry. *Journal of Plankton Research* **32:**119-37.

Fontana, A., d'Ippolito, G., Cutignano, A., Romano, G., Lamari, N., Gallucci, A. M., Cimino, G., Miralto, A. & Ianora, A. 2007. LOX-induced lipid peroxidation mechanism responsible for the detrimental effect of marine diatoms on zooplankton grazers. Chembiochem **8:** 1810-18.

Frada, M., Probert, I., Allen, M. J., Wilson, W. H. & de Vargas, C. 2008. The "Cheshire Cat" escape strategy of the coccolithophore *Emiliania huxleyi* in response to viral infection. *Proceedings of the National Academy of Sciences* **105:** 15944-49.

French, F. & Hargraves, P. E. 1980. Physiological characteristics of plankton diatom resting spores. *Marine Biology Letters* **1:** 185-95.

French III, F. W., & Hargraves, P. E. 1985. Spore formation in the life cycles of the diatoms *Chaetoceros diadema* and *Leptocylindrus danicus*1. *Journal of Phycology* **21(3):** 477-483.

Gaonkar, C. C., Kooistra, W. H., Lange, C. B., Montresor, M. & Sarno, D. 2017. Two new species in the *Chaetoceros socialis* complex (Bacillariophyta): *C. sporotruncatus* and *C. dichatoensis*, and characterization of its relatives, *C. radicans* and *C. cinctus*. *Journal of Phycology* **53.4:** 889-907.

Garrison, D. L. 1981. Monterey Bay phytoplankton. II. Resting spore cycles in coastal diatom populations. *Journal of Plankton Research* **3:** 137-56.

Geider, R. J. & La Roche, J. 2002. Redfield revisited: variability of C : N : P in marine microalgae and its biochemical basis. *European Journal of Phycology* **37:**1-17.

Gillard, J., Frenkel, J., Devos, V., Sabbe, K., Paul, C., Rempt, M., Inze, D., Pohnert, G., Vuylsteke, M. & Vyverman, W. 2013. Metabolomics enables the structure elucidation of a diatom sex pheromone. *Angewandte Chemie* (International ed. in English) **52:**854-7.

Godhe, A., Kremp, A. & Montresor, M. 2014. Genetic and microscopic evidence for sexual reproduction in the centric diatom *Skeletonema marinoi*. *Protist* **165:** 401-16.

Gran, H. 1912. Pelagic plant life. The depths of the ocean: 307-86.

Griffiths, J. A., Scialdone, A., Marioni, J. C. 2018. Using single- cell genomics to understand developmental processes and cell fate decisions. *Molecular systems biology* **14(4):** e8046.

Guillard, R. R. L. 1975. Culture of phytoplankton for feeding marine invertebrates. In: Smith, W. L. & Chanley, M. H. [Eds.] Culture of Marine Invertebrate Animals. Plenum Press, New York, pp. 29-60.

Haas, B. J., Papanicolaou, A., Yassour, M., Grabherr, M., Blood, P. D., Bowden, J., Couger, M. B., Eccles, D., Li, B., Lieber, M., MacManes, M. D., Ott, M., Orvis, J., Pochet, N., Strozzi, F., Weeks, N., Westerman, R., William, T., Dewey, C. N., Henschel, R., Leduc, R. D., Friedman, N. & Regev, A. 2013. De novo transcript sequence reconstruction from RNA-seq using the Trinity platform for reference generation and analysis. *Nature Protocols* **8:** 1494-512.

Hammer, Ø., Harper, D. & Ryan, P. 2001. PAST-Palaeontological statistics. www. uv. es/~ pardomv/pe/2001_1/past/pastprog/past. pdf, acessado em **25:**2009.

Hansen, H. P. & Grasshoff, K. 1983. Automated chemical analysis. In: Grasshoff, K., Ehrhardt, M. & Krernling, K. [Eds.] Methods of seawater analysis. *Verlag Chemie*, Weinheim, pp. 347-79.

Hansen, P. J. 2002. Effect of high pH on the growth and survival of marine phytoplankton: implications for species succession. *Aquatic Microbial Ecology* **28:** 279-88.

Hargraves, P. E. & French, F. W. 1983. Diatom resting spores: significance and strategies. In: Fryxell, G. A. [Ed.] Survival Strategies of the Algae. *Cambridge University Press*, Cambridge, pp. 49-68.

Hargraves, P. E. 1979. Studies on marine plankton Diatoms. IV. Morphology of *Chaetoceros* resting spores. *Nova Hedwigia Beihefte Series* **64:**99-120.

Härnström, K., Ellegaard, M., Andersen, T. J. & Godhe, A. 2011. Hundred years of genetic structure in a sediment revived diatom population. *Proceedings of the National Academy of Sciences* **108:** 4252-57.

Harrison, P., Zingone, A., Mickelson, M., Lehtinen, S., Ramaiah, N., Kraberg, A., Sun, J., McQuatters-Gollop, A. & Jakobsen, H. 2015. Cell Volumes of Marine Phytoplankton from Globally Distributed Coastal Data Sets. *Estuarine, Coastal and Shelf Science*, ***162*****:** 130-142.

Hasle, G. R. & Syvertsen, E. E. 1997. Marine diatoms. In: Tomas, C. R. [Ed.] Identifying marine phytoplankton. *Academic Press*, San Diego, pp. 5-385.

Hasle, G. R., Syvertsen, E. E., Steidinger, K. A., Tangen, K. & Tomas, C. R. 1996. Identifying marine diatoms and dinoflagellates. *Academic Press*, **11:**209-57.

Hedges, J. I. & Stern, J. H. 1984. Carbon and Nitrogen determination of carbonate containing solids. *Limnology and Oceanography* **29:** 657-63.

Hensen, V. 1887. Über die Bestimmung des Planktons oder des im Meere treibenden Material an Pflanzen und Tiere. Kommission zur wissenschaftlichen Untersuchungen der deutschen Meere in Kiel, 1882-1886. *V. Bericht, Jahrgang* **12-16:**1-107.

Hockin, N. L., Mock, T., Mulholland, F., Kopriva, S. & Malin, G. 2012. The response of diatom central carbon metabolism to nitrogen starvation is different to that of green algae and higher plants. *Plant physiology* pp-111.

Hollibaugh, J. T., Seibert, D. H. L. & Thomas, W. H. 1981. Observations on the survival and germination of resting spores of three *Chaetoceros* (Bacillariophyceae) species. *Journal of Phycology* **17:** 1-9.

Ianora, A., Bastianini, M., Carotenuto, Y., Casotti, R., Roncalli, V., Miralto, A., Romano, G., Gerecht, A., Fontana, A. & Turner, J. T. 2015. Non-volatile oxylipins can render some diatom blooms more toxic for copepod reproduction. *Harmful Algae* **44:** 1-7.

Ianora, A., Miralto, A. 2010. Toxigenic effects of diatoms on grazers, phytoplankton and other microbes: a review. E*cotoxicology*, **19(3):** 493-511.

Ianora, A., Miralto, A., Poulet, S. A., Carotenuto, Y., Buttino, I., Romano, G., Casotti, R., Pohnert, G., Wichard, T., Colucci-D'Amato, L., Terrazzano, G. & Smetacek, V. 2004. Aldehyde suppression of copepod recruitment in blooms of a ubiquitous planktonic diatom. *Nature* **429:** 403-07.

Ianora, A., Romano, G., Carotenuto, Y., Esposito, F., Roncalli, V., Buttino, I. & Miralto, A. 2011. Impact of the diatom oxylipin 15S-HEPE on the reproductive success of the copepod *Temora stylifera. Hydrobiologia* **666:** 265-75.

Imai, A., Matsuyama, T., Hanzawa, Y., Akiyama, T., Tamaoki, M., Saji, H., Shirano, Y., Kato, T., Hayashi, H. & Shibata, D. 2004. Spermidine synthase genes are essential for survival of *Arabidopsis*. *Plant Physiology* **135:** 1565-73.

Jacquet, S., Heldal, M., Iglesias-Rodriguez, D., Larsen, A., Wilson, W. & Bratbak, G. 2002. Flow cytometric analysis of an *Emiliana huxleyi* bloom terminated by viral infection. *Aquatic Microbial Ecology* **27:** 111-24.

Jaubert, M., Bouly, J. P., d'Alcalà, M. R. & Falciatorel, A. 2017. Light sensing and responses in marine microalgae. *Current Opinion in Plant Biology* **37:** 70-77.

Jewson, D. H., Granin, N. G., Zhdanov, A. A., Gorbunova, L. A., Bondarenko, N. A. & Gnatovsky, R. Y. 2008. Resting stages and ecology of the planktonic diatom *Aulacoseira skvortzowii* in Lake Baikal. *Limnology and Oceanography* **53:** 1125-36.

Jian, J. B., Zeng, D. Z., Wei, W., Lin, H. M., Li, P. & Liu, W. H. 2017. The Combination of RNA and Protein Profiling Reveals the Response to Nitrogen Depletion in *Thalassiosira pseudonana*. *Scientific Reports* **7**.

Jiang, S. C. & Paul, J. H. 1995. Viral contribution to dissolved DNA in the marine environment as determined by differential centrifugation and kingdom probing. *Applied and Environmental Microbiology* **61:** 317-25.

Jiang, S. C. & Paul, J. H. 1998. Gene transfer by transduction in the marine environment. *Applied and Environmental Microbiology* **64:** 2780-87.

Jones, S. E. & Lennon, J. T. 2010. Dormancy contributes to the maintenance of microbial diversity. *Proceedings of the National Academy of Sciences* **107:** 5881-86.

Kamp, A., de Beer, D., Nitsch, J. L., Lavik, G. & Stief, P. 2011. Diatoms respire nitrate to survive dark and anoxic conditions. *Proceedings of the National Academy of Sciences* **108:** 5649–54

Kaplan-Levy, R. N., Hadas, O., Summers, M. L., Rücker, J. & Sukenik, A. 2010. Akinetes: dormant cells of cyanobacteria. Dormancy and resistance in harsh environments. Springer, pp. 5-27.

Keeling, P. J., Burki, F., Wilcox, H. M., Allam, B., Allen, E. E., Amaral-Zettler, L. A., Armbrust, E. V., Archibald, J. M., Bharti, A. K., Bell, C. J., Beszteri, B., Bidle, K. D., Cameron, C. T., Campbell, L., Caron, D. A., Cattolico, R. A., Collier, J. L., Coyne, K., Davy, S. K., Deschamps, P., Dyhrman, S. T., Edvardsen, B., Gates, R. D., Gobler, C. J., Greenwood, S. J., Guida, S. M., Jacobi, J. L., Jakobsen, K. S., James, E. R., Jenkins, B., John, U., Johnson, M. D., Juhl, A. R., Kamp, A., Katz, L. A., Kiene, R., Kudryavtsev, A., Leander, B. S., Lin, S., Lovejoy, C., Lynn, D., Marchetti, A., McManus, G., Nedelcu, A. M., Menden-Deuer, S., Miceli, C., Mock, T., Montresor, M., Moran, M. A., Murray, S., Nadathur, G., Nagai, S., Ngam, P. B., Palenik, B., Pawlowski, J., Petroni, G., Piganeau, G., Posewitz, M. C., Rengefors, K., Romano, G., Rumpho, M. E., Rynearson, T., Schilling, K. B., Schroeder, D. C., Simpson, A. G. B., Slamovits, C. H., Smith, D. R., Smith, G. J., Smith, S. R., Sosik, H. M., Stief, P., Theriot, E., Twary, S., Umale, P. E., Vaulot, D., Wawrik, B., Wheeler, G. L., Wilson, W. H., Xu, Y., Zingone, A. & Worden, A. Z. 2014. The Marine Microbial Eukaryote Transcriptome Sequencing Project (MMETSP): Illuminating the Functional Diversity of Eukaryotic Life in the Oceans through Transcriptome Sequencing. *PLoS Biology* **12**.

Kimura, K. & Tomarua, Y. 2015. Discovery of Two Novel Viruses Expands the Diversity of Single-Stranded DNA and Single-Stranded RNA Viruses Infecting a Cosmopolitan Marine Diatom. *Applied and Environmental Microbiology* **81:** 1120-31.

Kooistra, W. H. C. F., Gersonde, R., Medlin, L. K. & Mann, D. G. 2007. The origin and evolution of the diatoms: their adaptation to a planktonic existence. In: Falkowski, P. G. & Knoll, A. H. [Eds.] Evolution of Primary Producers in the Sea Elsevier Academic Press, Burlington, pp. 207-50.

Kopylova, E., Noe, L. & Touzet, H. 2012. SortMeRNA: fast and accurate filtering of ribosomal RNAs in metatranscriptomic data. *Bioinformatics* **28:** 3211-17.

Kraml, M. & Herrmann, H. 1991. Red blue-interaction in mesotaenium chloroplast movement - blue seems to stabilize the transient memory of the phytochrome signal. *Photochemistry and Photobiology* **53:** 255-59.

Kuwata, A. & Takahashi, M. 1990. Life-form population responses of a marine planktonic diatom, *Chaetoceros pseudocurvisetus*, to oligotrophication in regionally upwelled waters. *Marine Biology* **107:** 503-12.

Kuwata, A. & Tsuda, A. 2005. Selection and viability after ingestion of vegetative cells, resting spores and resting cells of the marine diatom, *Chaetoceros pseudocurvisetus*, by two copepods. *Journal of Experimental Marine Biology and Ecology* **322:** 143– 51.

Kuwata, A., Hama, T. & Takahashi, M. 1993. Ecophysiological characterization of two life forms, resting spores and resting cells, of a marine planktonic diatom, *Chaetoceros pseudocurvisetus*, formed under nutrient depletion. *Marine Ecology Progress Series* **102:** 245-55.

Lakeman, M. B., von Dassow, P. & Cattolico, R. A. 2009. The strain concept in phytoplankton ecology. *Harmful Algae* **8:** 746-58.

Laloi, C., Apel, K., Danon, A. 2004. Reactive oxygen signalling: the latest news. *Current opinion in plant biology* **7(3):** 323-328.

Lang, A. S. & Beatty, J. T. 2007. Importance of widespread gene transfer agent genes in α-proteobacteria. *Trends in microbiology* **15:** 54-62.

Lauder, H. S. 1864. On new diatoms. *The Quarterly Journal of Microscopical Science* **4:** 6-8.

Lennon, J. T. & Jones, S. E. 2011. Microbial seed banks: the ecological and evolutionary implications of dormancy. *Nature Reviews Microbiology* **9:** 119-30.

Levitan, O., Dinamarca, J., Zelzion, E., Lun, D. S., Guerra, L. T., Kim, M. K., Kim, J., Van Mooy, B. A. S., Bhattacharya, D. & Falkowski, P. G. 2015. Remodeling of intermediate metabolism in the diatom *Phaeodactylum tricornutum* under nitrogen stress. *Proceedings of the National Academy of Sciences* **112:** 412-17.

Lewis, J., Harris, A. S. D., Jones, K. J. & Edmonds, R. L. 1999. Long term survival of marine planktonic diatoms and dinoflagellates in stored sediment samples. *Journal of Plankton Research* **21:** 343-54.

Li, Y., Boonprakob, A., Gaonkar, C. C., Kooistra, W., Lange, C. B., Hernandez-Becerrill, D., Chen, Z. Y., Moestrup, O. & Lundholm, N. 2017. Diversity in the Globally Distributed Diatom Genus *Chaetoceros* (Bacillariophyceae): Three New Species from Warm-Temperate Waters. *Plos One* **12**.

Lin, Q., Liang, J.-R., Huang, Q.-Q., Luo, C.-S., Anderson, D. M., Bowler, C., Chen, C.-P., Li, X.-S. & Gao, Y.-H. 2017a. Differential cellular responses associated with oxidative stress and cell fate decision under nitrate and phosphate limitations in *Thalassiosira pseudonana*: Comparative proteomics. *PloS one* **12**: e0184849.

Livingstone, D., & Jaworski, G. H. M. (1980). The viability of akinetes of blue-green algae recovered from the sediments of Rostherne Mere. *British Phycological Journal* **15(4):** 357-364.

Lund, J. 1954. The seasonal cycle of the plankton diatom, *Melosira italica* (Ehr.) Kutz. subsp. *subarctica* O. Mull. *The Journal of Ecology* pp151-79.

Malviya, S., Scalco, E., Audic, S., Vincenta, F., Veluchamy, A., Poulain, J., Wincker, P., Iudicone, D., de Vargas, C., Bittner, L., Zingone, A. & Bowler, C. 2016. Insights into global diatom distribution and diversity in the world's ocean. *Proceedings of the National Academy of Sciences* 201509523.

Marcus, N. 1996. Ecological and evolutionary significance of resting eggs in marine copepods: past, present, and future research. *Hydrobiologia* **320:** 141-52.

Marcus, N. H. & Boero, F. 1998. Minireview: The importance of benthic-pelagic coupling and the forgotten role of life cycles in coastal aquatic systems. *Limnology and Oceanography* **43:** 763-68.

Marcus, N. H. 2005. Calanoid copepods, resting eggs, and aquaculture. *Copepods in aquaculture*: 3-9.

Matrai, P., Thompson, B. & Keller, M. 2005. Circannual excystment of resting cysts of Alexandrium spp. from eastern Gulf of Maine populations. *Deep Sea Research Part II: Topical Studies in Oceanography* **52(19-21):** 2560-2568.

McKenney, P. T. & Eichenberger, P. 2012. Dynamics of spore coat morphogenesis in *Bacillus subtilis*. *Molecular Microbiology* **83:**245-60.

McKenney, P. T., Driks, A. & Eichenberger, P. 2013. The Bacillus subtilis endospore: assembly and functions of the multilayered coat. *Nature Reviews Microbiology* **11:** 33-44.

McQuoid, M. R. & Godhe, A. 2004. Recruitment of coastal planktonic diatoms from benthic versus pelagic cells: variations in bloom development and species composition. *Limnology and Oceanography* **49:** 1123-33.

McQuoid, M. R. & Hobson, L. A. 1996. Diatom resting stages. *Journal of Phycology* **32:** 889-902.

McQuoid, M. R. 2002. Pelagic and benthic environmental controls on the spatial distribution of a viable diatom propagule bank on the Swedish west coast. *Journal of Phycology* **38:** 881–93.

McQuoid, M. R., Godhe, A. & Nordberg, K. 2002. Viability of phytoplankton resting stages in the sediments of a coastal Swedish fjord. *European Journal of Phycology* **37:** 191-201.

Middelboe, M. & Lyck, P. G. 2002. Regeneration of dissolved organic matter by viral lysis in marine microbial communities. *Aquatic Microbial* ***Ecology*** **27:**187-94.

Miller, M. B. & Bassler, B. L. 2001. Quorum sensing in bacteria. *Annual Review of Microbiology* **55:** 165-99.

Mock, T., Samanta, M. P., Iverson, V., Berthiaume, C., Robison, M., Holtermann, K., Durkin, C., BonDurant, S. S., Richmond, K., Rodesch, M., Kallas, T., Huttlin, E. L., Cerrina, F., Sussmann, M. R. & Armbrust, E. V. 2008. Whole-genome expression profiling of the marine diatom *Thalassiosira pseudonana* identifies genes involved in silicon bioprocesses. *Proceedings of the National Academy of Sciences* **105:** 1579-84.

Moeys, S., Frenkel, J., Lembke, C., Gillard, J. T. F., Devos, V., Van den Berge, K., Bouillon, B., Huysman, M. J. J., De Decker, S., Scharf, J., Bones, A., Brembu, T., Winge, P., Sabbe, K., Vuylsteke, M., Clement, L., De Veylder, L., Pohnert, G. & Vyverman, W. 2016. A sex-inducing pheromone triggers cell cycle arrest and mate attraction in the diatom *Seminavis robusta*. *Scientific Reports* **6**.

Montresor, M. 1995. The life history of *Alexandrium pseudogonyaulax* (Gonyaulacales, Dinophyceae). *Phycologia* **34:** 444-48.

Montresor, M., Di Prisco, C., Sarno, D., Margiotta, F. & Zingone, A. 2013. Diversity and germination patterns of diatom resting stages at a coastal Mediterranean site. *Marine Ecology Progress Series* **484:** 79-95.

Montresor, M., Vitale, L., D'Alelio, D. & Ferrante, M. I. 2016. Sex in marine planktonic diatoms: insights and challenges. *Perspectives in Phycology* **3:** 61-75.

Moore, S. K., Bill, B. D., Hay, L. R., Emenegger, J., Eldred, K. C., Greengrove, C. L., Masura, J. E. & Anderson, D. M. 2015. Factors regulating excystment of *Alexandrium* in Puget Sound, WA, USA. *Harmful Algae* **43:** 103-10.

Mukamolova, G. V., Kaprelyants, A. S., Young, D. I., Young, M. & Kell, D. B. 1998. A bacterial cytokine. *Proceedings of the National Academy of Sciences* **95:** 8916-21.

Musacchia, F., Basu, S., Petrosino, G., Salvemini, M. & Sanges, R. 2015. Annocript: a flexible pipeline for the annotation of transcriptomes able to identify putative long noncoding RNAs. B*ioinformatics* **31:** 2199-201.

Nagasaki, K., Ando, M., Itakura, S., Imai, I. & Ishida, Y. 1994. Viral mortality in the final stage of *Heterosigma akashiwo* (Raphidophyceae) red tide. *Journal of Plankton Research* **16:** 1595-99.

Nagasaki, K., Tomaru, Y., Katanozaka, N., Shirai, Y., Nishida, K., Itakura, S. & Yamaguchi, M. 2004. Isolation and characterization of a novel single-stranded RNA virus infecting the bloom-forming diatom Rhizosolenia setigera. *Applied and Environmental Microbiology* **70:** 704-11.

Nagasaki, K., Tomaru, Y., Takao, Y., Nishida, K., Shirai, Y., Suzuki, H. & Nagumo, T. 2005. Previously unknown virus infects marine diatom. *Applied and Environmental Microbiology* **71:** 3528-35.

Nanjappa, D., Sanges, R., Ferrante, M. I. & Zingone, A. 2017. Diatom flagellar genes and their expression during sexual reproduction in Leptocylindrus danicus. *BMC genomics* **18(1):** 813.

Nedelcu, A. M. & Michod, R. E. 2003. Sex as a response to oxidative stress: the effect of antioxidants on sexual induction in a facultatively sexual lineage. *Proceedings of the Royal Society of London Series B: Biological Sciences* **270:**S136-S39.

Nedelcu, A. M. 2005. Sex as a response to oxidative stress: stress genes co-opted for sex. *Proceedings of the Royal Society of London Series B: Biological Sciences* **272:**1935-40.

Nedelcu, A. M., Marcu, O. & Michod, R. E. 2004. Sex as a response to oxidative stress: a twofold increase in cellular reactive oxygen species activates sex genes. *Proceedings of the Royal Society of London Series B-Biological Sciences* **271:**1591-96.

Newcombe, R. G. 1998. Interval estimation for the difference between independent proportions: Comparison of eleven methods. *Statistics in Medicine* **17:**873-90.

Not, F., Siano, R., Kooistra, W., Simon, N., Vaulot, D. & Probert, I. 2012. Diversity and Ecology of Eukaryotic Marine Phytoplankton. In: Piganeau, G. [Ed.] *Genomic Insights into the Biology of Algae.* pp. 1-53.

O'Donnell, D. R., Fey, S. B. & Cottingham, K. L. 2013. Nutrient availability influences kairomone-induced defenses in *Scenedesmus acutus* (Chlorophyceae). *Journal of Plankton Research* **35:**191-200.

Oku, O. & Kamatani, A. 1995. Resting spore formation and phosphorus composition of the marine diatom *Chaetoceros pseudocurvisetus* under various nutrient conditions. *Marine Biology* **123:**393-99.

Oku, O. & Kamatani, A. 1997. Resting spore formation of the marine planktonic diatom *Chaetoceros anastomosans* induced by high salinity and nitrogen depletion. *Marine Biology* **127:**515-20.

Oku, O. & Kamatani, A. 1999. Resting spore formation and biochemical composition of the marine planktonic diatom *Chaetoceros pseudocurvisetus* in culture: ecological significance of decreased nucleotide content and activation of the xanthophyll cycle by resting spore formation. *Marine Biology* **135:**425-36.

Onodera, J. & Ohsumi, Y. 2004. Ald6p is a preferred target for autophagy in yeast, *Saccharomyces cerevisiae*. *Journal of Biological Chemistry* **279:**16071-76.

Patil, S., Moeys, S., von Dassow, P., Huysman, M. J. J., Mapleson, D., De Veylder, L., Sanges, R., Vyverman, W., Montresor, M. & Ferrante, M. I. 2015. Identification of the meiotic toolkit in diatoms and exploration of meiosis-specific SPO11 and RAD51 homologs in the sexual species *Pseudo-nitzschia multistriata* and *Seminavis robusta*. BMC Genomics **16:**doi: 10.1186/s12864-015-1983-5.

Paul, J. H. 2008. Prophages in marine bacteria: dangerous molecular time bombs or the key to survival in the seas? *The ISME journal* **2:**579.

Peacock, L., Bailey, M., Carrington, M. & Gibson, W. 2014. Meiosis and haploid gametes in the pathogen *Trypanosoma brucei*. *Current Biology* **24:**181-86.

Peperzak, L. & Brussaard, C. P. 2011. Flow cytometric applicability of fluorescent vitality probes on phytoplankton. *Journal of Phycology* **47:**692-702.

Pickett-Heaps, J. D. 1998. Cell division and morphogenesis of the centric diatom *Chaetoceros decipiens* (Bacillariophyceae). I. Living cells. *Journal of Phycology* **34:**989-94.

Piredda, R., Sarno, D., Lange, C. B., Tomasino, M. P., Zingone, A. & Montresor, M. 2017. Diatom resting stages in surface sediments: a pilot study comparing Next Generation Sequencing and Serial Dilution Cultures. *Cryptogamie, Algologie,* **38:**31-46.

Pitcher, G. C. 1986. Sedimentary flux and the formation of resting spores of selected Chaetoceros species at two sites in the southern Benguela system. *South African Journal of Marine Science* **4:**231-44.

Plomp, M., Carroll, A. M., Setlow, P. & Malkin, A. J. 2014. Architecture and assembly of the *Bacillus subtilis* spore coat. *PLoS One* **9.9:**e108560.

Ragni, M. & Ribera D'Alcalà, M. 2004. Light as an information carrier underwater. *Journal of Plankton Research* **26:**433 - 43.

Read, B. A., Kegel, J., Klute, M. J., Kuo, A., Lefebvre, S. C., Maumus, F., Mayer, C., Miller, J., Monier, A., Salamov, A., Young, J., Aguilar, M., Claverie, J. M., Frickenhaus, S., Gonzalez, K., Herman, E. K., Lin, Y. C., Napier, J., Ogata, H., Sarno, A. F., Shmutz, J., Schroeder, D., de Vargas, C., Verret, F., von Dassow, P., Valentin, K., Van de Peer, Y., Wheeler, G., Dacks, J. B., Delwiche, C. F., Dyhrman, S. T., Glockner, G., John, U., Richards, T., Worden, A. Z., Zhang, X. Y., Grigoriev, I. V., Allen, A. E., Bidle, K., Borodovsky, M., Bowler, C., Brownlee, C., Cock, J. M., Elias, M., Gladyshev, V. N., Groth, M., Guda, C., Hadaegh, A., Iglesias-Rodriguez, M. D.,

Jenkins, J., Jones, B. M., Lawson, T., Leese, F., Lindquist, E., Lobanov, A., Lomsadze, A., Malik, S. B., Marsh, M. E., Mackinder, L., Mock, T., Mueller-Roeber, B., Pagarete, A., Parker, M., Probert, I., Quesneville, H., Raines, C., Rensing, S. A., Riano-Pachon, D. M., Richier, S., Rokitta, S., Shiraiwa, Y., Soanes, D. M., van der Giezen, M., Wahlund, T. M., Williams, B., Wilson, W., Wolfe, G., Wurch, L. L. & Emiliania Huxleyi, A. 2013. Pan genome of the phytoplankton *Emiliania* underpins its global distribution. *Nature* **499**:209-13.

Rembauville, M., Blain, S., Armand, L., Quéguiner, B. & Salter, I. 2015. Export fluxes in a naturally iron-fertilized area of the Southern Ocean-Part 2: Importance of diatom resting spores and faecal pellets for export. *Biogeosciences* **12(11):** 3171-3195.

Rembauville, M., Manno, C., Tarling, G., Blain, S. & Salter, I. 2016. Strong contribution of diatom resting spores to deep-sea carbon transfer in naturally iron-fertilized waters downstream of South Georgia. Deep Sea Research Part I: *Oceanographic Research Papers* **115:**22-35.

Ribalet, F., Bastianini, M., Vidoudez, C., Acri, F., Berges, J., Ianora, A., Miralto, A., Pohnert, G., Romano, G., Wichard, T. & Casotti, R. 2014. Phytoplankton Cell Lysis Associated with Polyunsaturated Aldehyde Release in the Northern Adriatic Sea. *PLoS ONE* **9:**e85947.

Ribalet, F., Intertaglia, L., Lebaron, P. & Casotti, R. 2008. Differential effect of three polyunsaturated aldehydes on marine bacterial isolates. *Aquatic Toxicology* **86:**249-55.

Ribera d'Alcalà, M., Conversano, F., Corato, F., Licandro, P., Mangoni, O., Marino, D., Mazzocchi, M., Modigh, M., Montresor, M. & Nardella, M. 2004. Seasonal patterns in plankton communities in a pluriannual time series at a coastal Mediterranean

site (Gulf of Naples): an attempt to discern recurrences and trends. *Scientia Marina* **68:**65-83.

Robinson, M. D., McCarthy, D. J. & Smyth, G. K. 2010. edgeR: a Bioconductor package for differential expression analysis of digital gene expression data. *Bioinformatics* **26:**139-40.

Rogato, A., Amato, A., Iudicone, D., Chiurazzi, M., Ferrante, M. I. & d'Alcalà, M. R. 2015. The diatom molecular toolkit to handle nitrogen uptake. *Marine genomics* **24:**95-108.

Rosenwasser, S., van Creveld, S. G., Schatz, D., Malitsky, S., Tzfadia, O., Aharoni, A., Levin Y., Gabashvili A., Feldmesser E., Vardi, A. (2014). Mapping the diatom redox-sensitive proteome provides insight into response to nitrogen stress in the marine environment. *Proceedings of the National Academy of Sciences* **111(7):** 2740-2745.

Roth, B. L., Poot, M., Yue, S. T., & Millard, P. J. 1997. Bacterial viability and antibiotic susceptibility testing with SYTOX green nucleic acid stain. *Applied and environmental microbiology* **63(6):** 2421-2431.

Round, F. E., Crawford, R. M. & Mann, D. G. 1990. Diatoms: biology and morphology of the genera. Cambridge University Press.

Rynearson, T. A., Richardson, K., Lampitt, R. S., Sieracki, M. E., Poulton, A. J., Lyngsgaard, M. M. & Perry, M. J. 2013. Major contribution of diatom resting spores to vertical flux in the sub-polar North Atlantic. *Deep Sea Research Part I: Oceanographic Research Papers* **82:**60-71.

Sandgren, C. D. & Flanagin, J. 1986. Heterothallic sexuality and density dependent encystment in the crysophycean alga *Synura petersenii* Korsh. *Journal of Phycology* **22:**206-16.

Scalco, E., Stec, K., Iudicone, D., Ferrante, M. I. & Montresor, M. 2014. The dynamics of sexual phase in the marine diatom *Pseudo-nitzschia multistria*ta (Bacillariophyceae). *Journal of Phycology* **50:**817-28.

Schindelin, J., Arganda-Carreras, I., Frise, E., Kaynig, V., Longair, M., Pietzsch, T., Preibisch, S., Rueden, C., Saalfeld, S. & Schmid, B. 2012. Fiji: an open-source platform for biological-image analysis. *Nature Methods* **9**:676-82.

Serafimidis, I., Bloomfield, G., Skelton, J., Ivens, A. & Kay, R. R. 2007. A new environmentally resistant cell type from *Dictyostelium*. *Microbiology* **153.2:** 619-630.

Sharoni, S., Trainic, M., Schatz, D., Lehahn, Y., Flores, M. J., Bidle, K. D., Ben-Dor, S., Rudich, Y., Koren, I. & Vardi, A. 2015. Infection of phytoplankton by aerosolized marine viruses. *Proceedings of the National Academy of Sciences* **112:**6643-47.

Shikata, T., Iseki, M., Matsunaga, S., Higashi, S.-i., Kamei, Y. & Watanabe, M. 2011. Blue and Red Light-Induced Germination of Resting Spores in the Red-Tide Diatom *Leptocylindrus danicus*. *Photochemistry and Photobiology* **87:**590-97.

Shikata, T., Nukata, A., Yoshikawa, S., Matsubara, T., Yamasaki, Y., Shimasaki, Y., Oshima, Y. & Honjo, T. 2009. Effects of light quality on initiation and development of meroplanktonic diatom blooms in a eutrophic shallow sea. *Marine Biology* **156:**875-89.

Shimizu, K., Del Amo, Y., Brzezinski, M. A., Stucky, G. D. & Morse, D. E. 2001. A novel fluorescent silica tracer for biological silicification studies. *Chemistry & Biology* **8:**1051-60.

Sicko-Goad, L., Stoermer, E. & Kociolek, J. 1989. Diatom resting cell rejuvenation and formation: time course, species records and distribution. *Journal of Plankton Research* **11:**375-89.

Simon, R. D. 1977. Macromolecular composition of spores from the filamentous cyanobacterium *Anabaena cylind*rica. *Journal of Bacteriology* **129:**1154.

Sineshchekov, O., Lebert, M. & Hader, D. P. 2000. Effects of light on gravitaxis and velocity in *Chlamydomonas reinhardtii*. *Journal of Plant Physiology* **157:**247-54.

Smith, H. 2000. Phytochromes and light signal perception by plants - an emerging synthesis. *Nature* **407:**585-91.

Snell, T. W., Burke, B. E. & Messur, S. D. 1983. Size and distribution of resting eggs in a natural population of the rotifer *Brachionus plicatilis*. *Gulf and Caribbean Research* **7:**285-87.

Speijer, D., Lukeš, J. & Eliáš, M. 2015. Sex is a ubiquitous, ancient, and inherent attribute of eukaryotic life. *Proceedings of the National Academy of Sciences* **112:**8827-34.

Stevenson, L. H. 1977. A case for bacterial dormancy in aquatic systems. *Marine Microbiology* **4:**127-33.

Sugie, K. & Kuma, K. 2008. Resting spore formation in the marine diatom *Thalassiosira nordenskioeldii* under iron- and nitrogen-limited conditions. *Journal of Plankton Research* **30:**1245-55.

Sutherland, J. M., Herdman, M. & Stewart, W. D. P. 1979. Akinetes of the cyanobacterium *Nostoc* PCC 7524: Macromolecular composition, structure and control of differentiation. *Journal of General Microbiology* **115:**273-87.

Suttle, C. A. 2005. Viruses in the sea. *Nature* **437:**356-61.

Suttle, C. A. 2007. Marine viruses - major players in the global ecosystem. *Nature Reviews Microbiology* **5:**801-12.

Syvertsen, E. E. 1979. Resting spore formation in clonal cultures of *Thalassiosira antarctica* Comber; *T. nordenskioeldii* Cleve and *Detonula confervacea* (Cleve) Gran. Nova Hedwigia Beihefte Series **64:**41-63.

Tai, V., Lawrence, J. E., Lang, A. S., Chan, A. M., Culley, A. I. & Suttle, C. A. 2003. Characterization of HaRNAV, a single-stranded RNA virus causing lysis of *Heterosigma akashiw*o (Raphidophyceae). *Journal of Phycology* **39:**343-52.

Tarutani, K., Nagasaki, K. & Yamaguchi, M. 2000. Viral impacts on total abundance and clonal composition of the harmful bloom-forming phytoplankton *Heterosigma akashiwo*. *Applied and Environmental Microbiology* **66:**4916-20.

Tarutani, K., Nagasaki, K. & Yamaguchi, M. 2006. Virus adsorption process determines virus susceptibility in *Heterosigma akashiwo* (Raphidophyceae). *Aquatic Microbial Ecology* **42:**209-13.

Tassan, S. & Ferrari, G. M. 1995. An alternative approach to absorption measurements of aquatic particles retained on filters. *Limnology and Oceanography* **40:**1358-68.

Thamatrakoln, K., Bailleul, B., Brown, C. M., Gorbunov, M. Y., Kustka, A. B., Frada, M., Joliot, P. A., Falkowski, P. G. & Bidle, K. D. 2013. Death-specific protein in

a marine diatom regulates photosynthetic responses to iron and light availability. *Proceedings of the National Academy of Sciences* **110:**20123-28.

Tomaru, Y. & Kimura, K. 2016. Rapid quantification of viable cells of the planktonic diatom *Chaetoceros tenuissimus* and associated RNA viruses in culture. *Plankton & Benthos Research* **11:**9-16.

Tomaru, Y., Shirai, Y., Suzuki, H., Nagumo, T. & Nagasaki, K. 2008. Isolation and characterization of a new single-stranded DNA virus infecting the cosmopolitan marine diatom *Chaetoceros debilis*. *Aquatic Microbial Ecology* **50:**103-12

Tomaru, Y., Takao, Y., Suzuki, H., Nagumo, T. & Nagasaki, K. 2009. Isolation and characterization of a single-stranded RNA virus infecting the bloom-forming diatom *Chaetoceros socialis*. *Applied and Environmental Microbiology* **75:**2375-81.

Tomaru, Y., Takao, Y., Suzuki, H., Nagumo, T., Koike, K. & Nagasaki, K. 2011. Isolation and Characterization of a Single-Stranded DNA Virus Infecting *Chaetoceros lorenzianus* Grunow. *Applied and Environmental Microbiology* **77:**5285-93.

Tomaru, Y., Tarutani, K., Yamaguchi, M. & Nagasaki, K. 2004. Quantitative and qualitative impacts of viral infection on a *Heterosigma akashiwo* (Raphidophyceae) bloom in Hiroshima Bay, Japan. *Aquatic Microbial Ecology* **34:**227-38.

Untergasser, A., Cutcutache, I., Koressaar, T., Ye, J., Faircloth, B. C., Remm, M. & Rozen, S. G. 2012. Primer3—new capabilities and interfaces. *Nucleic acids research* **40(15):**e115-e15.

van der Horst, M. A., & Hellingwerf, K. J. 2004. Photoreceptor proteins,"star actors of modern times": a review of the functional dynamics in the structure of

representative members of six different photoreceptor families. *Accounts of chemical research* **37(1):** 13-20.

van Gestel, J., Nowak, M. A. & Tarnita, C. E. 2012. The Evolution of Cell-to-Cell Communication in a Sporulating Bacterium. *PLoS computational biology* **8(12):** e1002818.

Vardi, A., Berman-Frank, I., Rozenberg, T., Hadas, O., Kaplan, A. & Levine, A. 1999. Programmed cell death of the dinoflagellate *Peridinium gatunense* is mediated by CO2 limitation and oxidative stress. *Current Biology* **9:**1061-64.

Vardi, A., Formiggini, F., Casotti, R., De Martino, A., Ribalet, F., Miralto, A. & Bowler, C. 2006. A stress surveillance system based on calcium and nitric oxide in marine diatoms. *Plos Biology* **4:**419-11.

Vardi, A., Haramaty, L., Van Mooy, B. A., Fredricks, H. F., Kimmance, S. A., Larsen, A. & Bidle, K. D. 2012. Host–virus dynamics and subcellular controls of cell fate in a natural coccolithophore population. *Proceedings of the National Academy of Sciences* **109:**19327-32.

von Dassow, P. & Montresor, M. 2011. Unveiling the mysteries of phytoplankton life cycles: patterns and opportunities behind complexity. *Journal of Plankton Research* **33:**3-12.

von Dassow, P., John, U., Ogata, H., Probert, I., Bendif, E. M., Kegel, J. U., Audic, S., Wincker, P., Da Silva, C. & Claverie, J.-M. 2015. Life-cycle modification in open oceans accounts for genome variability in a cosmopolitan phytoplankton. *The ISME journal* **9:**1365-77.

von Stosch, H. & Kowallik, K. 1969. Der von L. Geitler aufgestellte Satz über die Notwendigkeit einer Mitose für jede Schalenbildung von Diatomeen.

Beobachtungen über die Reichweite und Überlegungen zu seiner zellmechanischen Bedeutung. *Plant Systematics and Evolution* **116:**454-74.

von Stosch, H. A. & Drebes, G. 1964. Entwicklungsgeschichtliche Untersuchungen an zentrischen Diatomeen IV. *Helgoländer wissenschaftliche Meeresuntersuchungen* **11(3-4):** 209-257.

von Stosch, H. A. 1965. Manipulierung der zellgrösse von diatomeen in experiment. *Phycologia* **5:**21-44.

von Stosch, H. A., Theil, G. & Kowallik, K. 1973. Entwicklungsgeschichtliche Untersuchungen an zentrischen Diatomeen. V. Bau und Lebenszyklus von *Chaetoceros didymium*, mit Beobachtungen uber einige andere Arten der Gattung. *Helgolander Wiss. Meeresunters* **25:**384-445.

Weinbauer, M. G. 2004. Ecology of prokaryotic viruses. *FEMS Microbiology Reviews* **28:**127-81.

Wickham H. 2009. ggplot2: Elegant Graphics for Data Analysis. Ggplot2: Elegant Graphics for Data Analysis **doi:**10.1007/978-0-387-98141-3:1-212.

Wilhelm, S. W. & Suttle, C. A. 1999. Viruses and nutrient cycles in the sea: viruses play critical roles in the structure and function of aquatic food webs. *Bioscience* **49:**781-88.

Wilson, W. H., Tarran, G. A., Schroeder, D., Cox, M., Oke, J. & Malin, G. 2002. Isolation of viruses responsible for the demise of an *Emiliania huxley*i bloom in the English Channel. *Journal of the Marine Biological Association of the United Kingdom* **82:**369-77.

Winter, C., Bouvier, T., Weinbauer, M. G. & Thingstad, T. F. 2010. Trade-offs between competition and defense specialists among unicellular planktonic organisms: the "killing the winner" hypothesis revisited. *Microbiology and Molecular Biology Reviews* **74:**42-57.

Winterbourn, C. C., Hampton, M. B. 2008. Thiol chemistry and specificity in redox signaling. *Free Radical Biology and Medicine* ***45*****(5):** 549-561.

Wommack, K. E. & Colwell, R. R. 2000. Virioplankton: Viruses in aquatic ecosystems. *Microbiology and Molecular Biology Reviews* **64(1):** 69-114.

Wood, A. M., Everroad, R. & Wingard, L. 2005. Measuring growth rates in microalgal cultures. *Algal culturing techniques* **18:**269-85.

Wood, T. K., Knabel, S. J. & Kwan, B. W. 2013. Bacterial persister cell formation and dormancy. *Applied and environmental microbiology* **79(23):**7116-7121.

Zingone, A., Natale, F., Biffali, E., Borra, M., Forlani, G. & Sarno, D. 2006. Diversity in morphology, infectivity, molecular characteristics and induced host resistance between two viruses infecting Micromonas pusilla. *Aquatic microbial ecology* **45(1):** 1-1.

.

Appendix

Appendix

Appendix 5.1: Cytological comportments (CC) and molecular function (MF) up (green) and down (red) regulated in each comparison based on Gene Ontology.

T2T_T2C	T3T_T2C	T3T_T2T	T4T_T2C	T4T_T2T	T4T_T3T	Category	GO_id	GO_Name
					X	CC	GO:0000408	EKC/KEOPS complex
				X		CC	GO:0003755	peptidyl-prolyl cis-trans isomerase activity
				X		CC	GO:0004109	coproporphyrinogen oxidase activity
				X		CC	GO:0004314	[acyl-carrier-protein] S-malonyltransferase activity
				X		CC	GO:0004807	triose-phosphate isomerase activity
X	X	X	X	X		CC	GO:0005634	nucleus
			X			CC	GO:0005643	nuclear pore
X				X		CC	GO:0005654	nucleoplasm
X	X		X	X	X	CC	GO:0005730	nucleolus
					X	CC	GO:0005737	cytoplasm
	X					CC	GO:0005743	mitochondrial inner membrane
X		X				CC	GO:0005829	cytosol
	X	X				CC	GO:0005840	ribosome
	X			X		CC	GO:0005874	microtubule

				X			CC	GO:0005886	plasma membrane
				X			CC	GO:0008963	phospho-N-acetylmuramoyl-pentapeptide-transferase activity
	X	X	X	X			CC	GO:0009507	chloroplast
	X	X	X	X			CC	GO:0009523	photosystem II
	X	X	X	X			CC	GO:0009535	chloroplast thylakoid membrane
	X	X					CC	GO:0009654	photosystem II oxygen evolving complex
		X					CC	GO:0015934	large ribosomal subunit
		X					CC	GO:0015935	small ribosomal subunit
	X	X	X				CC	GO:0016021	integral component of membrane
				X			CC	GO:0016168	chlorophyll binding
	X	X					CC	GO:0019898	extrinsic component of membrane
	X	X					CC	GO:0022625	cytosolic large ribosomal subunit
	X	X			X		CC	GO:0022627	cytosolic small ribosomal subunit
	X	X	X	X			CC	GO:0030076	light-harvesting complex
X							CC	GO:0030686	90S preribosome
X							CC	GO:0030687	preribosome, large subunit precursor
X					X		CC	GO:0031428	box C/D snoRNP complex
X	X		X	X	X		CC	GO:0032040	small-subunit processome
		X					CC	GO:0042555	MCM complex

X	X		X				MF	GO:0003676	nucleic acid binding
X	X	X		X	X		MF	GO:0003677	DNA binding
		X					MF	GO:0003678	DNA helicase activity
X		X	X				MF	GO:0003723	RNA binding
	X	X					MF	GO:0003735	structural constituent of ribosome
						X	MF	GO:0003735	structural constituent of ribosome
	X	X	X				MF	GO:0003755	peptidyl-prolyl cis-trans isomerase activity
X							MF	GO:0003899	DNA-directed 5'-3' RNA polymerase activity
						X	MF	GO:0003995	acyl-CoA dehydrogenase activity
			X				MF	GO:0004004	ATP-dependent RNA helicase activity
	X						MF	GO:0004014	adenosylmethionine decarboxylase activity
						X	MF	GO:0004075	biotin carboxylase activity
	X	X	X				MF	GO:0004109	coproporphyrinogen oxidase activity
	X	X					MF	GO:0004314	[acyl-carrier-protein] S-malonyltransferase activity
	X						MF	GO:0004349	glutamate 5-kinase activity
	X						MF	GO:0004350	glutamate-5-semialdehyde dehydrogenase activity
X	X						MF	GO:0004386	helicase activity
						X	MF	GO:0004476	mannose-6-phosphate isomerase activity
X							MF	GO:0004488	methylenetetrahydrofolate dehydrogenase (NADP+) activity

	X					MF	GO:0004550	nucleoside diphosphate kinase activity
					X	MF	GO:0004550	nucleoside diphosphate kinase activity
	X		X			MF	GO:0004672	protein kinase activity
					X	MF	GO:0004719	protein-L-isoaspartate (D-aspartate) O-methyltransferase activity
					X	MF	GO:0004736	pyruvate carboxylase activity
		X				MF	GO:0004748	ribonucleoside-diphosphate reductase activity, thioredoxin disulfide as acceptor
X	X	X	X			MF	GO:0004807	triose-phosphate isomerase activity
					X	MF	GO:0004807	triose-phosphate isomerase activity
		X				MF	GO:0004853	uroporphyrinogen decarboxylase activity
				X		MF	GO:0005200	structural constituent of cytoskeleton
			X			MF	GO:0005215	transporter activity
					X	MF	GO:0005215	transporter activity
	X					MF	GO:0005506	iron ion binding
X	X		X	X		MF	GO:0005524	ATP binding
		X				MF	GO:0008097	5S rRNA binding
					X	MF	GO:0008440	inositol-1,4,5-trisphosphate 3-kinase activity
	X					MF	GO:0009055	electron carrier activity
					X	MF	GO:0009374	biotin binding

				X	MF	GO:0015098	molybdate ion transmembrane transporter activity
				X	MF	GO:0015204	urea transmembrane transporter activity
				X	MF	GO:0015930	glutamate synthase activity
	X	X	X		MF	GO:0016168	chlorophyll binding
				X	MF	GO:0016491	oxidoreductase activity
	X	X			MF	GO:0016836	hydro-lyase activity
				X	MF	GO:0016872	intramolecular lyase activity
X					MF	GO:0016887	ATPase activity
		X			MF	GO:0019843	rRNA binding
				X	MF	GO:0030170	pyridoxal phosphate binding
				X	MF	GO:0030515	snoRNA binding
	X		X		MF	GO:0031409	pigment binding
		X			MF	GO:0046429	4-hydroxy-3-methylbut-2-en-1-yl diphosphate synthase activity
X					MF	GO:0046872	metal ion binding
X					MF	GO:0046982	protein heterodimerization activity
				X	MF	GO:0031151	histone methyltransferase activity (H3-K79 specific)

Appendix 5.2: Top 20 transcripts up regulated in the comparison of T2T/T3T/T4T to control and relative fold change (Log FC) and p value.

			T2T_T2C		T3T_T2C		T4T_T2C	
TranscriptName	**DescriptionSP**	**OSNameSP**	**Log FC**	**P value**	**Log FC**	**P value**	**Log FC**	**P value**
TR1043|c0_g1_i1	UPF0187 protein alr2987	Nostoc sp. (strain PCC 7120 / SAG 25.82 / UTEX 2576)	8.958865326	7.05662E-10	10.72700385	2.00676E-13	12.11511459	2.43744E-15
TR25895|c0_g6_i1	Type-3 glutamine synthetase	Dictyostelium discoideum	8.859603913	1.29499E-08	9.653901601	1.98809E-10	8.785302309	6.28624E-09
TR4045|c0_g1_i2	Ribosome biogenesis protein BOP1 homolog	Oryza sativa subsp. japonica	8.913134202	4.85241E-11	9.300427935	2.49976E-12	11.27318671	1.10672E-15
TR17114|c0_g1_i1	Peroxiredoxin-6	Homo sapiens	-	-	13.13409194	4.54838E-12	-	-
TR3062|c0_g1_i2	Magnesium-chelatase subunit ChlD	Synechococcus elongatus (strain PCC 7942)	7.135658373	3.97647E-07	13.3150304	4.72649E-18	14.72998759	2.58104E-19
TR24256|c0_g2_i1	Heat shock cognate 70 kDa protein 1	Dictyostelium discoideum	8.908875538	4.46881E-08	12.42127947	4.23447E-13	13.3759878	5.81307E-14
TR8519|c0_g1_i1	2-oxoglutarate dehydrogenase mitochondrial	Dictyostelium discoideum	9.160377165	6.49238E-12	9.901775466	8.90048E-14	10.07441197	4.6716E-14
TR9540|c0_g1_i1	-	-	7.718160158	3.14065E-08	14.761536	5.34845E-19	15.72390497	1.05845E-19
TR7837|c0_g1_i4	-	-	8.588736472	2.64547E-07	8.015618338	8.46896E-07	7.942712324	1.16891E-06
TR6812|c0_g2_i3	-	-	8.571749517	3.30196E-09	11.16044252	2.55191E-14	11.69002811	4.69137E-15
TR6804|c0_g1_i2	-	-	-	-	13.09211049	3.70299E-18	13.01453751	4.51794E-18
TR6691|c0_g1_i1	-	-	9.043313121	1.00972E-10	12.20229587	2.23977E-16	11.78059477	8.03651E-

								16
TR6377|c0_g2_i1	-	-	8.980771254	0.000000005	10.2602796	1.49557E-11	9.188697284	9.48063E-10
TR4787|c0_g1_i1	-	-	8.698436258	9.21508E-09	8.486327683	8.87719E-09	8.232267859	2.66115E-08
TR4486|c0_g4_i1	-	-	6.619093449	1.93662E-06	13.47921217	9.59528E-19	14.97166044	4.91503E-20
TR4486|c0_g3_i1	-	-	-	-	10.59952429	1.96381E-13	12.12752571	1.92214E-15
TR4486|c0_g2_i2	-	-	5.066930894	0.001526809	13.09618606	3.12295E-18	13.80805838	6.19602E-19
TR4221|c0_g3_i1	-	-	-	-	8.118695378	0.000123066	15.38457767	8.90202E-10
TR4221|c0_g1_i1	-	-	5.454343445	0.003468578	7.476897384	7.66929E-07	14.91869111	8.33543E-17
TR4112|c0_g1_i1	-	-	6.430408944	0.000233882	11.3955439	5.16623E-13	15.59721886	7.50375E-17
TR3652|c0_g1_i2	-	-	8.627082563	6.64203E-09	6.882841317	2.78867E-06	7.508772832	2.53112E-07
TR31736|c0_g1_i1	-	-	5.644754643	0.00045352	13.62735799	7.61624E-18	14.42398412	1.49485E-18
TR31127|c0_g1_i1	-	-	-	-	6.575838326	0.008730701	15.59968354	1.45496E-08
TR30405|c0_g1_i2	-	-	8.462085975	2.9489E-10	11.33337552	4.54245E-16	11.43352803	3.32967E-16
TR30401|c0_g3_i18	-	-	8.572464047	5.48428E-10	10.99662384	5.40643E-15	11.33041082	1.76676E-15
TR30391|c0_g4_i1	-	-	5.793923337	8.33905E-05	12.89942344	2.9017E-18	12.81902355	3.59219E-18
TR3035|c0_g1_i1	-	-	7.372621001	1.98314E-05	12.81601659	1.9116E-13	15.14307177	3.12284E-15
TR29276|c0_g1_i1	-	-	5.359113342	0.001759396	13.83629446	1.82671E-17	15.41586231	9.87193E-19
TR29249|c1_g2_i9	-	-	6.44533733	1.42044E-05	13.02190721	1.46114E-17	14.21971071	1.04617E-

								18
TR29209|c0_g9_i1	-	-	6.329376201	0.000154115	13.51874724	2.676E-13	14.70461994	2.64105E-17
TR29209|c0_g3_i1	-	-	6.883777358	4.29991E-06	14.2406427	4.27341E-18	15.49485383	4.58823E-19
TR29202|c0_g1_i1	-	-	6.783424481	5.40749E-06	14.42322159	2.1318E-18	14.994599	7.52427E-19
TR28947|c0_g1_i3	-	-	8.552859003	0.000000001	8.484912592	4.49715E-10	10.30141064	2.32831E-13
TR28927|c0_g8_i1	-	-	6.562384928	5.56571E-05	12.71188171	9.18714E-16	14.7387455	1.25688E-17
TR28927|c0_g6_i1	-	-	6.651631018	4.30711E-06	13.18347359	7.83568E-18	15.38293234	1.02804E-19
TR28072|c0_g3_i1	-	-	5.506344527	0.00109356	13.74359893	1.40225E-17	14.20897486	5.39354E-18
TR27310|c1_g1_i2	-	-	8.376165926	3.85613E-09	13.45034928	3.39967E-17	16.52711116	1.52425E-19
TR27129|c1_g3_i1	-	-	8.700117464	1.91849E-09	10.70655236	1.33901E-13	11.34416138	1.51098E-14
TR27056|c0_g2_i1	-	-	6.684790133	9.65272E-06	13.07788346	3.31725E-17	13.7527349	7.15923E-18
TR2642|c0_g4_i1	-	-	7.961206681	2.38891E-08	14.34326712	5.10175E-18	17.38879958	4.61754E-20
TR26094|c0_g2_i1	-	-	9.158476544	7.42518E-10	5.764532807	0.000230847	8.501195623	5.21045E-09
TR23722|c2_g2_i2	-	-	8.494283694	2.48174E-08	9.092754669	7.77647E-10	9.194757266	5.39029E-10
TR23384|c0_g7_i1	-	-	8.595724076	1.22887E-08	12.81291351	2.29884E-15	16.94393143	1.50486E-18
TR23336|c1_g1_i1	-	-	6.678518626	0.001235215	13.39403663	2.11327E-11	14.85716819	2.71138E-12
TR21381|c0_g4_i2	-	-	9.090106052	6.29107E-10	8.678816912	1.45293E-09	8.589209929	2.24416E-09
TR18071|c0_g1_i2	-	-	-	-	6.100048234	0.000109296	14.52994638	4.47338E-

								17
TR18043|c0_g1_i1	-	-	5.762345269	0.00013412	13.1508732	4.59281E-18	14.33748657	3.5473E-19
TR11062|c0_g1_i1	-	-	9.6213084	5.38642E-10	9.121718979	1.83729E-09	8.827286497	6.2329E-09
TR10427|c0_g7_i1	-	-	7.30218316	2.97472E-05	12.13546842	1.11256E-12	16.28817428	8.35241E-16